Applications of Filippov's method to modelling avian influenza

Nyuk Sian Chong

Thesis submitted to the Faculty of Graduate and Postdoctoral Studies in partial fulfillment of the requirements for the degree of
Doctor of Philosophy in Mathematics[1]

Department of Mathematics and Statistics
Faculty of Science
University of Ottawa

[1]The Ph.D. program is a joint program with Carleton University, administered by the Ottawa-Carleton Institute of Mathematics and Statistics

Abstract

Avian influenza is a contagious viral disease caused by influenza virus type A. Avian influenza can be disastrous (if it occurs), due to the short incubation period (about 1–4 days). Thus it is important to study this disease so that we are more prepared to manage it in the future. A classical system of differential equations (the half-saturated incidence model) and three Filippov models — an avian-only model with culling of infected birds, an SIIR (Susceptible-Infected-Infected-Recovered) model with quarantine of infected humans and an avian-only model with culling both susceptible and infected birds — that are governed by ordinary differential equations with discontinuous right-hand sides (i.e., differential inclusion) are proposed to study the transmission of avian influenza. The effect of half-saturated incidence is investigated, and the outcome of this model is compared with the bilinear incidence model. Both models remain endemic whenever their respective basic reproduction numbers are greater than one. The half-saturated incidence model generates more infected individuals than the bilinear incidence model. This may be because the bilinear incidence model is underestimating the number of infected individuals at the outbreak. For the Filippov models, the number of infected individuals is used as a reference in applying control strategies. If this number is greater than a threshold value, a control measure has to be employed immediately to avoid a more severe outbreak. Otherwise, no action is necessary. We perform dynamical system analysis for all models. The existence of sliding modes and the flow on the discontinuity surfaces are determined. In addition, numerical simulations are conducted to illustrate the dynamics of the models. Our results suggest that if appropriate tolerance thresholds are chosen such that all trajectories of the Filippov models are converging to an equilibrium point that lies in the region below the infected tolerance threshold or on the discontinuity surface, then no control strategy is necessary as we consider the outbreak is tolerable. Otherwise, we have to apply control strategies to contain the outbreak. Hence a well-defined threshold policy is crucial for us to combat avian influenza effectively.

Dedications

This thesis is dedicated to my beloved parents, Yap Kiew and Heng Hui, my dearest husband, Kak Choon, and my lovely siblings, Nyuk Ling, Nyuk Yuin, Tze Huat and Tze Lung. Thank you for loving me unconditionally; thank you for being a constant source of encouragement during my challenging graduate life in abroad.

Acknowledgement

After a challenging five years of my Ph.D. study at University of Ottawa, now is the time for me to write this note of appreciation to whom I am greatly indebted.

My deepest gratitude goes to my supervisor, Dr. Robert J. Smith?, for his endless motivation and inspiring suggestions in my study and research work. I am truly grateful for his financial support to allow me to participate in several workshops and conferences throughout my studies. A special thanks to my co-supervisor, who is also the Director of Graduate Programs, Dr. Benoit Dionne, for his valuable comments to improve this thesis and his help in solving LaTeX problems that I had encountered.

I must acknowledge my two sponsors, Universiti Malaysia Terengganu and Ministry of Higher Education Malaysia, for the scholarship given to pursue my studies at University of Ottawa, Canada.

Special thanks go to my thesis committee, Dr. Christopher Bauch, Dr. David Sankoff, Dr. Victor Leblanc and Dr. David E. Amundsen, for their valuable feedback and comments, which have led to significant improvement of my thesis.

I would like to extend my appreciation to all the staff in the Department of Mathematics and Statistics. In particular Dr. Monica Nevins, Dr. Rafal Kulik, Diane Demers, Carolynne Roy, Chantal Giroux, Mayada El Maalouf, Janick Rainville and Rolland Fillion.

Two important people in my life that I am deeply thankful are Prof. Dr. Abu Osman bin Md Tap and Prof. Dr. Ong Boon Hua. Without their unconditional help and support, my dream to study in Canada would not be realized.

Thank you to my parents and family members for being good listeners and for their endless love. Kak Choon, my husband, also my colleague and classmate, I could not have completed this thesis without you. You have been so patient with me when I am frustrated and celebrate with me when things go right.

To Mr. Mohamed Amari and Mdm. Azidah Buang, I appreciate your assistant in our settlement in Ottawa and your continuous concern about my well-being here.

For both academic sharings and rock-solid support, I also thank Rachelle Miron, Kevin Church, Emily Campling, Jarno van der Kolk, Jeff Musgrave, Yuxiang Zhang, Jason Bramburger, Marc Beauparlant, Andrew Tomayer, Yue Dong and Bryson Hayes.

I would not be who am I today without you all.

Contents

List of Figures

List of Tables

Chapter 1

Introduction

The 1918 Spanish flu (H1N1), the 1957 Asian flu (H2N2) and the 1968 Hong Kong flu (H3N2) are the three great influenza A pandemics that happened in the twentieth century. The 1918 Spanish flu was extremely severe, causing approximately 50 million deaths (including 675,000 deaths in the United States alone) and infecting about one third of the world's population [1, 2, 3]. However, the 1957 Asian flu, which first emerged in China in February 1957, was not as disastrous as the 1918 Spanish flu; approximately 70,000 people died in the United States. This reduction was partly due to advances in laboratory technology to identify the new influenza virus as well as to develop new vaccines [1, 2, 4, 5]. Among these three influenza A pandemics in the 20th century, the 1968 Hong Kong flu was considered the mildest pandemic; roughly 34,000 people died in the United States [1, 6]. Influenza has a very short incubation period (1 to 4 days) and a large number of infectious influenza viruses are present in the respiratory secretions that are discharged by sneezing or coughing (airborne transmission) and through direct or indirect contact with infected individuals [7, 8, 9].

Additionally, humans may contract influenza disease from avian (bird) populations. Although avian influenza does not usually spread to humans, there are several cases of human infections from avian influenza that have been reported; for instance, H5N1 in Hong Kong (1997), H7N7 in the Netherlands (2004) and H7N9 in China (2013) [10, 11, 12, 13, 14, 15]. Before the H5N1 outbreak in Hong Kong in 1997, it was not known that avian influenza could infect humans. Six out of eighteen confirmed H5N1 infected individuals died during the first outbreak of avian influenza in Hong Kong in 1997. Humans contract H5N1 directly from chickens. More than 1.5 million chickens from all poultry markets and farms were culled by the end of December 1997 to stop the outbreak [12, 16]. In 2003, an outbreak of the highly pathogenic avian influenza H7N7 occurred in the Netherlands. The disease was transmitted from human to human. A total of 89 individuals were infected, 78 of whom had conjunctivitis. In order to control the outbreak, more than 30 million chickens were killed and other control strategies, such as personal protection, hygienic measures and antiviral

prophylaxis, were applied [13]. The recently reported avian influenza H7N9 outbreak in China in March 2013 caused 44 deaths out of 132 infected humans (one third of infections resulting in death). There was no evidence of human-to-human transmission. However, it is believed that humans contracted this disease from infected poultry or a contaminated environment, since most of the reported cases had poultry exposure and lived in the H7N9 contaminated areas [10, 17, 18].

As a result, it is crucial to study influenza A illness and viruses so that we may be better prepared to handle an outbreak in future. Mathematical modelling is one of the tools that has been widely used in the study of influenza. It can provide helpful information especially to public-health organisations and authorities; for instance, to determine when to apply control methods, which is the most efficient and cost-effective treatment, and how the influenza viruses is spreading [19, 20, 21, 22, 23, 24].

The influenza viruses are divided into three types, A, B and C, which all belong to the family of *Orthomyxoviridae*. Influenza type A is the most common type and is also the most prevalent. Wild birds are the natural hosts for the influenza A viruses. The influenza A viruses affect humans, pigs, horses, marine mammals and birds, while the influenza B viruses affect only humans, and the influenza C viruses affect humans and pigs [1, 25, 26]. Many people have difficulty telling the difference between a cold and the flu (also known as influenza) due to having similar symptoms, and mistakenly think that they are caused by the same virus. Flu is usually more severe than a cold, and it can generally lead to chronic conditions such as pneumonia and to hospitalization [1, 27, 28, 29]. Table 1.1 summarizes the difference between the common cold and influenza.

Influenza A virus is an enveloped virus whose external layer is covered by approximately 500 projecting spikes. These projecting spikes represent the glycoproteins; about 80% of these glycoproteins spikes are hemagglutinin (H), which is rod-shaped, and the rest are neuraminidase (N), which is mushroom-shaped. In addition, its virions (virus particles) contain:

(1) three membrane of proteins (H, N and the M_2 ion channel),

(2) a matrix protein M_1,

(3) NP (nucleocapsid) and

(4) a ribonucleoprotein core, which consists eight segments of RNA; each segment of RNA contains a transcriptase complex that made up of three additional viral polymerase proteins: PB1, PB2 and PA [1, 30].

Influenza A viruses are divided into subtypes, subject to the two glycoproteins on the surface of the virus — namely, hemagglutinin (H) and neuraminidase (N) — and are named according to the H and N glycoproteins on its surface. For instance, "H7N1"

Symptoms	The Common Cold	Influenza
Fever	Rare in adults and older children, but can be as high at 102°F in infants and small children	High (100 to 104°F), lasting 3–4 days
Headache	Rare	Prominent, sudden onset
General muscle aches and pain	Slight/mild	Common, often severe
Sore throat	Sometimes	Common
Cough, chest discomfort	Mild hacking cough	Common, can become severe
Sneezing	Often	Sometimes
Runny or stuffy nose	Often	Sometimes
Fatigue, weakness	Mild	Often extreme, lasting 2–3 weeks
Extreme exhaustion	Never	Sudden onset; can be severe
Complications	Sinus congestion or earache	Bronchitis, pneumonia
Prevention	None	Annual vaccination, antiviral drugs
Treatment	Temporary relief of symptoms	Antiviral drugs within 24–48 hours after onset of symptoms

Table 1.1: The difference between the common cold and influenza. Adapted from Shors [1], page 309.

describes a subtype of influenza A virus that has H7 and N1 proteins [1, 26, 30, 31]. There are 18 different H subtypes and 11 different N subtypes [26].

The knowledge of the subtype of the virus is crucial for vaccine preparation. Besides vaccination, antiviral medication is another option for the treatment of influenza. Currently, there are two types of influenza antivirals that are recommended for treatment: M_2 inhibitors and N inhibitors [1, 32]. The M_2 ion channel is important for virus replication, and hence it is the target for influenza antivirals. There are two types of M_2 inhibitors, amantadine and rimantadine, which block influenza A viruses from taking over the host cells by inhibiting the function of M_2 ion channel [1, 33]. However, the N inhibitors, Relenza (zanamivir) and Tamiflu (oseltamivir), inhibit the enzyme neuraminidase, which is responsible for cleaving the sialic acids from the surface of host cells or cell receptors. As a result, it inhibits the cell surface to release the newly formed virions [1, 33, 34].

In this thesis, we introduce a deterministic mathematical model with half-saturated incidence and models with a piecewise control strategy that takes into account a threshold policy in the study of avian influenza. The effect of half-saturated incidence on the spreading of avian influenza is investigated and compared to a model without half-saturated incidence. In addition, we propose both pharmaceutical and non-pharmaceutical control strategies for the human population in order to suppress the infection of avian influenza. We consider vaccination as a pharmaceutical control measure, whereas personal protection and isolation are non-pharmaceutical control

methods. The efficiency of these control measures are examined.

Next, we consider culling strategies for the bird population and quarantine for the human population. We use a threshold policy, also known as variable structure systems or on-off policy [35, 36], to represent culling and quarantine strategies. These mathematical models are governed by nonlinear ordinary differential equations with discontinuous right-hand sides, also known as differential inclusions. We propose an SIIR (Susceptible-Infected-Infected-Recovered) model incorporating a quarantine threshold policy and an avian-only model with culling either infected birds only or culling both susceptible and infected birds. In addition, by varying the threshold levels, all possible dynamics of these models are analyzed, and some numerical simulations are performed to illustrate the theoretical results.

An overview of ordinary differential equations with discontinuous right-hand sides based on the work of Aubin and Cellina [37], Filippov [38], Leine [39] and Utkin [36] is presented in Chapter 2. The behaviour of vector fields around the discontinuity surfaces, the types of regions on discontinuity surfaces, the existence of solutions, the methods of defining dynamical system on the discontinuity surfaces and the types of equilibrium points with their possible stability types will be discussed.

We investigate the half-saturated incidence rate model used in the study of the transmission of avian influenza in Chapter 3. The dynamics of the avian-only and avian–human half-saturated models are investigated. Moreover, the effect of half-saturated incidence on the avian-influenza transmission dynamics is examined when the basic reproduction number of the model is greater than one. Smith? [40] defines the basic reproduction number as "the average number of secondary infections caused by a single infectious individual during their entire infectious lifetime. It is a measure of how quickly a disease spreads in its initial phase and can predict whether a disease will become endemic or whether it will die out." We compare the total number of infected individuals predicted by the half-saturated incidence model with the total number predicted by the bilinear incidence model. Our results show that, although the half-saturated model predicts more infected people than the bilinear model, both models have decreasing number of infected people in the first approximately 225 days, and both models predict an endemic state at about 45 infected people. This shows that the disease-free equilibrium for these two models is not stable whenever their respective basic reproduction number is greater than one.

In Appendix A, we study the outcome for the half-saturated incidence model when the basic reproduction number of this model is less than one. This work has been published in the journal *Theory in Biosciences* [41]. In addition, we consider the implementation of several control methods for the human population to combat avian influenza; namely, pharmaceutical (vaccination) and non-pharmaceutical (personal protection and isolation) control measures. By solely implementing pharmaceutical protection, slightly more time is needed to reach disease eradication than by implementing solely a non-pharmaceutical protection or a combination of pharmaceutical

and non-pharmaceutical protections. In any case, by implementing a pharmaceutical protection, a non-pharmaceutical protection or a combination of both, the elimination of the disease is theoretically possible.

In Chapter 4, we focus our attention on the implementation of control measures on the infected populations. Two mathematical Filippov models with threshold policy are proposed: the avian-only model incorporating culling of infected birds and the SIIR (Susceptible-Infected-Infected-Recovered) model with quarantine for human population. For the avian-only Filippov model, the number of infected birds is used as a marker to determine the need for culling infected birds to manage the avian influenza outbreak. We assume that the outbreak is critical if the number of infected birds is more than a given tolerance threshold I_T. In this situation, we immediately employ a culling strategy to control and reduce the infection rate. However, if the number of infected birds is less than the tolerance threshold I_T, we consider the disease to be tolerable and no control measure is used.

The SIIR model with quarantine as a control measure consists of susceptible humans (S), humans infected with avian strain (I_a), humans infected with mutant strain (I_m) and humans who have recovered from avian and mutant strains (R). The number of infected humans (i.e., the total number of humans infected with either the avian strain or the mutant strain) is employed in the SIIR model as a marker to decide if a quarantine control strategy must be implemented. Infected humans are isolated to control the rate of transmission of the disease if the number of infected humans exceeds the tolerance threshold I_c. Otherwise, no control measure is implemented, as the disease is considered manageable. In addition, the dynamics of both the avian-only and SIIR models is analyzed when the value of the tolerance threshold is varied. Numerical simulations that depict the dynamics of these two models are also shown. We have published this work in the journal *Nonlinear Analysis: Real World Applications* [42].

In Chapter 5, we extend the depopulation threshold policy for the proposed avian-only model in Chapter 4 by considering not only the infected birds but also the susceptible birds. No control measure is applied when the number of infected birds is below the tolerance threshold I_b. However, culling is employed if the number of infected birds exceeds the tolerance threshold I_b. When the number of infected birds exceeds I_b and the number of susceptible birds is less than the tolerance threshold S_b, we only cull infected birds. However, when the numbers of infected birds and susceptible birds both exceed their respective thresholds, we cull both infected and susceptible birds. This is done to avoid that more susceptible birds contract avian influenza, which will make the outbreak worse and potentially uncontrollable. Furthermore, we examine the existence of equilibria, pseudoequilibria and pseudo-attractors and determine their stability as the tolerance thresholds are varied. This study has been published in the *Journal of Mathematical Biology* [43].

Finally, we end this thesis with a conclusion and a discusson of some future

avenues of research in Chapter 6.

Chapter 2

Review of ordinary differential equations with discontinuous right-hand sides: Differential Inclusions

In this chapter, we present several examples of the behaviour of a vector field around a discontinuity surface. Furthermore, we illustrate the types of discontinuity surfaces that we are interested in. We study the existence and uniqueness of solutions for discontinuous dynamical systems. We present some methods to describe the dynamics on discontinuous surfaces; in particular, the Filippov convex method and the Utkin equivalent control method. We end this chapter by presenting the types of equilibrium points that might exist for a discontinuous system and the types of stability that they may have. Much of the information in this chapter is summarized from [36, 38, 39]. Otherwise, we will specify it.

2.1 Review

Ordinary differential equations are widely used to model real-life phenomena in many disciplines such as biology, engineering, physics, ecology, chemistry, economic and finance. They can be used to describe the spread of diseases, population growth, mechanical system behaviour, trends in the stock market, motion of waves and molecules, and so on [39, 44, 45, 46, 47, 48].

In general, a classical dynamical system is represented by an ordinary differential equation as follows:

$$\dot{x} = f(x), \tag{2.1.1}$$

where $x \in \mathbb{R}^n$ is the n-dimensional state vector, f is the vector field and $\dot{x}$ is the

derivative of the state vector with respect to time t.

However, in many areas in applied mathematics, it is required to control the behaviour of the trajectories of a dynamical system. For instance, in disease management, it is necessary to apply control strategies to reduce the infection rate whenever the dynamics of a disease predicted by the model is within a critical region. No intervention is needed if the dynamics of the model predict that the number of infected individuals will stay in a safe region. Hence it is more appropriate to model this scenario with a dynamical system incorporating control parameters on the right-hand sides of the differential equations. In many situations, this breaks the continuity of the right-hand side in (2.1.1). The classical techniques for smooth dynamical systems cannot be used directly. A new approach is needed. We will use *differential inclusion* with the *Filippov convex method* or *Utkin equivalent control method* to describe the behaviour of the flow on the region of discontinuity of the dynamical system (2.1.1).

To formulate (2.1.1) as a differential inclusion, we replace the right-hand side $f(x)$ by a set-valued function $F(x)$, where $F(x) = \{f(x)\}$ whenever $f(x)$ is continuous at x. If $f(x)$ is discontinuous at x, the value of $F(x)$ is a set given by some topological restriction, as we will explain in Section 2.3. A solution $x(t)$ is continuous in time but may not be differentiable everywhere. The solution will not generally be unique. The following one-dimensional example describes the idea of extending a discontinuous differential equation to a differential inclusion.

Example 2.1.1. Consider the differential equation with discontinuous right-hand side:

$$\dot{x} = f(x) = -\Big(4\,\mathrm{sgn}\,(x) - 3\Big) = \begin{cases} 7 & \text{if } x < 0 \\ 3 & \text{if } x = 0 \\ -1 & \text{if } x > 0 \end{cases} \tag{2.1.2}$$

where

$$\mathrm{sgn}\,(x) = \begin{cases} -1 & \text{if } x < 0 \\ 0 & \text{if } x = 0 \\ 1 & \text{if } x > 0. \end{cases}$$

The solution of (2.1.2) with arbitrary initial condition $x(0) = x_0 \neq 0$ is

$$x(t) = \begin{cases} 7t + x_0, t < -\dfrac{x_0}{7} & \text{if } x_0 < 0 \\ -t + x_0, t < x_0 & \text{if } x_0 > 0, \end{cases}$$

which is illustrated in Figure 2.1. Since $\dot{x} > 0$ if $x < 0$ and $\dot{x} < 0$ if $x > 0$, we can see that each solution will approach $x = 0$ in finite time, and the solution will never leave $x = 0$ whenever it reaches $x = 0$. This suggests that $x = 0$ is an equilibrium for (2.1.2), but $x = 0$ is not a solution in the classical sense because $-(4\,\mathrm{sgn}\,(0) - 3) \neq 0$.

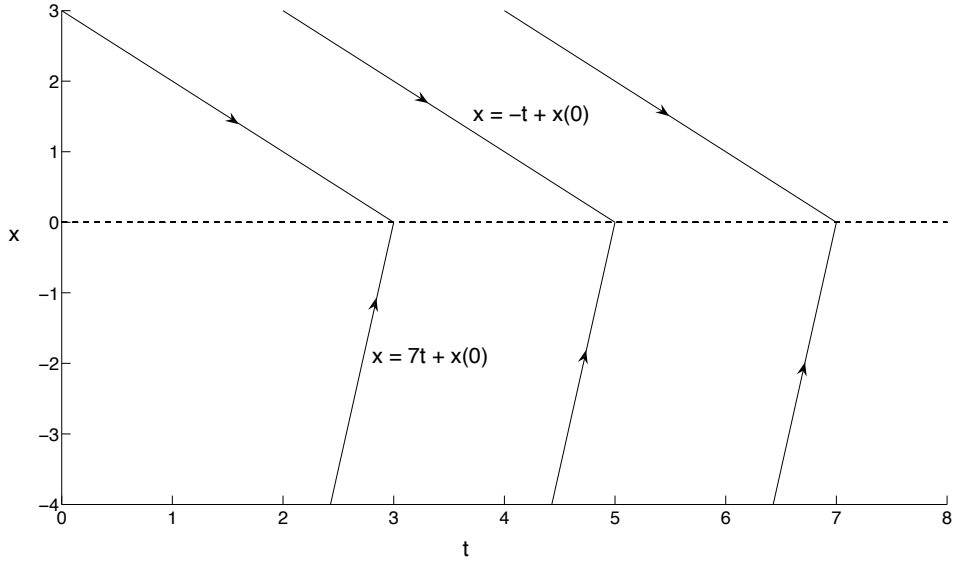

Figure 2.1: Solution of (2.1.2).

So, in this case, we replace $f(x)$ by a set-valued function $F(x)$ to obtain the differential inclusion

$$\dot{x} \in F(x) = \begin{cases} \{7\} & \text{if } x < 0 \\ [-1, 7] & \text{if } x = 0 \\ \{-1\} & \text{if } x > 0 \end{cases}$$

Hence, in this case, $x = 0$ is a solution.

We will explain in Section 2.3 how to select $F(x)$ when $f(x)$ is discontinuous at x.

2.2 Types of regions on the discontinuity surface

We consider an autonomous ordinary differential equation

$$\dot{x} = f(x), \qquad x \in \mathbb{R}^n, \tag{2.2.1}$$

where $f(x)$ is discontinuous at a surface M, which is defined by the equation

$$S(x) = 0,$$

where S is a smooth function. We assume that the surface M separates $\mathbb{R}^n$ into two domains: G^- and G^+. Let $f^+ = f\big|_{G^+}$ and $f^- = f\big|_{G^-}$. We assume that f^+ can be extended continuously to the closure $\overline{G^+}$ of G^+ and similarly for f^-. So f^+ and f^- are both defined on M but not necessarily equal.

There are three types of regions on the discontinuity surface M: sliding region, transversal (or sewing) region and escaping (or repulsion) region. Figure 2.2 illustrates the types of regions on M, and their definitions are given below. In this definition, $\langle x, y\rangle$ denotes the standard scalar product of two vectors x and y in $\mathbb{R}^n$.

Definition 2.2.1. *[49] Let $n = n(x)$ be the unit normal vector to M at x, where $n(x)$ points toward the region G^+.*

(a) If $\langle n, f^-\rangle > 0$ and $\langle n, f^+\rangle < 0$ on $\Omega \subset M$, then Ω is known as a sliding region.

(b) If $\langle n, f^-\rangle \cdot \langle n, f^+\rangle > 0$ (i.e., $\langle n, f^-\rangle$ and $\langle n, f^+\rangle$ have the same signs) on $\Omega_2 \subset M$, then Ω_2 is called a sewing region.

(c) If $\langle n, f^-\rangle < 0$ and $\langle n, f^+\rangle > 0$ on $\Omega_3 \subset M$, then Ω_3 is known as an escaping region.

We now show several examples of types of regions on the discontinuity surface. In this thesis, we focus our attention on the existence of sliding regions and the dynamical systems on them. Further discussion of sliding-mode scenarios will be conducted in the next section.

Example 2.2.2. Consider

$$\begin{aligned} \dot{x} &= 2 + \operatorname{sgn}(y-3) \\ \dot{y} &= 1 - 2\operatorname{sgn}(y-3). \end{aligned} \tag{2.2.2}$$

The right-hand side of (2.2.2) is

$$f(x,y) = \begin{pmatrix} 2 + \operatorname{sgn}(y-3) \\ 1 - 2\operatorname{sgn}(y-3) \end{pmatrix},$$

which is discontinuous along the line $M = \{(x,y) \in \mathbb{R}^2 : y = 3\}$. Let

$$G^- = \left\{(x,y) \in \mathbb{R}^2 : y < 3\right\} \quad \text{and} \quad G^+ = \left\{(x,y) \in \mathbb{R}^2 : y > 3\right\}.$$

Then

$$f^-(x,y) = f|_{G^-}(x,y) = \begin{pmatrix} 1 \\ 3 \end{pmatrix} \qquad \text{and} \qquad f^+(x,y) = f|_{G^+}(x,y) = \begin{pmatrix} 3 \\ -1 \end{pmatrix}.$$

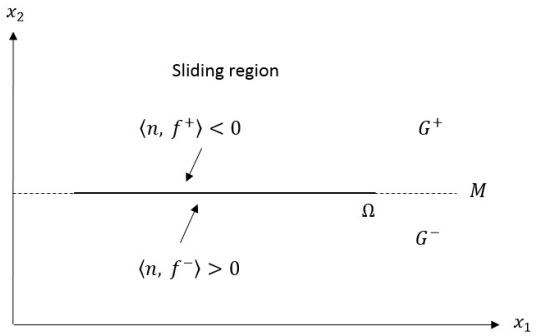

(a) A sliding region $\Omega \subset M$

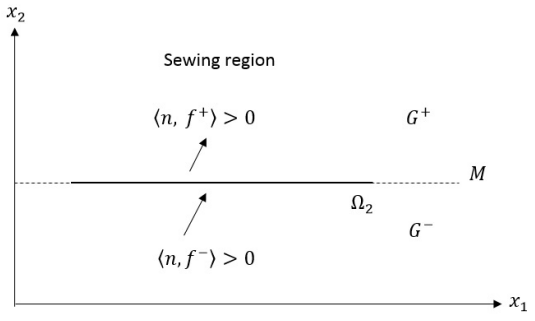

(b) A sewing region $\Omega_2 \subset M$

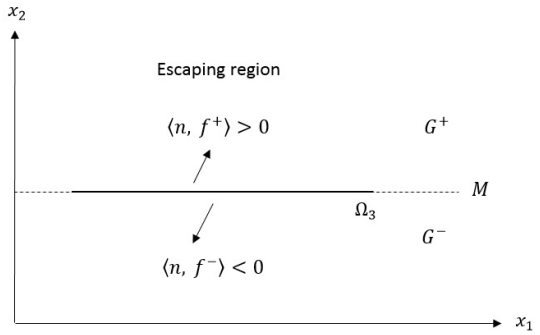

(c) An escaping region $\Omega_3 \subset M$

Figure 2.2: Types of regions on a discontinuity surface M.

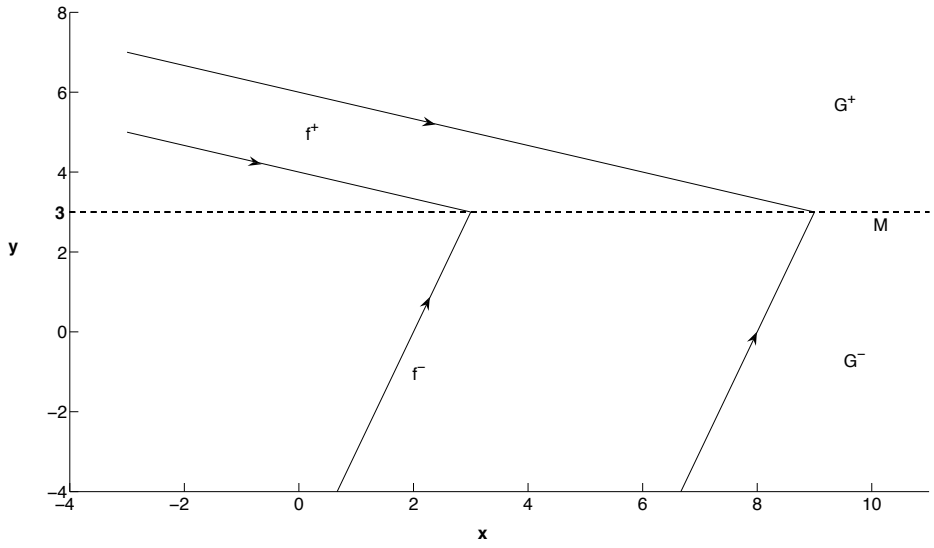

Figure 2.3: Sliding mode.

If $X = \begin{pmatrix} x & y \end{pmatrix}^\top$, then (2.2.2) can be written

$$\dot{X} = \begin{cases} \begin{pmatrix} 1 & 3 \end{pmatrix}^\top & \text{if } X \in G^- \\ \begin{pmatrix} 2 & 1 \end{pmatrix}^\top & \text{if } X \in M \\ \begin{pmatrix} 3 & -1 \end{pmatrix}^\top & \text{if } X \in G^+. \end{cases}$$

Let $n = \begin{pmatrix} 0 & 1 \end{pmatrix}^\top$ be the normal vector to M. The phase portrait of (2.2.2) is given in Figure 2.3. Since $\langle n, f^- \rangle = 3 > 0$ and $\langle n, f^+ \rangle = -1 < 0$, then $\Omega = M$ is a sliding domain for system (2.2.2) by Definition 2.2.1. Moreover, we can see from Figure 2.3 that the solutions for the discontinuous system (2.2.2) approach M in finite time, and they cannot leave the line M after that. Thus the flow will stay on and move along the line M. The sliding domain is $\Omega = M$. We call this type of phenomenon a sliding mode. The flow on the sliding domain will be studied in Section 2.3.

Example 2.2.3. Consider

$$\begin{aligned} \dot{x} &= 1 - 2\,\mathrm{sgn}\,(y-3) \\ \dot{y} &= -1 + 2\,\mathrm{sgn}\,(y-3). \end{aligned} \tag{2.2.3}$$

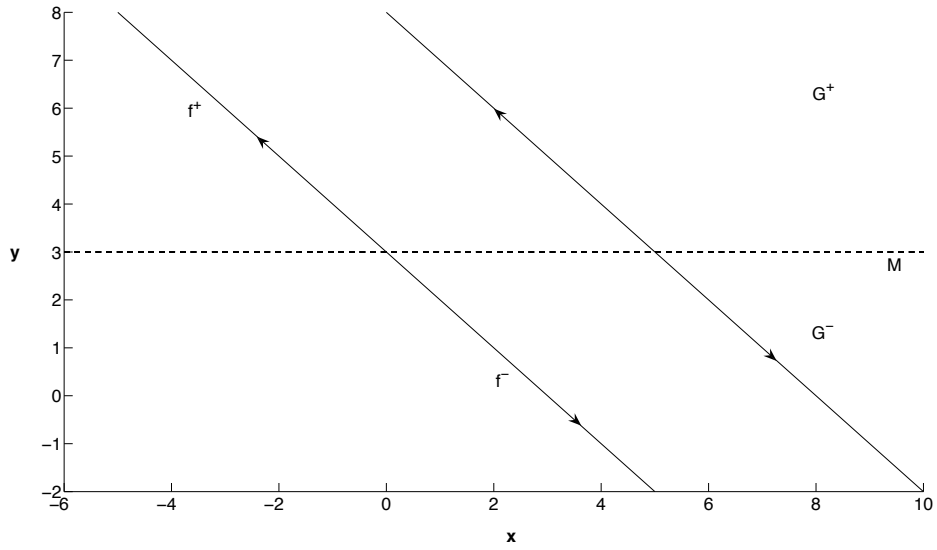

Figure 2.4: Escaping mode.

Using the same notation as in Example 2.2.2, we have

$$f^- = \begin{pmatrix} 3 \\ -3 \end{pmatrix} \quad \text{and} \quad f^+ = \begin{pmatrix} -1 \\ 1 \end{pmatrix}.$$

Since $\langle n, f^- \rangle = -3 < 0$ and $\langle n, f^+ \rangle = 1 > 0$, the solutions of (2.2.3) with initial conditions either in region G^- or G^+ will move away from the discontinuity line M as shown in Figure 2.4. However, a classical solution of (2.2.3) with initial conditions on M does not exist. We will define the concept of a solution for a differential inclusion later. Such solutions are unstable. This kind of phenomenon is known as an escaping mode.

Example 2.2.4. Consider

$$\begin{aligned} \dot{x} &= 2 + \operatorname{sgn}(y-3) \\ \dot{y} &= -2 + \operatorname{sgn}(y-3). \end{aligned} \tag{2.2.4}$$

The dynamical system in regions G^- and G^+ is governed by

$$f^- = \begin{pmatrix} 1 \\ -3 \end{pmatrix} \quad \text{and} \quad f^+ = \begin{pmatrix} 3 \\ -1 \end{pmatrix},$$

respectively. The phase portrait of (2.2.4) is given in Figure 2.5. Since the projections

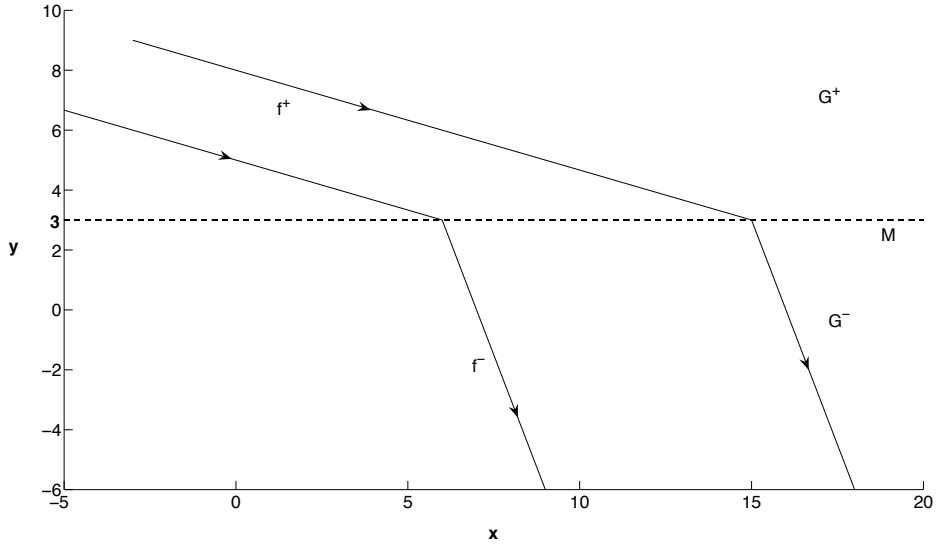

Figure 2.5: Transversal mode.

of f^- and f^+ on the normal to the discontinuity line M have the same sign (i.e., $\langle n, f^- \rangle = -3 < 0$ and $\langle n, f^+ \rangle = -1 < 0$), a transversal intersection occurs at M. So the solution of (2.2.4) with arbitrary initial conditions in region G^+ will cross M before moving into region G^-. Therefore the solution of this transversal system exists and is unique.

2.3 Existence of solutions

The existence and uniqueness of a solution for a classical system

$$\dot{x} = f(x, t) \tag{2.3.1}$$

is assured by the following theorem [50].

Theorem 2.3.1. *(Existence and uniqueness of solutions) Let $D \subset \mathbb{R}^n \times \mathbb{R}$ be an open set. Suppose that $f : D \to \mathbb{R}^n$ is continuous and that $(x_0, t_0) \in D$.*

(a) There exists a solution of (2.3.1) *on an open interval $(t_0 - \delta, t_0 + \delta)$, for some $\delta > 0$, satisfying $x(t_0) = x_0$.*

(b) If $f(x, t)$ is locally Lipschitz; namely, for any closed and bounded subset K of

D, there exists a constant $L = L_K > 0$ such that

$$||f(x,t) - f(y,t)|| \leq L||x - y|| \quad \forall\ (x,t),(y,t) \in K,$$

then there exists a unique solution of (2.3.1) *on* $(t_0 - \delta, t_o + \delta)$*, for some* $\delta > 0$*, satisfying* $x(t_0) = x_0$*.*

We consider an autonomous dynamical system defined by a piecewise continuous function f on a domain $G \subset \mathbb{R}^n$:

$$\dot{x} = f(x) \tag{2.3.2}$$

for $x \in G$. Suppose that the discontinuity surface M of (2.3.2) is defined by

$$M = \{x \in G : S_i(x) = 0 \quad \text{for } i = 1, \ldots, m\},$$

where $S_i : G \to \mathbb{R}$ are smooth functions. The solution of (2.3.2) exists and is unique on subsets V of $G \setminus M$, where there exists a Lipschitz constant $L = L_V$ such that

$$||f(x_2) - f(x_1)|| \leq L||x_2 - x_1|| \quad \forall x_1, x_2 \in V. \tag{2.3.3}$$

We replace (2.3.2) by the differential inclusion

$$\dot{x} \in F(x), \qquad x \in G, \tag{2.3.4}$$

where

$$F(x) = \bigcap_{\epsilon > 0} \bigcap_{\mu(N)=0} \overline{\text{co}} f\left(((x + \epsilon B) \cap G) \setminus N\right), \tag{2.3.5}$$

B is the unit ball in $\mathbb{R}^n$, μ is the Lebesgue measure on $\mathbb{R}^n$, N is any set and $\overline{\text{co}}A$ denotes the smallest closed and convex set containing A.

Let $P(\mathbb{R}^n)$ be the **power set** of $\mathbb{R}^n$; namely, the set of all subsets of $\mathbb{R}^n$.

Definition 2.3.2. *(Upper semi-continuity) [37] A set-valued function $F : G \to P(\mathbb{R}^n)$ is upper semi-continuous at $x \in G$ if, for any open neighbourhood W of $F(x)$, there exists an open neighbourhood $V \subset G$ of x such that $F(V) \subset W$. We say that F is upper semi-continuous on G if it is so at every $x \in G$.*

One can show that F defined in (2.3.5) is an upper semi-countinous set-valued function such that $F(x)$ is closed and convex for all x [37].

Example 2.3.3. If we apply the definition of F in (2.3.5) to the vector field f of Example 2.2.2, we find that

$$F(x,y) = \begin{cases} \{(1,3)\} & \text{if } y < 3 \text{ i.e. } (x,y) \in G^- \\ \{\lambda(3,-1) + (1-\lambda)(1,3) : 0 \leq \lambda \leq 1\} & \text{if } y = 3 \text{ i.e. } (x,y) \in M \\ \{(3,-1)\} & \text{if } y > 3 \text{ i.e. } (x,y) \in G^+. \end{cases}$$

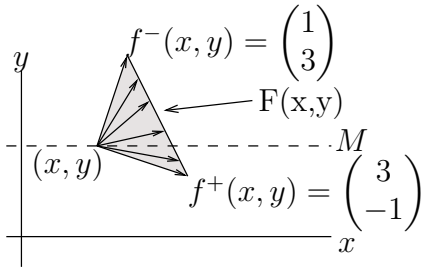

Figure 2.6: The image of F in Example 2.3.3 at a point on the region of discontinuity M. By tradition, we have drawn the vectors in $F(x,y)$ as arrows emanating from (x,y) instead of the origin.

That f in this example can be continuously expanded to $\overline{G^-}$ and $\overline{G^+}$ greatly simplifies F. The image of F at $(x,y) \in M$ is represented in Figure 2.6.

When f is continuous at x, we have $F(x) = \{f(x)\}$. Moreover, if f is Lebesgue measurable, then $f(x) \in F(x)$ almost everywhere in G [37]. The solutions of (2.3.4) will be expected to satisfy the following property.

Definition 2.3.4. *A function $\phi : [a,b] \to \mathbb{R}^n$ is absolutely continuous if, for every $\epsilon > 0$, there exists a $\delta > 0$ such that $\sum_{i \in I} \|\phi(b_i) - \phi(a_i)\| < \epsilon$ whenever $\{]a_i, b_i[; i \in I\}$ is a countable collection of mutually disjoint subintervals of $[a,b]$ satisfying $\sum_{i \in I} |b_i - a_i| < \delta$.*

Definition 2.3.5. *[39] An absolutely continuous function $x : [0,\tau] \to G$ is said to be a solution of (2.3.4) if*

$$\dot{x}(t) \in F(x(t))$$

for almost all $t \in [0,\tau]$.

We recall that an absolutely continuous function on an interval is differentiable almost everywhere on this interval (Theorem 8.19 of [51]).

We are interested on the conditions on F that guarantee the existence of solutions. The following theorem assures the existence of a solution.

Theorem 2.3.6. *(Existence of solutions) [37] Let $F : G \to P(\mathbb{R}^n)$ be a set-valued function. Assume that F is upper semi-continuous on G, and that $F(x)$ is a nonempty, closed, convex and bounded set for all $x \in G$. Then, for each $x_0 \in G$, there exists a $\tau > 0$ and an absolutely continuous function $x : [0,\tau] \to G$ that is a solution of the initial-value problem*

$$\dot{x}(t) \in F\big(x(t)\big), \quad x(0) = x_0. \tag{2.3.6}$$

Theorem 2.3.6 is proved in [37].

Before studying the dynamics of solutions for differential inclusion, we address the issue of the dependence of solutions on the initial conditions and the right-hand side of (2.3.4). For that, we need the following two concepts.

Definition 2.3.7. *Let $F_\delta(x) = (\operatorname{co} F(x+\delta B))+\delta B$, where $\delta \geq 0$ and B is the unit ball in $\mathbb{R}^n$. An approximate solution (with accuracy δ) of (2.3.4) is a function $y : \mathbb{R} \to G$ that is absolutely continuous on any given interval and satisfies $\dot{y}(t) \in F_\delta(y(t))$ almost everywhere.*

Definition 2.3.8. *The domain G of a set-valued function F satisfies the basic condition if $F(x)$ is nonempty, closed, bounded and convex for all $x \in G$ and F is upper semicontinuous on G.*

A proof of the existence of solutions for (2.3.4) and the studies of the dependence of solutions on initial conditions use approximation of solutions as defined above. In the next result that we state without proof, we are not only considering small perturbations on the right-hand side F in the domain where it is continuous but also on its entire domain, including the regions of discontinuity.

Theorem 2.3.9. *[38] Suppose that F in*

$$\dot{x}(t) \in F\big(x(t)\big), \quad x(t_0) = x_0 \tag{2.3.7}$$

satisfies the basic condition, $t_0 \in [a, b]$ and $x_0 \in G$. Suppose that all solutions of (2.3.7) exist for $a \leq t \leq b$ and their images are in G. Then, for every $\epsilon > 0$, there exists $\delta > 0$ such that, for $H : G \to P(\mathbb{R}^n)$ satisfying

$$H(x) \subset (F(x + \delta B) + \delta B)$$

for all $x \in G$ and the basic condition on G, $s_0 \in [a, b]$ satisfying $|s_0 - t_0| < \delta$ and $y_0 \in G$ satisfying $\|y_0 - x_0\| < \delta$, each solution $y(t)$ of

$$\dot{y}(t) \in H\big(y(t)\big), \quad y(s_0) = y_0$$

exists for $a \leq t \leq b$, and there is a solution x of (2.3.7) such that $\|x(t) - y(t)\| \leq \epsilon$ for all $a \leq t \leq b$.

We now present two approaches (among many) — the Filippov convex method in Section 2.3.1 and the Utkin equivalent control method in Section 2.3.2 — to describe the dynamics of (2.3.4) on the discontinuity region M.

2.3.1 Filippov Convex Method

We assume that the surface M separates G into two domains, G^- and G^+. We also assume that the subsets G^-, M and G^+ are defined by

$$G^- = \{x \in \mathbb{R}^n : S(x) < 0\} ,$$
$$M = \{x \in \mathbb{R}^n : S(x) = 0\}$$

and

$$G^+ = \{x \in \mathbb{R}^n : S(x) > 0\} .$$

As we did in the previous examples, we define the vector field on G^- as f^- and on G^+ as f^+.

Remark 2.3.10. If $x \in G^-$ or $x \in G^+$, then $F(x) = \{f(x)\}$ holds and we get the classical solution. If $x(t)$ is a solution on a sliding region along the discontinuity surface M, then $\dot{x} \in F(x)$.

Remark 2.3.11. If we assume that f can be extended continuously to $\overline{G^+}$ and $\overline{G^-}$, then (2.3.5) yields that $F(x)$ is the closure of the convex hull of

$$\left\{ z \in \mathbb{R}^n : z = \lim_{y \to x} f(y) \text{ for } y \in G \setminus M \right\}. \tag{2.3.8}$$

This procedure to generalize the differential equation (2.3.2) to a differential inclusion is due to Filippov [38].

The *Filippov convex method* is a method to select a potential vector field on M. We now describe this method. For $x \in M$, suppose that

$$f_x^- = \lim_{\substack{y \in G^- \\ y \to x}} f(y) \quad \text{and} \quad f_x^+ = \lim_{\substack{y \in G^+ \\ y \to x}} f(y)$$

exist. The set $F(x)$ is a linear segment joining the endpoints of vectors f_x^- and f_x^+. Assume that these vectors start from the point x. If this linear segment intersects the tangent plane P to M at x, then this intersection point is the endpoint of the vector $f_M(x)$ that describes the motion along the surface M (see Figure 2.7). If the function $x : \mathbb{R} \to M$ satisfies

$$\dot{x} = f_M(x), \tag{2.3.9}$$

then x is a solution of (2.3.4).

Let $n \equiv n(x)$ be the normal vector to M at x directed into G^+. We denote the projections of vectors f_x^- and f_x^+ onto n as $f_{x,n}^-$ and $f_{x,n}^+$, respectively. A sliding mode

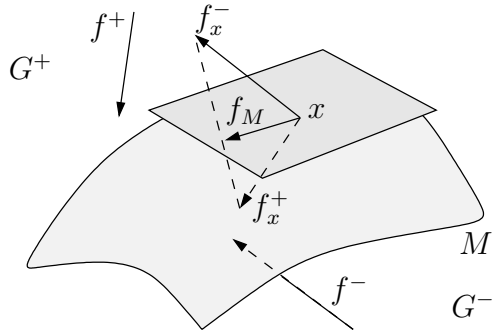

Figure 2.7: f^- and f^+ are the vector fields in regions G^- and G^+, respectively, whereas $f_M(x)$ is the vector field along the discontinuity surface M.

only exists if $f_{x,n}^+ < 0$ and $f_{x,n}^- > 0$; i.e., all vectors $f(x)$ for $x \in G \setminus M$ are directed toward M. All solutions will approach M from both sides, G^+ and G^-, as t increases. We have that

$$f_M(x) = \alpha f_x^+ + (1-\alpha) f_x^- \text{ where } \alpha = \frac{f_{x,n}^-}{f_{x,n}^- - f_{x,n}^+} \,. \tag{2.3.10}$$

We note that $0 \leq \alpha \leq 1$. If the surface M is given by the equation $S(x) = 0$ with S a continuously differentiable function, and f^- and f^+ are continuous on the closure of G^+ and G^- respectively, then

$$f_{\cdot,n}^- = \frac{\langle \nabla S, f^- \rangle}{|\nabla S|}, \quad f_{\cdot,n}^+ = \frac{\langle \nabla S, f^+ \rangle}{|\nabla S|} \quad \text{and} \quad \alpha = \frac{\langle \nabla S, f^- \rangle}{\langle \nabla S, f^- - f^+ \rangle}$$

when the gradient $\nabla S(x) \neq \vec{0}$, where $\langle \cdot, \cdot \rangle$ represents the standard scalar product on $\mathbb{R}^n$.

The system

$$\dot{x} = \begin{cases} f^- & ; x \in G^- \\ f_M & ; x \in M \\ f^+ & ; x \in G^+ \end{cases} \tag{2.3.11}$$

summarizes the Filippov convex method for (2.3.4) [38, 39]. The dynamic is governed by f^+ on G^+, by f^- on G^- and by f_M on M.

2.3.2 Utkin equivalent control method

We can also introduce a scalar or vector control parameter u into the discontinuous system (2.3.2) in order to improve the performance of the system or to control the behaviour of the dynamical system.

We assume that the control function $u : \mathbb{R}^n \to \mathbb{R}^m$ is at least continuous except on a set of measure zero. More precisely, we assume that each component u_i is discontinuous on an $n-1$ dimensional manifold M_i locally defined by $M_i = \{x : S_i(x) = 0\}$ for some continuously differentiable function $S_i : \mathbb{R}^n \to \mathbb{R}$.

A system of differential equations with a vector-valued control function u as above is defined by

$$\dot{x} = f(x, u) \ . \tag{2.3.12}$$

We assume that f is at least locally Lipschitz continuous in x and u. The discontinuity of the right-hand side of (2.3.12) comes from the discontinuity of the control function u.

Let M be a discontinuity surface. Without loss of generality, we may assume that

$$M = \left\{x \in \mathbb{R}^n : S_i(x) = 0 \text{ for all } i\right\} \ .$$

If some of the u_i are not discontinuous on M, we may include them in the definition of f and only consider the u_i that are discontinuous on M.

For an open neighbourhood of the discontinuity surface M, if the vector field $f(x, u)$ is directed toward M, then a sliding mode exists. The goal of the Utkin equivalent control method is to determine a continuous control function u_{eq} on M such that the flow on M defined by (2.3.12) with $u = u_{eq}$ is consistent with a regularization of the dynamical system.

First, we want to illustrate the choice of u_{eq}. Let us consider system (2.3.12) with a single discontinuity surface $S(x) = 0$. Let $u^-(x) = u(x)$ if $S(x) < 0$ and $u^+(x) = u(x)$ if $S(x) > 0$. We assume that u^- and u^+ can be extended to $\{x : S(x) \leq 0\}$ and $\{x : S(x) \geq 0\}$, respectively. The flow near $S(x) = 0$ is represented in Figure 2.8.

Suppose that $x : \mathbb{R} \to M$ is a solution of (2.3.12) with $u = u_{eq}$ and initial condition $x(0) = x_0 \in M$. Then $S\big(x(t)\big) = 0$ for all t (at least near 0). Hence

$$\frac{d}{dt} S\left((x(t)\right) = \mathrm{D}S\left(x(t)\right) \frac{dx}{dt} = \mathrm{D}S\left(x(t)\right) f\left(x(t), u\left(x(t)\right)\right) = 0$$

for all t where

$$\mathrm{D}S = \begin{pmatrix} \dfrac{\partial S_1}{\partial x_1} & \cdots & \dfrac{\partial S_1}{\partial x_n} \\ \vdots & \ddots & \vdots \\ \dfrac{\partial S_m}{\partial x_1} & \cdots & \dfrac{\partial S_m}{\partial x_n} \end{pmatrix}$$

is the Jacobian of S evaluated at $x(t)$. Thus u_{eq} is the solution of

$$W(x) f\big(x, u(x)\big) = 0 \tag{2.3.13}$$

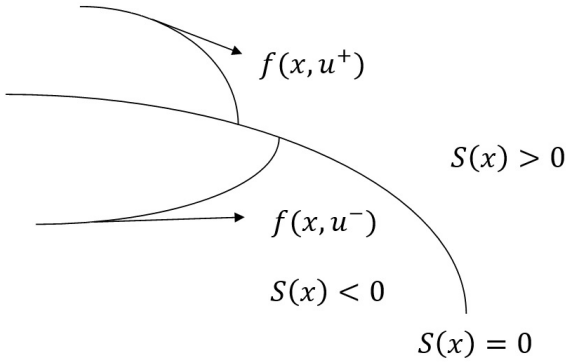

Figure 2.8: A sliding mode exists when the vector fields $f(x, u)$ is directed towards the discontinuous surface $S(x) = 0$.

for $x \in M$, where $W(x) = \mathrm{D}S(x)$.

Suppose that a solution u_{eq} of (2.3.13) exists. Substituting u with u_{eq} in (2.3.12), we obtain

$$\dot{x} = f(x, u_{eq}), \tag{2.3.14}$$

which governs the flow on the discontinuity surface M. The equation (2.3.14) is known as a *sliding-mode equation*.

From a geometric perspective, the Utkin equivalent control method defines a continuous control on the discontinuity boundary that regulates the velocity vector along this boundary. As an example, let us consider system (2.3.12) with a single discontinuity surface $S(x) = 0$, as we did to produce Figure 2.8. Let x_0 be a point on the surface $S(x) = 0$. By varying the scalar control u from u_0^+ to u_0^-, where

$$u_0^- = \lim_{\substack{S(y)<0 \\ y \to x_0}} u^-(y) \quad \text{and} \quad u_0^+ = \lim_{\substack{S(y)>0 \\ y \to x_0}} u^+(y),$$

we can draw the locus formed by the values $f(x_0, u)$ for u between u_0^- and u_0^+, and find the intersection point of this locus with the tangential plane to $S(x) = 0$ at x_0. This is illustrated in Figure 2.9. The value of u associated to this particular intersection point determines the equivalent control u_{eq}. By substituting u with u_{eq} in (2.3.12), we obtain the sliding-mode equation that describes the dynamics on the discontinuity surface $S(x) = 0$.

Since we use nonlinear systems with linear dependence on the control to study influenza A in this thesis, it is essential for us to discuss the Utkin equivalent control method for this type of dynamical system. Let us consider a nonlinear system with

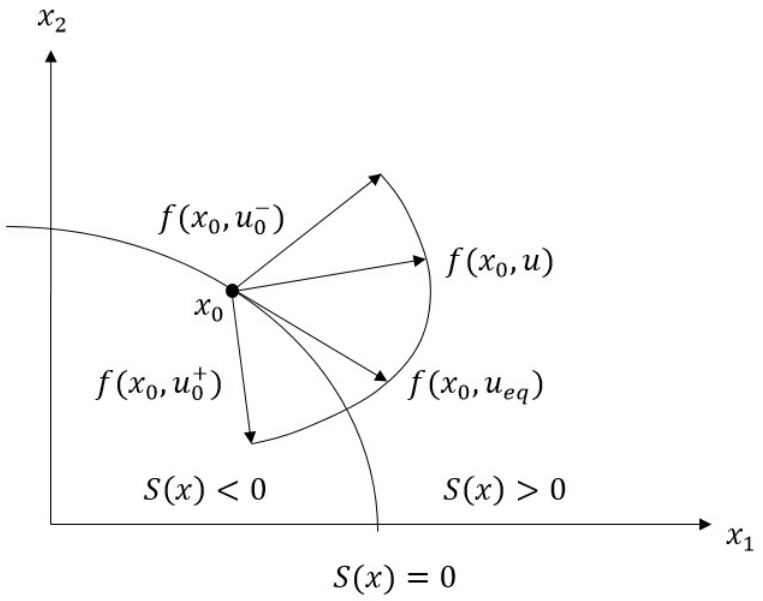

Figure 2.9: A geometric interpretation of the equivalent control u_{eq}. In this figure, $u_0^- < u < u_{eq} < u_0^+$.

linear dependence on a control function.

$$\dot{x} = f(x) + B(x)u(x), \tag{2.3.15}$$

where f is a Lipschitz-continuous vector-valued function from $\mathbb{R}^n$ to $\mathbb{R}^n$, B is a matrix valued function from $\mathbb{R}^n$ to the $n \times m$ matrices, and $u : \mathbb{R}^n \to \mathbb{R}^m$ is the control function that is discontinuous on the surface $M = \{x : S(x) = 0\}$ with $S : \mathbb{R}^n \to \mathbb{R}^m$ a continuously differentiable function.

The equivalent control u_{eq} for model (2.3.15) can be obtained as the solution of

$$W(x)\big(f(x) + B(x)u\big) = 0. \tag{2.3.16}$$

Assume that the $(m \times m)$-matrix WB has an inverse for all x. Then the equivalent control u_{eq} of model (2.3.15) obtained from (2.3.16) is

$$u_{eq} = -(WB)^{-1}Wf. \tag{2.3.17}$$

By substituting (2.3.17) into (2.3.15), we get the following sliding-mode equation on the discontinuity surface M.

$$\dot{x} = f - B(WB)^{-1}Wf. \tag{2.3.18}$$

However, if the inverse of WB does not exist, then we cannot apply the Utkin equivalent control method to define the sliding-mode equation on the discontinuity surface M, and we may have either infinitely many solutions or no solution for the control u_{eq}.

2.4 Equilibrium points

In this section, we use the notation introduced in Section 2.2. There are two types of equilibrium points that may exist in a Filippov system as (2.2.1): real equilibria and pseudoequilibria.

Definition 2.4.1. *[49]*

(a) $p \in \mathbb{R}^n \setminus M$ *is a real equilibrium if* $f(p) = 0$.

(b) $p \in M$ *is a pseudoequilibrium if* p *is an equilibrium point of a sliding mode dynamical system* $\dot{x} = f_M(x)$ *on* M*; i.e.,* $f_M(p) = 0$ *and* $S(p) = 0$.

2.4.1 Stability

There exist two types of stability for a differential inclusion system: stability and weak stability.

Definition 2.4.2. *Suppose that* $\varphi : [t_0, \infty[\to \mathbb{R}^n$ *is a solution of a differential inclusion* (2.3.4)*. The solution* φ *is called stable (weakly stable) if for every* $\epsilon > 0$ *there exists* $\delta > 0$ *such that, for all* x_0 *satisfying*

$$\left| x_0 - \varphi(t_0) \right| < \delta,$$

each solution (some solution) $\tilde{x}$ *with the initial condition* $\tilde{x}(t_0) = x_0$ *exists for* $t \geq t_0$ *and satisfies*

$$\left| \tilde{x}(t) - \varphi(t) \right| < \epsilon \qquad \forall t \geq t_0.$$

Moreover, the solution φ *is asymptotically stable (weakly asymptotically stable) if it is stable (weakly stable) and*

$$\tilde{x}(t) - \varphi(t) \to 0 \text{ as } t \to \infty.$$

The following example illustrates the types of stability of a differential inclusion.

Example 2.4.3. (page 153 of [38]) Consider

$$\dot{x} \in F(x) = \{y : kx \leq y \leq mx\} \subset \mathbb{R}.$$

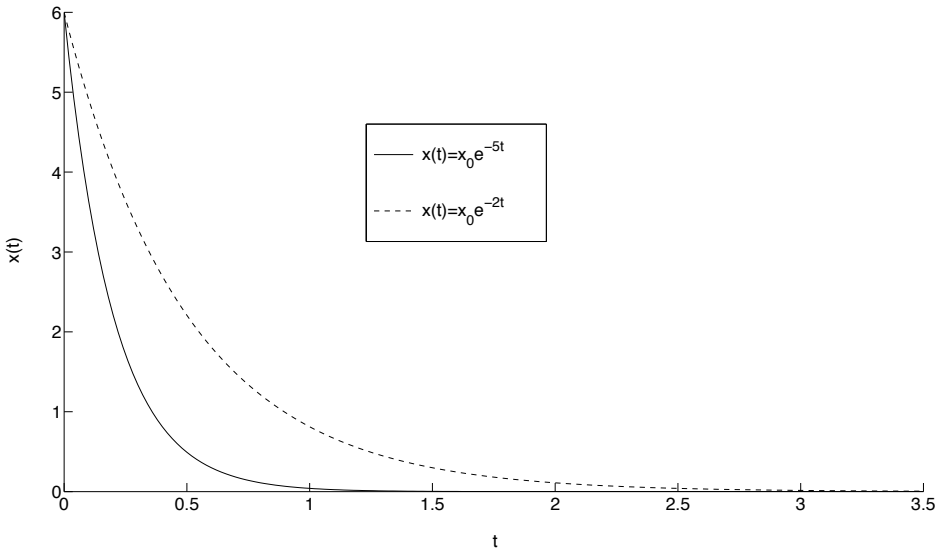

Figure 2.10: $\tilde{x} = 0$ is asymptotically stable whenever $k \leq m < 0$. Here $k = -5$ and $m = -2$ are chosen. Both solutions, $x(t) = x_0 e^{-5t}$ and $x(t) = x_0 e^{-2t}$, with $x_0 > 0$ approach $x = 0$ as t increases.

We have that $\tilde{x}(t) = 0$ for $t \in [0, \infty)$ is a solution of this system. The other solutions must satisfy $kx \leq \dot{x} \leq mx$. Since $\dot{x} = kx \implies x(t) = x_0 e^{kt}$ and $\dot{x} = mx \implies x(t) = x_0 e^{mt}$, where $x_0 = x(0)$, we get $x_0 e^{kt} \leq x(t) \leq x_0 e^{mt}$ for all t.

- If $k \leq m < 0$ and $x_0 > 0$ (resp. $x_0 < 0$), then $x_0 e^{kt} \leq x(t) \leq x_0 e^{mt}$ (resp. $x_0 e^{mt} \leq x(t) \leq x_0 e^{kt}$). For every $\epsilon > 0$ there exists $\delta > 0$ such that $|x_0 e^{kt}| < \epsilon$ and $|x_0 e^{mt}| < \epsilon$ for all t if $|x_0| < \delta$. Since $k \leq m < 0$, $x_0 e^{kt} \to 0$ and $x_0 e^{mt} \to 0$ as $t \to \infty$. Hence $\tilde{x}(t) \equiv 0$ is asymptotically stable as shown in Figure 2.10.

Below is the summary of the stability of the trivial solution for other possible values of k and m. We do not provide the proofs, since they are similar to the proof given above. The solution $\tilde{x}(t) = 0$ for all t is:

- stable if $k \leq m = 0$
- weakly asymptotically stable if $k < 0 < m$
- weakly stable if $k = 0 < m$
- unstable if $0 < k \leq m$.

2.4.2 Lyapunov stability

We first consider the dynamical system

$$\dot{x} = f(x), \tag{2.4.1}$$

where f is of class C^1 on the open subset $G \subset \mathbb{R}^n$. It is well known that we can at least define the flow $\phi : B \times [0, a] \to G$, where B is a small open subset of G, by $\phi(x_0, \cdot) : [0, a] \to G$, where ϕ is the unique solution of (2.4.1) with initial condition $\phi(x_0, 0) = x_0 \in B$.

Since the solution associated to an initial condition may no longer be unique for a differential inclusion, we need to modify the definition of ϕ. Under the conditions given in Theorem 2.3.6, we can define a function ψ from a neighbourhood B of an equilibrium point to subsets of $C([0, a], G)$ equipped with the uniform topology or $L^\infty([0, a], G)$ equipped with the weak*-topology [37]. In fact, the image will be a subset of

$$A([0, a], G) = \left\{x \in C([0, a], G) : x' \in L^\infty([0, a], \mathbb{R}^n)\right\} ,$$

where the derivative is in the sense of distribution. The function ψ defined by $\psi(x_0)$ is the set of all solutions curves (trajectories or orbits) $x : [0, a] \to G$ of the differential inclusion (2.3.4) with initial condition $x(0) = x_0 \in B$. A trajectory can be interpreted as a motion along a solution curve.

In this section, we present the theory of Lyapunov functions, which is one of the methods that can be used to determine the stability of an equilibrium point for a dynamical system. A good reference on this subject and its extension is [52]. A differentiable function $V : G \to \mathbb{R}$ that satisfies the hypothesis of Theorem 2.4.4 below is called a Lyapunov function.

To state Theorem 2.4.4, we need some new concepts. The upper and lower derivatives of a Lyapunov function $V : G \to \mathbb{R}$ with respect to the differential inclusion (2.3.4) are defined by

$$\dot{V}^*(x) = \sup_{\eta \in F(x)} (\nabla V(x) \cdot \eta) \quad \text{and} \quad \dot{V}_*(x) = \inf_{\eta \in F(x)} (\nabla V(x) \cdot \eta) ,$$

respectively, where $\nabla V \equiv \operatorname{grad} V$ [38]. If $\dot{V} = \nabla V\big(x(t)\big) \cdot \eta$, with $\eta \in F(x)$, then $\dot{V}_* \leq \dot{V} \leq \dot{V}^*$.

Theorem 2.4.4. *[38] Suppose that the basic condition (see Definition 2.3.8) is satisfied in an open neighbourhood B of an equilibrium $p \in G$; in particular $0 \in F(p)$. Moreover, suppose that there exists a function $V \in C^1(B)$ such that $V(p) = 0$ and $V(x) > 0$ for $B \setminus \{p\}$.*

(a) If $\dot{V}^*(x) \leq 0$ in B, then the solution $x(t) \equiv p$ of the differential inclusion (2.3.4) *is stable.*

(b) If $\dot{V}^*(x) < 0$ in B, then the solution $x(t) \equiv p$ is asymptotically stable.

Theorem 2.4.5. *[53] If the conditions of Theorem 2.4.4 are satisfied with $\dot{V}_*$ instead of $\dot{V}^*$, then the solution $x(t) \equiv p$ is weakly stable for case (a) and weakly asymptotically stable for case (b).*

Definition 2.4.6. *(Positively Invariant Set) A set $G \subset \mathbb{R}^n$ is said to be positively invariant with respect to the differential inclusion* (2.3.4) *if, for every initial condition $x_0 \in G$, the solutions x with $x(0) = x_0$ satisfy $x(t) \in G$ for almost all $t > 0$.*

Definition 2.4.7. *A point $p \in \mathbb{R}^n$ is a positive limit point of a solution curve x of* (2.3.4) *with the initial condition $x(0) = x_0$ if there exists a sequence $\{t_n\}$, where $t_n \to \infty$ as $n \to \infty$, such that $x(t_n) \to p$ as $n \to \infty$.*

The ω-limit set of a solution curve x of (2.3.4) *with the initial condition $x(0) = x_0$ is the set of all its positive limit points.*

By Theorem 2.4.4, the asymptotic stability of an equilibrium point p is guaranteed whenever the Lyapunov function is a strictly decreasing function along the orbits (i.e., $\dot{V}^*(x) < 0$) in the neighbourhood of p. However, it is not always trivial to find a Lyapunov function. The next theorem due to LaSalle requires only a function $V : G \to \mathbb{R}$ that is decreasing, but not necessarily strictly decreasing, along the orbits (i.e., $\dot{V}^*(x) \leq 0$) to locate the set Q of all ω-limit sets of points in G. If one can prove that $Q = \{p\}$, then p is an asymptotically stable equilibrium.

Theorem 2.4.8. *(LaSalle's Invariance Principle) [49, 54, 55, 56] Let $G \subset \mathbb{R}^n$ be a positively invariant compact set with respect to the differential inclusion* (2.3.4)*. Let V be a differentiable function such that the directional derivative $\dot{V}^*(x) \leq 0$ for all $x \in G$ and let $\Sigma := \left\{x \in G : \dot{V}^*(x) = 0\right\}$. If D is the largest positively invariant set in Σ (namely, the union of all the orbits that start in D and remains in D), then every solution curve $x : [0, \infty[\to G$ with $x(0) = x_0 \in G$ approaches D as $t \to \infty$.*

For a continuous dynamical system, the set Q of all ω-limit set of points in G is included in the set D given in the previous theorem.

2.4.3 Dulac's Theorem

Dulac's Theorem is a tool to prove the non-existence of limit cycle for a smooth dynamical system. We can also employ the idea of the proof of Dulac's Theorem, namely Green's Theorem, to show the non-existence of periodic solutions in a discontinuous dynamical system as in Chapters 4 and 5.

Theorem 2.4.9. *(Dulac's Theorem) [57] Suppose that*

$$\frac{dx}{dt} = f(x, y) \quad \text{and} \quad \frac{dy}{dt} = g(x, y), \tag{2.4.2}$$

where f and g are assumed to be functions of class C^1 in $\mathbb{R}^2$. If there exists a C^1 function B (called a Dulac function) defined on a simply connected region $R \subset \mathbb{R}^2$ such that

$$\frac{\partial(Bf)}{\partial x} + \frac{\partial(Bg)}{\partial y}$$

has constant sign and is not identically zero on R, then system (2.4.2) *does not have a periodic orbit lying entirely in R.*

Chapter 3

A mathematical model of avian influenza with half-saturated incidence

Several bilinear incidence mathematical models have been proposed to investigate the spreading of avian influenza in bird and human populations. Iwami *et al.* [58] showed that, based on the basic reproduction numbers of the proposed models and numerical results, there are two types of possible outbreaks that might occur if no action is taken to stop the spreading of this disease: avian influenza and mutant avian influenza outbreaks. The outbreak caused by avian influenza is not as severe as the outbreak caused by mutant avian influenza. Furthermore, it is suggested that, in order to prevent the transmission of avian influenza to the human population and the second outbreak caused by mutant avian influenza, infected birds should be exterminated and the contact rate of susceptible humans with mutant avian influenza should be reduced.

Iwami *et al.* [59] examined the relationship between the effect of virulence evolution and the efficacy of the intervention policies in combating avian influenza. Two intervention policies have been proposed: (1) eliminate infected birds with avian influenza and (2) quarantine infected humans with mutant avian influenza. By evaluating the total number of infected humans at equilibrium, they found that the quarantine policy is more effective if the number of virulent mutation that occurs is low; otherwise, the elimination policy is more effective. However, by calculating the total number of dead humans at equilibrium, they found that the elimination policy is more effective than quarantine if the virulent mutation rate is low. In addition, by considering a single mutation scenario — which is a better approach in modelling, since the number of infected humans with wild avian influenza is less and the probability for a mutation to occur is low in the real world — they found that the quarantine policy is the best plan compared to elimination policy. This is because elimination policy has

its positive and negative effects; they found that if the elimination policy reduces the total number of dead humans, then it increases the total number of infected humans at the same time; conversely, if the elimination policy reduces the total number of infected humans, then it increases the total number of dead humans.

Gumel [60] proposed a two-strain avian influenza model to study the spread of avian influenza in birds and humans for the purpose of assessing the effects of isolating infected humans with avian and mutant strains. Two types of equilibrium points are identified in this model: the disease-free and endemic equilibria. This model has a unique endemic equilibrium if the basic reproduction number of the avian-only model is greater than the unity. Otherwise, there is no endemic equilibrium in this model. Furthermore, this endemic equilibrium only exists by considering a special case of the avian-only model; namely, a reduced avian-only system. The stability of the disease-free and endemic equilibria (when they exist) of the proposed avian–human model depends on the basic reproduction number: the disease-free equilibrium is globally asymptotically stable if the basic reproduction numbers of the avian and human populations are less than one, whereas the endemic equilibrium is globally asymptotically stable if the basic reproduction number of the avian-only model is greater than one. Based on the numerical results, on average, isolating humans infected with the avian strain has more advantages than isolating humans infected with the mutant strain.

3.1 The half-saturated incidence model

In this chapter, we propose a half-saturated incidence model to study the transmission dynamics of avian influenza in birds and humans as follows:

$$\begin{aligned}
S_b'(t) &= \Lambda_b - \mu_b S_b - \frac{\beta_b S_b I_b}{H_b + I_b} \\
I_b'(t) &= \frac{\beta_b S_b I_b}{H_b + I_b} - (\mu_b + \delta_b) I_b \\
S_h'(t) &= \Lambda_h - \mu_h S_h - \frac{\beta_a S_h I_a}{H_a + I_a} - \frac{\beta_m S_h I_m}{H_m + I_m} - \frac{\beta_{bh} S_h I_b}{H_{bh} + I_b} \\
I_a'(t) &= \frac{\beta_{bh} S_h I_b}{H_{bh} + I_b} + \frac{\beta_a S_h I_a}{H_a + I_a} - (\mu_h + d + \epsilon + \gamma_a) I_a \\
I_m'(t) &= \frac{\beta_m S_h I_m}{H_m + I_m} + \epsilon I_a - (\mu_h + \alpha + \gamma_m) I_m \\
R_h'(t) &= \gamma_a I_a + \gamma_m I_m - \mu_h R_h.
\end{aligned} \tag{3.1.1}$$

The description of all variables and associated parameters is given in Table 3.1.

A brief insight of the effect of half-saturation constants in our proposed model is

Symbol	Description
$S_b(t)$	Susceptible birds
$I_b(t)$	Infected birds
$S_h(t)$	Susceptible humans
$I_a(t)$	Infected humans with avian strain
$I_m(t)$	Infected humans with mutant strain
$R_h(t)$	Recovered humans from avian and mutant strains
$N_b(t)$	Total bird population
$N_h(t)$	Total human population
Λ_b	Bird inflow
Λ_h	Human recruitment rate
μ_b	Natural death rate of birds
μ_h	Natural death rate of humans
β_a	Rate at which human-to-human avian influenza is contracted
β_m	Rate at which human-to-human mutant influenza is contracted
β_{bh}	Rate at which bird-to-human avian influenza is contracted
β_b	Rate at which birds contract avian influenza
H_a	Half-saturation constant for humans with avian strain
H_m	Half-saturation constant for humans with mutant strain
H_b	Half-saturation constant for birds with avian strain
H_{bh}	Half-saturation constant for humans with avian strain contracted from infected birds
α	Additional death rate mediated by mutant strain
ϵ	Mutation rate
d	Additional disease death rate due to avian strain in humans
δ_b	Additional disease death rate due to avian strain in birds
γ_a	Recovery rate of humans with avian strain
γ_m	Recovery rate of humans with mutant strain
ψ_a	Rate of isolation of humans with avian strain
ψ_m	Rate of isolation of humans with mutant strain

Table 3.1: Description of the variables and associated parameters.

as follows. Suppose that H is the half-saturation constant, S represents the susceptible population, I is the infected population and β is the infection rate. We obtain that $\beta S\,(I/(H+I))$ converges toward the peak of infection βS (linear infection) as H approaches zero. However, $\beta S\,(I/(H+I))$ converges to 0 as H converges to infinity, and there is no infection. It is so-named because half of the susceptible population will get infected when $H = I$.

We now identify the feasible and attracting regions of model (3.1.1).

Proposition 3.1.1. *The region of feasibility for* $(S_b, I_b, S_h, I_a, I_m, R_h)$ *is the flow-invariant set* $\mathbb{R}^6_+ = \{x \in \mathbb{R}^6 : x_i \geq 0 \quad \forall i\}$.

Proof: If $S_b(t) = 0$, then $S_b'(t) = \Lambda_b > 0$. Thus $S_b(t) \geq 0$ for all t if $S_b(0) \geq 0$. The surface $I_b = 0$ is flow invariant. So $I_b(t) > 0$ for all t if $I_b(0) > 0$. If $S_h(t) = 0$, then $S_h'(t) = \Lambda_b > 0$. Thus $S_h(t) \geq 0$ for all t if $S_h(0) \geq 0$. If $I_a(t) = 0$, then $I_a'(t) = (\beta_{bh} S_h(t) I_b(t))/(H_{bh} + I_b) \geq 0$ if $S_h(t)$ and $I_b(t)$ are non-negative. Thus $I_a(t) \geq 0$ for all t if $I_a(0)$, $I_b(0)$ and $S_h(0)$ are non-negative. If $I_m(t) = 0$, then $I_m'(t) = \epsilon I_a(t) \geq 0$ if $I_a(t)$ is non-negative. Thus $I_m(t) \geq 0$ for all t if $I_m(0)$, $I_a(0)$, $I_b(0)$ and $S_h(0)$ are non-negative. Finally, the solution of the differential equation for R_h in (3.1.1) is

$$R_h(t) = e^{-\mu_h t}\left(R_h(0) + \int_0^t \left(\gamma_a I_a(s) + \gamma_m I_m(s)\right) e^{\mu_h s}\, ds\right).$$

Thus $R_h(t) \geq 0$ if $R_h(0) \geq 0$ and $I_a(t)$ and $I_m(t)$ are non-negative for all t. ∎

Proposition 3.1.2. *The set*

$$\mathcal{D} = \left\{(S_b, I_b, S_h, I_a, I_m, R_h) \in \mathbb{R}^6_+ : N_b \leq \frac{\Lambda_b}{\mu_b} \text{ and } N_h \leq \frac{\Lambda_h}{\mu_h}\right\}$$

is a closed and bounded region in $\mathbb{R}^6_+$ *and is a flow invariant and attracting region for model* (3.1.1).

Proof: It is clear by construction that $\mathcal{D}$ is closed and bounded as a subset of $\mathbb{R}^6_+$.

From (3.1.1), we have

$$\frac{dN_b}{dt} = \Lambda_b - \mu_b N_b - \delta_b I_b \leq \Lambda_b - \mu_b N_b$$
$$\frac{dN_h}{dt} = \Lambda_h - \mu_h N_h - dI_a - \alpha I_m \leq \Lambda_h - \mu_h N_h.$$

If we multiply both sides of

$$\frac{\mathrm{d}N_b}{\mathrm{d}s} + \mu_b N_b \leq \Lambda_b$$

by $e^{\mu_b s}$ and integrate between 0 and t, we get

$$N_b(t) \leq N_b(0)e^{-\mu_b t} + \frac{\Lambda_b}{\mu_b}\left(1 - e^{-\mu_b t}\right)$$

for $t > 0$. Hence $\lim\limits_{t\to\infty} N_b(t) \leq \dfrac{\Lambda_b}{\mu_b}$. A similar reasoning yields $\lim\limits_{t\to\infty} N_h(t) \leq \dfrac{\Lambda_h}{\mu_h}$.

Since $\frac{\mathrm{d}N_b}{\mathrm{d}t}(t) < 0$ if $N_b(t) > \Lambda_b/\mu_b$ and $\frac{\mathrm{d}N_h}{\mathrm{d}t}(t) < 0$ if $N_h(t) > \Lambda_h/\mu_h$, no orbit starting in $\mathcal{D}$ can escape. ∎

By focusing on the avian-only model — Namely, on the first two equations of model (3.1.1) — we find that the disease-free equilibrium of this model is

$$E_b^0 = (S_b^0, I_b^0) = \left(\frac{\Lambda_b}{\mu_b}, 0\right),$$

and the endemic equilibrium is

$$E_b^* = (S_b^*, I_b^*) = \left(\frac{\Lambda_b + H_b(\mu_b + \delta_b)}{\mu_b + \beta_b}, \frac{\Lambda_b\beta_b - \mu_b H_b(\mu_b + \delta_b)}{(\mu_b + \beta_b)(\mu_b + \delta_b)}\right).$$

The basic reproduction number (see Chapter 1 and [61, 62] for further details) of this model is

$$R_b = \frac{\Lambda_b\beta_b}{\mu_b H_b(\mu_b + \delta_b)}.$$

To examine the stability of E_b^0 and E_b^*, we compute the Jacobian matrix of the avian-only model.

$$J_A(S_b, I_b) = \begin{pmatrix} -\mu_b - \dfrac{\beta_b I_b}{H_b + I_b} & -\dfrac{\beta_b S_b H_b}{(H_b + I_b)^2} \\ \dfrac{\beta_b I_b}{H_b + I_b} & \dfrac{\beta_b S_b H_b}{(H_b + I_b)^2} - (\mu_b + \delta_b) \end{pmatrix}.$$

Proposition 3.1.3. *E_b^0 is locally asymptotically stable if $R_b < 1$ and unstable if $R_b > 1$.*

Proof: The eigenvalues of $J_A(E_b^0)$ are $\lambda = -\mu_b < 0$ and $\lambda = \dfrac{\Lambda_b\beta_b - \mu_b H_b(\mu_b + \delta_b)}{\mu_b H_b}$.

Since

$$R_b < 1 \implies \Lambda_b\beta_b - \mu_b H_b(\mu_b + \delta_b) < 0$$

and

$$R_b > 1 \implies \Lambda_b\beta_b - \mu_b H_b(\mu_b + \delta_b) > 0,$$

we have that $\lambda = \dfrac{\Lambda_b\beta_b - \mu_b H_b(\mu_b + \delta_b)}{\mu_b H_b}$ is positive when $R_b > 1$ and negative when $R_b < 1$ because all associated parameters are positive. ∎

Proposition 3.1.4. *The disease-free equilibrium $E_b^0 = (\Lambda_b/\mu_b, 0)$ is globally asymptotically stable in $\mathbb{R}^2_+$ if $R_b < 1$.*

Proof: Consider the function

$$L(S_b, I_b) = S_b - \frac{\Lambda_b}{\mu_b} - \frac{\Lambda_b}{\mu_b}\ln\left(\frac{\mu_b S_b}{\Lambda_b}\right) + I_b \quad \text{for } S_b > 0, I_b \geq 0.$$

We have seen that the flow is crossing the line $S_b = 0$ to enter $\mathbb{R}^2_+$. We have also seen that the line $I_b = 0$ is flow invariant. Hence, L can play a role similar to a Lyapunov function for E_b^0 and the avian-only model if we can prove that L satisfies the three properties required by a Lyapunov function when $S_b > 0$ and $I_b \geq 0$. (Note that E_b^0 is located on the boundary of positive regions for S_b and I_b so L does not satisfy the Lyapunov property of positivity in an open neighbourhood of E_b^0.) We prove this below.

At E_b^0, we have $L(S_b^0, I_b^0) = L(\Lambda_b/\mu_b, 0) = 0$. In addition, $L(S_b, I_b) > 0$ for $I_b \geq 0$, $S_b > 0$ and $S_b \neq \Lambda_b/\mu_b$. This comes from the fact that

$$g(S_b) = S_b - \frac{\Lambda_b}{\mu_b} - \frac{\Lambda_b}{\mu_b}\ln\left(\frac{\mu_b S_b}{\Lambda_b}\right)$$

satisfies $g'(S_b) > 0$ if $S_b > \Lambda_b/\mu_b$ and $g'(S_b) < 0$ if $S_b < \Lambda_b/\mu_b$ with $g(\Lambda_b/\mu_b) = 0$. This proves that E_b^0 is a minimum point of L in $\mathbb{R}^2_+$.

Finally, if we derive L along any orbit in the region $S_b > 0$, $I_b \geq 0$, we get

$$\begin{aligned}
\frac{dL}{dt} &= \left(1 - \frac{\Lambda_b}{\mu_b S_b}\right)\left(\Lambda_b - \mu_b S_b - \frac{\beta_b S_b I_b}{H_b + I_b}\right) + \frac{\beta_b S_b I_b}{H_b + I_b} - (\mu_b + \delta_b) I_b \\
&= \frac{-(H_b + I_b)(\Lambda_b - \mu_b S_b)^2 + S_b I_b\left(\Lambda_b\beta_b - \mu_b H_b(\mu_b + \delta_b)\right) - \mu_b(\mu_b + \delta_b) S_b I_b^2}{\mu_b S_b (H_b + I_b)} \\
&< \frac{-(H_b + I_b)(\Lambda_b - \mu_b S_b)^2 - \mu_b(\mu_b + \delta_b) S_b I_b^2}{\mu_b S_b (H_b + I_b)} < 0
\end{aligned}$$

for $S_b > 0$ and $I_b \leq 0$ as long as $(S_b, I_b) \neq E_b^0$. The first inequality is a consequence of $R_b < 1$; namely, $\Lambda_b\beta_b - \mu_b H_b(\mu_b + \delta_b) < 0$.

Hence E_b^0 is globally asymptotically stable in $\mathbb{R}_+^2$ when $R_b < 1$. ∎

Note that Proposition 3.1.4 corrects the statement of Theorem 2 and its proof in the Appendix of [41].

Proposition 3.1.5. *The endemic equilibrium E_b^* is outside the feasibility domain if $R_b < 1$, and it is locally asymptotically stable if $R_b > 1$.*

Proof: Since

$$R_b < 1 \implies \Lambda_b\beta_b - \mu_b H_b(\mu_b + \delta_b) < 0,$$

we have $I_b^* = \dfrac{\Lambda_b\beta_b - \mu_b H_b(\mu_b + \delta_b)}{(\mu_b + \beta_b)(\mu_b + \delta_b)} < 0$ for $R_b < 1$ because all associated parameters are positive. There is no biological meaning for this equilibrium if I_b^* is negative. Hence E_b^* does not exist if $R_b < 1$.

Next, we prove the local stability of E_b^* if $R_b > 1$. The eigenvalues of $J_A(E_b^*)$ are

$$\lambda_\pm = \frac{1}{2}\Big(-X \pm \sqrt{Y}\Big)$$

where

$$X = \frac{\Lambda_b\beta_b(\mu_b + \beta_b) + (\mu_b + \delta_b)\big(\Lambda_b\beta_b - H_b\mu_b(\mu_b + \delta_b)\big)}{\beta_b\big(\Lambda_b + H_b(\mu_b + \delta_b)\big)}$$

and

$$Y = \left(\frac{\Lambda_b\beta_b(\mu_b + \beta_b) - (\mu_b + \delta_b)\big(\Lambda_b\beta_b - H_b\mu_b(\mu_b + \delta_b)\big)}{\beta_b\big(\Lambda_b + H_b(\mu_b + \delta_b)\big)}\right)^2 - \frac{4H_b(\mu_b + \beta_b)(\mu_b + \beta_b)(\mu_b + \delta_b)^2\big(\Lambda_b\beta_b - \mu_b H_b(\mu_b + \delta_b)\big)}{\beta_b\big(\Lambda_b + H_b(\mu_b + \delta_b)\big)^2}.$$

Since $\Lambda_b\beta_b - \mu_b H_b(\mu_b + \delta_b) > 0$ for $R_b > 1$, we obtain $X > 0$ and $Y < X^2$. Hence E_b^* is either a stable node (if $Y \geq 0$) or a stable spiral (if $Y < 0$) whenever $R_b > 1$. ∎

Proposition 3.1.6. *The endemic equilibrium E_b^* is globally asymptotically stable in $\mathbb{R}_+^2$ if $R_b > 1$.*

Proof: Let

$$f(S_b, I_b) = \begin{pmatrix} f_1 \\ f_2 \end{pmatrix} = \begin{pmatrix} \Lambda_b - \mu_b S_b - \dfrac{\beta_b S_b I_b}{H_b + I_b} \\ \dfrac{\beta_b S_b I_b}{H_b + I_b} - (\mu_b + \delta_b) I_b \end{pmatrix}$$

and $B(S_b, I_b) = \dfrac{1}{I_b}$.

Since

$$\nabla\big(Bf\big) = \frac{\partial}{\partial S_b}\big(Bf_1\big) + \frac{\partial}{\partial I_b}\big(Bf_2\big) = -\left(\frac{\mu_b}{I_b} + \frac{\beta_b}{H_b + I_b} + \frac{\beta_b S_b}{(H_b + I_b)^2}\right) < 0$$

for all (S_b, I_b) with $S_b, I_b > 0$, Dulac's Criteria [57] tells us that no periodic orbit can lie entirely in $\mathbb{R}^2_+$.

The S_b-nullcline of the avian-only model is

$$\left\{(S_b, I_b) \in \mathbb{R}^2_+ : I_b = \frac{H_b(\Lambda_b - \mu_b S_b)}{\beta_b S_b + \mu_b S_b - \Lambda_b}\right\},$$

and the I_b-nullclines are

$$\left\{(S_b, I_b) \in \mathbb{R}^2_+ : S_b = \frac{(\mu_b + \delta_b)(H_b + I_b)}{\beta_b}\right\} \text{ and } \Big\{(S_b, I_b) \in \mathbb{R}^2_+ : I_b = 0\Big\}.$$

E_b^* is the only stable equilibrium point in $\mathcal{D}$ whenever $R_b > 1$; recall that the disease-free equilibrium E_b^0 is unstable if $R_b > 1$ by Theorem 3.1.4. Since there is no periodic orbit in $\mathbb{R}^2_+$ and $\mathcal{D}$ is an attracting, flow-invariant, closed and bounded region for the avian-only model (which can be proved as in Proposition 3.1.2), we conclude from the Poincaré–Bendixson theorem [57] that E_b^* is globally asymptotically stable in $\mathbb{R}^2_+$ whenever $R_b > 1$. ∎

The S_b- and I_b-nullclines are represented by the asterisks and dashed lines, respectively, in Figure 3.1. From this figure, we can see that all trajectories with arbitrary initial points in $\mathbb{R}^2_+$ are converging to $E_b^* \in \mathcal{D}$. All the numerical results are simulated based on the parameter values in Table 3.2.

Proposition 3.1.6 corrects Theorem 3 in the appendix of [41].

The half-saturated incidence model (3.1.1) has a disease-free equilibrium $E_{ah}^0 = \big(S_b^0, I_b^0, S_h^0, I_a^0, I_m^0, R_h^0\big) = \left(\dfrac{\Lambda_b}{\mu_b}, 0, \dfrac{\Lambda_h}{\mu_h}, 0, 0, 0\right)$, and the basic reproduction number of

Parameter	Sample Value	Reference
Λ_b	1000 per day	[63]
Λ_h	30 per day	[63]
μ_b	1/100 per day	[60]
μ_h	$1/(70 \times 365)$ per day	[63]
β_a	0.4 per day	assumed
β_m	$0.3\beta_a$ per day	[60]
H_a	150000 individuals	assumed
H_m	150000 individuals	assumed
α	0.06 per day	assumed
ϵ	0.01 per day	[60]
d	1 per day	assumed
δ_b	5 per day	assumed
γ_a	0.05 per day	[60]
γ_m	0.01 per day	[60]
β_b	0.4 per day	assumed
H_b	180000 individuals	assumed
β_{bh}	0.2 per day	assumed
H_{bh}	120000 individuals	assumed

Table 3.2: Parameter values.

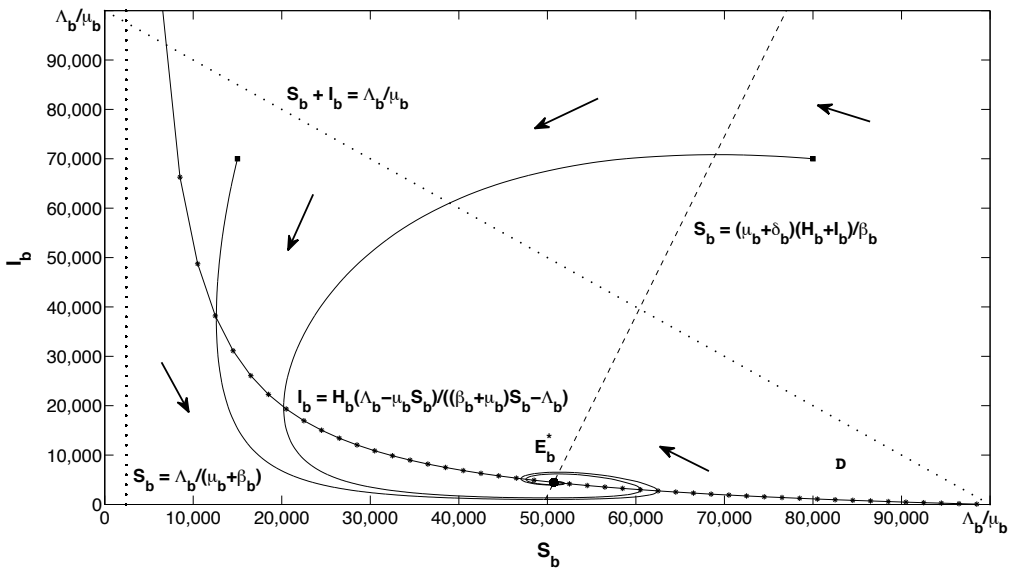

Figure 3.1: The endemic equilibrium E_b^* is globally asymptotically stable whenever $R_b > 1$.

this model is $R_{ah} = \max\{R_b, R_{h1}, R_{h2}\}$, where

$$R_b = \frac{\Lambda_b \beta_b}{H_b \mu_b(\mu_b + \delta_b)}, \qquad R_{h1} = \frac{\Lambda_h \beta_a}{H_a \mu_h(\mu_h + d + \epsilon + \gamma_a)}$$

and

$$R_{h2} = \frac{\Lambda_h \beta_m}{H_m \mu_h(\mu_h + \alpha + \gamma_m)}.$$

The local stability of E_{ah}^0 is examined in the following theorem.

Proposition 3.1.7. *The disease-free equilibrium E_{ah}^0 is locally asymptotically stable if $R_{ah} < 1$ and unstable if $R_{ah} > 1$.*

Proof: The Jacobian matrix for the avian-human half-saturated incidence model

(3.1.1) at E^0_{ah} is

$$J(E^0_{ah}) = \begin{pmatrix} -\mu_b & -\frac{\Lambda_b\beta_b}{\mu_b H_b} & 0 & 0 & 0 & 0 \\ 0 & J_{21} & 0 & 0 & 0 & 0 \\ 0 & -\frac{\Lambda_h\beta_{bh}}{\mu_h H_{bh}} & -\mu_h & -\frac{\Lambda_h\beta_a}{\mu_h H_a} & -\frac{\Lambda_h\beta_m}{\mu_h H_m} & 0 \\ 0 & \frac{\Lambda_h\beta_{bh}}{\mu_h H_{bh}} & 0 & J_{44} & 0 & 0 \\ 0 & 0 & 0 & \epsilon & J_{55} & 0 \\ 0 & 0 & 0 & \gamma_a & \gamma_m & -\mu_h \end{pmatrix},$$

where

$$J_{21} = \frac{\Lambda_b\beta_b - \mu_b H_b(\mu_b + \delta_b)}{\mu_b H_b}, \qquad J_{44} = \frac{\Lambda_h\beta_a - \mu_h H_a(\mu_h + d + \epsilon + \gamma_a)}{\mu_h H_a}$$

and

$$J_{55} = \frac{\Lambda_h\beta_m - \mu_h H_m(\mu_h + \alpha + \gamma_m)}{\mu_h H_m}.$$

The eigenvalues of $J(E^0_{ah})$ are $-\mu_b$, $-\mu_h$ (twice), J_{21}, J_{44} and J_{55}. Since $R_{ah} < 1$ implies that $\Lambda_b\beta_b - \mu_b H_b(\mu_b + \delta_b) < 0$, $\Lambda_h\beta_a - \mu_h H_a(\mu_h + d + \epsilon + \gamma_a) < 0$ and $\Lambda_h\beta_m - \mu_h H_m(\mu_h + \alpha + \gamma_m) < 0$ and all parameters are positive, it follows that all eigenvalues are negative. Hence E^0_{ah} is a locally asymptotically stable when $R_{ah} < 1$.

However, if $R_{ah} > 1$, the eigenvalues $\lambda = J_{21}$, J_{44} and J_{55} are positive. Thus E^0_{ah} is unstable if $R_{ah} > 1$. ∎

The attempt at proving that E^0_{ah} was globally asymptotically stable in Theorem 4 of [41] is unfortunately wrong. So we replace this result by the weaker stability result for E^0_{ah} in Proposition 3.1.7.

3.2 The effect of half-saturation constants on the dynamics of avian influenza

In order to examine the effect of half-saturated incidence on the dynamics of avian influenza infection, we compare the total number of infected humans generated by the half-saturated incidence model (3.1.1) with the following bilinear incidence model (3.2.1).

$$\begin{aligned}
S_b'(t) &= \Lambda_b - \mu_b S_b - \beta_B S_b I_b \\
I_b'(t) &= \beta_B S_b I_b - (\mu_b + \delta_b) I_b \\
S_h'(t) &= \Lambda_h - \mu_h S_h - \beta_A S_h I_a - \beta_M S_h I_m - \beta_{BH} S_h I_b \\
I_a'(t) &= \beta_{BH} S_h I_b + \beta_A S_h I_a - (\mu_h + d + \epsilon + \gamma_a) I_a \\
I_m'(t) &= \beta_M S_h I_m + \epsilon I_a - (\mu_h + \alpha + \gamma_m) I_m \\
R_h'(t) &= \gamma_a I_a + \gamma_m I_m - \mu_h R_h,
\end{aligned} \tag{3.2.1}$$

where β_B, β_A, β_M and β_{BH} are, respectively, the rates at which the birds contract avian influenza, human-to-human avian influenza is contracted, human-to-human mutant influenza is contracted and avian influenza is contracted from infected birds. All other parameters are defined in Table 3.1.

The infection parameter values of model (3.2.1) are stated in Table 3.3, whereas the remaining parameter values can be found in Table 3.2.

The disease-free equilibrium E_{AH} for model (3.2.1) is similar to the one for model (3.1.1); namely, $E_{AH}^0 = E_{ah}^0 = \left(\frac{\Lambda_b}{\mu_b}, 0, \frac{\Lambda_h}{\mu_h}, 0, 0, 0\right)$. The basic reproduction number of model (3.2.1) is defined by $R_{AH} = \max\{R_B, R_{H1}, R_{H2}\}$, where

$$R_B = \frac{\Lambda_b \beta_b}{\mu_b(\mu_b + \delta_b)}, \quad R_{H1} = \frac{\Lambda_h \beta_A}{\mu_h(\mu_h + d + \epsilon + \gamma_a)} \quad \text{and} \quad R_{H2} = \frac{\Lambda_h \beta_M}{\mu_h(\mu_h + \alpha + \gamma_m)}.$$

Furthermore, the Jacobian matrix of model (3.2.1) is

$$J_B = \begin{pmatrix}
-\mu_b - \beta_B I_b & -\beta_B S_b & 0 & 0 & 0 & 0 \\
\beta_B I_b & \beta_B S_b - (\mu_b + \delta_b) & 0 & 0 & 0 & 0 \\
0 & -\beta_{BH} S_h & \widehat{J}_{33} & -\beta_A S_h & -\beta_M S_h & 0 \\
0 & \beta_{BH} S_h & \beta_{BH} I_b + \beta_A I_a & \widehat{J}_{44} & 0 & 0 \\
0 & 0 & \beta_M I_m & \epsilon & \widehat{J}_{55} & 0 \\
0 & 0 & 0 & \gamma_a & \gamma_m & -\mu_h
\end{pmatrix},$$

where $\widehat{J}_{33} = -(\mu_h + \beta_A I_a + \beta_M I_m + \beta_{BH} I_b)$, $\widehat{J}_{44} = \beta_A S_h - (\mu_h + d + \epsilon + \gamma_a)$ and $\widehat{J}_{55} = \beta_M S_h - (\mu_h + \alpha + \gamma_m)$.

Proposition 3.2.1. *The disease-free equilibrium E_{AH}^0 of model (3.2.1) is locally asymptotically stable if $R_{AH} < 1$ and unstable if $R_{AH} > 1$.*

The proof of Proposition 3.2.1 is similar to Proposition 3.1.7. All eigenvalues of $J_B(E_{AH}^0)$ are negative if $R_{AH} < 1$. However, $J_B(E_{AH}^0)$ has positive and negative eigenvalues whenever $R_{AH} > 1$, which implies that E_{AH}^0 is unstable.

Parameter	Sample Value	Reference
β_A	0.4/200000 per individual per day	Assumed
β_M	$0.3\beta_A$ per individual per day	[60]
β_B	0.4/200000 per individual per day	Assumed
β_{BH}	0.2/100 per individual per day	Assumed

Table 3.3: The infection parameter values of bilinear incidence model (3.2.1).

Figure 3.2 shows the total number of infected humans (the sum of I_a and I_m) generated by the half-saturated and bilinear models. We considered the parameter values given in Tables 3.2 and 3.3 in order to produce the numerical results of models (3.1.1) and (3.2.1). Based on these parameter values, the basic reproduction numbers of these two models are greater than the unity ($R_{ah} > 1$ and $R_{AH} > 1$). From Figure 3.2, we can see that both models remain endemic; namely, the number of infected humans does not converge to zero as time $t \to \infty$. For the first approximately 225 days, both models have a decreasing number of infected humans, but the half-saturated incidence model (3.1.1) generates more infected people than the bilinear incidence model (3.2.1). After that, both models produce on average about the same number of infected people and stabilize at around $e^{3.8}$ infected people. This shows that both models will not converge to the disease-free equilibrium when their respective basic reproduction numbers are greater than unity, as predicted by Propositions 3.1.7 and 3.2.1. Furthermore, the bilinear incidence model (3.2.1) may be underestimating the number of infected individuals resulting from the outbreak.

Chong *et al.* [41] examined the outcome of model (3.1.1) by considering the basic reproduction number less than the unity (see Appendix A).

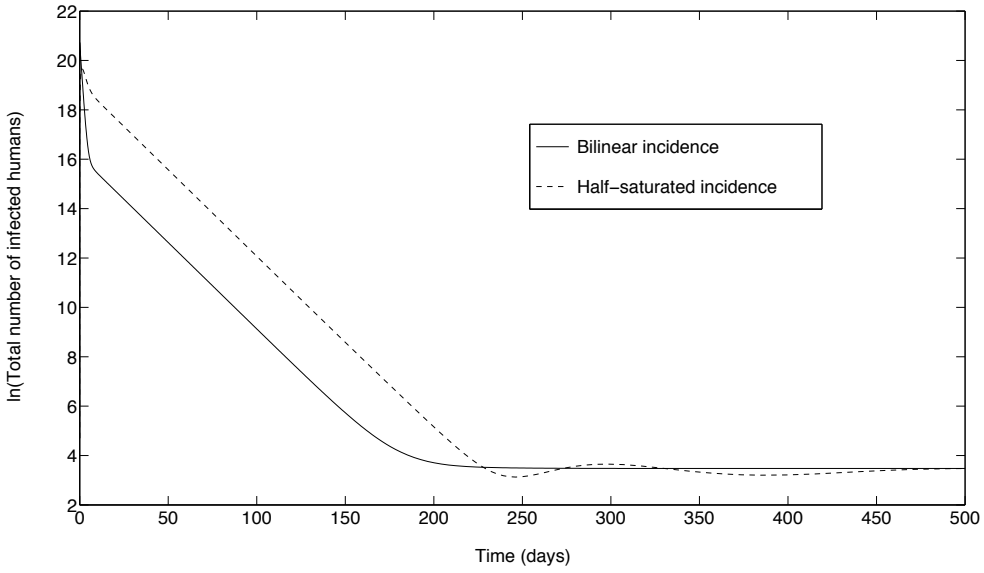

Figure 3.2: Comparison between the avian influenza transmission dynamics of models (3.1.1) and (3.2.1).

Chapter 4

Modelling avian influenza using Filippov systems to determine culling of infected birds and quarantine

In this chapter, we propose two mathematical models incorporating control strategies to study the transmission of avian influenza in the bird and human populations: an avian-only model with culling of infected domestic birds and an SIIR (Susceptible-Infected-Infected-Recovered) model with quarantine of infected humans. In order to control the spreading of avian influenza in the avian population and to mitigate the problem of over-killing birds, we will only execute a depopulation of infected birds when the number of infected birds exceeds the tolerance threshold I_T. Otherwise, no birds will be culled. For the human population, quarantine is considered to reduce the disease infection rate. The total number of infected humans with avian and mutant strains is used as a reference number in applying the quarantine strategy. No quarantine will be employed if the total number of infected humans is less than the tolerance threshold I_c. However, quarantine will be implemented immediately to isolate the infected humans from the susceptibles if the total number of infected humans is greater than I_c. These two proposed mathematical models are governed by nonlinear ordinary differential equations with discontinuous right-hand sides. We investigate the existence of equilibria and their stability as we vary the tolerance thresholds. In particular, we determine the existence of sliding modes on discontinuity surfaces and the dynamical system governing the dynamics on them. We also locate the sliding equilibria and investigate their stability.

We consider Filippov models in this paper instead of impulsive models for the following reasons. Impulsive models can be used to model avian influenza that incorporates control strategy like culling strategy if the strategy is carried out on a regular

fixed schedule. However, Gulbudak and Martcheva [64] mentioned that "employment of culling at fixed times may not be realistic for avian influenza since it ignores the fact that culling occurs as a response to outbreak". In addition, Gulbudak and Martcheva [64] also stated that, for the approach of state-dependent impulsive model, "impulsive culling would occur upon I reaching a threshold value, but culling effect would not vary beyond this impulse switch and limited qualitative results can be obtained in such a model", where I is the size of the infected population.

This paper was published in the Journal *Nonlinear Analysis: Real World Applications* [42]. Both authors designed the models. The first author did the analysis of the models, conducted all numerical results and wrote the initial manuscript. The second author edited the manuscript.

There are two mistakes in [42]. The references given to justify the values of β_d on page 201 and β_a on page 208 of the paper should be ignored. These parameter values were chosen by the authors.

The paper [42] is included at the end of this chapter.

4.1 An Avian-only Model with Culling of Infected Domestic Birds

In this section, we give a brief summary of the avian-only model with culling of infected domestic birds presented in [42]. More details and the computations can be found in [42]. The summary will be based on a phase-portrait analysis of the model, which was not emphasized in the paper.

In the paper, we propose the following avian-only model with culling of infected birds:

$$\begin{aligned} S_d'(t) &= \Lambda_d - \beta_d S_d I_d - \mu_d S_d \\ I_d'(t) &= \beta_d S_d I_d - (\mu_d + d_d) I_d - u_d c I_d \end{aligned} \tag{4.1.1}$$

with

$$u_d = \begin{cases} 0 & \text{for } I_d < I_T \\ 1 & \text{for } I_d > I_T, \end{cases} \tag{4.1.2}$$

where $I_T > 0$ is the tolerance threshold and all the variables and associated parameters are described in Table 4.1.

The space $(S_d, I_d) \in \mathbb{R}^2_+$ is divided into three regions as follows:

$$\begin{aligned} G_{1d} &= \{(S_d, I_d) \in \mathbb{R}^2_+; I_d < I_T\}, \\ G_{2d} &= \{(S_d, I_d) \in \mathbb{R}^2_+; I_d > I_T\}, \\ M_d &= \{(S_d, I_d) \in \mathbb{R}^2_+; I_d = I_T\}. \end{aligned}$$

We define the normal vector perpendicular to M_d as $n_d = \begin{pmatrix} 0 & 1 \end{pmatrix}^\top$, and the right-hand side of (4.1.1) in region G_{id} is denoted by f_{id} for $i = 1, 2$, where

$$\begin{pmatrix} S_d'(t) \\ I_d'(t) \end{pmatrix} = f_{1d}(S_d, I_d) = \begin{pmatrix} f_{1d,1}(S_d, I_d) \\ f_{1d,2}(S_d, I_d) \end{pmatrix} = \begin{pmatrix} \Lambda_d - S_d(\beta_d I_d + \mu_d) \\ I_d\left[\beta_d S_d - (\mu_d + d_d)\right] \end{pmatrix} \tag{4.1.3}$$

and

$$\begin{pmatrix} S_d'(t) \\ I_d'(t) \end{pmatrix} = f_{2d}(S_d, I_d) = \begin{pmatrix} f_{2d,1}(S_d, I_d) \\ f_{2d,2}(S_d, I_d) \end{pmatrix} = \begin{pmatrix} \Lambda_d - S_d(\beta_d I_d + \mu_d) \\ I_d\left[\beta_d S_d - (\mu_d + d_d + c)\right] \end{pmatrix}. \tag{4.1.4}$$

The dynamical system given in (4.1.3) has two equilibria: the endemic equilibrium

$$E_{11d} = \left(h_{1d}, h_{4d}\right) = \left(\frac{\mu_d + d_d}{\beta_d}, \frac{\Lambda_d\beta_d - \mu_d(\mu_d + d_d)}{\beta_d(\mu_d + d_d)}\right)$$

and the disease-free equilibrium $E_{10d} = (S_d, I_d) = (\Lambda_d/\mu_d, 0)$. The basic reproduction number for system (4.1.3) is

$$R_{1d} = \frac{\Lambda_d\beta_d}{\mu_d(\mu_d + d_d)}.$$

Proposition 4.1.1. *The endemic equilibrium E_{11d} does not exist if $R_{1d} < 1$.*

Proof: Since

$$R_{1d} < 1 \implies \Lambda_d\beta_d - \mu_d(\mu_d + d_d) < 0,$$

we obtain

$$h_{4d} = \frac{\Lambda_d\beta_d - \mu_d(\mu_d + d_d)}{\beta_d(\mu_d + d_d)} < 0$$

whenever $R_{1d} < 1$, because all associated parameters are positive. Therefore E_{11d} does not exist if $R_{1d} < 1$. There is no biological meaning for this equilibrium whenever h_{4d} is negative. ∎

For the dynamical system given in (4.1.4), we have a disease-free equilibrium E_{20d}, which is equal to the disease-free equilibrium in (4.1.3); namely $E_{20d} = E_{10d} = (\Lambda_d/\mu_d, 0)$. We also have an endemic equilibrium

$$E_{21d} = (h_{2d}, h_{3d}) = \left(\frac{\mu_d + d_d + c}{\beta_d}, \frac{\Lambda_d\beta_d - \mu_d(\mu_d + d_d + c)}{\beta_d(\mu_d + d_d + c)}\right).$$

The basic reproduction number for system (4.1.4) is

$$R_{2d} = \frac{\Lambda_d \beta_d}{\mu_d(\mu_d + d_d + c)}.$$

Proposition 4.1.2. *The endemic equilibrium E_{21d} does not exist if $R_{2d} < 1$.*

Since the proof of Proposition 4.1.2 is similar to the proof of Proposition 4.1.1, we omit it.

We prove in Lemma 2.1 of [42] that

$$D_d = \left\{ (S_d, I_d) \in \mathbb{R}^2_+; S_d + I_d \leq \frac{\Lambda_d}{\mu_d} \right\}$$

is attracting and flow-invariant in $\mathbb{R}^2_+$ for the model (4.1.1).

4.1.1 Sliding Domain

The existence of a sliding mode on M_d is proved in [42] and Filippov method is applied to define the flow on M_d as follows:

$$\begin{pmatrix} S'_d(t) \\ I'_d(t) \end{pmatrix} = f_d = \alpha f_{1d} + (1-\alpha) f_{2d} \text{ where } \alpha = \frac{\langle n_d, f_{2d} \rangle}{\langle n_d, f_{2d} - f_{1d} \rangle}.$$

So the flow on M_d is governed by

$$f_d = \begin{pmatrix} \Lambda_d - \beta_d S_d I_d - \mu_d S_d \\ 0 \end{pmatrix},$$

and the sliding domain of model (4.1.1) is defined by

$$\begin{aligned} \Omega_d &= \left\{ (S_d, I_d) \in M_d : \langle n_d, f_{1d} \rangle > 0 \text{ and } \langle n_d, f_{2d} \rangle < 0 \right\} \\ &= \left\{ (S_d, I_d) \in M_d : h_{1d} < S_d < h_{2d} \right\}. \end{aligned}$$

The dynamical system on Ω_d has an equilibrium at $E_d = \left(\frac{\Lambda_d}{\beta_d I_T + \mu_d}, I_T \right)$. We have that $E_d \in \Omega_d \subset M_d$ if $h_{3d} < I_T < h_{4d}$. Furthermore, E_d is locally asymptotically stable on Ω_d if we restrict the vector field f_d to Ω_d since

$$\frac{\partial}{\partial S_d}(\Lambda_d - \beta_d S_d I_d - \mu_d S_d)\Big|_{I_d = I_T} = -\beta_d I_T - \mu_d < 0,$$

Symbol	Description
$S_d(t)$	Susceptible domestic birds
$I_d(t)$	Infected domestic birds
$N_d(t)$	Total domestic bird population
Λ_d	Bird inflow
β_d	Rate at which domestic birds contract avian influenza
μ_d	Natural death rate of domestic birds
d_d	Additional disease death rate of domestic birds
c	Culling rate of infected domestic birds

Table 4.1: Description of the variables and associated parameters for the model (4.1.1).

where $\mu_d, \beta_d, I_T > 0$; namely, the eigenvalue of the linearization of the vector fields at E_d is $-\beta_d d I_T - \mu_d < 0$.

As we vary the tolerance threshold I_T, we investigate the existence of equilibrium points and their stability in the following subsections.

The S_d- and I_d-nullclines for (4.1.3) (resp. (4.1.4)) are given by $f_{1d,1} = 0$ and $f_{1d,2} = 0$ (resp. $f_{2d,1} = 0$ and $f_{2d,2} = 0$) respectively. We find that the S_d-nullcline for (4.1.3) and (4.1.4) is

$$\left\{ (S_d, I_d) \in \mathbb{R}^2_+ : I_d = \frac{\Lambda_d - \mu_d S_d}{\beta_d S_d} \right\},$$

whereas the I_d-nullclines for systems (4.1.3) are

$$\left\{ (S_d, I_d) \in \mathbb{R}^2_+ : S_d = h_{1d} \text{ and } I_d < I_T \right\} \text{ and } \left\{ (S_d, I_d) \in \mathbb{R}^2_+ : I_d = 0 \right\},$$

and the I_d-nullcline for (4.1.4) is

$$\left\{ (S_d, I_d) \in \mathbb{R}^2_+ : S_d = h_{2d} \text{ and } I_d > I_T \right\}.$$

4.1.2 Case 1: $I_T < h_{3d}$

For this case, E_{21d} is globally asymptotically stable as depicted in Figure 4.1. Since the region D_d is attracting and flow-invariant (see Lemma 2.1 in [42]), E_{21d} is the only locally stable (real) equilibrium that exists in D_d whenever $I_T < h_{3d}$ (see Theorem 2.5 of [42]). Since there is no periodic orbit in D_d (see Theorem 2.6 of [42]), we conclude from the Poincaré–Bendixson theorem that E_{21d} is globally asymptotically stable in $\mathbb{R}^2_+$. In addition, we can also consider LaSalle's Invariance Principle to show

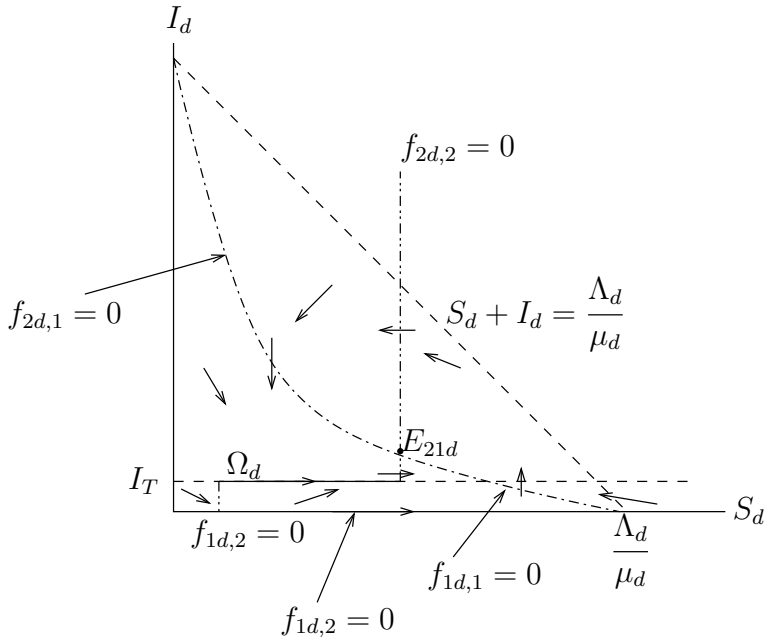

Figure 4.1: Vector field with nullclines and sliding mode when $I_T < h_{3d}$.

the global asymptotic stability of E_{21d} whenever $I_T < h_{3d}$ (see Theorem 2.8 of [42]).

4.1.3 Case 2: $h_{3d} < I_T < h_{4d}$

From Figure 4.2, we can see that $E_d \in \Omega_d \subset M_d$ is the only stable equilibrium point that exists for the model (4.1.1) whenever $h_{3d} < I_T < h_{4d}$. The justification for this case is similar to the previous case: E_d is the only locally stable equilibrium that exists in region D_d, and there is no periodic orbit in D_d. Thus we conclude that E_d is globally asymptotically stable in $\mathbb{R}^2_+$.

4.1.4 Case 3: $I_T > h_{4d}$

In Figure 4.3, we notice that E_{11d} is the only (real) equilibrium that exists whenever $I_T > h_{4d}$. By Theorem 2.3 of [42], it is shown that E_{11d} is locally stable if it exists. Again, there is no periodic orbit in D_d (in fact, this is true for all cases in this section); hence we conclude that E_{11d} is globally asymptotically stable. In Theorem 2.7 of [42], LaSalle's Invariance Principle is used to prove the global stability of E_{11d}. Theorem 2.7 in [42] is a consequence of LaSalle's Invariance Principle (Theorem 2.4.8), with

- $G = \mathbb{R}^2_+$,
- $\Sigma \subset \{(S_d, I_d) : S_d = h_{1d} \text{ and } I_d > 0\}$,

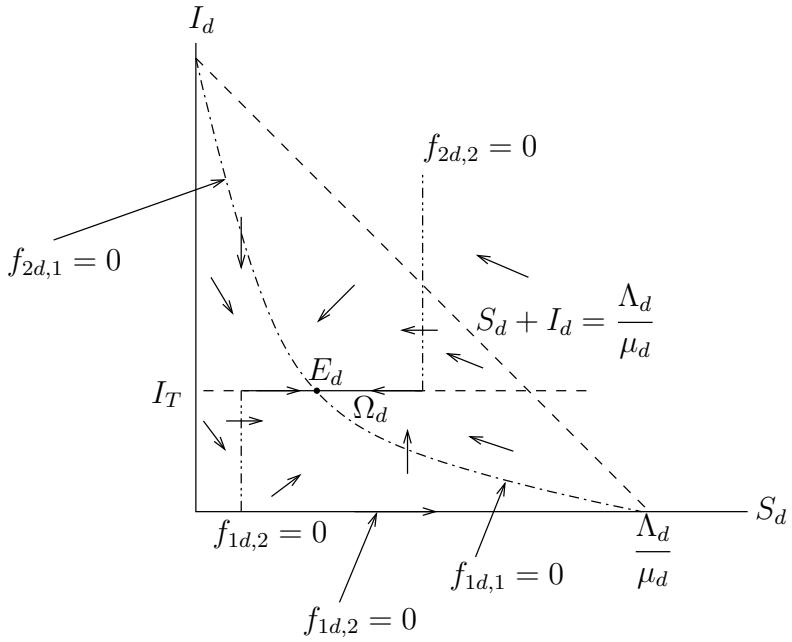

Figure 4.2: Vector field with nullclines and sliding mode when $h_{3d} < I_T < h_{4d}$.

- $D = D_d = \{E_{11d}\}$,
- f given by the right-hand side of (4.1.1) and
- the function

$$V(S_d, I_d) = S_d - \frac{\mu_d + d_d}{\beta_d}\left(1 + \ln\left(\frac{\beta_d S_d}{\mu_d + d_d}\right)\right) + I_d - \frac{\Lambda_d \beta_d \mu_d (\mu_d + d_d)}{\beta_d(\mu_d + d_d)}\left(1 + \ln\left(\frac{\beta_d(\mu_d + d_d) I_d}{\Lambda_d \beta_d \mu_d (\mu_d + d_d)}\right)\right)$$

given as V_1 in (2.13) of [42].

4.2 The SIIR Model with Quarantine as Control Measure

In this section, we summarize the results of [42] on the SIIR model with quarantine as control measure. We also expand our understanding of the dynamics of this system with some new results.

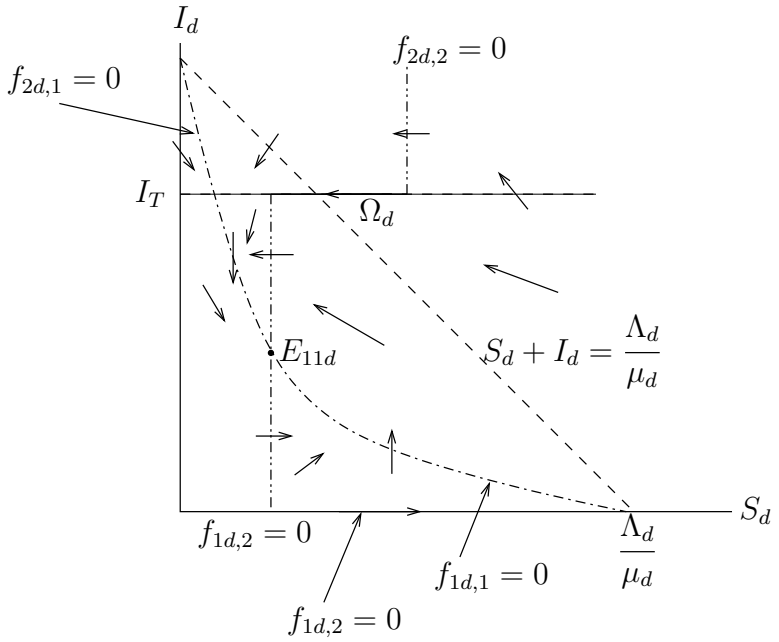

Figure 4.3: Vector field with nullclines and sliding mode when $h_{4d} < I_T$.

The SIIR model with quarantine of infected humans is formulated as follows:

$$\begin{aligned} S'(t) &= \Lambda - \beta_a(1-qu)SI_a - \beta_m(1-qu)SI_m - \mu S \\ I_a'(t) &= \beta_a(1-qu)SI_a - (\mu + d + \gamma + \epsilon)I_a \\ I_m'(t) &= \beta_m(1-qu)SI_m + \epsilon I_a - (\mu + d + \gamma)I_m \\ R'(t) &= \gamma(I_a + I_m) - \mu R \end{aligned} \tag{4.2.1}$$

with

$$u = \begin{cases} 0 & \text{for } I_a + I_m < I_c \\ 1 & \text{for } I_a + I_m > I_c, \end{cases} \tag{4.2.2}$$

where $I_c > 0$ is the critical threshold for the total number of infected humans. The description of the variables and parameters is given in Table 4.2. We assume that $\beta_a > \beta_m$ and $q \in (0, 1)$.

We first observe that we may ignore the last equation of (4.2.1) if we are only studying equilibria.

Suppose that $(\tilde{S}, \tilde{I_a}, \tilde{I_m})$ is an equilibrium of

$$\begin{aligned} S'(t) &= \Lambda - \beta_a(1-qu)SI_a - \beta_m(1-qu)SI_m - \mu S \\ I_a'(t) &= \beta_a(1-qu)SI_a - (\mu + d + \gamma + \epsilon)I_a \\ I_m'(t) &= \beta_m(1-qu)SI_m + \epsilon I_a - (\mu + d + \gamma)I_m. \end{aligned} \tag{4.2.3}$$

This equilibrium is associated to an equilibrium $\tilde{P} = (\tilde{S}, \tilde{I_a}, \tilde{I_m}, \tilde{R})$ of (4.2.1) with

$$\tilde{R} = \frac{\gamma(\tilde{I_a} + \tilde{I_m})}{\mu}.$$

All equilibria of (4.2.1) are of this form. Since

$$\frac{\partial}{\partial R}\Big(\gamma(I_a + I_m) - \mu R\Big)\Big|_{(S,I_a,I_m,R)=\tilde{P}} = -\mu < 0,$$

we have that $R \to \tilde{R}$ as $t \to \infty$. So the stability of an equilibrium of (4.2.1) is determined by the stability of the associated equilibrium of (4.2.3). Hence we consider only the first three equations of model (4.2.1) in analyzing the stability of the equilibria of model (4.2.1).

The space of $(S, I_a, I_m) \in \mathbb{R}^3_+$ is divided into three regions as follows:

$$\begin{aligned} G_1 &= \{(S, I_a, I_m) \in \mathbb{R}^3_+; I_a + I_m < I_c\}, \\ G_2 &= \{(S, I_a, I_m) \in \mathbb{R}^3_+; I_a + I_m > I_c\}, \\ M &= \{(S, I_a, I_m) \in \mathbb{R}^3_+; I_a + I_m = I_c\}. \end{aligned}$$

The normal vector perpendicular to M that we choose is $n = \begin{pmatrix} 0 & 1 & 1 \end{pmatrix}^\top$.

From (4.2.3), we obtain the following dynamical systems on the region G_i for $i = 1, 2$:

$$\begin{pmatrix} S' \\ I_a' \\ I_m' \end{pmatrix} = \begin{pmatrix} f_{1,1}(S, I_a, I_m) \\ f_{1,2}(S, I_a, I_m) \\ f_{1,3}(S, I_a, I_m) \end{pmatrix} = \begin{pmatrix} \Lambda - \beta_a SI_a - \beta_m SI_m - \mu S \\ \beta_a SI_a - (\mu + d + \gamma + \epsilon)I_a \\ \beta_m SI_m + \epsilon I_a - (\mu + d + \gamma)I_m \end{pmatrix} \tag{4.2.4}$$

$$\begin{pmatrix} S' \\ I_a' \\ I_m' \end{pmatrix} = \begin{pmatrix} f_{2,1}(S, I_a, I_m) \\ f_{2,2}(S, I_a, I_m) \\ f_{2,3}(S, I_a, I_m) \end{pmatrix} = \begin{pmatrix} \Lambda - (1-q)\beta_a SI_a - (1-q)\beta_m SI_m - \mu S \\ (1-q)\beta_a SI_a - (\mu + d + \gamma + \epsilon)I_a \\ (1-q)\beta_m SI_m + \epsilon I_a - (\mu + d + \gamma)I_m \end{pmatrix}. \tag{4.2.5}$$

Proposition 4.2.1. *The set* $\widehat{D} \equiv \left\{(S, I_a, I_m) \in \mathbb{R}^3_+ : S + I_a + I_m \leq \frac{\Lambda}{\mu}\right\}$ *is flow in-*

Symbol	Description
S	Susceptible humans
I_a	Humans infected with avian strain
I_m	Humans infected with mutant avian
R	Humans who have recovered from avian and mutant strains
Λ	Human recruitment rate
μ	Natural mortality rate of humans
β_a	Transmission rate of human-to-human with avian strain
β_m	Transmission rate of human-to-human with mutant strain
d	Additional disease death rate of humans due to avian influenza
γ	Recovery rate of humans with avian influenza
ϵ	Mutation rate
q	Quarantine rate

Table 4.2: Descriptions of the associated variables and parameters in SIIR model (4.2.1).

variant and attracting for (4.2.3).

The proof of Proposition 4.2.1 is similar to the proof of Lemma 3.1 in [42], so we do not include the proof of this proposition. The region $\widehat{D}$ in $\mathbb{R}^3_+$ is depicted in Figure 4.4; in Figure 4.5, we illustrate the space $\mathbb{R}^3_+$ with the three regions: G_1, G_2 and M.

The S-, I_a- and I_m-nullclines for system (4.2.4) are given by $f_{1,1} = 0$, $f_{1,2} = 0$ and $f_{1,3} = 0$, respectively. That is, the S-nullcline is

$$\left\{(S, I_a, I_m) \in \mathbb{R}^3_+ : S = \frac{\Lambda}{\beta_a I_a + \beta_m I_m + \mu} \text{ and } I_a + I_m < I_c\right\},$$

the I_a-nullclines are

$$\left\{(S, I_a, I_m) \in \mathbb{R}^3_+ : I_a = 0 \text{ and } I_a + I_m < I_c\right\}$$

and

$$\left\{(S, I_a, I_m) \in \mathbb{R}^3_+ : S = \frac{\mu + d + \gamma + \epsilon}{\beta_a} \text{ and } I_a + I_m < I_c\right\},$$

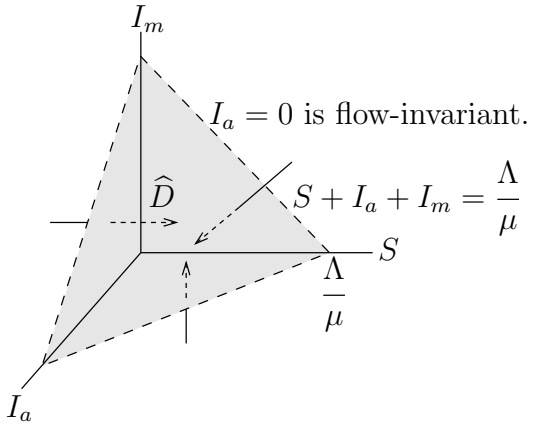

Figure 4.4: $\widehat{D}$ is flow-invariant.

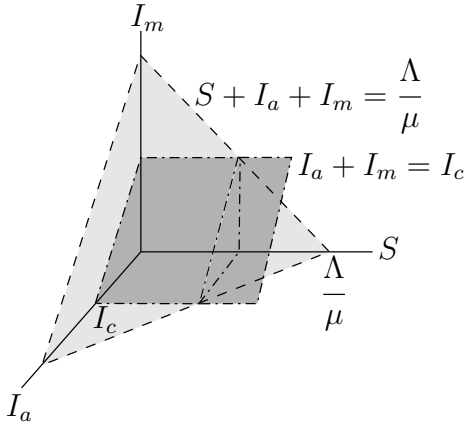

Figure 4.5: G_1 is below the plane $I_a + I_m = I_c$ and G_2 is above.

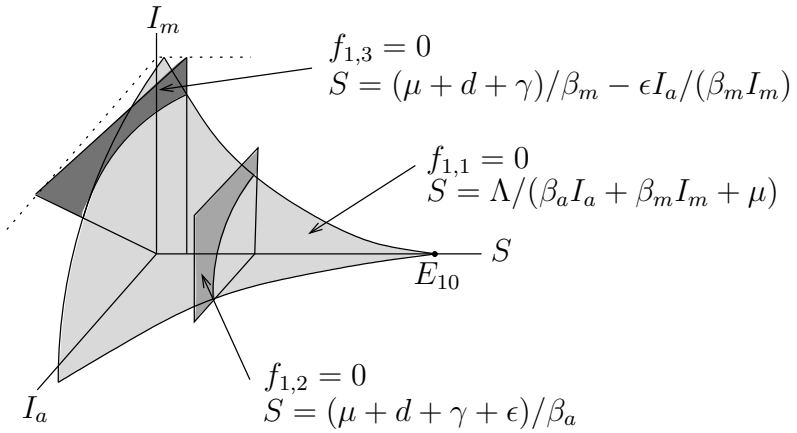

Figure 4.6: Nullclines for f_1 if $(\mu + d + \gamma)(\beta_a - \beta_m) - \beta_m \epsilon < 0$ and $R_{1a} > 1$.

and the I_m-nullcline is

$$\left\{ (S, I_a, I_m) \in \mathbb{R}^3_+ : S = \frac{\mu + d + \gamma}{\beta_m} - \frac{\epsilon I_a}{\beta_m I_m} \text{ and } I_a + I_m < I_c \right\}.$$

The nullclines are represented in Figure 4.6 if $(\mu + d + \gamma)(\beta_a - \beta_m) - \beta_m \epsilon < 0$, and in Figure 4.7 if $(\mu + d + \gamma)(\beta_a - \beta_m) - \beta_m \epsilon > 0$. Proposition 4.2.2 below says that only the second case is interesting.

The dynamical system (4.2.4) has two equilibria in $\mathbb{R}^3_+$: a disease-free equilibrium, $E_{10} = (\Lambda/\mu, 0, 0)$, and an endemic equilibrium, $E_{11} = (E_{11,S}, E_{11,I_a}, E_{11,I_m})$, where

$$\begin{aligned}
E_{11,S} &= \frac{\mu + d + \gamma + \epsilon}{\beta_a}, \\
E_{11,I_m} &= \frac{\epsilon \left(\Lambda \beta_a - \mu(\mu + d + \gamma + \epsilon) \right)}{(\beta_a - \beta_m)(\mu + d + \gamma)(\mu + d + \gamma + \epsilon)}, \\
E_{11,I_a} &= \frac{\left(\Lambda \beta_a - \mu(\mu + d + \gamma + \epsilon) \right) \left((\mu + d + \gamma)(\beta_a - \beta_m) - \epsilon \beta_m \right)}{\beta_a (\beta_a - \beta_m)(\mu + d + \gamma)(\mu + d + \gamma + \epsilon)}, \\
&= \frac{\left((\mu + d + \gamma)(\beta_a - \beta_m) - \epsilon \beta_m \right) E_{11,I_m}}{\epsilon \beta_a}.
\end{aligned}$$

The basic reproduction number of the dynamical system (4.2.4) is defined as $R_1 = \max\{R_{1a}, R_{1m}\}$, where

$$R_{1a} = \frac{\Lambda \beta_a}{\mu(\mu + d + \gamma + \epsilon)} \text{ and } R_{1m} = \frac{\Lambda \beta_m}{\mu(\mu + d + \gamma)}.$$

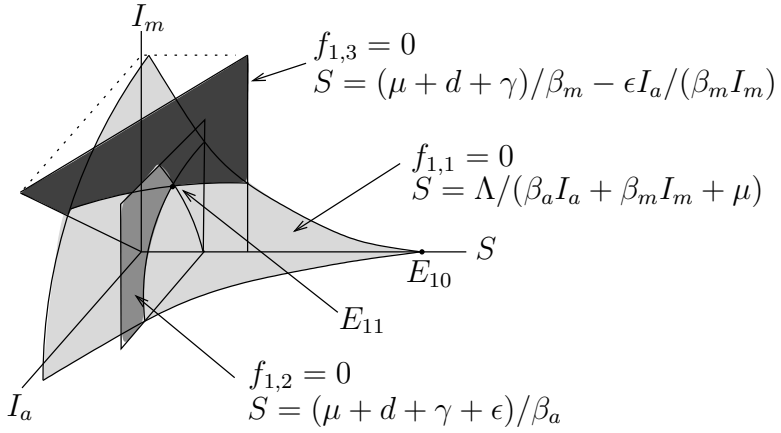

Figure 4.7: Nullclines for f_1 if $(\mu + d + \gamma)(\beta_a - \beta_m) - \beta_m\epsilon > 0$ and $R_{1a} > 1$.

Proposition 4.2.2. *The endemic equilibrium $E_{11} \in \mathbb{R}^3_+$ exists if and only if $R_{1a} > 1$ and $(\mu + d + \gamma)(\beta_a - \beta_m) - \epsilon\beta_m > 0$.*

Proof: Note that all parameters are positive and $\beta_a > \beta_m$. Since all parameters are positive, $E_{11,S}$ is always positive.

If $R_{1a} < 1$, then $\Lambda\beta_a - \mu(\mu + d + \gamma + \epsilon) < 0$ and $E_{11,I_m} < 0$. Note that E_{11} is not biologically meaningful whenever E_{11,I_m} is negative.

If $R_{1a} > 1$, then $\Lambda\beta_a - \mu(\mu + d + \gamma + \epsilon) > 0$. If we assume that $(\mu + d + \gamma)(\beta_a - \beta_m) - \epsilon\beta_m < 0$, we have that E_{11,I_m} is positive (recall that $\beta_a > \beta_m$ by general assumption) but E_{11,I_a} is negative. Thus E_{11} has no biological meaning. From Figure 4.6, we can see that E_{11} does not exist if $R_{1a} > 1$ and $(\mu + d + \gamma)(\beta_a - \beta_m) - \epsilon\beta_m < 0$.

Finally, if $R_{1a} > 1$ and $(\mu + d + \gamma)(\beta_a - \beta_m) - \epsilon\beta_m > 0$, then we have that both E_{11,I_m} and E_{11,I_a} are positive. Hence $E_{11} \in \mathbb{R}^3_+$ exists whenever $R_{1a} > 1$ and $(\mu + d + \gamma)(\beta_a - \beta_m) - \epsilon\beta_m > 0$ as illustrated in Figure 4.7. ∎

The local stability of E_{11} when present is proven in Theorem 3.3 of [42].

Because of the similar structure of the dynamical systems (4.2.4) and (4.2.5), the observations that we have made about the dynamical system (4.2.4) on G_1 can also be made with a slight adaptation about the dynamical system (4.2.5).

The S-, I_a- and I_m-nullclines for system (4.2.5) are given by $f_{2,1} = 0$, $f_{2,2} = 0$ and $f_{2,3} = 0$, respectively. That is, the S-nullcline is

$$\left\{ (S, I_a, I_m) \in \mathbb{R}^3_+ : S = \frac{\Lambda}{(1-q)(\beta_a I_a + \beta_m I_m) + \mu} \text{ and } I_a + I_m > I_c \right\};$$

the I_a-nullclines are

$$\left\{(S, I_a, I_m) \in \mathbb{R}^3_+ : I_a = 0 \text{ and } I_a + I_m > I_c\right\}$$

and

$$\left\{(S, I_a, I_m) \in \mathbb{R}^3_+ : S = \frac{\mu + d + \gamma + \epsilon}{\beta_a(1-q)} \text{ and } I_a + I_m > I_c\right\};$$

and the I_m-nullcline is

$$\left\{(S, I_a, I_m) \in \mathbb{R}^3_+ : S = \frac{(\mu + d + \gamma)I_m - \epsilon I_a}{(1-q)\beta_m I_m} \text{ and } I_a + I_m > I_c\right\}.$$

The diagram of nullclines for the dynamical system (4.2.5) is qualitatively similar to the diagram of nullclines for the dynamical system (4.2.4).

For the dynamical system (4.2.5) on G_2, we have a disease-free equilibrium $E_{20} = E_{10} = \left(\frac{\Lambda}{\mu}, 0, 0\right)$ and an endemic equilibrium $E_{21} = (E_{21,S}, E_{21,I_a}, E_{21,I_m})$, where

$$\begin{aligned}
E_{21,S} &= \frac{\mu + d + \gamma + \epsilon}{\beta_a(1-q)}, \\
E_{21,I_m} &= \frac{\epsilon\left(\Lambda\beta_a(1-q) - \mu(\mu + d + \gamma + \epsilon)\right)}{(1-q)(\beta_a - \beta_m)(\mu + d + \gamma)(\mu + d + \gamma + \epsilon)}, \\
E_{21,I_a} &= \frac{\left(\Lambda\beta_a(1-q) - \mu(\mu + d + \gamma + \epsilon)\right)\left((\mu + d + \gamma)\beta_a - (\mu + d + \gamma + \epsilon)\beta_m\right)}{\beta_a(1-q)(\beta_a - \beta_m)(\mu + d + \gamma)(\mu + d + \gamma + \epsilon)} \\
&= \frac{\left((\mu + d + \gamma)\beta_a - (\mu + d + \gamma + \epsilon)\beta_m\right) E_{21,I_m}}{\epsilon\beta_a}.
\end{aligned}$$

The basic reproduction number for the dynamical system (4.2.5) is $R_2 = \max\{R_{2a}, R_{2m}\}$, where

$$R_{2a} = \frac{\Lambda\beta_a(1-q)}{\mu(\mu + d + \gamma + \epsilon)} \text{ and } R_{2m} = \frac{\Lambda\beta_m(1-q)}{\mu(\mu + d + \gamma)}.$$

Proposition 4.2.3. *The endemic equilibrium $E_{21} \in \mathbb{R}^3_+$ exists if and only if $R_{2a} > 1$ and $(\mu + d + \gamma)(\beta_a - \beta_m) - \epsilon\beta_m > 0$.*

We omit the proof of Proposition 4.2.3 since it is similar to the proof of Proposition 4.2.2.

We show that E_{21} is locally asymptotically stable in Theorem 3.5 of [42] when it is present.

4.2.1 Sliding Domain

We determine in [42] the existence of a sliding mode on the discontinuity surface M and its dynamical system for model (4.2.3).

A sliding mode exists if $\langle n, f_1\rangle > 0$ and $\langle n, f_2\rangle < 0$. We have

$$\langle n, f_1\rangle > 0 \quad \text{if} \quad S > h_1(I_a) = \frac{(\mu + d + \gamma)I_c}{(\beta_a - \beta_m)I_a + \beta_m I_c}$$

and

$$\langle n, f_2\rangle < 0 \quad \text{if} \quad S < h_2(I_a) = \frac{(\mu + d + \gamma)I_c}{(1-q)\left[(\beta_a - \beta_m)I_a + \beta_m I_c\right]}.$$

So the sliding domain $\Omega \subset M$ is defined as

$$\Omega = \left\{(S, I_a, I_m) \in M : h_1(I_a) < S < h_2(I_a) \text{ and } I_a + I_m = I_c\right\}.$$

We use the Utkin equivalent control method to determine the sliding mode equations and find that the dynamical system on the discontinuity surface M is governed by the following equations.

$$\begin{aligned} S'(t) &= \Lambda - (\mu + d + \gamma)I_c - \mu S \\ I_a'(t) &= \beta_a I_a \left(\frac{(\mu + d + \gamma)I_c}{(\beta_a - \beta_m)I_a + \beta_m I_c}\right) - (\mu + d + \gamma + \epsilon)I_a \\ I_m'(t) &= -I_a'(t). \end{aligned} \tag{4.2.6}$$

All the details to determine the sliding mode equation (4.2.6) can be found in [42]. Furthermore, there is a sliding equilibrium $E_s = (E_{s,S}, E_{s,I_a}, E_{s,I_m})$ for system (4.2.6), where

$$\begin{aligned} E_{s,S} &= \frac{\Lambda - (\mu + d + \gamma)I_c}{\mu}, \\ E_{s,I_a} &= \frac{I_c\left(\beta_a(\mu + d + \gamma) - \beta_m(\mu + d + \gamma + \epsilon)\right)}{(\beta_a - \beta_m)(\mu + d + \gamma + \epsilon)} \end{aligned}$$

and

$$E_{s,I_m} = \frac{\epsilon\beta_a I_c}{(\beta_a - \beta_m)(\mu + d + \gamma + \epsilon)}.$$

Obviously, $E_s \in \Omega \subset M$ if $h_1(I_a) < E_{s,S} < h_2(I_a)$; namely, if

$$h_1(I_a) < \frac{\Lambda - (\mu + d + \gamma)I_c}{\mu} < h_2(I_a)$$

is satisfied. The local stability of E_s on Ω is proven in Theorem 3.6 of [42].

We summarize in the next sections the stability of model (4.2.3) when the tolerance threshold I_c is varying.

Proposition 4.2.4. *$E_{11,I_a} + E_{11,I_m}$ is larger than $E_{21,I_a} + E_{21,I_m}$.*

Proof: Following simplification, we have

$$E_{11,I_a} + E_{11,I_m} = \frac{\Lambda}{\mu + d + \gamma} - \frac{\mu(\mu + d + \gamma + \epsilon)}{\beta_a(\mu + d + \gamma)}$$

and

$$E_{21,I_a} + E_{21,I_m} = \frac{\Lambda}{\mu + d + \gamma} - \frac{\mu(\mu + d + \gamma + \epsilon)}{(1 - q)\beta_a(\mu + d + \gamma)}.$$

Since $0 < 1 - q < 1$, then we obtain

$$\frac{\Lambda}{\mu + d + \gamma} - \frac{\mu(\mu + d + \gamma + \epsilon)}{(1 - q)\beta_a(\mu + d + \gamma)} < \frac{\Lambda}{\mu + d + \gamma} - \frac{\mu(\mu + d + \gamma + \epsilon)}{\beta_a(\mu + d + \gamma)},$$

which proves that $E_{21,I_a} + E_{21,I_m} < E_{11,I_a} + E_{11,I_m}$. ∎

4.2.2 Case 1: $E_{21,I_a} + E_{21,I_m} < E_{11,I_a} + E_{11,I_m} < I_c$

The only equilibrium for the model (4.2.3) is $E_{11} \in G_1$. The local stability of E_{11} is proved in Theorem 3.8 of [42].

4.2.3 Case 2: $E_{21,I_a} + E_{21,I_m} < I_c < E_{11,I_a} + E_{11,I_m}$

There is no real equilibrium in regions G_1 and G_2, but there is the sliding equilibrium $E_s \in \Omega \subset M$. Hence E_s is locally asymptotically stable (see Theorem 3.7 of [42]).

4.2.4 Case 3: $I_c < E_{21,I_a} + E_{21,I_m} < E_{11,I_a} + E_{11,I_m}$

$E_{21} \in G_2$ is the only equilibrium point, and we prove that it is locally stable in Theorem 3.9 of [42].

4.2.5 Conjecture and conclusions

Based on the numerical evidence presented in [42], we may conjecture that the local stability for the equilibria in the previous section can be replaced by global stability.

A conclusion and discussion of this study can be found in [42]. We attach the manuscript [42] below.

Nonlinear Analysis: Real World Applications 24 (2015) 196–218

Contents lists available at ScienceDirect

Nonlinear Analysis: Real World Applications

journal homepage: www.elsevier.com/locate/nonrwa

Modeling avian influenza using Filippov systems to determine culling of infected birds and quarantine

Nyuk Sian Chong [a,b], Robert J. Smith? [c,*]

[a] Department of Mathematics, The University of Ottawa, 585 King Edward Ave, Ottawa ON K1N 6N5, Canada
[b] School of Informatics & Applied Mathematics, Universiti Malaysia Terengganu, 21030 Kuala Terengganu, Malaysia
[c] Department of Mathematics and Faculty of Medicine, The University of Ottawa, 585 King Edward Ave, Ottawa ON K1N 6N5, Canada

ARTICLE INFO

Article history:
Received 17 March 2014
Received in revised form 10 February 2015
Accepted 21 February 2015
Available online 18 March 2015

Keywords:
Avian influenza
Filippov model
Threshold policy
Culling of infected birds
Quarantine

ABSTRACT

The growing number of reported avian influenza cases has prompted awareness of the effectiveness of pharmaceutical or/and non-pharmaceutical interventions that aim to suppress the transmission rate. We propose two Filippov models with threshold policy: the avian-only model with culling of infected birds and the SIIR (Susceptible–Infected–Infected–Recovered) model with quarantine. The dynamical systems of these two models are governed by nonlinear ordinary differential equations with discontinuous right-hand sides. The solutions of these two models will converge to either one of the two endemic equilibria or the sliding equilibrium on the discontinuous surface. We prove that the avian-only model achieves global stability. Moreover, by choosing an appropriate quarantine threshold level I_c in the SIIR model, this model converges to an equilibrium in the region below I_c or a sliding equilibrium, suggesting the outbreak can be controlled. Therefore a well-defined threshold policy is important for us to combat the influenza outbreak efficiently.

1. Introduction

Recently, a new bird flu H7N9 has been reported as a threat to the public health across China. As an early stage of precaution, the China Health and Family Planning Commission has alerted the WHO (World Health Organization) about this infection [1,2]. Further, epidemiological investigations have been carried out to identify the root of the infection so that the disease can be controlled in the most effective and efficient way [2]. The public are also advised to take care of their personal hygiene, avoiding any contact with the sick or bird carcasses, reducing contact with wild birds and limiting unnecessary visits to poultry farms [3,2]. Humans can be infected by avian influenza through direct contact with dead or infected poultry and wild birds. People who have been infected by avian influenza may initially develop several symptoms such as fever, sore throat, muscle aches, cough, having breathing difficulties and conjunctivitis [4–6].

The spread of the new highly pathogenic avian influenza A viruses has not only triggered a major loss of life but has also cost a significant amount of money. Governments worldwide have spent billions of dollars to treat the infected patients and invest in prevention to control the disease [7]. Thus it is crucial to identify any possible effective control measures that

* Corresponding author.
E-mail address: rsmith43@uottawa.ca (R.J. Smith?).

http://dx.doi.org/10.1016/j.nonrwa.2015.02.007
1468-1218/

can eradicate the disease or at least to bring down the impact of the outbreak to a minimum level. That is, minimizing the number of infected is always a priority.

A significant number of mathematical modeling studies have been initiated to evaluate the effectiveness and the role of control measures in combating avian influenza [8–13]. Ferguson et al. [14] examined the effectiveness of targeted prophylaxis antiviral drug and social distancing measures in fighting an emerging influenza outbreak in Southeast Asia. Nuño et al. [15] assessed the basic public-health control strategies (such as using protective tools like gloves and masks, isolation in hospital wards and quarantine of suspected patients) in order to minimize the infection rate in hospitals and communities. The use of antiviral drugs and vaccination in combating a potential flu pandemic had also been discussed. Gulbudak and Martcheva [16] incorporated various approaches to culling of domestic birds: mass, modified and selective culling approaches. They concluded that, besides culling of domestic birds, timely employment of temporary control methods such as separation of poultry from wild birds, increasing biosecurity and prohibiting poultry movement and hatching eggs will either reduce the number of infected domestic birds or eradicate the disease in poultry.

Further, Agusto [17] applied optimal control theory to a system of ordinary differential equations to describe the transmission of two-strain avian influenza. Isolation of individuals with avian and mutant strains is represented by a pair of control variables. Moreover, cost-effectiveness of all possible combinations of the control measures is calculated. The results show that the combination strategy of isolating individuals with both avian and mutant strains is the most cost-effectiveness and provides more benefits towards disease eradication compared to only using one control strategy. Chong et al. [18] suggested that a combination of pharmaceutical (vaccination) and non-pharmaceutical (personal protection and isolation) interventions can combat avian influenza more effectively.

Several conventional control methods such as pharmaceutical or non-pharmaceutical interventions may be employed if the number of infected individuals exceeds a certain tolerant threshold, say I_c, in order to control or suppress the transmission rate of an emerging infectious disease. Thus, whenever the number of infected is below the threshold level I_c, the infection is considered tolerable. However, once the number of infected reaches I_c, we assume that an outbreak might occur. Henceforth, we call this type of disease management strategy a threshold policy [19–21].

Xiao et al. [22] extended the classical SIR model to a Filippov SIR model incorporating behavioral change of general individuals and implementation of necessary control measures by public authorities. They showed that the model solutions will either converge to one of the two endemic equilibria or the sliding equilibrium on the discontinuous surface. In order to preclude the outbreak or to stabilize the infection at a desired level, Xiao et al. suggested that choosing a proper combination of threshold level and control intensities is crucial.

Tang et al. [19] designed a piecewise HIV virus dynamic model with $CD4^+$ T cell counts to evaluate the strategies of structured treatment interruptions (STIs) of antiretroviral therapies. The dynamic models for drug-on and drug-off states with a single threshold and two thresholds (i.e., threshold window) are studied. Both models for STIs with single threshold and threshold window show that the $CD4^+$ T cell counts are preserved above a safe level. However, numerical results show that, by picking different lower and upper tolerant thresholds, it will either converge to a stable level or fluctuate. To conclude, an appropriate tolerant threshold of $CD4^+$ T cell counts and an individualized STI strategy based on the initial value of $CD4^+$ T cell counts for each individual patient are essential to compute the duration of drug on/off states for a patient.

In addition, Zhao et al. [23] proposed two Filippov plant disease models with cultural control strategy; a plant-disease model with replanting and roguing, and a Lotka–Volterra Filippov plant disease model with proportional planting rate. For the former model, a roguing rate that is proportional to the number of infected plants is considered. The global dynamic behavior of these models is discussed. Further, the global stability of five types of equilibria is thoroughly investigated.

An HPAI (highly pathogenic avian influenza) outbreak brings losses to the poultry business especially in commercialized poultry-processing industries. Besides the great loss in these business ventures, a significant number of birds will be destroyed [24,25]. The H5N1 outbreak in Hong Kong during 1997 caused an estimated loss of $13 million and the culling of 1.4 millions birds. In the 2001 H5N1 outbreak in Hong Kong, 1.2 million birds were killed, resulting in a total loss of $3.8 million. The H7N7 outbreak in 2003 in several European countries caused a loss of $314 million and 30 million birds [26,27].

HPAI viruses (H5 and H7 subtypes) usually cause infection among common bird species, such as chickens, ducks, pigeons, quails, turkeys and others. HPAI viruses can result in a very high mortality rate (90%–100%). Avian influenza viruses can be found mostly in the feces, saliva and nasal secretions of birds. Due to limited space of birds in the farm, avian influenza viruses can be spread easily among poultry flocks through aerosol or fecal-oral route [8,26,28]. Poultry, mainly chicken meat and eggs, are a valuable source of protein for many people, especially for lower-income groups, since chicken meat is the cheapest of all farm animals [29]. Hence, it is important for us to study avian influenza infections.

Here we would like to propose two mathematical models with piecewise control strategy that relate to threshold policy: an avian-only model with culling of infected birds as a control strategy in Section 2 and an SIIR model with quarantine as the control measure in Section 3. The dynamical systems of these two models are governed by nonlinear ordinary differential equations with discontinuous right-hand sides. The local asymptotic stability of disease-free and endemic equilibria in the regions below and above the threshold level are analyzed in each model. Further, the existence of a sliding mode, its dynamics and the global stability of the equilibria (if it exists) will also be investigated in each model. Finally, we will discuss the implications of our results in Section 4.

2. The avian-only model with culling of infected domestic birds

In this section, we consider an avian-only model incorporating culling of infected birds as a control strategy. Here we only consider domestic birds for the avian population. In order to manage the disease, the number of infected birds is used as an index of reference in applying the control strategy. The disease is considered to be manageable and the implementation of control methods is not required if the number of infected birds is below the tolerant threshold I_T. However, the action of culling the infected birds has to be employed immediately when the number of the infected birds exceeds the threshold level I_T. This action is essential to control the outbreak before the situation becomes more severe.

The avian-only model is driven by two compartments: susceptible domestic birds (S_d) and infected domestic birds (I_d). The total population of domestic birds, $N_d(t)$, is the sum of $S_d(t)$ and $I_d(t)$ at time t. Here, we represent the bird inflow, natural death and disease death by the parameters Λ_d, μ_d and d_d, respectively. The differential equations for this model are formulated as follows:

$$\begin{aligned} S_d'(t) &= \Lambda_d - \beta_d S_d I_d - \mu_d S_d \\ I_d'(t) &= \beta_d S_d I_d - (\mu_d + d_d) I_d - u_d c I_d \end{aligned} \tag{2.1}$$

with

$$u_d = \begin{cases} 0 & \text{for } I_d < I_T \Leftrightarrow \sigma_d(I_d) = I_d - I_T < 0 \\ 1 & \text{for } I_d > I_T \Leftrightarrow \sigma_d(I_d) = I_d - I_T > 0, \end{cases} \tag{2.2}$$

where $I_T > 0$ is the tolerance threshold, β_d is the rate at which domestic birds contract avian influenza and c is the culling rate of infected domestic birds.

Moreover, we divide $(S_d, I_d) \in \mathbb{R}^2_+$ into three regions as follows:

$$\begin{aligned} G_{1d} &:= \{(S_d, I_d) \in \mathbb{R}^2_+; I_d < I_T\} \\ G_{2d} &:= \{(S_d, I_d) \in \mathbb{R}^2_+; I_d > I_T\} \\ M_d &:= \{(S_d, I_d) \in \mathbb{R}^2_+; I_d = I_T\}. \end{aligned}$$

We define the normal vector perpendicular to M_d as $n_d = (0, 1)^T$ and the right-hand sides of (2.1) in region G_{id} are denoted by f_{id} for $i = 1, 2$, where

$$\begin{aligned} f_{1d} &= f_{1d}(S_d, I_d) = \begin{pmatrix} \Lambda_d - S_d(\beta_d I_d + \mu_d) \\ I_d\,[\beta_d S_d - (\mu_d + d_d)] \end{pmatrix} \\ f_{2d} &= f_{2d}(S_d, I_d) = \begin{pmatrix} \Lambda_d - S_d(\beta_d I_d + \mu_d) \\ I_d\,[\beta_d S_d - (\mu_d + d_d + c)] \end{pmatrix}. \end{aligned}$$

Lemma 2.1. *The set* $D_d = \left\{(S_d, I_d) \in \mathbb{R}^2_+; S_d + I_d \le \frac{\Lambda_d}{\mu_d}\right\}$ *is a positively invariant and attracting region for model* (2.1) *with any given initial conditions in* $\mathbb{R}^2_+$.

Proof. By adding both $S_d'(t)$ and $I_d'(t)$ of model (2.1), we get

$$N_d' = \Lambda_d - \mu_d S_d - (\mu_d + d_d) I_d - u_d c I_d \le \Lambda_d - \mu_d N_d. \tag{2.3}$$

Solving (2.3) by using an integrating factor, we obtain

$$\begin{aligned} &\int_0^t \frac{d}{d\zeta}\left(N_d e^{\mu_d \zeta}\right) d\zeta = \int_0^t \Lambda_d e^{\mu_d \zeta}\, d\zeta \\ &N_d(t) e^{\mu_d t} = N_d(0) + \frac{\Lambda_d}{\mu_d}\left(e^{\mu_d t} - 1\right) \\ &N_d(t) \le \frac{\Lambda_d}{\mu_d} \quad \text{if } N_d(0) = S_d(0) + I_d(0) \le \frac{\Lambda_d}{\mu_d}. \end{aligned}$$

Thus we obtain $N_d(t) \le \frac{\Lambda_d}{\mu_d}$ if $N_d(0) \le \frac{\Lambda_d}{\mu_d}$. Hence the region D_d is positively invariant.

Next, to show that D_d is an attracting region for model (2.1), let $N_d(t) > \frac{\Lambda_d}{\mu_d}$ and $\frac{\Lambda_d}{\mu_d} = \psi_d \Longrightarrow \Lambda_d = \mu_d \psi_d$. From (2.3), we have

$$N_d' \le \Lambda_d - \mu_d N_d = \mu_d(\psi_d - N_d) < 0.$$

We infer that the total population of domestic birds (i.e., $N_d = S_d + I_d$) of (2.1) is bounded by $\frac{\Lambda_d}{\mu_d}$. Moreover, every solution of model (2.1) with initial conditions in D_d will remain in D_d for $t > 0$. It is noteworthy to mention that every solution with initial conditions in $\mathbb{R}^2_+ \setminus D_d$ will approach D_d as $t \to \infty$. Hence the ω-limit sets of (2.1) are contained in D_d. ■

Since D_d is a positively invariant and attracting region for model (2.1), the solution of model (2.1) exists in $D_d \forall t > 0$ and this model is mathematically and epidemiologically well-posed in D_d [30]. So it is sufficient to consider the dynamics of this model in D_d.

2.1. Analysis in region G_{1d}

In this section, we begin with the calculation of the basic reproduction number and then analyze the stability of the equilibria in region G_{1d}. The dynamics in region G_{1d} can be described by the following nonlinear ordinary differential equations:

$$\begin{pmatrix} S_d'(t) \\ I_d'(t) \end{pmatrix} = \begin{pmatrix} \Lambda_d - \beta_d S_d I_d - \mu_d S_d \\ \beta_d S_d I_d - (\mu_d + d_d) I_d \end{pmatrix} \equiv f_{1d}. \tag{2.4}$$

There are two equilibria involved in (2.4), the DFE (disease-free equilibrium), $E_{10d} = (S_d, I_d) = \left(\frac{\Lambda_d}{\mu_d}, 0\right)$ and a unique positive EE (endemic equilibrium), $E_{11d} = \left(\frac{\mu_d + d_d}{\beta_d}, \frac{\Lambda_d \beta_d - \mu_d(\mu_d + d_d)}{\beta_d(\mu_d + d_d)}\right)$. The basic reproduction number (see [31,32] for further details) for model (2.4), R_{1d}, is given as follows:

$$R_{1d} = \frac{\Lambda_d \beta_d}{\mu_d(\mu_d + d_d)}.$$

In addition, we would like to show that the DFE and EE of model (2.4) achieve local asymptotic stability in the following theorems, and the Jacobian matrix for this model is

$$J_{1d}(S_d, I_d) = \begin{pmatrix} -\beta_d I_d - \mu_d & -\beta_d S_d \\ \beta_d I_d & \beta_d S_d - (\mu_d + d_d) \end{pmatrix}.$$

Theorem 2.2. *The DFE, E_{10d}, of model (2.4) is locally asymptotically stable if $R_{1d} < 1$.*

Proof. By solving the characteristic equation $|J_{1d}(E_{10d}) - \lambda I| = 0$, we obtain

$$(-\mu_d - \lambda)\left[\frac{\Lambda_d \beta_d}{\mu_d} - (\mu_d + d_d) - \lambda\right] = 0 \quad \Longrightarrow \lambda = -\mu_d < 0$$

$$\lambda = \frac{\Lambda_d \beta_d - \mu_d(\mu_d + d_d)}{\mu_d} < 0$$

if $R_{1d} < 1$. We conclude that, at the DFE, all eigenvalues of (2.4) are negative if $R_{1d} < 1$. Hence E_{10d} is locally asymptotically stable if $R_{1d} < 1$. ■

Theorem 2.3. *The EE, E_{11d}, of model (2.4) is locally asymptotically stable if $R_{1d} > 1$.*

Proof. The eigenvalues of $J_{1d}(E_{11d})$ are

$$\lambda = \frac{1}{2}\left(-\frac{\Lambda_d \beta_d}{\mu_d + d_d} \pm \sqrt{\Delta_{1d}}\right) \quad \text{where } \Delta_{1d} = \left(\frac{\Lambda_d \beta_d}{\mu_d + d_d}\right)^2 - 4\left[\Lambda_d \beta_d - \mu_d(\mu_d + d_d)\right].$$

If $R_{1d} > 1$, we obtain $\Lambda_d \beta_d - \mu_d(\mu_d + d_d) > 0$. Thus all λ are complex eigenvalues with negative real parts if $\Delta_{1d} < 0$ since all associated parameters are positive. Otherwise, if $\Delta_{1d} > 0$, then $\Delta_{1d} < \left(\frac{\Lambda_d \beta_d}{\mu_d + d_d}\right)^2$, so all λ are negative real numbers.

It follows that E_{11d} is either a stable spiral or stable node. Hence E_{11d} achieves local asymptotic stability whenever $R_{1d} > 1$. ■

2.2. Analysis in region G_{2d}

A similar analysis as shown in Section 2.1 will be carried out in this section. The following equations describe the dynamics in region G_{2d}.

$$\begin{pmatrix} S_d'(t) \\ I_d'(t) \end{pmatrix} = \begin{pmatrix} \Lambda_d - \beta_d S_d I_d - \mu_d S_d \\ \beta_d S_d I_d - (\mu_d + d_d + c) I_d \end{pmatrix} \equiv f_{2d}. \tag{2.5}$$

In G_{2d}, we found two equilibria: the DFE, $E_{20d} = (S_d, I_d) = \left(\frac{\Lambda_d}{\mu_d}, 0\right)$, and a unique positive EE, $E_{21d} = \left(\frac{\mu_d + d_d + c}{\beta_d}, \frac{\Lambda_d \beta_d - \mu_d(\mu_d + d_d + c)}{\beta_d(\mu_d + d_d + c)}\right)$. Moreover, the basic reproduction number (refer to [31,32] for further details) for model (2.5), R_{2d}, is thus

$$R_{2d} = \frac{\Lambda_d \beta_d}{\mu_d(\mu_d + d_d + c)}.$$

Further, the local asymptotic stability of the DFE and EE of model (2.5) are shown in the following theorems.

Theorem 2.4. *The DFE E_{20d} of model (2.5) is locally asymptotically stable if $R_{2d} < 1$.*

We use a similar method as in the proof of Theorem 2.2 to demonstrate that all eigenvalues of (2.5) at E_{20d} are negative or have negative real parts whenever $R_{2d} < 1$. Therefore, we claim that E_{20d} is locally asymptotically stable if $R_{2d} < 1$.

Theorem 2.5. *The EE E_{21d} of model (2.5) is locally asymptotically stable if $R_{2d} > 1$.*

The same method as Theorem 2.3 can be used to prove Theorem 2.5, so we omit the proof here.

2.3. Existence of a sliding mode and its dynamics

Definition 2.1 ([23]). If $\langle n_d, f_{1d}\rangle > 0$ and $\langle n_d, f_{2d}\rangle < 0$ on $\Omega_d \subset M_d$, then Ω_d is the sliding region.

Types of regions on discontinuity surfaces are given in Appendix A.

The existence of a sliding mode is assured if $\langle n_d, f_{1d}\rangle > 0$ and $\langle n_d, f_{2d}\rangle < 0$. In this case, we have

$$\langle n_d, f_{1d}\rangle > 0 \quad \text{if } S_d > h_{1d} \equiv \frac{\mu_d + d_d}{\beta_d} \quad \text{and} \quad \langle n_d, f_{2d}\rangle < 0 \quad \text{if } S_d < h_{2d} \equiv \frac{\mu_d + d_d + c}{\beta_d}.$$

Note that we have $h_{1d} < h_{2d}$ whenever $c > 0$. So the sliding domain $\Omega_d \subset M_d$ is defined as follows:

$$\Omega_d = \left\{(S_d, I_d) \in M_d;\ \frac{\mu_d + d_d}{\beta_d} < S_d < \frac{\mu_d + d_d + c}{\beta_d}\right\} = \{(S_d, I_d) \in M_d;\ h_{1d} < S_d < h_{2d}\}.$$

Next, we find the sliding mode equations using Filippov convex method [33,34], which is demonstrated as follows:

$$\begin{aligned} &f_d = \alpha f_{1d} + (1-\alpha) f_{2d} \quad \text{where } f_d = \begin{pmatrix} S_d'(t) \\ I_d'(t) \end{pmatrix} \quad \text{and} \quad \alpha = \frac{\langle n_d, f_{2d}\rangle}{\langle n_d, f_{2d} - f_{1d}\rangle} \\ &\therefore f_d = \begin{pmatrix} S_d'(t) \\ I_d'(t) \end{pmatrix} = \begin{pmatrix} \Lambda_d - \beta_d S_d I_d - \mu_d S_d \\ 0 \end{pmatrix}. \end{aligned} \tag{2.6}$$

Since the sliding mode only exists on $\Omega_d \in M_d$ and there is no change of I_d with respect to time t, we can rewrite (2.6) on Ω_d in following manner.

$$S_d'(t) = \Lambda_d - \beta_d S_d I_T - \mu_d S_d. \tag{2.7}$$

The sliding equilibrium, $E_d = \left(\frac{\Lambda_d}{\beta_d I_T + \mu_d}, I_T\right)$, is a unique pseudoequilibrium (refer to Appendix B for further discussion of types of equilibrium points for a Filippov system) if

$$\frac{\mu_d + d_d}{\beta_d} < \frac{\Lambda_d}{\beta_d I_T + \mu_d} < \frac{\mu_d + d_d + c}{\beta_d}. \tag{2.8}$$

By manipulating (2.8), we infer that E_d lies on Ω_d if

$$h_{3d} \equiv \frac{\Lambda_d \beta_d - \mu_d(\mu_d + d_d + c)}{\beta_d(\mu_d + d_d + c)} < I_T < \frac{\Lambda_d \beta_d - \mu_d(\mu_d + d_d)}{\beta_d(\mu_d + d_d)} \equiv h_{4d}.$$

In conclusion, E_d is locally asymptotically stable on Ω_d since $\frac{\partial}{\partial S_d}(\Lambda_d - \beta_d S_d I_d - \mu_d S_d) = -\beta_d I_T - \mu_d < 0$ where $\mu_d, \beta_d, I_T > 0$; i.e., the eigenvalue of (2.7) is negative.

2.4. Global stability of the endemic equilibria

We divide $(S_d, I_d) \in \mathbb{R}^2_+$ into three regions, G_{1d}, M_d and G_{2d}. For each region, there exists equilibrium points, E_d, E_{11d} and E_{21d}, which are located in regions M_d, G_{1d} and G_{2d}, respectively. In this section, we represent E_d, E_{11d}, E_{21d} and the initial point in Figs. 2–6 by symbols ○, ●, × and ■, respectively. Next, the stability of equilibria E_d, E_{11d} and E_{21d} is discussed in the following subsections and some numerical simulations have been shown to depict the stability of the equilibrium point. All parameters are given in Table 1, unless otherwise stated.

2.4.1. Case 1: E_{11d} and E_{21d} are virtual equilibria if $h_{3d} < I_T < h_{4d}$

Let us denote the virtual equilibria E_{11d} and E_{21d} as E^V_{11d} and E^V_{21d}. These two equilibria are located in regions G_{2d} and G_{1d}, respectively. In this case, we claim that $E_d \in \Omega_d \subset M_d$ is globally asymptotically stable if $h_{3d} < I_T < h_{4d}$ in the following theorem. So if a limit cycle does not exist in model (2.1), then our claim is valid.

Table 1
Avian-only model (2.1) parameters.

Parameter	Description	Sample value	Units	Reference
Λ_d	Bird inflow	$\frac{2060}{365}$	Individuals per day	[35]
μ_d	Natural death of birds	$\frac{1}{2\times 365}$	per day	[36]
β_d	Rate at which birds contract avian influenza	0.4	per individual per day	[37]
d_d	Disease death rate due to avian influenza in birds	0.1	per day	[36]
c	Culling rate of infected birds	1.5	per day	Assumed

Theorem 2.6. *$E_d \in \Omega_d \subset M_d$ is globally asymptotically stable if $h_{3d} < I_T < h_{4d}$.*

Proof. Let $g_1 = \Lambda_d - \beta_d S_d I_d - \mu_d S_d$, $g_2 = \beta_d S_d I_d - (\mu_d + d_d) I_d$, $g_3 = \beta_d S_d I_d - (\mu_d + d_d + u_d c) I_d$ and $g_4 = \beta_d S_d I_d - (\mu_d + d_d + c) I_d$. Consider a Dulac function, $B(S_d, I_d) = \frac{1}{S_d I_d}$ for regions $I_d < I_T$ and $I_d > I_T$ where $I_T > 0$ and $(S_d, I_d) \in \mathbb{R}^2_+$.

For regions $I_d < I_T$ and $I_d > I_T$, we obtain

$$\begin{aligned}\frac{\partial(Bg_1)}{\partial S_d} + \frac{\partial(Bg_3)}{\partial I_d} &= \frac{\partial}{\partial S_d}\left(\frac{\Lambda_d}{S_d I_d} - \beta_d - \frac{\mu_d}{I_d}\right) + \frac{\partial}{\partial I_d}\left(\beta_d - \frac{\mu_d + d_d + u_d c}{S_d}\right)\\ &= -\frac{\Lambda_d}{S_d^2 I_d}\\ &< 0 \quad \forall (S_d, I_d) \in \mathbb{R}^2_+ \setminus M_d. \end{aligned} \tag{2.9}$$

We refer to [22], which has demonstrated that Dulac's theorem (see Theorem C.3 in Appendix C for more details) can be used to prove the non-existence of a limit cycle for a discontinuous dynamical system. In this case, the dynamical system (2.1) with (2.2) is discontinuous at the line $I_d = I_T$ and (2.9) is satisfied for $I_d \neq I_T$. In order to show the non-existence of limit cycle Γ that surrounds the sliding equilibrium E_d, we have to show that $\iint_{G_{id}} \left[\frac{\partial(Bg_1)}{\partial S_d} + \frac{\partial(Bg_3)}{\partial I_d}\right] dS_d dI_d < 0$ for $i = 1, 2$, by Green's Theorem. We would like to show this by contradiction. Assume that there exists a limit cycle Γ that passes through the discontinuous manifold M_d containing E_d and the sliding domain Ω_d in its interior. Suppose this limit cycle Γ has period T and direction as shown in Fig. 1. Let us denote the intersection points of Γ and M_d (i.e., the line $I_d = I_T$) as P and Q, the intersection points of Γ and the line $I_d = I_T - \delta$ as $P_1 = P + a_1(\delta)$ and $Q_1 = Q - a_2(\delta)$, and the intersection points of Γ and the line $I_d = I_T + \delta$ as $P_2 = P + b_1(\delta)$ and $Q_2 = Q - b_2(\delta)$ where $\delta > 0$ is sufficiently small. Moreover, we assume that $a_1(\delta)$, $a_2(\delta)$, $b_1(\delta)$ and $b_2(\delta)$ are continuous with respect to δ and $\lim_{\delta\to 0} a_i(\delta) = \lim_{\delta\to 0} b_i(\delta) = 0$ for $i = 1, 2$ are satisfied. The region G_{1d} is bounded by Γ_1 and segment P_1Q_1, whereas the region G_{2d} is bounded by Γ_2 and segment P_2Q_2. Furthermore, the nonlinear ordinary differential equations in region G_{1d} are denoted by g_1 and g_2. Let ∂G_{1d} denote the boundary of G_{1d}. By Green's Theorem, we obtain the following:

$$\begin{aligned}\iint_{G_{1d}}\left[\frac{\partial(Bg_1)}{\partial S_d} + \frac{\partial(Bg_2)}{\partial I_d}\right] dS_d dI_d &= \iint_{G_{1d}} \frac{\partial(Bg_1)}{\partial S_d} dS_d dI_d + \iint_{G_{1d}} \frac{\partial(Bg_2)}{\partial I_d} dS_d dI_d\\ &= \oint_{\partial G_{1d}} (Bg_1) dI_d - \oint_{\partial G_{1d}} (Bg_2) dS_d\\ &= \int_{\Gamma_1} Bg_1 dI_d + \int_{\overrightarrow{Q_1P_1}} Bg_1 dI_d - \left(\int_{\Gamma_1} Bg_2 dS_d + \int_{\overrightarrow{Q_1P_1}} Bg_2 dS_d\right)\\ &= \int_{\Gamma_1} \left(Bg_1 \cdot g_2 - Bg_2 \cdot g_1\right) dt - \int_{\overrightarrow{Q_1P_1}} Bg_2 dS_d\\ &= -\int_{\overrightarrow{Q_1P_1}} Bg_2 dS_d \end{aligned} \tag{2.10}$$

where $\frac{dS_d}{dt} = g_1 \Longrightarrow dS_d = g_1 dt$, $\frac{dI_d}{dt} = g_2 \Longrightarrow dI_d = g_2 dt$ and there are no changes of I_d in the segment $P_1Q_1 \Longrightarrow \int_{\overrightarrow{Q_1P_1}} Bg_1 dI_d = \int_{I_T-\delta}^{I_T-\delta} Bg_1 dI_d = 0$.

Similarly, in G_{2d} the dynamical system is represented by g_1 and g_4. By Green's Theorem, we have

$$\iint_{G_{2d}}\left[\frac{\partial(Bg_1)}{\partial S_d} + \frac{\partial(Bg_4)}{\partial I_d}\right] dS_d dI_d = -\int_{\overrightarrow{P_2Q_2}} Bg_4 dS_d. \tag{2.11}$$

Suppose $G_{20} \subset G_{2d}$. Let $\zeta = \iint_{G_{20}} \left[\frac{\partial(Bg_1)}{\partial S_d} + \frac{\partial(Bg_4)}{\partial I_d}\right] dS_d dI_d = \oint_{\partial G_{20}} \left(Bg_1 dI_d - Bg_4 dS_d\right) < 0$ from (2.9). Thus we have

$$0 > \zeta > -\left(\int_{\overrightarrow{Q_1P_1}} Bg_2 dS_d + \int_{\overrightarrow{P_2Q_2}} Bg_4 dS_d\right). \tag{2.12}$$

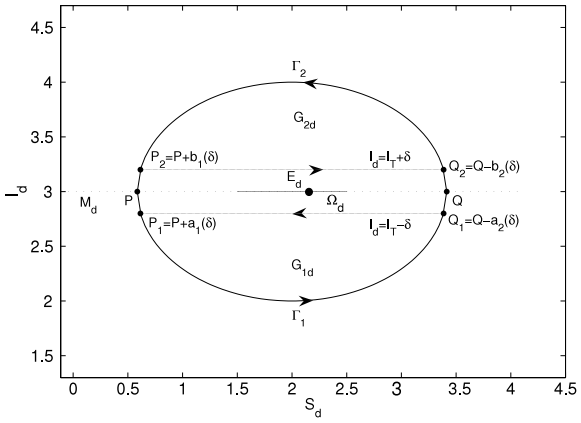

Fig. 1. Limit cycle Γ.

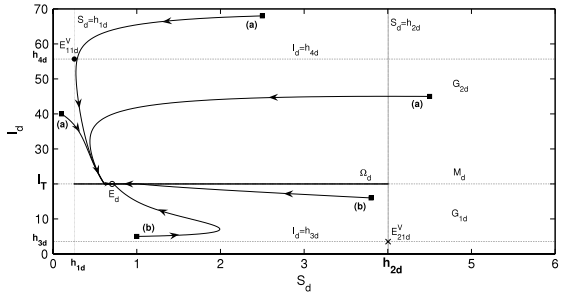

Fig. 2. $E_d \in \Omega_d \subset M_d$ is globally asymptotically stable if $h_{3d} < I_T < h_{4d}$.

Moreover, by taking the limit $\delta \to 0$ of the addition of (2.10) and (2.11), we obtain

$$\begin{aligned}
&\lim_{\delta\to 0}\left(-\int_{\overrightarrow{Q_1P_1}} Bg_2 dS_d - \int_{\overrightarrow{P_2Q_2}} Bg_4 dS_d\right)\\
&= \lim_{\delta\to 0}\left[\int_{P+a_1(\delta)}^{Q-a_2(\delta)}\left(\beta_d - \frac{\mu_d + d_d}{S_d}\right)dS_d - \int_{P+b_1(\delta)}^{Q-b_2(\delta)}\left(\beta_d - \frac{\mu_d + d_d + c}{S_d}\right)dS_d\right]\\
&= \left[\beta_d S_d - (\mu_d + d_d)\ln S_d\right]_P^Q - \left[\beta_d S_d - (\mu_d + d_d + c)\ln S_d\right]_P^Q\\
&= c(\ln Q - \ln P) > 0
\end{aligned}$$

since $Q > P$, which contradicts (2.12). Thus there are no limit cycles surrounding the sliding domain Ω_d and the sliding equilibrium E_d. Hence $E_d \in \Omega_d \subset M_d$ is globally asymptotically stable if $h_{3d} < I_T < h_{4d}$. ■

Fig. 2 shows that all the trajectories with arbitrary initial conditions in $\mathbb{R}^2_+$ will converge to $E_d \in \Omega_d \subset M_d$ if $h_{3d} < I_T < h_{4d}$, as per Theorem 2.6. We pick $I_T = 20$ in this figure. Trajectories denoted by (a) will hit and slide to the right of Ω_d before converging to E_d. Meanwhile, trajectories (b) will hit and slide to the left of Ω_d and then move towards E_d.

Since $\frac{\Lambda_d}{\mu_d}$ (from Table 1) is large, it is unlikely we can show clearly that Case 1 will remain in the positively invariant and attracting region, $D_d = \left\{(S_d, I_d) \in \mathbb{R}^2_+ ; I_d + S_d \le \frac{\Lambda_d}{\mu_d}\right\}$, as $t \to \infty$. For this reason, we increase μ_d to 0.3 in Fig. 3 to depict the convergence of solutions of Case 1 in region D_d and define $I_T = 8$. From Fig. 3, we found that the possible trajectories for this case are

(a) a trajectory that hits Ω_d from the region G_{1d} slides to the left of Ω_d and moves towards E_d.
(b) a trajectory with initial point located either inside or outside the attraction region D_d will cross M_d from G_{1d} to G_{2d}. Then the trajectory hits and slides to the left of Ω_d before converging to E_d.
(c) a trajectory with initial point located in G_{2d} either inside or outside of the attraction region D_d will hit and slide to the right of Ω_d before moving towards E_d.

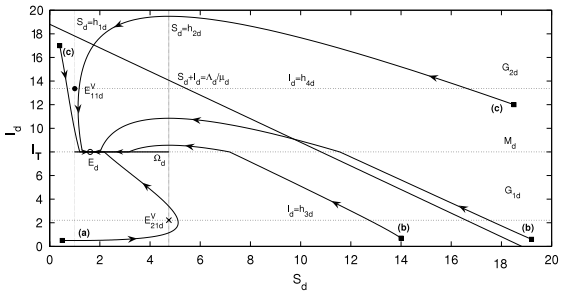

Fig. 3. All trajectories move towards $E_d \in \Omega_d \subset M_d$ in the positively invariant and attracting region $D_d = \left\{(S_d, I_d) \in \mathbb{R}^2_+; I_d + S_d \leq \frac{\Lambda_d}{\mu_d}\right\}$ if $h_{3d} < I_T < h_{4d}$ is fulfilled.

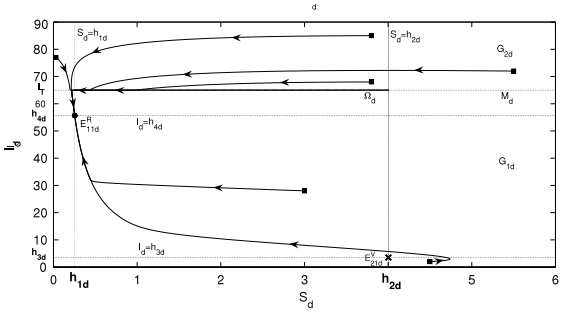

Fig. 4. $E^R_{11d} \in G_{1d}$ is globally asymptotically stable if $I_T > h_{4d}$.

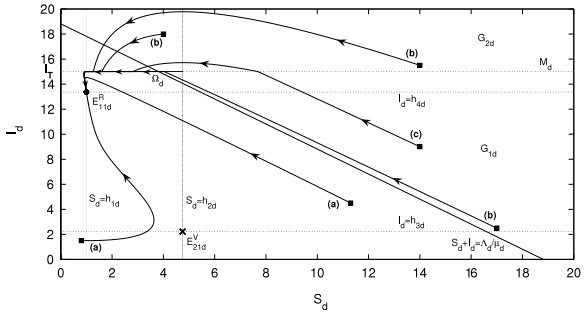

Fig. 5. All solutions of Case 2, where $I_T > h_{4d}$, will approach $E^R_{11d} \in G_{1d}$ in region $D_d = \left\{(S_d, I_d) \in \mathbb{R}^2_+; I_d + S_d \leq \frac{\Lambda_d}{\mu_d}\right\}$ as $t \to \infty$.

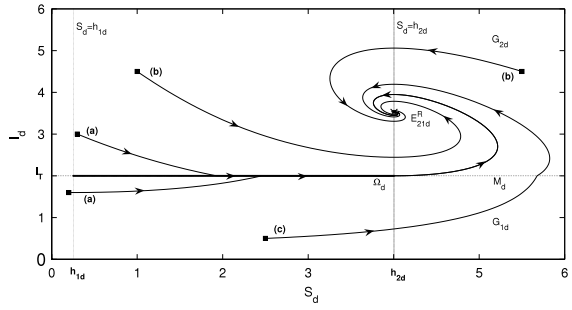

Fig. 6. $E^R_{21d} \in G_{2d}$ is globally asymptotically stable if $I_T < h_{3d}$.

2.4.2. Case 2: E_{11d} is a real equilibrium, whereas E_{21d} is a virtual equilibrium if $I_T > h_{4d}$

Let us denote E^R_{11d} as a real equilibrium and E^V_{21d} as a virtual equilibrium. Both of these equilibria are located in region G_{1d} and there is no equilibrium lying in region G_{2d}. Further, we claim that E^R_{11d} achieves global asymptotic stability if $I_T > h_{4d}$. In order to show the global behavior of E^R_{11d} in this case, we would like to consider the following Lyapunov functions for model (2.1), which have given rise to Theorem 2.7:

$$V_1 = V_1(S_d, I_d) = S_d - \frac{\mu_d + d_d}{\beta_d} - \frac{\mu_d + d_d}{\beta_d} \ln\left(\frac{\beta_d S_d}{\mu_d + d_d}\right) + I_d - \frac{\Lambda_d\beta_d - \mu_d(\mu_d + d_d)}{\beta_d(\mu_d + d_d)} - \frac{\Lambda_d\beta_d - \mu_d(\mu_d + d_d)}{\beta_d(\mu_d + d_d)} \ln\left[\frac{\beta_d(\mu_d + d_d)I_d}{\Lambda_d\beta_d - \mu_d(\mu_d + d_d)}\right]$$

and

$$V_2 = V_2(S_d, I_d) = S_d - \frac{\mu_d + d_d + c}{\beta_d} - \frac{\mu_d + d_d + c}{\beta_d} \ln\left(\frac{\beta_d S_d}{\mu_d + d_d + c}\right) + I_d - \frac{\Lambda_d\beta_d - \mu_d(\mu_d + d_d + c)}{\beta_d(\mu_d + d_d + c)} - \frac{\Lambda_d\beta_d - \mu_d(\mu_d + d_d + c)}{\beta_d(\mu_d + d_d + c)} \ln\left[\frac{\beta_d(\mu_d + d_d + c)I_d}{\Lambda_d\beta_d - \mu_d(\mu_d + d_d + c)}\right]. \tag{2.13}$$

Theorem 2.7. *The function*

$$V(S_d, I_d) = \begin{cases} V_1(S_d, I_d); & I_d < I_T \\ V_1(S_d, I_T) + V_2(S_d, I_d) - V_2(S_d, I_T); & I_d = I_T \text{ and } S_d \le \dfrac{\mu_d + d_d}{\beta_d} \\ V_1(S_d, I_T); & I_d = I_T \text{ and } S_d > \dfrac{\mu_d + d_d}{\beta_d} \\ V_1(S_d, I_d); & I_d > I_T \end{cases} \tag{2.14}$$

is a Lyapunov function on $\mathbb{R}^2_+$ for (2.1) and $\{E^R_{11d}\}$ is globally asymptotically stable if $I_T > h_{4d}$.

Proof. If $I_T > h_{4d}$, it follows that $\Lambda_d\beta_d < \beta_d(\mu_d + d_d)I_T + \mu_d(\mu_d + d_d) \Leftrightarrow \Lambda_d\beta_d < (\mu_d + d_d)(\beta_d I_T + \mu_d)$.

(a) We want to show that if $(S_d, I_d) \in G_{1d} := \{(S_d, I_d) \in \mathbb{R}^2_+; I_d < I_T\}$, then $\langle \nabla V, f_{1d}\rangle \le 0$.

In this particular case, we have the fact that $V_1(S_d, I_d) > 0 \forall (S_d, I_d) \in G_{1d}$ and $V_1(E^R_{11d}) = 0$. Then

$$\begin{aligned} \langle \nabla V, f_{1d}\rangle &= \langle \nabla V_1, f_{1d}\rangle \\ &= \frac{[\beta_d S_d - (\mu_d + d_d)][\Lambda_d - S_d(\beta_d I_d + \mu_d)]}{\beta_d S_d} + \frac{[(\mu_d + d_d)(\beta_d I_d + \mu_d) - \Lambda_d\beta_d][\beta_d S_d - (\mu_d + d_d)]}{\beta_d(\mu_d + d_d)} \\ &= \frac{-\Lambda_d[\beta_d S_d - (\mu_d + d_d)]^2}{\beta_d S_d(\mu_d + d_d)} \\ &\le 0 \quad \forall (S_d, I_d) \in G_{1d} \end{aligned}$$

where $\langle \nabla V, f_{1d}\rangle = 0$ when $S_d = \frac{\mu_d + d_d}{\beta_d}$. Otherwise, $\langle \nabla V, f_{1d}\rangle < 0$.

(b) We claim that if $(S_d, I_d) \in \left\{(S_d, I_d) \in M_d; S_d \le \frac{\mu_d + d_d}{\beta_d}\right\}$ is satisfied, then we obtain $\sup_{0\le\alpha\le1}\langle \nabla V, \alpha f_{1d} + (1-\alpha) f_{2d}\rangle = 0$.

For $I_d = I_T$ and $S_d \le \frac{\mu_d + d_d}{\beta_d}$, we have $V_1(S_d, I_T) + V_2(S_d, I_d) - V_2(S_d, I_T) > 0$. We find that, when $I_d = I_T$,

$$\langle \nabla V, f_{1d}\rangle = \frac{\Lambda_d[\beta_d S_d - (\mu_d + d_d)][(\mu_d + d_d + c) - \beta_d S_d]}{\beta_d S_d(\mu_d + d_d + c)} \le 0$$

where, for all $S_d \le \frac{\mu_d + d_d}{\beta_d}$, we have $\beta_d S_d - (\mu_d + d_d) \le 0$ and $(\mu_d + d_d + c) - \beta_d S_d > 0$. It follows that $\langle \nabla V, f_{1d}\rangle = 0$ when $S_d = \frac{\mu_d + d_d}{\beta_d}$. Otherwise, $\langle \nabla V, f_{1d}\rangle < 0$.

Again, we compute

$$\begin{aligned}
\langle \nabla V, f_{2d}\rangle &= \frac{[\beta_d S_d - (\mu_d + d_d)]\,[\Lambda_d - S_d(\beta_d I_d + \mu_d)]}{\beta_d S_d} \\
&\quad + \frac{[(\mu_d + d_d + c)(\beta_d I_d + \mu_d) - \Lambda_d \beta_d]\,[\beta_d S_d - (\mu_d + d_d + c)]}{\beta_d(\mu_d + d_d + c)} \\
&< \frac{(\mu_d + d_d + c)\,[\beta_d S_d - (\mu_d + d_d)]\,[\Lambda_d - S_d(\beta_d I_T + \mu_d)]}{\beta_d S_d(\mu_d + d_d + c)} \\
&\quad + \frac{S_d\,[(\mu_d + d_d + c)(\beta_d I_T + \mu_d) - \Lambda_d \beta_d]\,[\beta_d S_d - (\mu_d + d_d)]}{\beta_d S_d(\mu_d + d_d + c)} \\
&\quad \text{where } I_d = I_T,\ (\mu_d + d_d + c)(\beta_d I_T + \mu_d) - \Lambda_d \beta_d > 0 \text{ and} \\
&\quad \times [(\mu_d + d_d + c)(\beta_d I_T + \mu_d) - \Lambda_d \beta_d]\,[\beta_d S_d - (\mu_d + d_d + c)] \\
&< [(\mu_d + d_d + c)(\beta_d I_T + \mu_d) - \Lambda_d \beta_d]\,[\beta_d S_d - (\mu_d + d_d)] \\
&= \frac{\Lambda_d\,[\beta_d S_d - (\mu_d + d_d)]\,[(\mu_d + d_d + c) - \beta_d S_d]}{\beta_d S_d(\mu_d + d_d + c)} \\
&\leq 0 \quad \forall S_d \leq \frac{\mu_d + d_d}{\beta_d}
\end{aligned}$$

where $\beta_d S_d - (\mu_d + d_d) \leq 0$, $(\mu_d + d_d + c) - \beta_d S_d > 0\ \forall S_d \leq \frac{\mu_d + d_d}{\beta_d}$ and $\langle \nabla V, f_{2d}\rangle = 0$ when $S_d = \frac{\mu_d + d_d}{\beta_d}$.

Hence $\sup_{0\leq\alpha\leq 1} \langle \nabla V, \alpha f_{1d} + (1-\alpha) f_{2d}\rangle = 0$.

(c) We claim that, under the condition of $(S_d, I_d) \in \left\{(S_d, I_d) \in M_d;\ S_d > \frac{\mu_d + d_d}{\beta_d}\right\}$, we have $\sup_{0\leq\alpha\leq 1}\langle \nabla V, \alpha f_{1d} + (1-\alpha) f_{2d}\rangle < 0$.

For $I_d = I_T$ and $S_d > \frac{\mu_d + d_d}{\beta_d}$, we obtain $V_1(S_d, I_T) > 0$. Next,

$$\begin{aligned}
\langle \nabla V, f_{1d}\rangle &= \langle \nabla V, f_{2d}\rangle \\
&= \frac{[\beta_d S_d - (\mu_d + d_d)][\Lambda_d - S_d(\beta_d I_T + \mu_d)]}{\beta_d S_d} \quad \text{where } I_d = I_T \\
&< \frac{[\beta_d S_d - (\mu_d + d_d)]\left(\Lambda_d - \frac{\Lambda_d \beta_d S_d}{\mu_d + d_d}\right)}{\beta_d S_d} \quad \text{where } -(\beta_d I_T + \mu_d) < -\frac{\Lambda_d \beta_d}{\mu_d + d_d} \\
&= \frac{-\Lambda_d[\beta_d S_d - (\mu_d + d_d)]^2}{\beta_d S_d(\mu_d + d_d)} \\
&< 0 \quad \forall S_d > \frac{\mu_d + d_d}{\beta_d}.
\end{aligned}$$

Hence, $\sup_{0\leq\alpha\leq 1} \langle \nabla V, \alpha f_{1d} + (1-\alpha) f_{2d}\rangle < 0$.

(d) We want to show that, whenever the condition $(S_d, I_d) \in G_{2d} := \{(S_d, I_d) \in \mathbb{R}^2_+;\ I_d > I_T\}$ is satisfied, we obtain $\langle \nabla V, f_{2d}\rangle < 0$.

For $I_d > I_T$, it follows that $V_1(S_d, I_d) > 0$. Next,

$$\begin{aligned}
\langle \nabla V, f_{2d}\rangle &= \langle \nabla V_1, f_{2d}\rangle \\
&= \frac{-\Lambda_d\,[\beta_d S_d - (\mu_d + d_d)]^2 - cS_d\,[(\mu_d + d_d)(\mu_d + \beta_d I_d) - \Lambda_d \beta_d]}{\beta_d S_d(\mu_d + d_d)} \\
&< \frac{-\Lambda_d\,[\beta_d S_d - (\mu_d + d_d)]^2 - cS_d\,[(\mu_d + d_d)(\mu_d + \beta_d I_T) - \Lambda_d \beta_d]}{\beta_d S_d(\mu_d + d_d)} \\
&< 0 \quad \forall (S_d, I_d) \in G_{2d}
\end{aligned}$$

since $-cS_d\,[(\mu_d + d_d)(\mu_d + \beta_d I_d) - \Lambda_d \beta_d] < -cS_d\,[(\mu_d + d_d)(\mu_d + \beta_d I_T) - \Lambda_d \beta_d]$ and $(\mu_d + d_d)(\mu_d + \beta_d I_T) - \Lambda_d \beta_d > 0$.

We obtain $\dot{V}^* \equiv \max_{\eta \in f_{id}(S_d, I_d)} \langle \nabla V, \eta\rangle \leq 0\ \forall (S_d, I_d) \in \mathbb{R}^2_+$ and with equality only if $S_d = \frac{\mu_d + d_d}{\beta_d}$ where $i = 1, 2$ and

$$f_{id}(S_d, I_d) := \begin{cases} f_{1d}; & (S_d, I_d) \in G_{1d} \\ \alpha f_{1d} + (1-\alpha) f_{2d}; & (S_d, I_d) \in M_d \text{ where } \alpha \in [0, 1] \\ f_{2d}; & (S_d, I_d) \in G_{2d}. \end{cases}$$

Thus $V(S_d, I_d)$ is a Lyapunov function on D_d and, by Lemma 2.1, D_d is compact. Let $\Sigma_{1d} := \{(S_d, I_d) \in \mathbb{R}^2_+;\ \dot{V}^* = 0\} = G_{1d} \bigcup \left(\frac{\mu_d + d_d}{\beta_d}, I_T\right)$. So the largest positively invariant subset of $\overline{\Sigma}_{1d}$ is $\{E^R_{11d}\}$. Hence, by LaSalle's Invariance Principle and

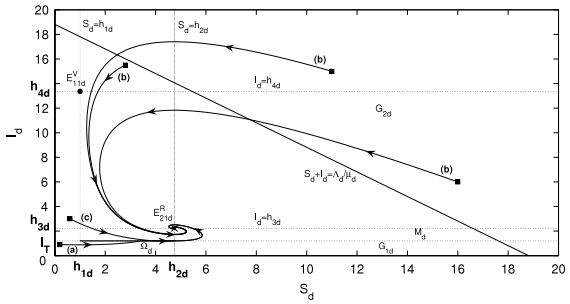

Fig. 7. All trajectories will remain in region $D_d = \left\{(S_d, I_d) \in \mathbb{R}^2_+; I_d + S_d \leq \frac{\Lambda_d}{\mu_d}\right\}$ and converge to $E^R_{21d} \in G_{2d}$ as $t \to \infty$ if $I_T < h_{3d}$ is satisfied.

Corollary C.2 (see Appendix C), every solution of (2.1) with initial conditions in $\mathbb{R}^2_+$ will approach E^R_{11d} as $t \to \infty$ if $I_T > h_{4d}$. Therefore E^R_{11d} is globally asymptotically stable if $I_T > h_{4d}$. ■

Fig. 4 describes the possible trajectories for Case 2 with $I_T = 65$. The solutions for Case 2 with initial points in G_{1d} will move to E^R_{11d} in G_{1d}, whereas trajectories with initial conditions in G_{2d} will either converge to E^R_{11d} after crossing M_d or hit and slide to the left of Ω_d before moving towards E^R_{11d}.

By applying the same reasoning as in Case 1, we choose $\mu_d = 0.3$ and $I_T = 15$ in Fig. 5. The possible trajectories, which are illustrated in Fig. 5, are as follows:

(a) a trajectory with initial point located in G_{1d} within D_d will converge directly to E^R_{11d}.
(b) a trajectory with initial point located either in G_{1d} or G_{2d} and outside the attracting region D_d will hit and slide to the left of Ω_d before moving towards E^R_{11d} in region G_{1d}.
(c) a trajectory that begins in region G_{1d} outside the attracting region D_d will cross the discontinuous surface M_d. Then it will hit and slide to the left of Ω_d before converging to E^R_{11d} in G_{1d}.

2.4.3. Case 3: E_{21d} is a real equilibrium, whereas E_{11d} is a virtual equilibrium if $I_T < h_{3d}$

Let us denote E^R_{21d} as a real equilibrium and E^V_{11d} as a virtual equilibrium. Both of these equilibria are located in region G_{2d}, and there is no equilibrium lying in region G_{1d}. Further, we claim that E^R_{21d} achieves global asymptotic stability if $I_T < h_{3d}$. In order to show the global behavior of E^R_{21d}, we consider the Lyapunov function $V_2(S_d, I_d)$ (2.13) for model (2.1) and the construction of Theorem 2.8.

Theorem 2.8. *The function $V_2(S_d, I_d)$ (2.13) is a Lyapunov function on $\mathbb{R}^2_+$ for (2.1) and $\{E^R_{21d}\}$ is globally asymptotically stable if $I_T < h_{3d}$.*

The proof of Theorem 2.8 is similar to that of Theorem 2.7.

We depict Theorem 2.8 numerically in Fig. 6. It is clearly shown that every solution of Case 3 will approach E^R_{21d} as $t \to \infty$ with arbitrary initial conditions in $\mathbb{R}^2_+$. Trajectories, which are depicted in Fig. 6, are

(a) a trajectory that starts in region G_{1d} or G_{2d} will hit and slide to the right of Ω_d before moving towards E^R_{21d}.
(b) a trajectory with initial condition in G_{2d} will approach E^R_{21d} as $t \to \infty$.
(c) a trajectory with initial point in G_{1d} may pass through M_d and then proceed towards E^R_{21d} in region G_{2d}.

We increase the parameter μ_d to 0.3 in Fig. 7 to show that the numerical solutions of Case 3 remain in region D_d and converge to E^R_{21d} as $t \to \infty$. In this simulation, we select $I_T = 1.2$. From Fig. 7, we can see that

(a) a trajectory with initial point located in G_{1d} within D_d will hit and slide to the right of $\Omega_d \subset M_d$ before moving towards E^R_{21d} in region G_{2d}.
(b) a trajectory with initial point located in G_{2d} and either within or outside of the attraction region D_d will approach to E^R_{21d} directly.
(c) a trajectory that begins from G_{2d} might hit $\Omega_d \subset M_d$ and slide to the right before moving towards E^R_{21d}.

For Fig. 8, we set $\Lambda_d = 100$, $\mu_d = 0.3$, $\beta_d = 0.01$, $d_d = 0.05$, $c = 0.5$ and $I_T = 50$. We observe that all trajectories with arbitrary initial conditions converge to E^R_{21d}, which agrees with the theoretical result shown in Theorem 2.8.

In conclusion, the solutions of model (2.1) will converge to either one of the two endemic equilibria (i.e., either E^R_{11d} in G_{1d} or E^R_{21d} in G_{2d}) or the sliding equilibrium E_d on sliding domain $\Omega_d \subset M_d$ if the requirement of (2.8) is met. We do not have to apply any control methods whenever $h_{3d} < I_T < h_{4d}$ (Case 1) or $I_T > h_{4d}$ (Case 2) is satisfied. This is due to the number of infected birds, which always remain below the given threshold level I_T since we have proclaimed that the infection is tolerable. Therefore, in this particular case, the trajectory of model (2.1) either converges to E^R_{11d} in G_{1d} or stabilizes at E_d

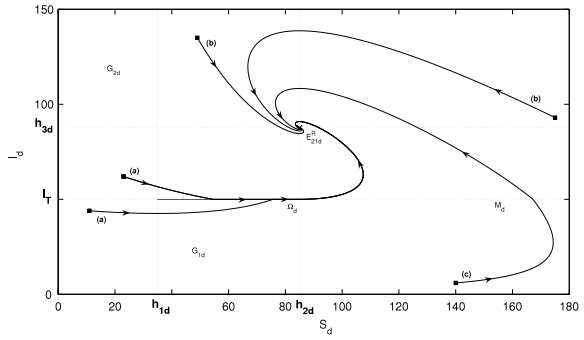

Fig. 8. $E^R_{21d} \in G_{2d}$ achieves global asymptotic stability whenever $I_T < h_{3d}$.

on $\Omega_d \subset M_d$. However, the solution of (2.1) converges to E^R_{21d} in G_{2d} if $I_T < h_{3d}$ (Case 3). For this case, the application of control methods will be triggered as the number of infected birds reaches the critical level (i.e., greater than the tolerance threshold level I_T), beyond which we proclaim that an outbreak will occur. In order to inhibit the occurrence of an outbreak or stabilize the infection at a satisfactory level, by virtue of Theorem 2.6, we need a proper combination of control intensity and tolerance level. Hence, in order to combat an outbreak effectively, we require a well-defined threshold policy.

3. The SIIR model with quarantine as a control measure

When six people were reported dead and 18 people infected by H5N1 in Hong Kong in 1997, it changed the general belief that avian influenza viruses were believed to be non-infectious to humans. Most avian influenza viruses do not spread to humans; however, H5N1, H7N2, H7N3, H7N7 and H7N9 are known to cause severe infections in humans [26,38,39]. Avian influenza viruses transmit easily to humans through direct contact with dead or infected birds. However, there are some reported cases that humans might be infected by the lethal virus indirectly via contaminated water, food that has been stained by the virus or other objects contaminated with infected birds' feces [26,40].

There are many types of control methods that have been employed to reduce the infection rate of avian influenza, such as practicing personal protection, isolation, prescription of antiviral drugs and vaccination [18,14,15]. So in this section, we would like to consider a Filippov SIIR avian influenza model incorporating quarantine as a control measure. This model consists of susceptibles (S), humans infected with avian strain (I_a), humans infected with mutant strain (I_m) and humans who have recovered from avian and mutant strains (R). Here, we assume that when the total number of infected humans, $I_a + I_m$, is greater than some threshold level I_c, infected humans with either avian or mutant strain will be isolated from susceptibles. In other words, quarantine will be implemented in order to control the spread of the disease and the quarantined individuals will not return to the susceptible population; that is, the immunity was permanent. However, if the total number of infected humans is below the tolerance threshold I_c, then quarantine is not required. The SIIR model equations can be expressed as:

$$\begin{aligned} S'(t) &= \Lambda - \beta_a(1-qu)SI_a - \beta_m(1-qu)SI_m - \mu S \\ I_a'(t) &= \beta_a(1-qu)SI_a - (\mu + d + \gamma + \epsilon)I_a \\ I_m'(t) &= \beta_m(1-qu)SI_m + \epsilon I_a - (\mu + d + \gamma)I_m \\ R'(t) &= \gamma(I_a + I_m) - \mu R \end{aligned} \tag{3.1}$$

with

$$u = \begin{cases} 0 & \text{for } I_a + I_m < I_c \Leftrightarrow \sigma(I_a, I_m) = I_a + I_m - I_c < 0 \\ 1 & \text{for } I_a + I_m > I_c \Leftrightarrow \sigma(I_a, I_m) = I_a + I_m - I_c > 0, \end{cases} \tag{3.2}$$

where q is the quarantine rate and $I_c > 0$ is the critical threshold of the total number of infected humans. Table 2 shows the descriptions of the associated parameters in model (3.1) and sample values.

Since R decouples from the remaining equations in model (3.1), we consider only the first three equations of model (3.1) with (3.2). It should be noted that R always preserves local stability; i.e., the associated eigenvalue is $\lambda = -\mu < 0$ where $\mu > 0$. We further assume that $\beta_a > \beta_m$ [37]. Furthermore, we define

$$\begin{aligned} G_1 &:= \{(S, I_a, I_m) \in \mathbb{R}^3_+ ; I_a + I_m < I_c\} \\ G_2 &:= \{(S, I_a, I_m) \in \mathbb{R}^3_+ ; I_a + I_m > I_c\} \\ M &:= \{(S, I_a, I_m) \in \mathbb{R}^3_+ ; I_a + I_m = I_c\}. \end{aligned}$$

Table 2
Descriptions of the associated parameters in SIIR model (3.1) and sample values.

Parameter	Description	Sample value	Units	Reference
Λ	Human recruitment rate	$\frac{1000}{365}$	Individuals per day	[36]
μ	Natural mortality rate of humans	$\frac{1}{65\times365}$	per day	[36]
β_a	Transmission rate of human-to-human with avian strain	0.4	per individual per day	[37]
β_m	Transmission rate of human-to-human with mutant strain	$0.3\times\beta_a$	per individual per day	[37]
d	Additional disease death rate of humans due to avian influenza	0.15	per day	[36]
γ	Recovery rate of humans with avian influenza	0.2669	per day	[41]
ϵ	Mutation rate	0.01	per day	[37]
q	Quarantine rate	0.6	Assumed	

The manifold M is a discontinuous surface and it divides $\mathbb{R}^3_+$ into two regions, G_1 and G_2. We denote the normal vector that is perpendicular to M as $n = (0, 1, 1)^T$ and all the right-hand sides of (3.1) in region G_i by f_i for $i = 1, 2$. The dynamical systems in regions G_1 and G_2 are thus represented by

$$\begin{aligned} f_1 &= f_1(S, I_a, I_m) = \begin{pmatrix} \Lambda - \beta_a S I_a - \beta_m S I_m - \mu S \\ \beta_a S I_a - (\mu + d + \gamma + \epsilon) I_a \\ \beta_m S I_m + \epsilon I_a - (\mu + d + \gamma) I_m \end{pmatrix} \\ f_2 &= f_2(S, I_a, I_m) = \begin{pmatrix} \Lambda - (1-q)\beta_a S I_a - (1-q)\beta_m S I_m - \mu S \\ (1-q)\beta_a S I_a - (\mu + d + \gamma + \epsilon) I_a \\ (1-q)\beta_m S I_m + \epsilon I_a - (\mu + d + \gamma) I_m \end{pmatrix}. \end{aligned} \tag{3.3}$$

Lemma 3.1. *The set* $D = \left\{(S, I_a, I_m, R) \in \mathbb{R}^4_+ ; N = S + I_a + I_m + R \le \frac{\Lambda}{\mu}\right\}$ *is a positively invariant and attracting region for* (3.1) *with any initial conditions in* $\mathbb{R}^4_+$.

We can use a similar method as shown in Lemma 2.1 to prove Lemma 3.1; hence we omit the proof of this lemma.

Since D is a positively invariant and attracting region for model (3.1), the solution of (3.1) exists in $D\ \forall t > 0$ and model (3.1) is mathematically and epidemiologically well-posed in D [30]. Thus it is sufficient to consider the dynamics of this model in D.

3.1. Analysis in region G_1

The dynamical systems in region G_1 can be described by the following nonlinear ordinary differential equations.

$$\begin{pmatrix} S'(t) \\ I_a'(t) \\ I_m'(t) \end{pmatrix} = \begin{pmatrix} \Lambda - \beta_a S I_a - \beta_m S I_m - \mu S \\ \beta_a S I_a - (\mu + d + \gamma + \epsilon) I_a \\ \beta_m S I_m + \epsilon I_a - (\mu + d + \gamma) I_m \end{pmatrix} := f_1. \tag{3.4}$$

There are two equilibria in G_1, the DFE $E_{10} = (S, I_a, I_m) = \left(\frac{\Lambda}{\mu}, 0, 0\right)$ and a unique positive EE

$$E_{11} = (E_{11}S, E_{11}I_a, E_{11}I_m)$$

where

$$\begin{aligned} E_{11}S &= \frac{\mu + d + \gamma + \epsilon}{\beta_a} \\ E_{11}I_m &= \frac{\epsilon\left[\Lambda\beta_a - \mu(\mu + d + \gamma + \epsilon)\right]}{(\beta_a - \beta_m)(\mu + d + \gamma)(\mu + d + \gamma + \epsilon)} \\ E_{11}I_a &= \frac{\left[\Lambda\beta_a - \mu(\mu + d + \gamma + \epsilon)\right]\left[(\mu + d + \gamma)(\beta_a - \beta_m) - \epsilon\beta_m\right]}{\beta_a(\beta_a - \beta_m)(\mu + d + \gamma)(\mu + d + \gamma + \epsilon)} \\ &= \frac{\left[(\mu + d + \gamma)(\beta_a - \beta_m) - \epsilon\beta_m\right]E_{11}I_m}{\epsilon\beta_a}. \end{aligned}$$

In $G_1 := \left\{(S, I_a, I_m) \in \mathbb{R}^3_+ ; I_m < -I_a + I_c\right\}$, we have $E_{11} \in \mathbb{R}^3_+$, and this implies that

$$\begin{aligned} E_{11}S &= \frac{\mu + d + \gamma + \epsilon}{\beta_a} > 0 \\ E_{11}I_m &= \frac{\epsilon\left[\Lambda\beta_a - \mu(\mu + d + \gamma + \epsilon)\right]}{(\beta_a - \beta_m)(\mu + d + \gamma)(\mu + d + \gamma + \epsilon)} > 0, \end{aligned} \tag{3.5}$$

which implies $\Lambda\beta_a - \mu(\mu + d + \gamma + \epsilon) > 0$ since $\beta_a > \beta_m$ and

$$E_{11}I_a = \frac{[(\mu + d + \gamma)(\beta_a - \beta_m) - \epsilon\beta_m]E_{11}I_m}{\epsilon\beta_a} > 0, \tag{3.6}$$

which implies $(\mu + d + \gamma)\beta_a - (\mu + d + \gamma + \epsilon)\beta_m > 0$ since $\beta_a > \beta_m$ and $E_{11}I_m > 0$.

The transmission matrix F_1 and transition matrix V_1 of model (3.4) are defined as

$$F_1 = \begin{pmatrix} \beta_a S & 0 \\ 0 & \beta_m S \end{pmatrix} \quad \text{and} \quad V_1 = \begin{pmatrix} \mu + d + \gamma + \epsilon & 0 \\ -\epsilon & \mu + d + \gamma \end{pmatrix}, \quad \text{respectively.}$$

At the DFE, we have

$$F_1V_1^{-1} = \begin{pmatrix} \dfrac{\Lambda\beta_a}{\mu(\mu + d + \gamma + \epsilon)} & 0 \\ \dfrac{\Lambda\beta_m\epsilon}{\mu(\mu + d + \gamma)(\mu + d + \gamma + \epsilon)} & \dfrac{\Lambda\beta_m}{\mu(\mu + d + \gamma)} \end{pmatrix}$$

and the basic reproduction number (see [31,32] for more details) of G_1 is given as follows:

$$R_1 := \max\left\{\frac{\Lambda\beta_a}{\mu(\mu + d + \gamma + \epsilon)}, \frac{\Lambda\beta_m}{\mu(\mu + d + \gamma)}\right\} = \max\{R_{1a}, R_{1m}\}$$

where $R_{1a} = \frac{\Lambda\beta_a}{\mu(\mu+d+\gamma+\epsilon)}$ and $R_{1m} = \frac{\Lambda\beta_m}{\mu(\mu+d+\gamma)}$.

The Jacobian matrix of model (3.4) is

$$J_1(S, I_a, I_m) = \begin{pmatrix} -\beta_a I_a - \beta_m I_m - \mu & -\beta_a S & -\beta_m S \\ \beta_a I_a & \beta_a S - (\mu + d + \gamma + \epsilon) & 0 \\ \beta_m I_m & \epsilon & \beta_m S - (\mu + d + \gamma) \end{pmatrix}.$$

Further, the local asymptotic stability of E_{10} and E_{11} is shown in the following theorems.

Theorem 3.2. *For model (3.4), the DFE E_{10} is locally asymptotically stable if $R_1 < 1$.*

As in the proof of Theorem 2.2, we can show that all eigenvalues of (3.4) at E_{10} are negative if $R_1 < 1$. Hence E_{10} achieves local asymptotic stability whenever $R_1 < 1$.

Theorem 3.3. *For model (3.4), the endemic equilibrium E_{11} is locally asymptotically stable if $R_1 > 1, a_1, a_2, a_3 > 0$ and $a_1a_2 > a_3$, where*
$a_1 = \frac{\Lambda\beta_a}{\mu+d+\gamma+\epsilon} + \frac{(\mu+d+\gamma)\beta_a-(\mu+d+\gamma+\epsilon)\beta_m}{\beta_a}$,
$a_2 = \frac{[\Lambda\beta_a-\mu(\mu+d+\gamma+\epsilon)][\beta_a(\mu+d+\gamma)-\epsilon\beta_m]}{\beta_a(\mu+d+\gamma)} + \frac{\Lambda[\beta_a(\mu+d+\gamma)-\beta_m(\mu+d+\gamma+\epsilon)]}{\mu+d+\gamma+\epsilon}$ *and*
$a_3 = \frac{[\Lambda\beta_a-\mu(\mu+d+\gamma+\epsilon)][(\mu+d+\gamma)\beta_a-(\mu+d+\gamma+\epsilon)\beta_m]}{\beta_a}$.

Proof. At E_{11}, the Jacobian matrix is

$$J_1(E_{11}) = \begin{pmatrix} A_{11} & A_{12} & A_{13} \\ A_{21} & A_{22} & A_{23} \\ A_{31} & A_{32} & A_{33} \end{pmatrix}$$

where $A_{11} = -\frac{\Lambda\beta_a}{\mu+d+\gamma+\epsilon}, A_{12} = -(\mu + d + \gamma + \epsilon), A_{13} = -\frac{\beta_m(\mu+d+\gamma+\epsilon)}{\beta_a}, A_{21} = \frac{[\Lambda\beta_a-\mu(\mu+d+\gamma+\epsilon)][(\mu+d+\gamma)\beta_a-(\mu+d+\gamma+\epsilon)\beta_m]}{(\beta_a-\beta_m)(\mu+d+\gamma)(\mu+d+\gamma+\epsilon)}$,
$A_{22} = A_{23} = 0, A_{31} = \frac{\epsilon\beta_m[\Lambda\beta_a-\mu(\mu+d+\gamma+\epsilon)]}{(\beta_a-\beta_m)(\mu+d+\gamma)(\mu+d+\gamma+\epsilon)}, A_{32} = \epsilon$ and $A_{33} = \frac{(\mu+d+\gamma+\epsilon)\beta_m-(\mu+d+\gamma)\beta_a}{\beta_a}$.

By solving the characteristic equation $|J_1(E_{11}) - \lambda I| = 0$, we obtain

$$\begin{aligned} &\lambda^3 + \left[\frac{\Lambda\beta_a}{\mu + d + \gamma + \epsilon} + \frac{(\mu + d + \gamma)\beta_a - (\mu + d + \gamma + \epsilon)\beta_m}{\beta_a}\right]\lambda^2 \\ &+ \left\{\frac{\Big[\Lambda\beta_a - \mu(\mu + d + \gamma + \epsilon)\Big]\Big[\beta_a(\mu + d + \gamma) - \epsilon\beta_m\Big]}{\beta_a(\mu + d + \gamma)} + \frac{\Lambda\Big[\beta_a(\mu + d + \gamma) - \beta_m(\mu + d + \gamma + \epsilon)\Big]}{\mu + d + \gamma + \epsilon}\right\}\lambda \\ &+ \frac{\Big[\Lambda\beta_a - \mu(\mu + d + \gamma + \epsilon)\Big]\Big[(\mu + d + \gamma)\beta_a - (\mu + d + \gamma + \epsilon)\beta_m\Big]}{\beta_a} = 0. \end{aligned} \tag{3.7}$$

If $R_1 > 1 \Longrightarrow R_{1a} > 1 \Longrightarrow \Lambda\beta_a - \mu(\mu + d + \gamma + \epsilon) > 0$ and $\beta_a(\mu + d + \gamma) - \beta_m(\mu + d + \gamma + \epsilon) > 0$ from (3.6) $\Longrightarrow \beta_a(\mu + d + \gamma) - \epsilon\beta_m > 0$, then we obtain $a_1, a_2, a_3 > 0$. Moreover, if we also have $a_1a_2 > a_3$, then, by the Routh–Hurwitz Criterion [42], all roots of (3.7) are negative or have negative real parts. Hence E_{11} is locally asymptotically stable if $R_1 > 1$ and $a_1a_2 > a_3$. ■

3.2. Analysis in region G_2

The dynamics in region G_2 can be represented by nonlinear ordinary differential equations as follows:

$$\begin{pmatrix} S'(t) \\ I_a'(t) \\ I_m'(t) \end{pmatrix} = \begin{pmatrix} \Lambda - \beta_a(1-q)SI_a - \beta_m(1-q)SI_m - \mu S \\ \beta_a(1-q)SI_a - (\mu + d + \gamma + \epsilon)I_a \\ \beta_m(1-q)SI_m + \epsilon I_a - (\mu + d + \gamma)I_m \end{pmatrix} := f_2. \tag{3.8}$$

In G_2, we have two equilibria: the DFE, $E_{20} = (S, I_a, I_m) = \left(\frac{\Lambda}{\mu}, 0, 0\right)$, and a unique positive EE,

$$E_{21} = (E_{21}S, E_{21}I_a, E_{21}I_m),$$

where

$$\begin{aligned} E_{21}S &= \frac{\mu + d + \gamma + \epsilon}{\beta_a(1-q)} \\ E_{21}I_m &= \frac{\epsilon\left[\Lambda\beta_a(1-q) - \mu(\mu + d + \gamma + \epsilon)\right]}{(1-q)(\beta_a - \beta_m)(\mu + d + \gamma)(\mu + d + \gamma + \epsilon)} \\ E_{21}I_a &= \frac{\left[\Lambda\beta_a(1-q) - \mu(\mu + d + \gamma + \epsilon)\right]\left[(\mu + d + \gamma)\beta_a - (\mu + d + \gamma + \epsilon)\beta_m\right]}{\beta_a(1-q)(\beta_a - \beta_m)(\mu + d + \gamma)(\mu + d + \gamma + \epsilon)} \\ &= \frac{\left[(\mu + d + \gamma)\beta_a - (\mu + d + \gamma + \epsilon)\beta_m\right]E_{21}I_m}{\epsilon\beta_a}. \end{aligned}$$

Furthermore, we have $E_{21} \in \mathbb{R}^3_+$, and this implies that

$$\begin{aligned} E_{21}S &= \frac{\mu + d + \gamma + \epsilon}{\beta_a(1-q)} > 0 \\ E_{21}I_m &= \frac{\epsilon\left[\Lambda\beta_a(1-q) - \mu(\mu + d + \gamma + \epsilon)\right]}{(1-q)(\beta_a - \beta_m)(\mu + d + \gamma)(\mu + d + \gamma + \epsilon)} > 0, \end{aligned}$$

which implies $\Lambda\beta_a(1-q) - \mu(\mu + d + \gamma + \epsilon) > 0$, where $0 < 1 - q < 1$ and $\beta_a > \beta_m \Longrightarrow \beta_a - \beta_m > 0$ and

$$E_{21}I_a = \frac{\left[(\mu + d + \gamma)\beta_a - (\mu + d + \gamma + \epsilon)\beta_m\right]E_{21}I_m}{\epsilon\beta_a} > 0,$$

which implies $(\mu + d + \gamma)\beta_a - (\mu + d + \gamma + \epsilon)\beta_m > 0$ with $E_{21}I_m > 0$.

The transmission matrix, F_2, and transition matrix, V_2, of model (3.8) are

$$F_2 = \begin{pmatrix} \beta_a(1-q)S & 0 \\ 0 & \beta_m(1-q)S \end{pmatrix} \quad \text{and} \quad V_2 = \begin{pmatrix} \mu + d + \gamma + \epsilon & 0 \\ -\epsilon & \mu + d + \gamma \end{pmatrix}, \quad \text{respectively.}$$

At the DFE E_{20}, we have

$$F_2V_2^{-1} = \begin{pmatrix} \dfrac{\Lambda\beta_a(1-q)}{\mu(\mu + d + \gamma + \epsilon)} & 0 \\ \dfrac{\epsilon\Lambda\beta_m(1-q)}{\mu(\mu + d + \gamma)(\mu + d + \gamma + \epsilon)} & \dfrac{\Lambda\beta_m(1-q)}{\mu(\mu + d + \gamma)} \end{pmatrix}$$

and the basic reproduction number (see [31,32] for further details) of G_2 is

$$R_2 := \max\left\{\frac{\Lambda\beta_a(1-q)}{\mu(\mu + d + \gamma + \epsilon)}, \frac{\Lambda\beta_m(1-q)}{\mu(\mu + d + \gamma)}\right\} = \max\{R_{2a}, R_{2m}\}$$

where $R_{2a} = \frac{\Lambda\beta_a(1-q)}{\mu(\mu+d+\gamma+\epsilon)}$ and $R_{2m} = \frac{\Lambda\beta_m(1-q)}{\mu(\mu+d+\gamma)}$.

In addition, the Jacobian matrix of model (3.8) is

$$J_2(S, I_a, I_m) = \begin{pmatrix} B_{11} & B_{12} & B_{13} \\ B_{21} & B_{22} & B_{23} \\ B_{31} & B_{32} & B_{33} \end{pmatrix}$$

where $B_{11} = -\beta_a(1-q)I_a - \beta_m(1-q)I_m - \mu$, $B_{12} = -\beta_a(1-q)S$, $B_{13} = -\beta_m(1-q)S$, $B_{21} = \beta_a(1-q)I_a$, $B_{22} = \beta_a(1-q)S - (\mu + d + \gamma + \epsilon)$, $B_{23} = 0$, $B_{31} = \beta_m(1-q)I_m$, $B_{32} = \epsilon$ and $B_{33} = \beta_m(1-q)S - (\mu + d + \gamma)$.

Furthermore, the local asymptotic stability of E_{21} and E_{21} is shown in the following theorems.

Theorem 3.4. *For model (3.8), the DFE E_{20} is locally asymptotically stable if $R_2 < 1$.*

We use a similar method as shown in Theorem 3.2 to prove Theorem 3.4; i.e., to show that all eigenvalues of model (3.8) at E_{20} are negative if $R_2 < 1$.

Theorem 3.5. *For model (3.8), the endemic equilibrium E_{21} is locally asymptotically stable if $R_2 > 1$, $b_1, b_2, b_3 > 0$ and $b_1 b_2 > b_3$, where*

$$\begin{aligned} b_1 &= \frac{\Lambda\beta_a(1-q)}{\mu+d+\gamma+\epsilon} + \frac{(\mu+d+\gamma)\beta_a - (\mu+d+\gamma+\epsilon)\beta_m}{\beta_a} \\ b_2 &= \frac{[\Lambda\beta_a(1-q) - \mu(\mu+d+\gamma+\epsilon)][\beta_a(\mu+d+\gamma) - \epsilon\beta_m]}{\beta_a(\mu+d+\gamma)} \\ &\quad + \frac{\Lambda(1-q)[\beta_a(\mu+d+\gamma) - \beta_m(\mu+d+\gamma+\epsilon)]}{\mu+d+\gamma+\epsilon} \\ b_3 &= \frac{[\Lambda\beta_a(1-q) - \mu(\mu+d+\gamma+\epsilon)][(\mu+d+\gamma)\beta_a - (\mu+d+\gamma+\epsilon)\beta_m]}{\beta_a}. \end{aligned}$$

Similar methods as Theorem 3.3 can be used to demonstrate the proof of Theorem 3.5; thus we omit the proof of this theorem.

3.3. Existence of sliding mode and its dynamical systems

We need to compute

$$\begin{aligned} \langle n, f_1\rangle &= \left\langle \begin{pmatrix} 0 \\ 1 \\ 1 \end{pmatrix}, \begin{pmatrix} \Lambda - \beta_a SI_a - \beta_m SI_m - \mu S \\ \beta_a SI_a - (\mu+d+\gamma+\epsilon)I_a \\ \beta_m SI_m + \epsilon I_a - (\mu+d+\gamma)I_m \end{pmatrix} \right\rangle \\ &= \beta_a SI_a + \beta_m SI_m - (\mu+d+\gamma)(I_a+I_m) \\ &= \beta_a SI_a + \beta_m SI_m - (\mu+d+\gamma)I_c \end{aligned} \tag{3.9}$$

where, on M, we have $I_m = -I_a + I_c$ and

$$\begin{aligned} \langle n, f_2\rangle &= \left\langle \begin{pmatrix} 0 \\ 1 \\ 1 \end{pmatrix}, \begin{pmatrix} \Lambda - \beta_a(1-q)SI_a - \beta_m(1-q)SI_m - \mu S \\ \beta_a(1-q)SI_a - (\mu+d+\gamma+\epsilon)I_a \\ \beta_m(1-q)SI_m + \epsilon I_a - (\mu+d+\gamma)I_m \end{pmatrix} \right\rangle \\ &= \beta_a(1-q)SI_a + \beta_m(1-q)SI_m - (\mu+d+\gamma)(I_a+I_m) \\ &= \beta_a(1-q)SI_a + \beta_m(1-q)S(I_c - I_a) - (\mu+d+\gamma)I_c \\ &= (\beta_a - \beta_m)(1-q)SI_a + \beta_m(1-q)SI_c - (\mu+d+\gamma)I_c. \end{aligned} \tag{3.10}$$

A sliding mode exists if $\langle n, f_1\rangle > 0$ and $\langle n, f_2\rangle < 0$. Thus

$$\begin{aligned} \langle n, f_1\rangle > 0 \quad &\text{if } S > h_1(I_a) := \frac{(\mu+d+\gamma)I_c}{(\beta_a-\beta_m)I_a + \beta_m I_c} \\ \langle n, f_2\rangle < 0 \quad &\text{if } S < h_2(I_a) := \frac{(\mu+d+\gamma)I_c}{(1-q)[(\beta_a-\beta_m)I_a + \beta_m I_c]} \end{aligned}$$

where $0 < 1-q < 1$. Since $\beta_a > \beta_m$, $0 < 1-q < 1$ and $I_a, I_c > 0$, then we obtain $h_2(I_a) = \frac{h_1(I_a)}{1-q}$ and $h_1(I_a) < h_2(I_a)$. So the sliding domain $\Omega \subset M$ is defined as

$$\Omega := \{(S, I_a, I_m) \in M;\, h_1(I_a) < S < h_2(I_a), I_a + I_m = I_c\}.$$

Further, we can find sliding mode equations by using the Utkin equivalent control method [43]. From (3.2), we have $\sigma(I_a, I_m) = I_a + I_m - I_c$. Then,

$$\begin{aligned} \frac{d\sigma}{dt} &= \frac{\partial\sigma}{\partial I_a}\cdot\frac{dI_a}{dt} + \frac{\partial\sigma}{\partial I_m}\cdot\frac{dI_m}{dt} \\ &= (1-qu)S(\beta_a I_a + \beta_m I_m) - (\mu+d+\gamma)(I_a+I_m) \quad \text{from (3.1).} \end{aligned}$$

By setting $\frac{d\sigma}{dt} = 0$ and solving for u, we obtain

$$u = \frac{S[(\beta_a-\beta_m)I_a + \beta_m I_c] - (\mu+d+\gamma)I_c}{qS[(\beta_a-\beta_m)I_a + \beta_m I_c]} \tag{3.11}$$

where, on M, we have $I_m = -I_a + I_c$.

From $\frac{d\sigma}{dt} = 0$, we also have $I_a'(t) + I_m'(t) = 0$. By substituting (3.11) into (3.1), we have

$$\begin{aligned} S'(t) &= \Lambda - (\mu + d + \gamma)I_c - \mu S; \\ I_a'(t) &= \beta_a I_a \left[\frac{(\mu + d + \gamma)I_c}{(\beta_a - \beta_m)I_a + \beta_m I_c}\right] - (\mu + d + \gamma + \epsilon)I_a. \end{aligned} \tag{3.12}$$

So the sliding mode equations on $\Omega \subset M$ are

$$\begin{aligned} S'(t) &= \Lambda - (\mu + d + \gamma)I_c - \mu S \\ I_a'(t) &= \beta_a I_a \left[\frac{(\mu + d + \gamma)I_c}{(\beta_a - \beta_m)I_a + \beta_m I_c}\right] - (\mu + d + \gamma + \epsilon)I_a \\ I_m'(t) &= -I_a'(t). \end{aligned} \tag{3.13}$$

For model (3.13), there exists a unique positive pseudoequilibrium point, $E_s = (E_sS, E_sI_a, E_sI_m)$, where $E_sS = \frac{\Lambda - (\mu+d+\gamma)I_c}{\mu}$, $E_sI_a = \frac{I_c[\beta_a(\mu+d+\gamma) - \beta_m(\mu+d+\gamma+\epsilon)]}{(\beta_a-\beta_m)(\mu+d+\gamma+\epsilon)}$ and $E_sI_m = \frac{\epsilon\beta_a I_c}{(\beta_a-\beta_m)(\mu+d+\gamma+\epsilon)}$. E_s is in $\Omega \subset M$ if the following constraint is satisfied.

$$h_1(I_a) < E_sS < h_2(I_a) \Leftrightarrow h_1(I_a) < \frac{\Lambda - (\mu + d + \gamma)I_c}{\mu} < h_2(I_a).$$

A reduced dynamical system of (3.13) is defined as in (3.12), and the local asymptotic stability of E_s is shown in the following theorem.

Theorem 3.6. *$E_s \in \Omega$ is locally asymptotically stable if $\beta_a(\mu + d + \gamma) - \beta_m(\mu + d + \gamma + \epsilon) > 0$.*

A similar approach as in Theorem 2.2 can be employed to demonstrate that all eigenvalues of (3.12) at E_s are negative if $\beta_a(\mu + d + \gamma) - \beta_m(\mu + d + \gamma + \epsilon) > 0$, so we omit the proof of this theorem.

3.4. Local stability of the endemic equilibria

$(S, I_a, I_m) \in \mathbb{R}^3_+$ is divided into three regions, G_1, M and G_2. There exists an equilibrium point in each region, E_{11}, E_s and E_{21} in regions G_1, $\Omega \subset M$ and G_2, respectively. In this section, let us denote the real and virtual equilibria with superscripts R and V, respectively. We will discuss the stability of E_s, E_{11} and E_{21} in the following subsections. Note that, in order to illustrate the theoretical results, some numerical simulations are carried out in this section. All parameters shown in Table 2 are used in the numerical simulations, unless otherwise stated.

3.4.1. Case 1: E_{11} and E_{21} are virtual equilibria

If (3.14) is satisfied, then both E_{11} and E_{21} are virtual equilibria.

$$E_{11}I_a + E_{11}I_m > I_c \quad \text{and} \quad E_{21}I_a + E_{21}I_m < I_c. \tag{3.14}$$

Here E_{11}^V and E_{21}^V are located in regions G_2 and G_1, respectively. In this case, we have $E_s \in \Omega \subset M$, which is locally asymptotically stable. All trajectories will converge to E_s if (3.14) is satisfied.

Theorem 3.7. *The pseudoequilibrium E_s cannot coexist with E_{11}^R and E_{21}^R. In addition, $E_s \in \Omega \subset M$ is locally asymptotically stable if it exists.*

Proof. Note that $E_sS - h_1(E_sI_a) > (<)0 \Longrightarrow \Lambda\beta_a - \mu(\mu + d + \gamma + \epsilon) > (<)\beta_a(\mu + d + \gamma)I_c$, $E_sS - h_2(E_sI_a) < (>)0 \Longrightarrow \Lambda\beta_a(1 - q) - \mu(\mu + d + \gamma + \epsilon) < (>)\beta_a(1 - q)(\mu + d + \gamma)I_c$ where $0 < 1 - q < 1$ and all associated parameters are positive, $E_{11}I_a + E_{11}I_m = \frac{\Lambda\beta_a - \mu(\mu+d+\gamma+\epsilon)}{\beta_a(\mu+d+\gamma)}$ and $E_{21}I_a + E_{21}I_m = \frac{\Lambda\beta_a(1-q) - \mu(\mu+d+\gamma+\epsilon)}{\beta_a(1-q)(\mu+d+\gamma)}$. We refer to [44] to prove that the pseudoequilibrium E_s cannot coexist with E_{11}^R and E_{21}^R. So we have to show that (a) if $E_s \in \Omega \subset M$ is a pseudoequilibrium, then E_{11} and E_{21} are virtual equilibria, and (b) if E_s is not a pseudoequilibrium, then E_{11} and E_{21} are real equilibria.

(a) If $E_s \in \Omega \subset M$ is a pseudoequilibrium (i.e., $h_1(E_sI_a) < E_sS < h_2(E_sI_a) \Longrightarrow E_sS - h_1(E_sI_a) > 0$ and $E_sS - h_2(E_sI_a) < 0$), then $E_{11}I_a + E_{11}I_m > I_c$ and $E_{21}I_a + E_{21}I_m < I_c$ indicate that E_{11} and E_{21} are virtual equilibria.

$$E_{11}I_a + E_{11}I_m = \frac{\Lambda\beta_a - \mu(\mu + d + \gamma + \epsilon)}{\beta_a(\mu + d + \gamma)} > \frac{\beta_a(\mu + d + \gamma)I_c}{\beta_a(\mu + d + \gamma)} = I_c$$

where $E_sS - h_1(E_sI_a) > 0 \Longrightarrow \Lambda\beta_a - \mu(\mu + d + \gamma + \epsilon) > \beta_a(\mu + d + \gamma)I_c$.

$$E_{21}I_a + E_{21}I_m = \frac{\Lambda\beta_a(1 - q) - \mu(\mu + d + \gamma + \epsilon)}{\beta_a(1 - q)(\mu + d + \gamma)} < \frac{\beta_a(1 - q)(\mu + d + \gamma)I_c}{\beta_a(1 - q)(\mu + d + \gamma)} = I_c$$

where $E_sS - h_2(E_sI_a) < 0 \Longrightarrow \Lambda\beta_a(1 - q) - \mu(\mu + d + \gamma + \epsilon) < \beta_a(1 - q)(\mu + d + \gamma)I_c$. Thus the existence of pseudoequilibrium E_s implies the non-existence of real equilibria E_{11} and E_{21}.

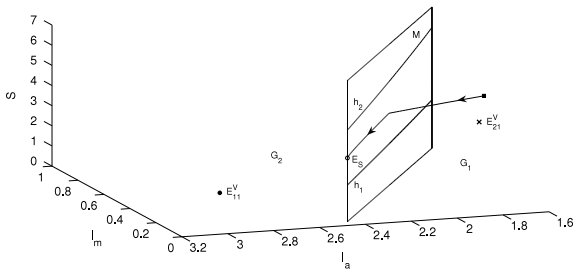

(a) A trajectory with initial point in G_1 will hit and slide to the left on $\Omega \subset M$ before moving towards E_s.

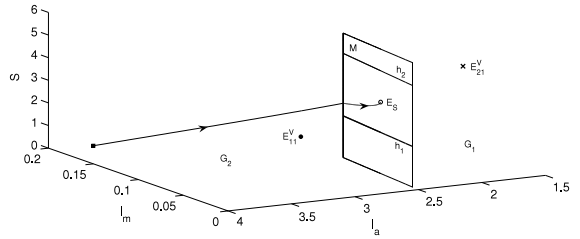

(b) A trajectory which begins in region G_2 will converge to E_s after it hits and slides to the right on $\Omega \subset M$.

Fig. 9. $E_s \in \Omega \subset M$ is locally asymptotically stable if (3.14) is satisfied.

(b) If E_s is not a pseudoequilibrium (i.e., $E_s \notin \Omega \subset M \Longrightarrow E_sS - h_1(E_sI_a) < 0$ and $E_sS - h_2(E_sI_a) > 0$) then $E_{11}I_a + E_{11}I_m < I_c$ and $E_{21}I_a + E_{21}I_m > I_c$ indicate that E_{11} and E_{21} are real equilibria.

$$E_{11}I_a + E_{11}I_m = \frac{\Lambda\beta_a - \mu(\mu + d + \gamma + \epsilon)}{\beta_a(\mu + d + \gamma)} < \frac{\beta_a(\mu + d + \gamma)I_c}{\beta_a(\mu + d + \gamma)} = I_c$$

where $E_sS - h_1(E_sI_a) < 0 \Longrightarrow \Lambda\beta_a - \mu(\mu + d + \gamma + \epsilon) < \beta_a(\mu + d + \gamma)I_c$.

$$E_{21}I_a + E_{21}I_m = \frac{\Lambda\beta_a(1-q) - \mu(\mu + d + \gamma + \epsilon)}{\beta_a(1-q)(\mu + d + \gamma)} > \frac{\beta_a(1-q)(\mu + d + \gamma)I_c}{\beta_a(1-q)(\mu + d + \gamma)} = I_c$$

where $E_sS - h_2(E_sI_a) > 0 \Longrightarrow \Lambda\beta_a(1-q) - \mu(\mu + d + \gamma + \epsilon) > \beta_a(1-q)(\mu + d + \gamma)I_c$.

So E_{11} and E_{21} are real equilibria whenever $E_s \notin \Omega \subset M$. Therefore, the pseudoequilibrium E_s cannot coexist with the real equilibria E_{11} and E_{21}.

Next, we would like to discuss the stability of $E_s \in \Omega \subset M$. We have shown that $E_s \in \Omega \subset M$ achieves local asymptotic stability in Theorem 3.6. For any choice of threshold level I_c in between $E_{21}I_a + E_{21}I_m$ and $E_{11}I_a + E_{11}I_m$, the local asymptotic stability of E_s in the sliding domain always holds. Hence, E_s is locally asymptotically stable in the sliding domain $\Omega \subset M$ if it exists. ■

Since the difference between $E_{11}I_a + E_{11}I_m$ and $E_{21}I_a + E_{21}I_m$ $\left(\text{i.e., } \frac{q\mu(\mu+d+\gamma+\epsilon)}{\beta_a(1-q)(\mu+d+\gamma)}\right)$ with $\mu = \frac{1}{65\times365}$ is considerably small (0.0001619), then we select $\mu = 0.3$ and $I_c = 2.5$ while other parameters are defined in Table 2 in order to depict Case 1 clearly; i.e., $E_s \in \Omega \subset M$ achieves local asymptotic stability if (3.14) is fulfilled. Fig. 9 shows that any trajectory that begins either in region G_1 or G_2 will converge to $E_s \in \Omega \subset M$ if (3.14) is satisfied.

3.4.2. Case 2: E_{11} is a real equilibrium, whereas E_{21} is a virtual equilibrium

If the following constraint is satisfied, then E_{11} is a real equilibrium and E_{21} is a virtual equilibrium.

$$E_{11}I_a + E_{11}I_m < I_c \quad \text{and} \quad E_{21}I_a + E_{21}I_m < I_c. \tag{3.15}$$

Both E_{11}^R and E_{21}^V are located in region G_1. In this case, we have an equilibrium point located in G_1 (i.e., E_{11}) and there is no equilibrium point located in region G_2. If (3.15) is satisfied, then all trajectories in this case will converge to E_{11}^R. Hence, E_{11}^R achieves local asymptotic stability.

Theorem 3.8. *E_{11}^R is locally asymptotically stable if (3.15) is satisfied.*

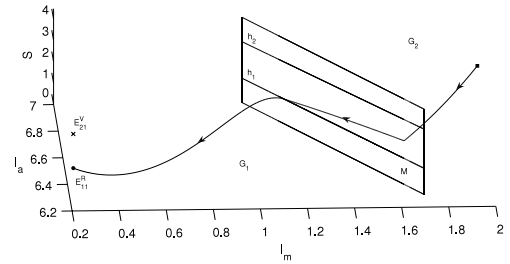

(a) A trajectory with initial point in G_2 will hit and slide to the right on $\Omega \subset M$ before moving towards E_{11}^R.

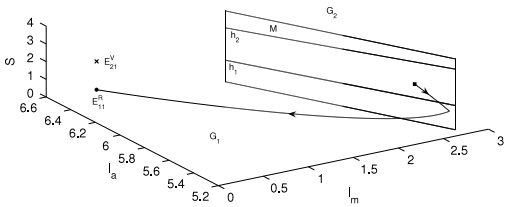

(b) A trajectory will cross the region $S < h_1$ on M from the direction of G_2 before moving towards E_{11}^R.

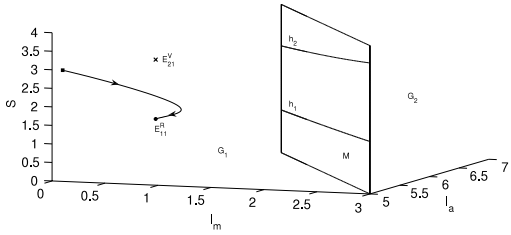

(c) A trajectory that begins in region G_1 will converge to E_{11}^R without hitting or passing through manifold M.

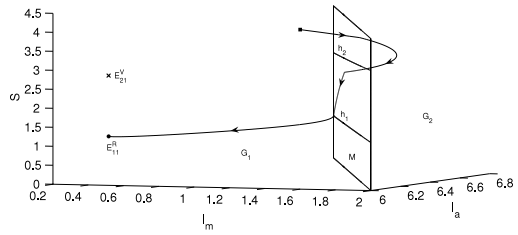

(d) A trajectory will pass through M moving towards G_2 from G_1 and hit manifold M again from the direction of G_2. Then it will slide down on $\Omega \subset M$ before converging to E_{11}^R in G_1.

Fig. 10. $E_{11}^R \in G_1$ is locally asymptotically stable if (3.15) is fulfilled.

We discover that E_{11}^R is located in region G_1 if (3.15) is fulfilled. Since we have proved that the equilibrium point $E_{11} \in G_1$ achieves local asymptotic stability in Theorem 3.3, we omit the proof of Theorem 3.8.

Case 2 is depicted in Fig. 10 with $I_c = 8$. Any trajectory with initial point in region G_1 or G_2 will converge directly to E_{11}^R either without hitting the manifold M or it will hit the manifold M, slide and then move towards the equilibrium E_{11}^R.

3.4.3. Case 3: E_{21} is a real equilibrium, whereas E_{11} is a virtual equilibrium

E_{21} is a real equilibrium and E_{11} is a virtual equilibrium if (3.16) is satisfied.

$$E_{11}I_a + E_{11}I_m > I_c \quad \text{and} \quad E_{21}I_a + E_{21}I_m > I_c. \tag{3.16}$$

In this case, both E_{11}^V and E_{21}^R are located in region G_2. There is no equilibrium point that can be found in region G_1, but there is one equilibrium point (i.e., E_{21}) that lies in region G_2. All trajectories will converge to E_{21}^R if (3.16) is fulfilled. So E_{21}^R achieves local asymptotic stability in this case.

Theorem 3.9. *E_{21}^R achieves local asymptotic stability if the requirement of (3.16) is met.*

Note that E_{21}^R is located in region G_2 if (3.16) is satisfied. In Theorem 3.5, we have proved that the equilibrium point $E_{21} \in G_2$ is locally asymptotically stable. So we omit the proof of Theorem 3.9.

The result of Theorem 3.9 is illustrated in Fig. 11. All trajectories in this case with $I_c = 6$ will either hit or do not hit the manifold M before converging to E_{21}^R.

4. Conclusion and discussion

Two Filippov models that are governed by nonlinear ordinary differential equations with discontinuous right-hand sides have been proposed; notably the avian-only model with culling of infected birds and the SIIR model with quarantine as control measure. At the initial stage of an outbreak, many people are not aware of the existence of the disease. This usually leads to rapid disease outbreak since no disease preventions have been practiced by the public. When the emerging infectious disease has reached a critical stage, known as the "threshold level", people may start to take necessary precautions to prevent themselves from being infected [22]. Sliding mode control is one of the desirable methods to depict this type of disease-management phenomenon [21].

An HPAI outbreak in avian population can create havoc in the poultry industry; a large number of birds will have to be killed since culling birds is one of the primary strategy to eradicate an avian flu outbreak, especially among the infected avian population. Studies on culling have been carried out to identify the most effective approach to eradicating the disease

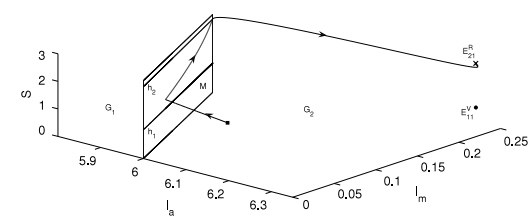

(a) A trajectory will hit M from the direction of G_2. Then it will slide to right on $\Omega \subset M$ before moving towards E_{21}^R in G_2.

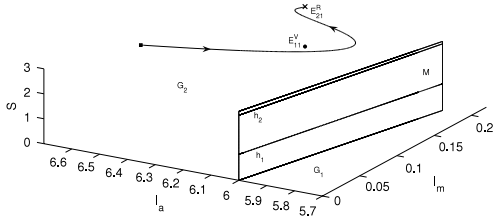

(b) A trajectory with initial point in region G_2 converges to E_{21}^R directly.

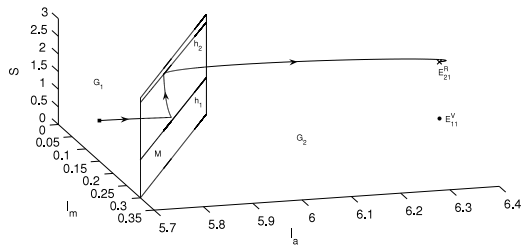

(c) A trajectory hits $\Omega \subset M$ from G_1 and then moves up on Ω before converging to E_{21}^R in G_2.

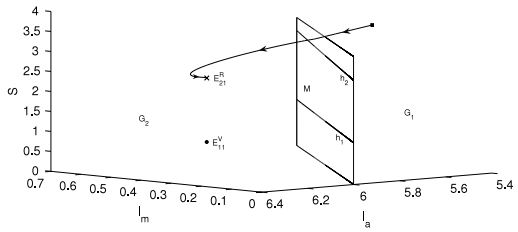

(d) A trajectory crosses manifold M from G_1 to G_2 and then moves towards E_{21}^R.

Fig. 11. $E_{21}^R \in G_2$ is locally asymptotically stable if (3.16) is satisfied.

and reducing the socio-economic impact [16,45]. Hence it is essential for us to look closely at which culling threshold level should be chosen in order to eliminate the disease or at least to stabilize the infection. For instance, in the avian-only Filippov model (2.1), whenever the trajectory is found to be converging to E_{11d} in G_{1d} or $E_d \in \Omega_d \subset M_d$, we proclaim that the infection of avian influenza in the avian population is still bearable. However, if the solution of model (2.1) converges to E_{21d} in G_{2d}, we assume that an outbreak is emerging. As a response to the outbreak, control methods have to be implemented in order to suppress the transmission and contain the disease. In addition, the theoretical results and numerical simulations in Section 2 show that model (2.1) achieves global asymptotic stability.

Due to the influenza pandemic history, HPAI outbreaks, mainly H5N1, have caused severe infections in humans and resulted in many human deaths [46]. Many types of interventions have been applied to minimize the impact of avian influenza. Quarantine is one of the conventional control methods that has been widely used, especially in the absence of medicines and vaccines, during the onset of the outbreak to reduce the transmission rate of the disease. However, quarantine policy (e.g., location of quarantine, timeframe, who can set up quarantine, the use of legal orders and who has the authority to issue the orders and so on), limitations of resources (e.g., food, clean drinking water and medical equipments) and the lack of health-care workers are some of the most critical issues for public-health authorities [47,48]. Hence, an SIIR model with quarantine as a control measure is designed to assess an appropriate quarantine threshold level that will lead to disease elimination. In Section 3, it is shown that the solutions of model (3.1) will converge to either one of the two endemic equilibria or the sliding equilibrium. In order to inhibit an outbreak or to stabilize the infection, we have to choose a suitable tolerance threshold I_c such that the trajectory of model (3.1) is approaching E_{11} in G_1 or a sliding equilibrium E_s on $\Omega \subset M$.

There are several limitations of these two models that should be mentioned here. Throughout the model simulations, fixed constants of bird inflow and human recruitment have been applied in avian-only and SIIR models. We have made assumptions that the immunity of humans was permanent (i.e., recovered humans will not move to susceptible class) and the human-to-human transmission rate with avian strain is greater than the human-to-human transmission rate with mutant strain. For the avian population, infected birds are presumed to stay infected; i.e., infected birds will not move to other classes such as susceptible and recovered compartments. It is also noteworthy that we assumed humans with avian and mutant strains have the same values of recovery and additional disease death rate.

Our findings show that we can either preclude the influenza outbreak or stabilize the infection at a desired level by choosing an appropriate threshold level. A well-defined threshold policy is essential to us in order to combat an outbreak effectively and efficiently.

Acknowledgments

NSC acknowledges support from the Ministry of Higher Education, Malaysia, and School of Informatics and Applied Mathematics, Universiti Malaysia Terengganu. RJS? is supported by an NSERC Discovery Grant. For citation purposes, please note that the question mark in "Smith?" is part of his name.

Appendix A. Types of regions on a discontinuity surface M

Suppose an ordinary differential equation

$$\dot{x} = f(x, t) \tag{A.1}$$

with threshold policy is discontinuous on a surface M that is defined by equation

$$\sigma(x) = 0$$

where $x \in \mathbb{R}^n$. The surface M separates the x space into domains G^- and G^+. Let us denote the differential equations that represent the dynamics in the regions G^- and G^+ as $f^-(x, t)$ and $f^+(x, t)$, respectively.

There are three types of regions on M: sliding, sewing and escaping regions [23], which are defined as follows.

Definition A.1 ([23]).

(a) If $\langle n, f^- \rangle > 0$ and $\langle n, f^+ \rangle < 0$ on $\Omega \subset M$, then Ω is known as a sliding region.
(b) If $\langle n, f^- \rangle \cdot \langle n, f^+ \rangle > 0$, i.e., $\langle n, f^- \rangle$ and $\langle n, f^+ \rangle$ have the same signs on $\Omega_2 \subset M$, then Ω_2 is called as a sewing region.
(c) If $\langle n, f^- \rangle < 0$ and $\langle n, f^+ \rangle > 0$ on $\Omega_3 \subset M$, then Ω_3 is known as an escaping region.

Note that escaping and sliding regions cannot exist simultaneously; it is impossible that $\langle n, f^- \rangle < 0$ and $\langle n, f^+ \rangle > 0$ exist at the same time with $\langle n, f^- \rangle > 0$ and $\langle n, f^+ \rangle < 0$.

Appendix B. Types of equilibrium points for a Filippov system

In this appendix, we will use similar notations as in Appendix A. Let us denote the sliding mode equation that describes the motion in the sliding region $\Omega \subset M$ by $f^0(x, t)$. Suppose there exists an equilibrium point in each region G^-, G^+ and Ω, denoted by E_1, E_2 and E_s, respectively. There are four types of equilibria that might exist in a model of ordinary differential equations with threshold policy: real, virtual, pseudoequilibrium and boundary equilibria [23].

Definition B.1 ([23]).

(a) E^R is a real equilibrium if $f^-(E^R) = 0$ and $\sigma(E^R) < 0$ or $f^+(E^R) = 0$ and $\sigma(E^R) > 0$.
(b) E^V is a virtual equilibrium if $f^-(E^V) = 0$ and $\sigma(E^V) > 0$ or $f^+(E^V) = 0$ and $\sigma(E^V) < 0$.
(c) E^B is a boundary equilibrium if $f^-(E^B) = 0$ and $\sigma(E^B) = 0$ or $f^+(E^B) = 0$ and $\sigma(E^B) = 0$.
(d) E^P is a pseudoequilibrium if E^P is an equilibrium point on the sliding mode; i.e., $f^0(E^P) = 0$ and $\sigma(E^P) = 0$.

Note that a stable virtual equilibrium will not be achieved as the dynamics will change once the trajectory hits the discontinuous manifold [23].

Appendix C. Lyapunov function and theories on global stability of the Filippov system

Consider a differential equation (A.1) with $f \in C^1(G)$ where G is an open subset of $\mathbb{R}^n$. The solution $\phi(t, x_0)$ of the initial-value problem (A.1) with $x_0 \in G$ will be a dynamical system on G if and only if $\forall x_0 \in G$, $\phi(t, x_0)$ is defined $\forall t \in \mathbb{R}$. The function $\phi(\cdot, x) : \mathbb{R} \to G$ for $x \in G$ defines a solution curve, trajectory or orbit of (A.1) with initial point $x_0 \in G$. A trajectory with $x_0 \in G$ can be described as a motion along the curve $\Gamma = \{x \in G; x = \phi(t, x_0), t \in \mathbb{R}\}$, which is defined by (A.1) (refer to [49] for further details).

Definition C.1 ([49]). A point $E \in G$ is an ω-limit point of the trajectory $\phi(\cdot, x)$ of (A.1) if there is a sequence $t_n \to \infty$ such that $\lim_{n\to\infty} \phi(t_n, x) = E$. The set of all ω-limit points of a trajectory Γ is called the ω-limit set of Γ and it is denoted by $\omega(\Gamma)$.

Definition C.2 ([49]). Let G be an open subset of $\mathbb{R}^n$, $f \in C^1(G)$ and $\phi_t : G \to G$ be the flow of the differential equation (A.1) defined $\forall t \in \mathbb{R}$. Then a set $S \subset G$ is called invariant with respect to the flow ϕ_t if $\phi_t(S) \subset S$ $\forall t \in \mathbb{R}$ and S is called positively invariant with respect to the flow ϕ_t if $\phi_t(S) \subset S$ $\forall t \geq 0$.

Let $\Gamma_1(t) := \{x \in \mathbb{R}^n_+; x = \phi(t, x_0)$ for some $x_0 \in G\}$ and $\zeta(G) := \bigcup_{t\geq 0} \Gamma_1(t)$.

Definition C.3 ([50,23]). A function $V \in C^1(\mathbb{R}^n)$ is called a Lyapunov function of (A.1) on $G \subset \mathbb{R}^n$ if it is non-negative on G and, $\forall x \in G$,

$$\dot{V}^*(x) := \max_{\eta \in g(x)} \langle \nabla V(x), \eta \rangle \leq 0 \quad \text{where}$$

$$g(x) := \begin{cases} f^-(x); & x \in G^- \\ \alpha f^+(x) + (1-\alpha) f^-(x); & x \in M \text{ where } \alpha \in [0, 1] \\ f^+(x); & x \in G^+. \end{cases}$$

Proposition C.1 (*[50,23, LaSalle's Invariance Principle]*). *Suppose $G \subset \mathbb{R}^n$ is an open set that satisfies $\omega(G) := \bigcup_{x\in G} \omega(x) \subset \zeta(G)$. Let every Filippov solution $\phi(t, x_0)$ of (A.1) be unique and defined $\forall t \geq 0$ and $x_0 \in G$. Suppose $V : \mathbb{R}^n \to \mathbb{R}$ is a Lyapunov function of (A.1) on $\zeta(G)$. Then $\omega(G)$ is a subset of the largest positively invariant subset of $\overline{\Sigma}$ where $\Sigma := \{x \in \overline{G}; \dot{V}^*(x) = 0\}$.*

Corollary C.2 (*[50,23]*). *Assume that G and $V : \mathbb{R}^n \to \mathbb{R}$ satisfy Proposition C.1 and $\mathbb{R}^n \setminus G$ is repelling in the sense that all solutions stay in $\mathbb{R}^n \setminus G$ for only a finite time. Let $\omega(\mathbb{R}^n) = \omega(G)$ be bounded. Then $\overline{\omega(\mathbb{R}^n)}$ is globally asymptotically stable.*

Theorem C.3 (*[49, Dulac's Theorem]*). *Suppose*

$$\frac{dx}{dt} = f(x, y) \quad \text{and} \quad \frac{dy}{dt} = g(x, y) \tag{C.1}$$

where $f(x, y)$ and $g(x, y)$ are assumed to be C^1 functions. If there exists a C^1 function $B(x, y)$ (where $B(x, y)$ is also known as a Dulac function) in a simply connected region R such that $\frac{\partial(Bf)}{\partial x} + \frac{\partial(Bg)}{\partial y}$ has constant sign and is not identically zero in any subregion, then system (C.1) does not have a periodic orbit lying entirely in R.

References

[1] R. Goodwin, S. Sun, Public perceptions and reactions to H7N9 in Mainland China, J. Infect. 67 (2013) 458–462.
[2] World Health Organization. 2013. Human infection with influenza A (H7N9) virus in China-update. http://www.who.int/csr/don/2013_04_03/en/index.html (Accessed October 28, 2013).
[3] Centers for Disease Control and Prevention. 2013. Avian influenza A (H7N9) virus. http://www.cdc.gov/flu/avianflu/h7n9-virus.htm (Accessed October 30, 2013).
[4] Centers for Disease Control and Prevention. 2010. Key facts about avian influenza (bird flu) and highly pathogenic avian influenza A (H5N1) virus. http://www.cdc.gov/flu/avian/gen-info/facts.htm (Accessed October 30, 2013).
[5] World Health Organization. 2011. New: WHO comment on the importance of global monitoring of variant influenza viruses. http://www.who.int/influenza/human_animal_interface/avian_influenza/h5n1-2011_12_19/en/index.html (Accessed October 30, 2013).
[6] World Health Organization. 2012. H5N1 avian influenza: Timeline of major events. http://www.who.int/influenza/human_animal_interface/avian_influenza/H5N1_avian_influenza_update.pdf (Accessed October 30, 2013).
[7] D. Zilberman, J. Otte, D. Roland-Host, D. Pfeiffer, The cost of saving a statistical life: a case for influenza prevention and control, Nat. Resour. Manag. Policy 36 (2012) 135–141.
[8] F.B. Agusto, A.B. Gumel, Qualitative dynamics of lowly- and highly-pathogenic avian influenza strains, Math. Biosci. 243 (2013) 147–162.
[9] M.E. Alexander, S.M. Moghadas, J. Wu, A delay differential model for pandemic influenza with antiviral treatment, Bull. Math. Biol. 70 (2008) 382–397.
[10] T.C. Germann, K. Kadau, I.M. Longini, C.A. Macken, Mitigation strategies for pandemic influenza in the United States, Proc. Natl. Acad. Sci. USA 103 (2006) 5935–5940.
[11] E. Jung, S. Iwami, Y. Takeuchi, T.-C. Jo, Optimal control strategy for prevention of avian influenza pandemic, J. Theoret. Biol. 260 (2009) 220–229.
[12] K.I. Kim, Z. Lin, L. Zhang, Avian-human influenza epidemic model with diffusion, Nonlinear Anal. RWA 11 (2010) 313–322.
[13] M. Lipsitch, T. Cohen, M. Murray, B.R. Levin, Antiviral resistance and the control of pandemic influenza, PLoS Med. 4 (2007) e15.
[14] N.M. Ferguson, D.A.T. Cummings, S. Cauchemez, C. Fraser, S. Riley, A. Meeyai, S. Iamsirithaworn, D.S. Burke, Strategies for containing an emerging influenza pandemic in Southeast Asia, Nature 437 (2005) 209–214.
[15] M. Nuño, G. Chowell, A.B. Gumel, Assessing the role of basic control measures, antivirals and vaccine in curtailing pandemic influenza: scenarios for the US, UK and the Netherlands, J. R. Soc. Interface 4 (2006) 505–521.
[16] H. Gulbudak, M. Martcheva, Forward hysteresis and backward bifurcation caused by culling in an avian influenza model, Math. Biosci. (2013) http://dx.doi.org/10.1016/j.mbs.2013.09.001.
[17] F.B. Agusto, Optimal isolation control strategies and cost-effectiveness analysis of a two-strain avian influenza model, Biosystems 113 (2013) 155–164.
[18] N.S. Chong, J.M. Tchuenche, R.J. Smith?, A mathematical model of avian influenza with half-saturated incidence, Theory Biosci. 133 (2014) 23–38.
[19] S. Tang, Y. Xiao, N. Wang, H. Wu, Piecewise HIV virus dynamic model with $CD4^+$ T cell count-guided therapy: I, J. Theoret. Biol. 308 (2012) 123–134.
[20] A. Wang, Y. Xiao, A Filippov system describing media effects on the spread of infectious diseases, Nonlinear Anal. Hybrid Syst. 11 (2014) 84–97.
[21] Y. Xiao, T. Zhao, Dynamics of an infectious diseases with media/psychology induced non-smooth incidence, Math. Biosci. Eng. 10 (2) (2013) 445–461.
[22] Y. Xiao, X. Xu, S. Tang, Sliding mode control of outbreaks of emerging infectious diseases, Bull. Math. Biol. 74 (2012) 2403–2422.
[23] T. Zhao, Y. Xiao, R.J. Smith?, Non-smooth plant disease models with economic thresholds, Math. Biosci. 241 (2013) 34–48.
[24] G. Matei, M. Decun, G.H. Ontanu, A comparative risk consequences assessment for avian influenza outbreaks occurred in Romania, Lucr. Ştiinţ. Med. Vet. XI (2007) 10–15.
[25] G. Sun, H. Yang, A study on the space–time dynamic of global avian influenza and relationship with bird migration, Int. J. Bus. Manag. 3 (2) (2008) 10–17.
[26] The Center for Food Security and Public Health. 2013. High pathogenicity avian influenza. http://www.cfsph.iastate.edu/DiseaseInfo/notes/AvianInfluenza.pdf (Accessed October 30, 2013).
[27] M. Koopmans, B. Wilbrink, M. Conyn, G. Natrop, et al., Transmission of H7N7 avian influenza A virus to human beings during a large outbreak in commercial poultry farms in the Netherlands, Lancet 363 (2004) 587–593.
[28] World Health Organization. 2010. Reducing the risk of emergence of pandemic influenza. http://www.who.int/influenza/resources/research/research_agenda_influenza_stream_1_reducing_risk.pdf (Accessed October 30, 2013).
[29] Food and Agriculture Organization of the United Nations. 2013. Poultry and human nutrition. http://www.fao.org/ag/againfo/themes/en/poultry/hh_nutrition.html (Accessed October 30, 2013).
[30] H.W. Hethcote, The mathematics of infectious diseases, SIAM Rev. 42 (4) (2000) 599–653.
[31] P. van den Driessche, J. Watmough, Reproduction numbers and sub-threshold endemic equilibria for compartmental models of disease transmission, Math. Biosci. 180 (2002) 29–48.
[32] J. Li, D. Blakeley, R.J. Smith?, The failure of R_0, Comput. Math. Methods Med. 2011 (2011) Article ID 527610.
[33] A.F. Filippov, Differential Equations with Discontinuous Right-hand Sides, Kluwer Academic, Dordrecht, The Nertherlands, 1988.
[34] R.I. Leine, Bifurcations in discontinuous mechanical systems of Filippov-type. The Universiteitsdrukkerij TU Eindhoven, The Netherlands, 2000.
[35] M. Martcheva, Avian flu: modeling and implications for control. AMS Subject Classification: 92D30, 92D40, 2011.
[36] N. Tuncer, M. Martcheva, Modeling seasonality in avian influenza H5N1, J. Biol. Syst. 21 (2013) Article ID 1340004.
[37] A.B. Gumel, Global dynamics of a two-strain avian influenza model, Int. J. Comput. Math. 86 (2009) 85–108.
[38] World Health Organization. 2013. Frequently asked questions on human infection caused by the avian influenza A (H7N9) virus. http://www.who.int/influenza/human_animal_interface/faq_H7N9/en/ (Accessed October 28, 2013).

[39] World Health Organization. 2013. Influenza at the human-animal interface. http://www.who.int/influenza/human_animal_interface/Influenza_Summary_IRA_HA_interface_7October13.pdf (Accessed October 28, 2013).
[40] World Health Organization. Avian influenza: food safety issues. http://www.who.int/foodsafety/micro/avian/en/index1.html (Accessed October 28, 2013).
[41] J. Lucchetti, M. Roy, M. Martcheva, A dynamic avian flu model and its fit to human avian influenza cases, in: J.M. Tchuenche, Z. Mukandavire (Eds.), Advances in Disease Epidemiology, Nova Science Publishers, New York, 2009, pp. 1–30.
[42] X. Yang, Generalized form of Routh–Hurwitz criterion and Hopf bifurcation of higher order, J. Appl. Math. Lett. 15 (2001) 615–621.
[43] V.I. Utkin, Sliding Modes in Control and Optimization, Springer-Verlag, Berlin, Heidelberg, 1992.
[44] J. Yang, S. Tang, R.A. Cheke, Global stability and sliding bifurcations of a non-smooth Gause predator–prey system, J. Appl. Math. Comput. 224 (2001) 9–20.
[45] A. Le Menach, E. Vergu, R.F. Grais, D.L. Smith, A. Flahault, Key strategies for reducing spread of avian influenza among commercial poultry holdings: lessons for transmission to humans, Proc. R. Soc. B 273 (2006) 2467–2475.
[46] World Health Organization. 2011. Avian influenza. http://www.who.int/mediacentre/factsheets/avian_influenza/en/ (Accessed November 5, 2013).
[47] National Association of County and City health Officials. 2006. Issues to consider isolation and quarantine. http://www.naccho.org/toolbox/_toolbox/IssuestoConsiderIsolation&Quarantine.pdf.
[48] North Country Regional Public Health Emergency Annex. 2011. Appendix 6—Isolation and quarantine. http://www.nchcnh.org/images/NCHCuplds/files/Appendix%206%20Isolation%20&%20Quarantine%20v4_0.pdf.
[49] L. Perko, Differential Equations and Dynamical Systems, third ed., Springer-Verlag, New York, 2001.
[50] D.S. Boukal, V. Křivan, Lyapunov functions for Lotka–Volterra predator–prey models with optimal foraging behavior, Math. Biol. 39 (1999) 493–517.

Chapter 5

An avian-only Filippov model incorporating culling of both susceptible and infected birds in combating avian influenza

We extend our previous work on the avian-only model [42] by proposing culling of both susceptible and infected birds instead of only infected birds. We consider the depopulation of susceptible or infected birds when the susceptible or infected bird populations exceed their respective tolerance thresholds. The reason why stamping out susceptible birds is considered in our culling strategy, on top of stamping out the infected birds, is that we wish to prevent more birds from getting infected later and hence to reduce the seriousness of the avian influenza outbreak. We study the dynamics of this model as the tolerance thresholds of infected and susceptible birds vary.

This work is published in the *Journal of Mathematical Biology* [43]. The contribution of each author is as follows. The first author designed the study, analyzed the model, conducted all numerical simulations and wrote the manuscript. The second and third authors wrote part of the conclusion and discussion and edited the manuscript.

There is a mistake in [43] concerning the reference for the value of the parameter β. This parameter value was chosen by the authors and not taken from [60].

The statement of Theorem 3.2 should be "There is no periodic solution inside the region D, whose path may contain (part of) a sliding domain" and not the present statement which is in fact the statement of Theorem 3.6. The proof of Theorem 3.6 requires the result of Theorem 3.2 combined with the phase portrait of the system.

The paper [43] is included in the following pages.

J. Math. Biol.
DOI 10.1007/s00285-016-0971-y

Mathematical Biology

An avian-only Filippov model incorporating culling of both susceptible and infected birds in combating avian influenza

Nyuk Sian Chong[1,2] · **Benoit Dionne**[1] · **Robert Smith?**[1,3]

Received: 7 June 2015 / Revised: 5 November 2015

Abstract Depopulation of birds has always been an effective method not only to control the transmission of avian influenza in bird populations but also to eliminate influenza viruses. We introduce a Filippov avian-only model with culling of susceptible and/or infected birds. For each susceptible threshold level S_b, we derive the phase portrait for the dynamical system as we vary the infected threshold level I_b, focusing on the existence of endemic states; the endemic states are represented by real equilibria, pseudoequilibria and pseudo-attractors. We show generically that all solutions of this model will approach one of the endemic states. Our results suggest that the spread of avian influenza in bird populations is tolerable if the trajectories converge to the equilibrium point that lies in the region below the threshold level I_b or if they converge to one of the pseudoequilibria or a pseudo-attractor on the surface of discontinuity. However, we have to cull birds whenever the solution of this model converges to an equilibrium point that lies in the region above the threshold level I_b in order to control the outbreak. Hence a good threshold policy is required to combat bird flu successfully and to prevent overkilling birds.

✉ Robert Smith?

Nyuk Sian Chong

Benoit Dionne

[1] Department of Mathematics and Statistics, University of Ottawa, 585 King Edward Ave, Ottawa, ON K1N 6N5, Canada

[2] School of Informatics and Applied Mathematics, Universiti Malaysia Terengganu, 21030 Kuala Terengganu, Malaysia

[3] Faculty of Medicine, University of Ottawa, 451 Smyth Rd, Ottawa, ON K1H 8M5, Canada

Published online: 10 February 2016

Keywords Dynamical systems · Avian influenza · Filippov model · Culling · Threshold policy

Mathematics Subject Classification 34C05 · 92D30

1 Introduction

Avian influenza is induced by type A viruses. These viruses can be classified into two categories: low pathogenic avian influenza (LPAI) and highly pathogenic avian influenza (HPAI) (Public Health Agency of Canada 2006; Canadian Food Inspection Agency 2012; Centers for Disease Control and Prevention 2012). Infection by LPAI viruses usually causes mild or no illness at all, whereas infection by HPAI viruses can cause severe disease with high disease-death rate. These two types of viruses can potentially infect domesticated birds (such as chickens, quails and turkeys) rapidly, as well as wild birds and humans (Public Health Agency of Canada 2006; Canadian Food Inspection Agency 2012; Centers for Disease Control and Prevention 2012).

Waterfowl are carriers of the avian influenza viruses but do not show any symptoms. They spread the virus through excretions; the virus can be easily spread to domesticated birds when they come in contact with waterfowl or via contaminated area/objects. As a result, this allows the virus to proliferate, which may further induce viral mutation (Public Health Agency of Canada 2006; Centers for Disease Control and Prevention 2012; Jacob et al. 2013).

Currently, there is no effective treatment for birds infected with avian influenza. Although vaccination, biosecurity and surveillance measures reduce the infection rate, these measures do not eliminate the virus (Canadian Food Inspection Agency 2012; International Animal Health Organisation 2015; Jacob et al. 2013). Thus, whenever a highly pathogenic avian influenza outbreak occurs, culling birds is usually an effective method to control the spread of the disease. However, susceptible birds are also at risk of being killed in the course of preventing the disease (FAO 2006, 2008, 2011; Centers for Disease Control and Prevention 2012; International Animal Health Organisation 2015; Kimman et al. 2013; Perez and Garcia-Sastre 2013). Hence an efficient culling strategy is needed to avoid overkilling and reduce the economic impact, particularly where the poultry business is concerned (FAO 2008, 2011; Centers for Disease Control and Prevention 2012; Gulbudak and Martcheva 2013).

A number of studies involving the culling strategy in bird populations to combat avian influenza have been carried out (Dorigatti et al. 2010; Gulbudak and Martcheva 2013; Iwami et al. 2008, 2009; Menach et al. 2006; Shim and Galvani 2009). Menach et al. (2006) proposed a model that employs stochastic and deterministic processes to examine the impact and efficiency of control strategies. For instance, the spread of the disease within a farm is modelled stochastically by discrete-time model formulation, whereas the changes of farm's disease status is studied by using a deterministic model. Based on the results obtained, an immediate culling of infected flocks upon an accurate and quick diagnosis will be better at controlling the outbreak compared to the strategy of only stamping out the surrounding flocks.

Shim and Galvani (2009) proposed a mathematical model parameterized by clinical, epidemiological and poultry data to assess the evolutionary consequences of mass avian depopulation on both host and pathogen. They also investigated the selection of a dominant allele that confers resistance against avian influenza and the level of pathogenicity of influenza. Their results showed that, by increasing the culling rate, less host resistance is needed to eradicate the disease and the selection for the resistant allele would be reduced. As a consequence, the implementation of mass depopulation would elevate the virulence level of influenza. So, although an avian influenza outbreak can be eliminated by employing mass avian culling control strategy, it brings several detrimental evolutionary consequences such as the decreasing of influenza resistance and the increasing of host mortality and influenza virulence.

Dorigatti et al. (2010) considered an SEIR (Susceptible-Exposed-Infected-Removed) model with a spatial transmission kernel to model the diffusion of H7N1 in Italy. The infection of H7N1 between farms was investigated. They found that the transmissibility of virus between the first phase and the subsequent phases is decreasing, and there is a variation of susceptibility in between poultry species. Further, they discovered that banning restocking on empty farms was the most effective control method.

During the emerging phase of an infectious disease, applying control measures to prevent the infection may be disregarded by the public. However, when the number of infected individuals has gone beyond a certain threshold level, the public will be alerted and immediate actions have to be taken in order to avoid a deadly outbreak. Hence a good threshold policy is required to provide useful information in disease-management strategy not only to the public but also to the public authorities, so that the disease can be eradicated or at least reduced to a minimum level (Tang et al. 2012; Xiao et al. 2012; Zhao et al. 2013).

Xiao et al. (2013) proposed an infectious disease model with a piecewise smooth incidence rate that incorporated media/psychology effects by converting the implicitly defined classical model based on the properties of the Lambert W function. The global dynamics of this system were analyzed. They discovered that the disease-free equilibrium is globally asymptotically stable if the basic reproduction number is less than one, whereas the endemic equilibrium is globally stable whenever the basic reproduction number is larger than one. Moreover, the effect of media does not affect the epidemic threshold or disease eradication. However, it does reduce the number of infected individuals and the prevalence significantly.

Furthermore, Wang and Xiao (2014) designed a Filippov SIR (Susceptible-Infected-Recovered) model to describe the media effects on the spread of infectious diseases. The mass media will have an effect whenever the number of infected individuals reaches a certain threshold level. A bifurcation analysis was conducted and all possible dynamic behaviours were determined. Based on the primary results, the model will achieve stability either at the two endemic equilibria or the pseudoequilibrium. They inferred that a good threshold policy with media coverage can assist in controlling and combating an emerging infectious disease.

In Sect. 2 of this paper, we propose a Filippov avian-only model incorporating culling of susceptible and/or infected birds. We extend our previous work on the

avian-only model (Chong and Smith? 2015) by considering not only culling of infected birds but also the effort to stamp out susceptible birds if the numbers of susceptible and infected birds exceed certain threshold levels. Previously, we only considered culling of infected birds for the avian-only model as a control measure (Chong and Smith? 2015). In Sects. 3–6, we analyse all the possible dynamics of this model by varying the threshold levels of the infected and susceptible birds. We prove the existence of equilibria, *pseudoequilibria* and *pseudo-attractors*. The prefix *pseudo* was added to equilibria and attractors to distinguish them from the standard equilibria and attractors. For a pseudoequilibrium, some orbits may converge to it in a finite time. For the pseudo-attractor, all orbits will converge to it in a finite time. Finally, Sect. 7 will present several concluding remarks together with the discussion pertaining to the study.

2 The avian-only Filippov model

In this section, we propose a threshold policy in an avian-only model with culling of susceptible and/or infected birds. We only consider domestic birds for the avian population. To control the spread of the disease and reduce the transmission level, immediate action (i.e., a culling strategy) has to be taken once the numbers of susceptible and infected birds exceed the threshold levels.

In this paper, we will focus on the effects of tolerance thresholds of susceptible birds S_b and infected birds I_b, which can provide useful information for disease management. Namely, in which cases do we have to apply culling of susceptible and/or infected birds in order to suppress the infection rate? We use a Filippov model to determine threshold criteria for culling. Filippov models consist of ordinary differential equations with discontinuous conditions on the derivatives, whereby the solution undergoes a rapid change in motion when certain conditions are met.

We assume that the infection is within the tolerable range when the number of infected birds I is less than the tolerance threshold I_b, so no control strategy is required under this condition, and that an outbreak might occur if $I > I_b$, which requires a control strategy to reduce the infection to a safer level. In this model, we do not apply any control strategies when $I < I_b$. However, for $I > I_b$, we kill only infected birds at a rate of c_2 if the number of susceptible birds S is less than the threshold level S_b, and we cull both susceptible and infected birds at rates of c_1 and c_3 respectively if $S > S_b$. We assume that $c_2 < c_3$ and $c_1, c_2, c_3 > 0$ in this model. We not only consider culling infected birds with a higher cull rate c_3 when $S > S_b$ but we also reduce the population of susceptible birds. The reason for this choice is that we may have a lot of susceptible birds that may get infected by avian influenza later and more severely affect the outbreak.

We consider an avian-only population that is divided into susceptible and infected birds. Infected birds are assumed to remain in the infected class in this model. The sum of $S(t)$ and $I(t)$ is the total population of domestic birds $N(t)$ at time t. This avian-only Filippov model is governed by nonlinear ordinary differential equations with discontinuous right-hand sides as follows:

$$\begin{pmatrix} S' \\ I' \end{pmatrix} = F(S, I) \equiv \begin{pmatrix} \Lambda - \beta SI - (\mu + u_1)S \\ \beta SI - (\mu + d + u_2)I \end{pmatrix} \tag{2.1}$$

with

$$(u_1, u_2) = \begin{cases} (0, 0) & \text{for } I < I_b \\ (0, c_2) & \text{for } S < S_b \text{ and } I > I_b \\ (c_1, c_3) & \text{for } S > S_b \text{ and } I > I_b, \end{cases} \tag{2.2}$$

where S_b, $I_b > 0$ are the tolerance thresholds, Λ (individual/day) is the bird inflow, β (/day $\times$ /individual) is the rate at which birds contract avian influenza, μ (/day) is the natural death rate of birds, and d (/day) is the additional disease-specific death rate due to avian influenza in birds.

We divide the S, I space $\mathbb{R}^2_+$ into five regions as follows:

$$\begin{aligned} G_1 &\equiv \left\{(S, I) \in \mathbb{R}^2_+ : I < I_b\right\} \\ G_2 &\equiv \left\{(S, I) \in \mathbb{R}^2_+ : S < S_b \text{ and } I > I_b\right\} \\ G_3 &\equiv \left\{(S, I) \in \mathbb{R}^2_+ : S > S_b \text{ and } I > I_b\right\} \\ M_1 &\equiv \left\{(S, I) \in \mathbb{R}^2_+ : I = I_b\right\} \end{aligned}$$

and

$$M_2 \equiv \{(S, I) \in \mathbb{R}^2_+ : S = S_b \text{ and } I > I_b\}.$$

The dynamics in region G_i are governed by f_i, for $i = 1, 2$ and 3, where

$$f_1(S, I) = \begin{pmatrix} \Lambda - \beta SI - \mu S \\ I\big(\beta S - (\mu + d)\big) \end{pmatrix} \tag{2.3}$$

$$f_2(S, I) = \begin{pmatrix} \Lambda - \beta SI - \mu S \\ I\big(\beta S - (\mu + d + c_2)\big) \end{pmatrix} \tag{2.4}$$

and

$$f_3(S, I) = \begin{pmatrix} \Lambda - \beta SI - (\mu + c_1)S \\ I\big(\beta S - (\mu + d + c_3)\big) \end{pmatrix}. \tag{2.5}$$

Moreover, the normal vectors that are perpendicular to M_1 and M_2 are defined as $n_1 = (0, 1)^T$ and $n_2 = (1, 0)^T$, respectively.

To give a sense of the flow of the dynamical system on the boundaries M_i between the regions G_i, we use Filippov's convex method (Filippov 1988). The basic idea of Filippov's method is to replace the vector field F in (2.1) by the set-valued function $\hat{F}$, where $\hat{F}(S, I)$ is the closed convex hull of the set

$$\left\{ \begin{pmatrix} U \\ V \end{pmatrix} : \begin{pmatrix} U \\ V \end{pmatrix} = \lim_{(u,v)\to(S,I)} F(u, v) \text{ for } (u, v) \in G_i \right\}.$$

Then (2.1) becomes

$$\begin{pmatrix} S' \\ I' \end{pmatrix} \in \hat{F}(S, I).$$

There is a theory of existence and uniqueness of solutions for such systems. Since $F|_{G_i}$ is continuously differentiable on the closure of G_i, we may give a simple interpretation of Filippov's method. At the points (S, I) where F is continuous, $\hat{F}(S, I) = \{F(S, I)\}$, and hence we may still use the formulation in (2.1). To be able to write

$$\begin{pmatrix} S' \\ I' \end{pmatrix} = F(S, I).$$

at the points $(S, I) \in M_i$ ($i = 1$ or 2) where F is discontinuous, we choose a representative value for $\hat{F}(S, I)$ as follows. Let $F_+(S, I) = \lim_{(u,v)\to(S,I)} F(u, v)$ for (u, v) on one side of M_i and $F_-(S, I) = \lim_{(u,v)\to(S,I)} F(u, v)$ for (u, v) on the other side of M_i. Then

$$\hat{F}(S, I) = \{\alpha F_+(S, I) + (1 - \alpha)F_-(S, I) : 0 \le \alpha \le 1\}.$$

At a point (S, I) of M_i where the flow of F approaches (S, I) on one side of M_i and moves away from (S, I) on the other side of M_i, we may choose any vector in $\hat{F}(S, I)$. This will not influence the dynamics because this vector will point in the local direction of the vector field.

The more interesting situation is when the flow of F approaches M_i from all sides or moves away from M_i from all sides.

Definition 2.1 The set of all points (S, I) on M_i such that the flow of F (outside M_i) approaches (S, I) from all sides is an attraction sliding mode. When the attraction sliding mode is formed of only one point, we call this point a pseudo-attractor. The repulsion sliding mode is the set of all points (S, I) on M_i such that the flow of F (outside M_i) moves away from (S, I).

At a point (S, I) on M_i where the flow of F approaches (S, I) from both sides (or moves away from both sides), we choose $F(S, I) = \alpha F_+(S, I) + (1 - \alpha)F_-(S, I)$, where $\alpha = (n_i^\top F_-(S, I))/(n_i^\top (F_-(S, I) - F_+(S, I)))$ and n_i is a normal vector to M_i. With this choice, the flow entering the sliding mode will remain on it for at least a finite time. We have $n_1 = (0, 1)^T$ and $n_2 = (1, 0)^T$.

The vector field F that we defined on sliding modes may have an equilibrium point; such an equilibrium point is called a *pseudoequilibrium*. The major difference between this type of equilibrium point and the classical equilibrium points for a continuously differentiable vector field in $\mathbb{R}^2$ is that some of the orbits inside G_i may converge to this equilibrium in a finite period as time increases or decreases.

We now identify the existence of a positively invariant and globally (in $\mathbf{R}^2_+$) attracting region for the system (2.1).

Lemma 2.2 *$D \equiv \{(S, I) \in \mathbb{R}^2_+ : S + I \le \frac{A}{\mu}\}$ is a positively invariant and attracting region in $\mathbf{R}^2_+$ for the system* (2.1).

If you ignore the lines M_1 and M_2, where the vector field F is discontinuous, the proof will look like this. Let $N = S + I$. Taking the sum of S' and I' given by (2.1) yields

$$N' = \Lambda - \mu(S + I) - u_1 S - (d + u_2)I \leq \Lambda - \mu N.$$

Thus

$$\frac{d}{ds}\big(N(s)e^{\mu s}\big) = e^{\mu s}(N'(s) + \mu N(s)) \leq \Lambda e^{\mu s}.$$

Integrating both sides between 0 and t gives

$$N(t)e^{\mu t} - N(0) = \int_0^t \frac{d}{ds}\big(N(s)e^{\mu s}\big)ds \leq \int_0^t \Lambda e^{\mu s} ds = \frac{\Lambda}{\mu}\left(e^{\mu t} - 1\right).$$

If $N(0) \leq \frac{\Lambda}{\mu}$, then we get

$$N(t)e^{\mu t} \leq N(0) + \frac{\Lambda}{\mu}\left(e^{\mu t} - 1\right) \leq \frac{\Lambda}{\mu}e^{\mu t},$$

and thus $N(t) \leq \frac{\Lambda}{\mu}$. This proves that D is positively invariant.

To prove that D is attractive, let's suppose that $N > \frac{\Lambda}{\mu}$ and let $\phi = \frac{\Lambda}{\mu}$. We have proved above that $N' \leq \Lambda - \mu N$. Thus $N' \leq \mu\phi - \mu N = \mu(\phi - N) < 0$.

A simple but lengthy justification could be given to handle the situation where the vector field F is discontinuous.

We have from the lemma that the ω-limit sets of (2.1) are contained in D.

2.1 The system f_1

In this section, we study the dynamics of f_1 given by (2.3) on $\mathbb{R}^2_+$. In particular, we examine the linear stability of the two equilibria of this system: the disease-free equilibrium (DFE) $E_{10} = \left(\frac{\Lambda}{\mu}, 0\right)$ and the endemic equilibrium (EE)

$$E_{11} \equiv (h_1, g_1) = \left(\frac{\mu + d}{\beta}, \frac{\Lambda\beta - \mu(\mu + d)}{\beta(\mu + d)}\right).$$

The basic reproduction number (Driessche and Watmough 2002; Li et al. 2011) of this system is

$$R_1 = \frac{\Lambda\beta}{\mu(\mu + d)}.$$

The Jacobian matrix for (2.3) is

$$J_1(S, I) = \begin{pmatrix} -\beta I - \mu & -\beta S \\ \beta I & \beta S - (\mu + d) \end{pmatrix}.$$

Theorem 2.3 *E_{10} is locally asymptotically stable for $R_1 < 1$ and unstable for $R_1 > 1$.*

Proof The eigenvalues of $J_1(E_{10})$ are obtained from

$$|J_1(E_{10}) - \lambda I| = -(\mu + \lambda)\left(\frac{\Lambda\beta - \mu(\mu + d)}{\mu} - \lambda\right) = 0.$$

Thus $\lambda = -\mu < 0$ and $\lambda = \frac{\Lambda\beta - \mu(\mu+d)}{\mu}$ is negative for $R_1 < 1$ and positive for $R_1 > 1$, where all parameters are positive. □

Theorem 2.4 *E_{11} is locally asymptotically stable for $R_1 > 1$.*

Proof The eigenvalues of $J_1(E_{11})$ are

$$\lambda_{\pm} = \frac{1}{2}\left(-\frac{\Lambda\beta}{\mu + d} \pm \sqrt{\nu}\right), \quad \text{where } \nu = \left(\frac{\Lambda\beta}{\mu + d}\right)^2 - 4\left(\Lambda\beta - \mu(\mu + d)\right).$$

For $R_1 > 1$, we have $\Lambda\beta - \mu(\mu + d) > 0$. Hence $\nu < \left(\frac{\Lambda\beta}{\mu+d}\right)^2$ and $\lambda_{\pm} < 0$. □

2.2 The system f_2

This time, we study the dynamics of f_2 given by (2.4) on $\mathbb{R}^2_+$. There are two equilibria for this system: the EE,

$$E_{21} \equiv (h_2, g_2) = \left(\frac{\mu + d + c_2}{\beta}, \frac{\Lambda\beta - \mu(\mu + d + c_2)}{\beta(\mu + d + c_2)}\right),$$

and the DFE, $E_{20} = \left(\frac{\Lambda}{\mu}, 0\right)$. To determine their linear stability, we need the basic reproduction number

$$R_2 = \frac{\Lambda\beta}{\mu(\mu + d + c_2)}$$

of this model. The Jacobian matrix of (2.4) is

$$J_2(S, I) = \begin{pmatrix} -\beta I - \mu & -\beta S \\ \beta I & \beta S - (\mu + d + c_2) \end{pmatrix}.$$

Theorem 2.5 *The DFE E_{20} is locally asymptotically stable if $R_2 < 1$ and unstable if $R_2 > 1$.*

The proof of this theorem is similar to the proof of Theorem 2.3.

Theorem 2.6 *The EE E_{21} is locally asymptotically stable if $R_2 > 1$.*

Proceeding as in the proof of Theorem 2.4, one can show that E_{21} is either a stable spiral or a stable node if $R_2 > 1$.

2.3 The system f_3

Finally, we study the dynamics of f_3 given by (2.5) on $\mathbb{R}^2_+$. There are two equilibria for this system, the DFE, $E_{30} = (\frac{\Lambda}{\mu+c_1}, 0)$, and the EE, $E_{31} \equiv (h_3, g_3) = (\frac{\mu+d+c_3}{\beta}, \frac{\Lambda\beta-(\mu+c_1)(\mu+d+c_3)}{\beta(\mu+d+c_3)})$. The basic reproduction number of (2.5) is $R_3 = \frac{\Lambda\beta}{(\mu+c_1)(\mu+d+c_3)}$.

Theorem 2.7 *The DFE E_{30} is locally asymptotically stable if $R_3 < 1$ and unstable whenever $R_3 > 1$.*

Theorem 2.7 is proved as Theorem 2.3 is proved.

Theorem 2.8 *The EE E_{31} is locally asymptotically stable if $R_3 > 1$.*

A proof similar to the proof of Theorem 2.4 shows that all eigenvalues of the linearization of (2.5) at E_{31} are either negative real numbers or complex numbers with negative real parts.

3 Case A: $S_b < h_1$

In this and the following three sections, we determine the existence of sliding modes on M_1 and M_2 and study the dynamics of (2.1) and (2.2). We have $h_1 < h_2 < h_3$ and $g_3 < g_2 < g_1$. We consider the 16 cases generated by $S_b < h_1$, $h_1 < S_b < h_2$, $h_2 < S_b < h_3$ and $h_3 < S_b$, and $I_b < g_3$, $g_3 < I_b < g_2$, $g_2 < I_b < g_1$ and $g_1 < I_b$. They each require a distinct mathematical analysis. However, we will show in the conclusion that many of these cases are identical from a biological point of view. The endemic equilibrium may mathematically change from one case to the other but may still produce the same biological phenomena.

The conclusions of the results in Sects. 3–6 are summarized in the table at the end of the paper. We list the equilibria of the dynamical system (2.1) when the thresholds S_b and I_b vary, as well as the corresponding culling strategy to be implemented.

3.1 Existence of a sliding mode on M_1 and its dynamics

There are several types of regions on a discontinuity surface and several types of equilibrium points for a Filippov system. See Appendices A and B of Chong and Smith? (2015), respectively.

Proposition 3.1 (Zhao et al. 2013) *If* $\langle n_1, f_1\rangle > 0$ *and* $\langle n_1, f_3\rangle < 0$ *on* $\Omega_1 \subset M_1$, *then* Ω_1 *is a sliding region.*

From $\langle n_1, f_1\rangle > 0$ and $\langle n_1, f_3\rangle < 0$, we get

$$h_1 = \frac{\mu + d}{\beta} < S < \frac{\mu + d + c_3}{\beta} = h_3.$$

Thus

$$\Omega_1 = \{(S, I) \in M_1 : S_b < h_1 < S < h_3\}. \tag{3.1}$$

Sliding-mode equations can be found by using Filippov convex method (Filippov 1988; Leine 2000) as follows:

$$\begin{pmatrix} S' \\ I' \end{pmatrix} = \psi f_1 + (1 - \psi) f_3 \quad \text{, where } \psi = \frac{\langle n_1, f_3\rangle}{\langle n_1, f_3 - f_1\rangle}.$$

Thus

$$\begin{pmatrix} S' \\ I' \end{pmatrix} = \begin{pmatrix} \Lambda - \beta SI - (\mu + c_1)S + \dfrac{c_1 S\left((\mu + d + c_3) - \beta S\right)}{c_3} \\ 0 \end{pmatrix}. \tag{3.2}$$

The differential equation for S has two steady states, given by

$$S = \frac{B \pm \sqrt{B^2 - 4AC}}{2\beta c_1}, \quad \text{where } A = -\beta c_1,\ B = c_1(\mu + d) - c_3(\beta I_b + \mu) \text{ and } C = \Lambda c_3.$$

However, $B^2 - 4AC > B^2 > 0$ because $A < 0$ and $C > 0$. Thus there is only one positive steady state, given by

$$S = h_4 \equiv \frac{B + \sqrt{B^2 - 4AC}}{2\beta c_1}.$$

Hence $E_{S1} = (h_4, I_b) \in \Omega_1 \subset M_1$ is an equilibrium for (3.2) if $h_1 < h_4 < h_3$. It is locally asymptotically stable because

$$\frac{\partial}{\partial S}\left(\frac{-\beta c_1 S^2 + (c_1(\mu + d) - c_3(\beta I_b + \mu))\, S + \Lambda c_3}{c_3}\right)\Bigg|_{E_{S1}} = \frac{-\sqrt{B^2 - 4AC}}{c_3} < 0.$$

We now show that E_{S1} is globally asymptotically stable if

$$g_3 < I_b < g_1. \tag{3.3}$$

We note that the equilibria E_{11}, E_{21} and E_{31} for f_1, f_2 and f_3, respectively, do not appear in this case, because they are outside the considered domain for f_1, f_2 and f_3. For this reason, we call them *virtual equilibria* for (2.1).

Theorem 3.2 *$E_{S1} \in \Omega_1 \subset M_1$ is globally asymptotically stable if $g_3 < I_b < g_1$ and $R_1 > 1$.*

Proof We first prove that there cannot be any periodic solution entirely included in one of the regions G_i. Consider a Dulac function $B_1(S, I) = \frac{1}{SI}$ for $(S, I) \in \mathbb{R}^2_+$. Then

$$\frac{\partial(B_1 f_{1,1})}{\partial S} + \frac{\partial(B_1 f_{1,2})}{\partial I} = \frac{\partial}{\partial S}\left(\frac{\Lambda}{SI} - \beta - \frac{\mu}{I}\right) + \frac{\partial}{\partial I}\left(\beta - \frac{\mu + d}{S}\right) = -\frac{\Lambda}{S^2 I} < 0$$

on $\mathbb{R}^2_+$, where $f_{1,1}$ is the first component of f_1 and $f_{1,2}$ is the second component of f_1. We have a similar result for f_2 and f_3. From Dulac's Theorem (Perko 2001), we know that there will not be any periodic solution included in $\mathbb{R}^2_+ \setminus \{M_1, M_2\}$.

Because the vector field F in (2.1) is discontinuous, we cannot use Dulac's Theorem to prove that there are no periodic solution crossing the regions M_i. However, proceeding as in the proof of Dulac's Theorem, using Green's Theorem, we can reach this conclusion for our system as we now show.

Suppose that Γ is a periodic orbit around Ω_1 as in Fig. 1. Let $\Gamma = \Gamma_1 + \Gamma_2 + \Gamma_3$, where $\Gamma_i = \Gamma \cap G_i$. Let H be the bounded region delimited by Γ and $H_i = H \cap G_i$ for $i = 1, 2$ and 3. Then

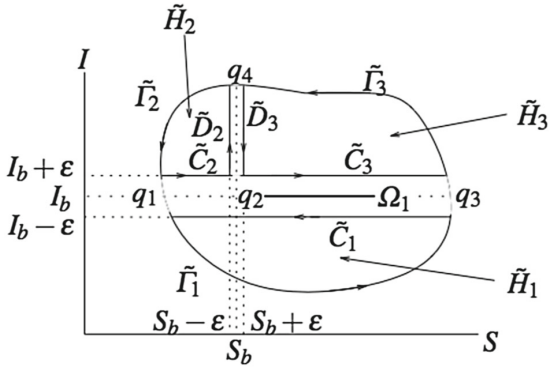

Fig. 1 Limit cycle Γ

$$\iint_H \left(\frac{\partial(B_1F_1)}{\partial S} + \frac{\partial(B_1F_2)}{\partial I}\right) dSdI$$
$$= \sum_{i=1}^{3} \iint_{H_i} \left(\frac{\partial(B_1 f_{i,1})}{\partial S} + \frac{\partial(B_1 f_{i,2})}{\partial I}\right) dSdI < 0, \tag{3.4}$$

where F_1 is the first component of F and F_2 is the second component of F. We have

$$\iint_{H_i} \left(\frac{\partial(B_1 f_{i,1})}{\partial S} + \frac{\partial(B_1 f_{i,2})}{\partial I}\right) dSdI = \lim_{\epsilon \to 0} \iint_{\tilde{H}_i} \left(\frac{\partial(B_1 f_{i,1})}{\partial S} + \frac{\partial(B_1 f_{i,2})}{\partial I}\right) dSdI,$$

where $\tilde{H}_i$ is the region bounded by the curves $\tilde{\Gamma}_i$, $\tilde{C}_i$ and $\tilde{D}_i$ (if necessary) as illustrated in Fig. 1. $\tilde{H}_i$ and $\tilde{\Gamma}_i$ depend on ϵ and converge to H_i and Γ_i as ϵ approaches 0.

By applying Green's Theorem to the region $\tilde{H}_1$, we get

$$\iint_{\tilde{H}_1} \left(\frac{\partial(B_1 f_{1,1})}{\partial S} + \frac{\partial(B_1 f_{1,2})}{\partial I}\right) dSdI = \oint_{\partial \tilde{H}_1} B_1 f_{1,1} dI - B_1 f_{1,2} dS$$
$$= \int_{\tilde{\Gamma}_1} B_1 f_{1,1} dI - B_1 f_{1,2} dS + \int_{\tilde{C}_1} B_1 f_{1,1} dI - B_1 f_{1,2} dS$$
$$= -\int_{\tilde{C}_1} B_1 f_{1,2} dS \tag{3.5}$$

because $dS = f_{1,1}dt$ and $dI = f_{1,2}dt$ along $\tilde{\Gamma}_1$, and $dI = 0$ along $\tilde{C}_1$. Note that $\partial \tilde{H}_1$ denotes the boundary of $\tilde{H}_1$.

Proceeding as we just did, we get

$$\iint_{\tilde{H}_2} \left(\frac{\partial(B_1 f_{2,1})}{\partial S} + \frac{\partial(B_1 f_{2,2})}{\partial I}\right) dSdI = \int_{\tilde{D}_2} B_1 f_{2,1} dI - \int_{\tilde{C}_2} B_1 f_{2,2} dS \tag{3.6}$$

and

$$\iint_{\tilde{H}_3} \left(\frac{\partial(B_1 f_{3,1})}{\partial S} + \frac{\partial(B_1 f_{3,2})}{\partial I}\right) dSdI = \int_{\tilde{D}_3} B_1 f_{3,1} dI - \int_{\tilde{C}_3} B_1 f_{3,2} dS. \tag{3.7}$$

From (3.4) to (3.7), we see that

$$0 > \sum_{i=1}^{3} \iint_{H_i} \left(\frac{\partial(B_1 f_{i,1})}{\partial S} + \frac{\partial(B_1 f_{i,2})}{\partial I}\right) dSdI$$
$$= \lim_{\epsilon \to 0} \left(-\int_{\tilde{C}_1} B_1 f_{1,2} dS + \int_{\tilde{D}_2} B_1 f_{2,1} dI - \int_{\tilde{C}_2} B_1 f_{2,2} dS + \int_{\tilde{D}_3} B_1 f_{3,1} dI - \int_{\tilde{C}_3} B_1 f_{3,2} dS \right).$$

If q_1 and q_3 are the intersections of Γ with the line $I = I_b$, q_4 is the intersection of Γ with the line $S = S_b$ with $I > I_b$ and $q_2 = (S_b, I_b)$, then the previous inequality can be written

$$\begin{aligned} 0 > &-\int_{q_{3,1}}^{q_{1,1}} \left(\beta - \frac{\mu + d}{S}\right) dS + \int_{q_{2,2}}^{q_{4,2}} \left(\frac{\Lambda}{SI} - \beta - \frac{\mu}{I}\right) dI - \int_{q_{1,1}}^{q_{2,1}} \left(\beta - \frac{\mu + d + c_2}{S}\right) dS \\ &+ \int_{q_{4,2}}^{q_{2,2}} \left(\frac{\Lambda}{SI} - \beta - \frac{\mu + c_1}{I}\right) dI - \int_{q_{2,1}}^{q_{3,1}} \left(\beta - \frac{\mu + d + c_3}{S}\right) dS \\ &= c_1(\ln q_{4,2} - \ln I_b) + c_2(\ln S_b - \ln q_{1,1}) + c_3(\ln q_{3,1} - \ln S_b) > 0 \end{aligned}$$

since $q_{1,1} < S_b < q_{3,1}$ and $q_{4,2} > I_b$. This is a contradiction. So the periodic solution Γ cannot exist.

Similar computations show that no periodic orbit can cross only M_1 or only M_2.

The condition $R_1 > 1$ implies that E_{10} is unstable. This condition is always satisfied in the model that we consider. □

Remark It should be noted that Dulac's Theorem relies on continuity and hence cannot be applied directly to Filippov systems. However, our proof follows the same idea as Dulac's Theorem, by using Green's Theorem and considering the boundary to be away from the discontinuities, in order to produce the result.

3.2 Sliding mode on M_2 and its dynamics

Proposition 3.3 (Zhao et al. 2013) *The sliding region Ω_2 is the set of all points on M_2 such that $\langle n_2, f_2\rangle > 0$ and $\langle n_2, f_3\rangle < 0$.*

We have $\langle n_2, f_2\rangle > 0$ for $I < g_4 \equiv (\Lambda - \mu S_b)/(\beta S_b)$ and $\langle n_2, f_3\rangle < 0$ for $I > g_5 \equiv \big(\Lambda - (\mu + c_1)S_b\big)/(\beta S_b)$. We have $g_5 < g_4$ because $c_1 > 0$. So, as long as $I_b < g_4$, we get the sliding domain $\Omega_2 \subset M_2$ defined as

$$\Omega_2 = \Big\{(S, I) \in M_2 : \max\{g_5, I_b\} < I < g_4\Big\}. \tag{3.8}$$

The condition $S_b < h_1$ implies that $g_3 < g_5$ because $c_3 > 0$, and $g_1 < g_4$. Thus

$$g_3 < g_1, g_5 < g_4. \tag{3.9}$$

There is no sliding domain on M_2 for $I_b > g_4$.

Again, by the Filippov convex method, the sliding mode equation on Ω_2 is given by

$$\begin{pmatrix} S' \\ I' \end{pmatrix} = \psi_2 f_2 + (1 - \psi_2) f_3, \quad \text{where } \psi_2 = \frac{\langle n_2, f_3\rangle}{\langle n_2, f_3 - f_2\rangle}.$$

Thus

$$\begin{pmatrix} S' \\ I' \end{pmatrix} = \begin{pmatrix} 0 \\ I\left(\beta S - (\mu + d + c_3) + \dfrac{(c_3 - c_2)\,(\beta SI + (\mu + c_1)S - \Lambda)}{c_1 S}\right) \end{pmatrix}. \quad (3.10)$$

System (3.10) has an obvious equilibrium point given by $E_{S2} \equiv (S_b, g_6)$, where

$$g_6 = \frac{c_1 S_b\,((\mu + d + c_3) - \beta S_b) + (c_3 - c_2)\,(\Lambda - S_b(\mu + c_1))}{\beta S_b (c_3 - c_2)}.$$

This becomes a pseudoequilibrium in our system only if

$$\max\{g_5, I_b\} < g_6 < g_4. \quad (3.11)$$

However, it is unstable on Ω_2.

Theorem 3.4 *E_{S2} is an unstable sliding equilibrium on $\Omega_2 \subset M_2$. This is true independently of the value of S_b.*

Proof

$$\frac{\partial}{\partial I}\left(\frac{I\left(c_1 S_b\left(\beta S_b - (\mu + d + c_3)\right) + (c_3 - c_2)\left(S_b(\mu + c_1) - \Lambda\right) + \beta S_b (c_3 - c_2) I\right)}{c_1 S_b}\right)\Bigg|_{g_6}$$
$$= \frac{c_1 S_b\left((\mu + d + c_3) - \beta S_b\right) + (c_3 - c_2)\left(\Lambda - S_b(\mu + c_1)\right)}{c_1 S_b} > 0$$

because $g_6 > 0$ and $c_3 > c_2$. □

3.3 Stability of the endemic states

In this section, we are going to investigate the stability of endemic states with a fixed tolerance threshold $S_b < h_1$ as we vary the tolerance threshold I_b. Since $S_b < h_1 < h_2$ in Case A, the equilibrium E_{21} is not present in the system (it is a virtual equilibrium) for any values of I_b. So there is no real equilibrium in region G_2. However, equilibria E_{11} and E_{31} may be present depending on the value of the tolerance threshold I_b.

Moreover, we assume that $R_1 > 1$. Thus the equilibrium E_{10} on the S-axis is unstable according to Theorem 2.3.

3.3.1 Case 1: $I_b < g_3 < g_2 < g_1$

In this case, E_{11} and E_{21} are not present in the system (2.1) but E_{31} is. $E_{S1} \notin \Omega_1 \subset M_1$ since (3.3) is not satisfied. Moreover, since $S_b < h_1 = \frac{\mu + d}{\beta}$, we have

$$g_6 = g_4 + \frac{c_1(\mu + d + c_2 - \beta S_b)}{\beta(c_3 - c_2)} > g_4.$$

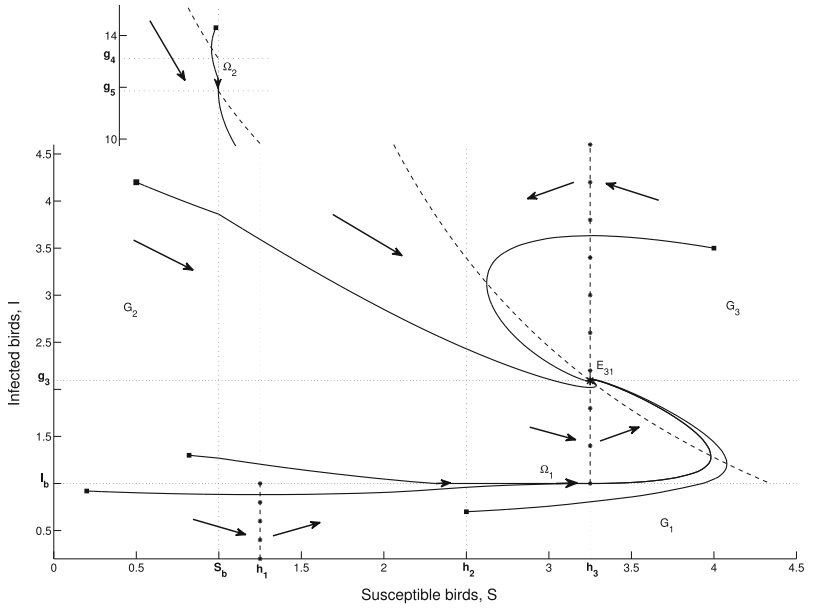

Fig. 2 E_{31} is globally asymptotically stable if $R_1 > 1$, $S_b < h_1$ and $I_b < g_3 < g_2 < g_1$. *Inset* Behaviour when the number of infected birds is large

Thus E_{S2} is not in Ω_2. We claim that E_{31} is globally asymptotically stable if $I_b < g_3 < g_2 < g_1$.

Theorem 3.5 *E_{31} is globally asymptotically stable if $I_b < g_3 < g_2 < g_1$ and $R_1 > 1$.*

Proof The proof is identical to the proof of Theorem 3.2. □

From Fig. 2, where $I_b = 1$ is chosen, we can see that all solutions of model (2.1) will approach E_{31} as $t \to \infty$ as stated in Theorem 3.5. Note that for the chosen parametric values, we have $R_1 > 1$ and E_{10} is unstable.

Throughout this paper, the S-nullclines and I-nullclines of model (2.1) are represented by the dashed curves and asterisk dashed lines, respectively. The curve $\{(S, I) \in \mathbb{R}^2_+ : I = \frac{1}{\beta}(\frac{\Lambda}{S} - \mu)\}$ is the S-nullcline of systems f_1 and f_2, whereas the curve $\{(S, I) \in \mathbb{R}^2_+ : I = \frac{1}{\beta}(\frac{\Lambda}{S} - (\mu + c_1))\}$ is the S-nullcline of system f_3. Furthermore, $S = h_1, h_2$ and h_3 are the I-nullclines of systems f_1, f_2 and f_3, respectively. All associated parameters that are used in the numerical simulations are stated in Table 1. Nevertheless, there is one exception: to get all figures of manageable size, we define $\mu = 0.4$. For Case A, we pick $S_b = 1$.

3.3.2 Case 2: $g_3 < I_b < g_2 < g_1$ or $g_3 < g_2 < I_b < g_1$

In both cases, E_{11}, E_{21} and E_{31} are virtual equilibria because $g_1 > I_b$, $h_2 > S_b$ and $g_3 < I_b$ respectively. Thus, E_{11}, E_{21} and E_{31} are not present in system (2.1).

Table 1 Avian-only model (2.1) parameters

	Description	Sample value	Units	References
Λ	Bird inflow	2060/365	Individuals per day	Martcheva (2014)
μ	Natural death of birds	$1/(2 \times 365)$	Per day	Tuncer and Martcheva (2013)
β	Rate at which birds contract avian influenza	0.4	Per individual per day	Gumel (2009)
d	Disease death rate due to avian influenza in birds	0.1	Per day	Tuncer and Martcheva (2013)
c_1	Culling rate of susceptible birds for $S > S_b$ and $I > I_b$	0.5	Per day	Assumed
c_2	Culling rate of infected birds for $S < S_b$ and $I > I_b$	0.5	Per day	Assumed
c_3	Culling rate of infected birds for $S > S_b$ and $I > I_b$	0.8	Per day	Assumed

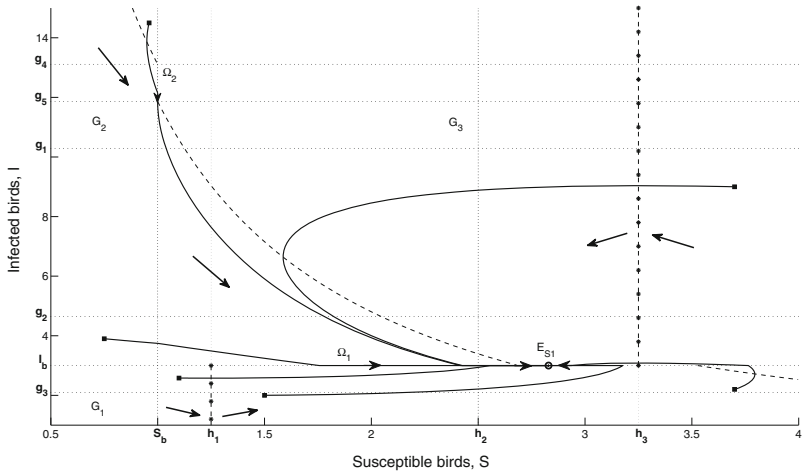

Fig. 3 $E_{S1} \in \Omega_1 \subset M_1$ is globally asymptotically stable if $S_b < h_1$, $g_3 < I_b < g_2 < g_1$ and $R_1 > 1$

$E_{S1} \in \Omega_1 \subset M_1$ is a pseudoequilibrium since (3.3) is satisfied. Moreover, E_{S1} is globally asymptotically stable according to Theorem 3.2.

Theorem 3.6 *E_{S1} is a globally asymptotically stable pseudoequilibrium if $g_3 < I_b < g_2 < g_1$ or $g_3 < g_2 < I_b < g_1$, and $R_1 > 1$.*

The phase portrait for Case 2 with $g_3 < I_b < g_2 < g_1$ is represented in Fig. 3, where $I_b = 3$ is chosen. The phase portrait for $g_3 < g_2 < I_b < g_1$ is similar to Fig. 3 and will not be given.

3.3.3 Case 3: $g_3 < g_2 < g_1 < I_b$

We have the equilibrium $E_{11} \in G_1$ because $g_3 < g_2 < g_1 < I_b$. However, this condition also implies that E_{21} and E_{31} are not present in the system. Moreover, $E_{S1} \notin \Omega_1 \subset M_1$ since (3.3) is not satisfied.

Theorem 3.7 *There is no closed orbit lying in region* G_1.

Proof We have $f_{1,1} = \Lambda - \beta SI - \mu S$ and $f_{1,2} = \beta SI - (\mu + d)I$. Consider a Dulac function $B_1(S, I) = \frac{1}{SI}$ for all $(S, I) \in G_1$. We get

$$\begin{aligned}\frac{\partial\big(B_1 f_{1,1}\big)}{\partial S} + \frac{\partial\big(B_1 f_{1,2}\big)}{\partial I} &= \frac{\partial}{\partial S}\Big(\frac{\Lambda}{SI} - \beta - \frac{\mu}{I}\Big) + \frac{\partial}{\partial I}\Big(\beta - \frac{\mu + d}{S}\Big)\\ &= -\frac{\Lambda}{S^2 I}\\ &< 0 \quad \forall (S, I) \in G_1.\end{aligned}$$

Therefore, by the Bendixson–Dulac theorem, there is no closed orbit lying entirely within region G_1. □

Theorem 3.8 E_{11} *is globally asymptotically stable if* $g_3 < g_2 < g_1 < I_b$ *and* $R_1 > 1$.

Proof We define regions D_1, D_2, D_3 and D_4 as follows:

$$\begin{aligned}D_1 &= \big\{(S, I) \in \mathbb{R}^2_+ : S \le h_3 \text{ and } I > I_b\big\},\\ D_2 &= \big\{(S, I) \in \mathbb{R}^2_+ : S > h_3 \text{ and } I > I_b\big\},\\ D_3 &= \left\{(S, I) \in \mathbb{R}^2_+ : I > \frac{1}{\beta}\left(\frac{\Lambda}{S} - \mu\right) \text{ and } I \le I_b\right\} \text{ and}\\ D_4 &= \left\{(S, I) \in \mathbb{R}^2_+ : I < \frac{1}{\beta}\left(\frac{\Lambda}{S} - \mu\right) \text{ and } I \le I_b\right\}.\end{aligned}$$

The vector field in each region is denoted by arrows, as shown in Fig. 4 with $S_b = 1$ and $I_b = 12$. The flow to the right of the S-nullcline is moving to the left, while to the left of the S-nullcline it is moving to the right.

In addition, by Theorems 2.4 and 3.7, E_{11} is locally asymptotically stable and there is no limit cycle in region G_1. The possible trajectories for this case are as follows:

(i) A trajectory with initial point in region D_4 either converges to E_{11} directly or moves downward for $S < h_1$, then upward for $S > h_1$ and finally crosses the S-nullcline to enter the region D_3 and converge to E_{11}.

(ii) A trajectory with initial point in region D_3 converges to E_{11} directly or moves upward for $S > h_1$, then downward for $S < h_1$ and finally crosses the S-nullcline to enter the region D_4 and converge to E_{11}. An orbit starting in D_3 may also go up until it enters the region D_2 through $I = I_b$ or reaches the sliding domain. In both cases, the orbit goes on to enter D_3 or D_4 with $S < h_1$ and converges to E_{11}.

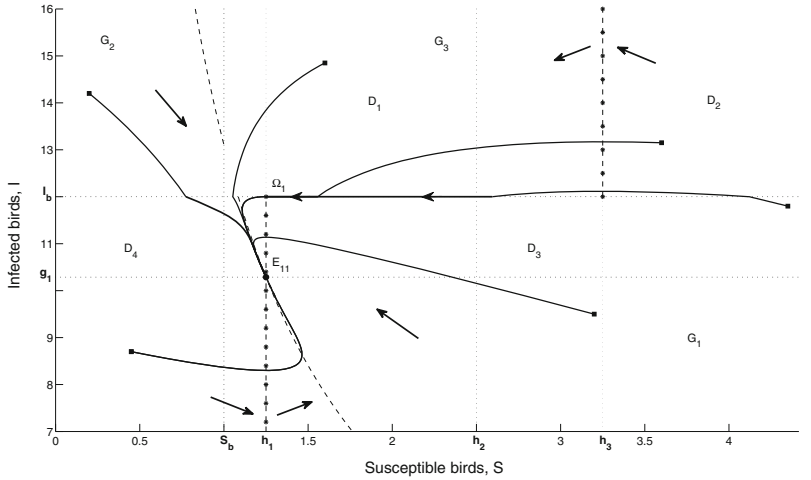

Fig. 4 E_{11} is globally asymptotically stable if $S_b < h_1$, $g_3 < g_2 < g_1 < I_b$ and $R_1 > 1$

(iii) A trajectory that begins in region D_1 moves downward to either enter the region D_3 through $I = I_b$ or the region D_4.
(iv) A trajectory with initial condition in region D_2 moves to the left to either enter the region D_1 through the line $S = h_3$ and then heads to region D_3 or D_4 with $S < h_1$. In all cases, the orbit finally converges to E_{11}.

Since E_{10} is unstable whenever $R_1 > 1$, we conclude that E_{11} is globally asymptotically stable in $\mathbb{R}^2_+$ if $g_3 < g_2 < g_1 < I_b$. □

4 Case B: $h_1 < S_b < h_2$

We will proceed as in Sect. 3 to study the dynamics of (2.1) including the sliding mode on M_1 and M_2 and the stability of endemic states.

4.1 Sliding mode on M_1 and its dynamics

For Case B, we have two sliding domains on M_1.

$$\Omega_3 = \{(S, I) \in M_1; h_1 < S < S_b\}$$

and

$$\Omega_4 = \{(S, I) \in M_1; S_b < S < h_3\}.$$

The dynamics on $\Omega_4 \subset M_1$ are described by (3.2), whereas on $\Omega_3 \subset M_1$, they are governed by

$$\begin{pmatrix} S' \\ I' \end{pmatrix} = \begin{pmatrix} \Lambda - \beta I_b S - \mu S \\ 0 \end{pmatrix}. \tag{4.1}$$

There is a sliding equilibrium for (4.1) at $E_{S3} = (h_5, I_b)$, where $h_5 = \frac{\Lambda}{\beta I_b + \mu}$, and a sliding equilibrium for (3.2) at $E_{S1} = (h_4, I_b)$.

E_{S3} is a pseudoequilibrium if

$$h_1 < h_5 < S_b \tag{4.2}$$

and E_{S1} is a pseudoequilibrium if

$$S_b < h_4 < h_3. \tag{4.3}$$

Proposition 4.1 *We have*

$$h_1 < h_5 < S_b \Leftrightarrow g_4 < I_b < g_1 \tag{4.4}$$

and

$$S_b < h_4 < h_3 \Leftrightarrow g_3 < I_b < g_8 \equiv g_4 + \frac{c_1(\mu + d - \beta S_b)}{\beta c_3}. \tag{4.5}$$

The proof is lengthy, but trivial.

In (4.5), $g_3 < g_2 - \frac{c_1 c_2}{\beta c_3} < g_8 < g_4 < g_1$ since $h_1 < S_b < h_2$ yields $-\frac{c_1 c_2}{\beta c_3} < \frac{c_1(\mu + d - \beta S_b)}{\beta c_3} < 0$.

Corollary 4.2 *The pseudoequilibria E_{S1} and E_{S3} are mutually exclusive.*

We note that $h_1 < S_b < h_2$ implies that $g_2 < g_4 < g_1$; this last inequality will play a crucial role in the cases below.

4.2 Sliding mode on M_2 and its dynamics

By Definition 3.3, the sliding domain $\Omega_2 \subset M_2$ for $I < g_4$ is given by (3.8), and there is no sliding domain for $I > g_4$. As we have seen, we get $g_2 < g_4 < g_1$ from $h_1 < S_b < h_2$. Moreover, $h_1 < S_b < h_2$ yields

$$g_3 < \frac{\Lambda\beta - (\mu + c_1)(\mu + d + c_2)}{\beta(\mu + d + c_2)} < g_5 < \frac{\Lambda\beta - (\mu + d)(\mu + c_1)}{\beta(\mu + d)} < g_1.$$

The sliding mode on Ω_2 is governed by Eq. (3.10) and the sliding equilibrium $E_{S2} = (S_b, g_6)$, if present in the system, is unstable on $\Omega_2 \subset M_2$ as proven in Theorem 3.4. Since $g_6 = g_4 - \frac{c_1}{\beta} + \frac{c_1(\mu + d + c_3 - \beta S_b)}{\beta(c_3 - c_2)} > g_4$ whenever $h_1 < S_b < h_2$, then $E_{S2} \notin \Omega_2 \subset M_2$.

4.3 Stability of the endemic states

For a fixed threshold level S_b such that $h_1 < S_b < h_2$, E_{21} is a virtual equilibrium and so it is not present in system (2.1). However, E_{11} and E_{31} are real equilibria if $E_{11} \in G_1$ and $E_{31} \in G_3$, respectively. In the following subsections, we are going to study the stability of the endemic states that we will illustrate with several numerical simulations. The associated parameters involved in the numerical simulations are defined in Table 1.

4.3.1 Case 4: $I_b < g_3 < g_2 < g_1$

Under these conditions, E_{11} and E_{21} are virtual equilibria, whereas E_{31} is a real equilibrium. It follows from Proposition 4.1 that E_{S1} and E_{S3} are not pseudoequilibria; namely, $E_{S1} \notin \Omega_4$ and $E_{S3} \notin \Omega_3$.

Proceeding as we did for Theorem 3.5, we get the following result.

Theorem 4.3 *E_{31} is globally asymptotically stable for $I_b < g_3 < g_2 < g_1$ and $R_1 > 1$.*

Theorem 4.3 is illustrated in Fig. 5 with $S_b = 2$ and $I_b = 1$. All solutions with any initial conditions in $\mathbb{R}^2_+$ converge to E_{31} as t increases.

4.3.2 Case 5: $g_3 < I_b < g_2 < g_1$

In the present case, E_{11}, E_{21} and E_{31} are virtual equilibria and so not present in the system (2.1). This case must be divided in two subcases: $g_8 > g_2$ and $g_8 < g_2$.

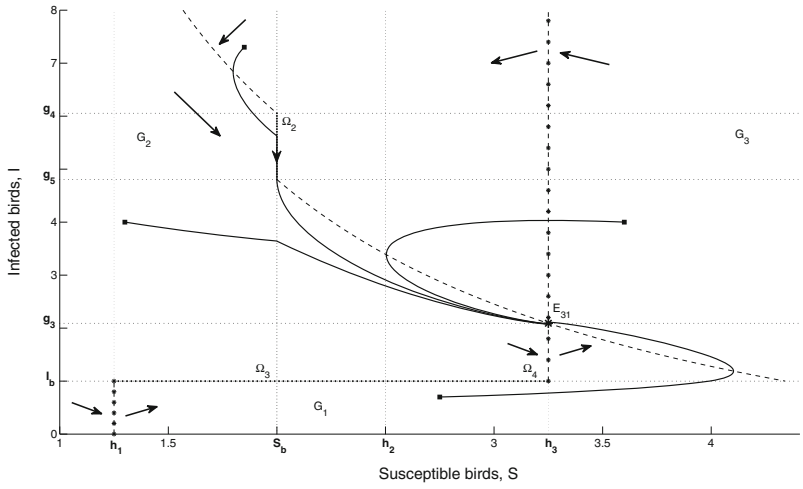

Fig. 5 E_{31} is globally asymptotically stable for $h_1 < S_b < h_2$, $I_b < g_3 < g_2 < g_1$ and $R_1 > 1$

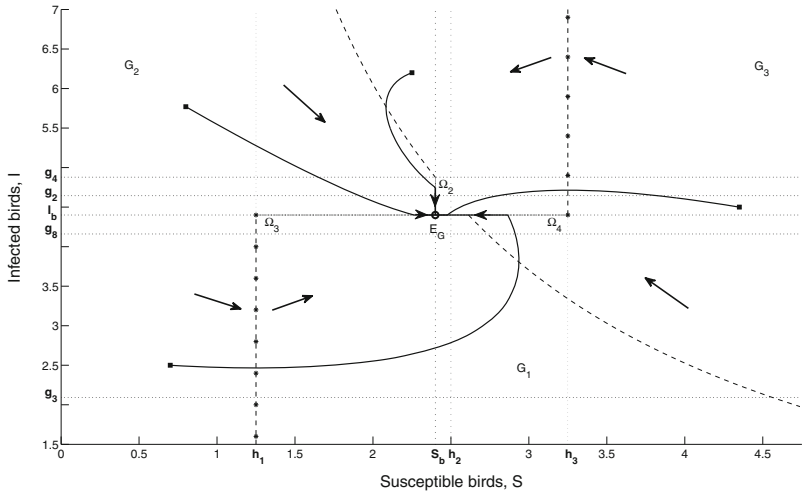

Fig. 6 E_G is a global pseudo-attractor whenever $h_1 < S_b < h_2$, $g_3 < g_8 < I_b < g_2 < g_1$ and $R_1 > 1$

First, we note that E_{S3} is not a pseudoequilibrium in the present case. Moreover, using a technique similar to the one used in the proof of the non-existence of limit cycles in Theorem 3.2, the reader can prove the following theorem.

Theorem 4.4 *Since $g_3 < I_b < g_8$, then $E_{S1} \in \Omega_4 \subset M_1$ is globally asymptotically stable if $R_1 > 1$.*

If $g_3 < I_b < g_2 < g_8 < g_1$, the point $E_{S1} \in \Omega_4 \subset M_1$ is a globally asymptotically stable pseudoequilibrium. The phase space in this case is similar to the phase portrait represented in Fig. 3 and will not be given.

If $g_3 < I_b < g_8 < g_2$, then we have the same dynamic as above. However, if $g_3 < g_8 < I_b < g_2$, no equilibrium exists in the system. However, all orbits will converge in a finite time to $E_G = (S_b, I_b)$; we call such an attracting point a pseudo-attractor. The phase portrait in this case is represented in Fig. 6 with $S_b = 2.4$ and $I_b = 4.4$.

4.3.3 Case 6: $g_3 < g_2 < I_b < g_1$

We have that E_{11}, E_{21} and E_{31} are virtual equilibria; so, they are not present in (2.1). As in Case 5, we have to consider $g_8 < g_2$ and $g_8 > g_2$.

Recall that $g_2 < g_4 < g_1$ in Case B. If $g_4 < I_b < g_1$, independently of $g_8 < g_2$ or $g_8 > g_2$, it follows from (4.4) that E_{S3} is a pseudoequilibrium. Again, using an approach similar to the one used in the proof of the non-existence of limit cycles in Theorem 3.2, we get the following theorem.

Theorem 4.5 *If $g_4 < I_b < g_1$, then $E_{S3} \in \Omega_3 \subset M_1$ is globally asymptotically stable if $R_1 > 1$.*

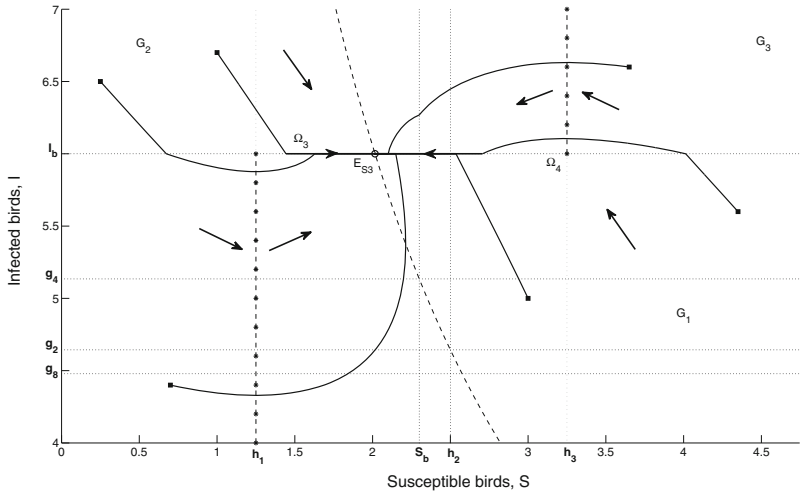

Fig. 7 $E_{S3} \in \Omega_3 \subset M_1$ is a globally asymptotically stable pseudoequilibrium if $h_1 < S_b < h_2$, $g_3 < g_8 < g_2 < g_4 < I_b < g_1$ and $R_1 > 1$

If $g_8 < g_2 < g_4 < I_b < g_1$ or $g_2 < g_8 < g_4 < I_b < g_1$, we get the same phase space. So for this case, we only depict the numerical result of $g_3 < g_8 < g_2 < g_4 < I_b < g_1$ with $S_b = 2.3$ and $I_b = 6$, which is as shown in Fig. 7.

If $g_2 < g_8 < I_b < g_4 < g_1$ or $g_8 < g_2 < I_b < g_4 < g_1$, then no equilibrium can be found in this system and E_G becomes again a global pseudo-attractor. The phase portrait for the case $g_2 < g_8 < I_b < g_4 < g_1$ is given in Fig. 8, where $S_b = 2.2$ and $I_b = 5$.

Finally, if $g_2 < I_b < g_8$, then we may use Theorem 4.4 to conclude that E_{S1} is a globally asymptotically stable pseudoequilibrium. The point E_{S3} is not a pseudoequilibrium according to (4.4). The phase portrait of this case is similar to the phase portrait in Fig. 3.

4.3.4 Case 7: $g_3 < g_2 < g_1 < I_b$

In this case, E_{21} and E_{31} are not equilibria for (2.1), but E_{11} is an equilibrium. Moreover, E_{S3} and E_{S1} are not pseudoequilibria as the requirements of (4.2) and (4.3) are not met, according to Proposition 4.1.

Theorem 4.6 *The equilibrium E_{11} is globally asymptotically stable if $I_b > g_1$ and $R_1 > 1$.*

The proof of this theorem is identical to the proof of Theorem 3.8 since E_{11} is asymptotically stable in G_1 by Theorem 2.4. It is globally asymptotically stable because there are no periodic orbits in G_1 and, eventually, all orbits enter the region G_1 and do not leave it. The phase portrait for this case is similar to Fig. 4.

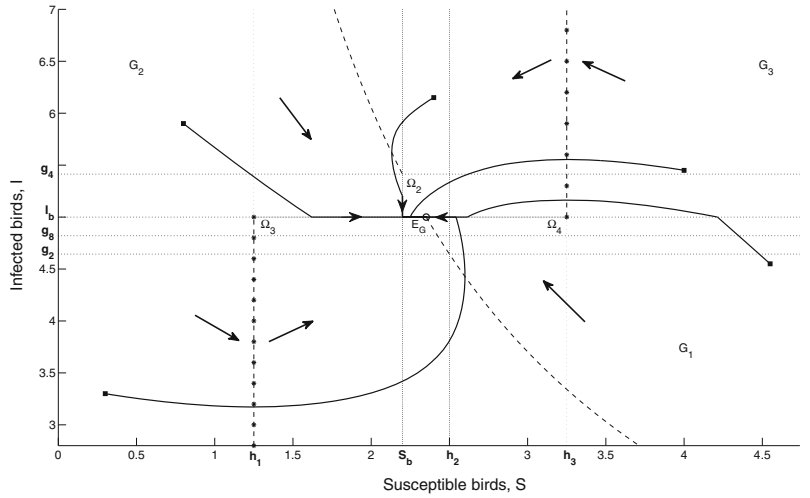

Fig. 8 E_G is a global attractor if $h_1 < S_b < h_2$ and $g_3 < g_2 < g_8 < I_b < g_4 < g_1$

5 Case C: $h_2 < S_b < h_3$

5.1 Sliding mode on M_1 and its dynamics

The sliding domains on M_1 are

$$\Omega_5 = \{(S, I) \in M_1; h_1 < S < h_2\} \quad \text{and} \quad \Omega_6 = \{(S, I) \in M_1; S_b < S < h_3\}.$$

The dynamics on Ω_5 are governed by (4.1), whereas the dynamics on Ω_6 are governed by (3.2).

$E_{S3} = (h_5, I_b)$ and $E_{S1} = (h_4, I_b)$ are the sliding equilibria on Ω_5 and Ω_6, respectively. The following proposition gives the conditions for E_{S3} and E_{S1} to be pseudoequilibria.

Proposition 5.1 *Let* $g_7 = g_4 - \frac{c_1[\beta S_b - (\mu+d)]}{\beta c_3}$. *Since* $h_2 < S_b < h_3$, *we have* $g_3 < g_7 < g_4 < g_2$. *Moreover,*

$$S_b < h_4 < h_3 \Leftrightarrow g_3 < I_b < g_7 \tag{5.1}$$

and

$$h_1 < h_5 < h_2 \Leftrightarrow g_2 < I_b < g_1. \tag{5.2}$$

Thus E_{S1} is a pseudoequilibrium if $g_3 < I_b < g_7$ and E_{S3} is a pseudoequilibrium if $g_2 < I_b < g_1$.

5.2 Sliding mode on M_2 and its dynamics

Everything from Sect. 3.2 is still valid. In particular, the sliding region $\Omega_2 \subset M_2$ is defined in (3.8). There is a pseudoequilibrium $E_{S2} = (S_b, g_6)$ only if (3.11) is satisfied. It is always unstable.

We note that $h_2 < S_b < h_3$ yields $g_3 < g_5 < g_4 < g_2$. Moreover, since $S_b < h_3 = \frac{\mu+d+c_3}{\beta}$, we get

$$g_6 = \frac{c_1(\mu + d + c_3 - \beta S_b)}{\beta(c_3 - c_2)} + \frac{\Lambda - (\mu + c_1)S_b}{\beta S_b} > \frac{\Lambda - (\mu + c_1)S_b}{\beta S_b} = g_5,$$

and since $S_b > h_2 = \frac{\mu+d+c_2}{\beta}$, we get

$$g_6 = \frac{c_1(\mu + d + c_3 - \beta S_b)}{\beta(c_3 - c_2)} + \frac{\Lambda - (\mu + c_1)S_b}{\beta S_b} = g_4 + \frac{c_1(\mu + d + c_2 - \beta S_b)}{\beta(c_3 - c_2)} < g_4.$$

The condition (3.11) is therefore always satisfied and the pseudoequilibrium E_{S2} is always present if $I_b < g_6$.

5.3 Stability of the endemic states

A similar analysis as exhibited in Sects. 3.3 and 4.3 is applied here. For Case C, we pick $S_b = 3$ to execute several numerical simulations in order to demonstrate the theoretical results.

5.3.1 Case 8: $I_b < g_3 < g_2 < g_1$

In the present case, E_{21} and E_{31} are real equilibria, whereas E_{11} is a virtual equilibrium. Furthermore, there is no pseudoequilibrium other than E_{S2} whenever $I_b < g_3 < g_2 < g_1$. In the following theorem, it is proven that E_{21} and E_{31} are locally asymptotically stable.

Theorem 5.2 *If $h_2 < S_b < h_3$, then E_{21} is locally asymptotically stable for $I_b < g_2$ and E_{31} is locally asymptotically stable for $I_b < g_3$.*

Proof The linearization $J_2(E_{21})$ of (2.1) at E_{21} has the eigenvalues

$$\lambda_{\pm} = \frac{1}{2}\left\{-\frac{\Lambda\beta}{\mu + d + c_2} \pm \sqrt{\triangle_2}\right\}$$

where

$$\triangle_2 = \left(\frac{\Lambda\beta}{\mu + d + c_2}\right)^2 - 4\big[\Lambda\beta - \mu(\mu + d + c_2)\big].$$

Since $I_b < g_2$, we have $\Lambda\beta - \mu(\mu + d + c_2) > \beta I_b(\mu + d + c_2) > 0$, where all associated parameters are positive. Thus $\triangle_2 < \left(\frac{\Lambda\beta}{\mu+d+c_2}\right)^2$. Hence the real part of $\lambda_\pm$ is always negative. We can have $\triangle_2 \geq 0$ or $\triangle_2 < 0$; thus E_{21} is either a stable node in the first case or a stable spiral in the latter case.

A similar argument shows that E_{31} is also locally asymptotically stable if $I_b < g_3 < g_2 < g_1$. □

Since there are no periodic orbits in $\mathbb{R}^2_+$, almost all solutions of (2.1) in $\mathbb{R}^2_+$ will converge to either E_{21} or E_{31} as $t \to \infty$. The exceptions are the two orbits associated to the stable manifold of the equilibrium E_{S2}; together, they form the separatrix between the ω-limit sets of E_{21} and E_{31}.

Figure 9 displays the phase portrait for Case 8 with $I_b = 1$.

5.3.2 Case 9: $g_3 < I_b < g_2 < g_1$

In this case, E_{21} is a real equilibrium, but E_{11} and E_{31} are virtual equilibria. We also have that E_{S2} is an unstable pseudoequilibrium as long as $I_b < g_6$.

A simple computation gives

$$h_2 < S_b < h_3 \Leftrightarrow g_5 < g_7 < g_4 - \frac{c_1 c_2}{\beta c_3}.$$

Proposition 5.3 *Since* $c_3 > c_2 > 0$ *and* $h_2 < S_b < h_3$, *then*

$$g_6 = g_7 + \frac{c_1 c_2\,(\mu + d + c_3 - \beta S_b)}{\beta c_3 (c_3 - c_2)} > g_7.$$

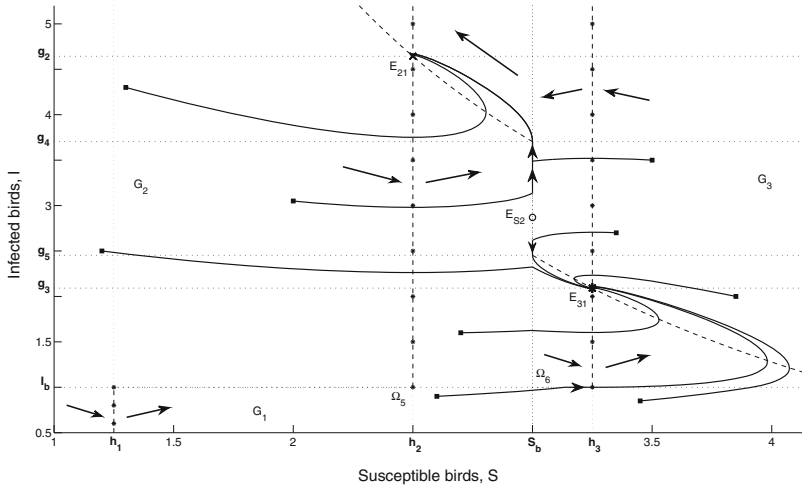

Fig. 9 E_{21} and E_{31} are locally asymptotically stable if $h_2 < S_b < h_3$, $I_b < g_3 < g_2 < g_1$ and $R_1 > 1$

Hence $g_3 < g_5 < g_7 < g_6 < g_4 < g_2 < g_1$.

This is a consequence of the fact that $h_2 < S_b < h_3$ implies $0 < \mu + d + c_3 - \beta S_b < c_3 - c_2$.

If $g_3 < I_b < g_7$, we have one equilibrium, E_{21}, and two pseudoequilibria, E_{S1} and E_{S2}. We have seen in Theorem 5.2 that E_{21} is locally asymptotically stable, and in Theorem 3.4 that E_{S2} is always unstable. The following theorem addresses the stability of E_{S1}.

Theorem 5.4 *$E_{S1} \in \Omega_6 \subset M_1$ is locally asymptotically stable if $g_3 < I_b < g_7$.*

Proof $E_{S1} \in \Omega_6 \subset M_1$ is locally asymptotically stable since

$$\frac{\partial}{\partial S}\left(\frac{-\beta c_1 S^2 + (c_1(\mu+d) - c_3(\beta I_b + \mu))S + \Lambda c_3}{c_3}\right)\Bigg|_{h_4}$$
$$= \frac{-2\beta c_1 S + c_1(\mu+d) - c_3(\mu+\beta I_b)}{c_3}\Bigg|_{h_4} = \frac{-\sqrt{B^2 - 4AC}}{c_3} < 0,$$

where $c_3, \sqrt{B^2 - 4AC} > 0$. □

Hence the orbits in $\mathbb{R}^2_+$ of the system (2.1) will either converge to E_{S1} or E_{21} as t increases except for the two orbits associated to the stable manifold of the unstable pseudoequilibrium E_{S2}. The phase portrait for this case can be found in Fig. 10 with $I_b = 2.3$.

If $g_7 < I_b < g_6$, the system (2.1) has a pseudo-attractor E_G, a locally asymptotically stable equilibrium E_{21} and an unstable pseudoequilibrium E_{S2}. All trajectories

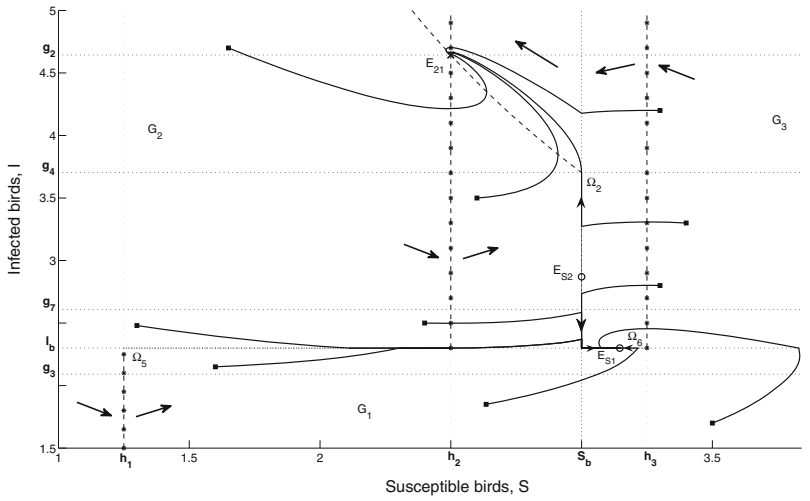

Fig. 10 E_{21} and $E_{S1} \in \Omega_6 \subset M_1$ are locally asymptotically stable if $h_2 < S_b < h_3$ and $g_3 < I_b < g_7 < g_6 < g_4 < g_2 < g_1$

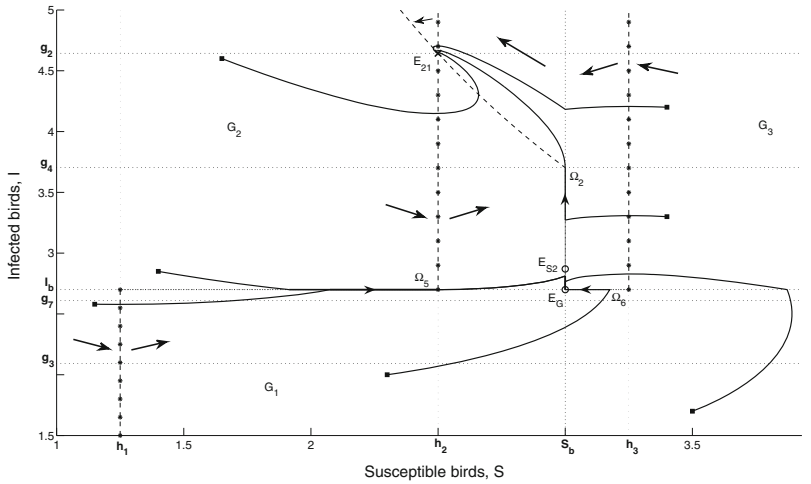

Fig. 11 E_{21} is locally asymptotically stable and E_G is a pseudo-attractor if $h_2 < S_b < h_3$ and $g_3 < g_7 < I_b < g_6 < g_4 < g_2 < g_1$

with arbitrary initial points in $\mathbb{R}^2_+$ will either converge to E_{21} or E_G as t increases. The two orbits associated to the stable manifold of the unstable pseudoequilibrium E_{S2} form a separatrix between the ω-limit sets of E_{21} and E_G. The phase portrait of this system is given in Fig. 11, where $I_b = 2.7$.

If $g_6 < I_b < g_2$, we have only the equilibrium E_{21}. Therefore E_{21} is globally asymptotically stable. The phase portrait of the system for $g_6 < I_b < g_4 < g_2$ is given in Fig. 12, where $I_b = 3.2$. The phase portrait for the case $g_6 < g_4 < I_b < g_2$ is qualitatively similar to the one given in Fig. 12 and is not given here.

5.3.3 Case 10: $g_3 < g_2 < I_b < g_1$

E_{11}, E_{21} and E_{31} are all virtual equilibria. Moreover, from (4.5), we find that E_{S1} is not a pseudoequilibrium because $I_b > g_2 > g_7$ and the sliding domain on M_2 (i.e., Ω_2) does not exist as $I_b > g_2 > g_4$. The system (2.1) has only the pseudoequilibrium E_{S3} since (5.2) is fulfilled.

The following theorem proves that $E_{S3} \in \Omega_5 \subset M_1$ is globally asymptotically stable.

Theorem 5.5 *$E_{S3} \in \Omega_5 \subset M_1$ is globally asymptotically stable if $h_2 < S_b < h_3$, $g_3 < g_2 < I_b < g_1$ and $R_1 > 1$.*

The proof of Theorem 5.5 is similar to the proof of Theorem 3.2.

Furthermore, the phase portrait of Case 10 is described in Fig. 13, where $I_b = 7$.

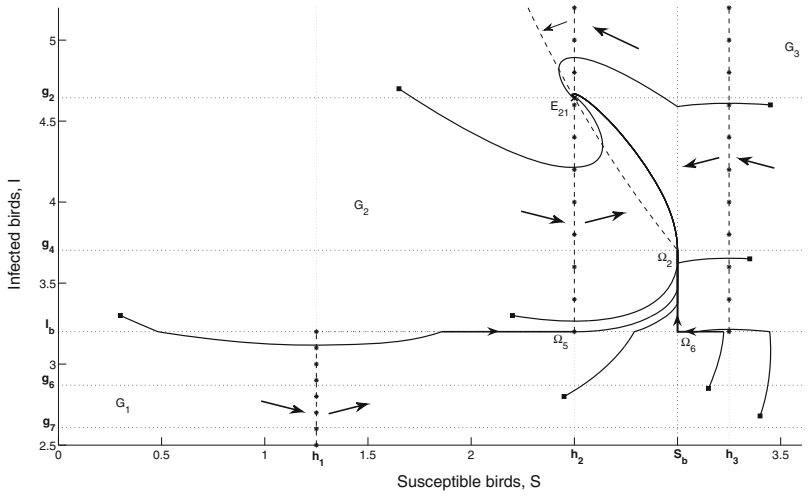

Fig. 12 E_{21} is globally asymptotically stable if $h_2 < S_b < h_3$ and $g_3 < g_7 < g_6 < I_b < g_4 < g_2 < g_1$

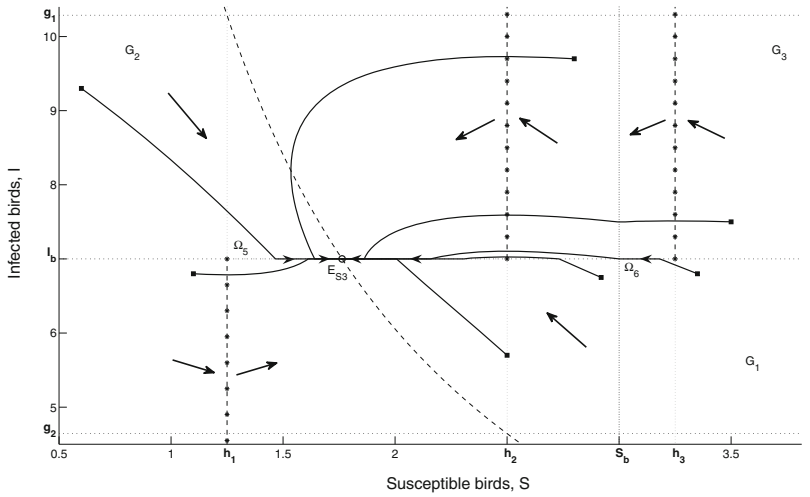

Fig. 13 $E_{S3} \in \Omega_5 \subset M_1$ is globally asymptotically stable if $h_2 < S_b < h_3$, $g_3 < g_2 < I_b < g_1$ and $R_1 > 1$

5.3.4 Case 11: $g_3 < g_2 < g_1 < I_b$

E_{21} and E_{31} are virtual equilibria, and E_{11} is a real equilibrium. It also follows from Sects. 5.1 and 5.2 that there are no pseudoequilibria. We show below that E_{11} is globally asymptotically stable. Case 11 is similar as Case 7.

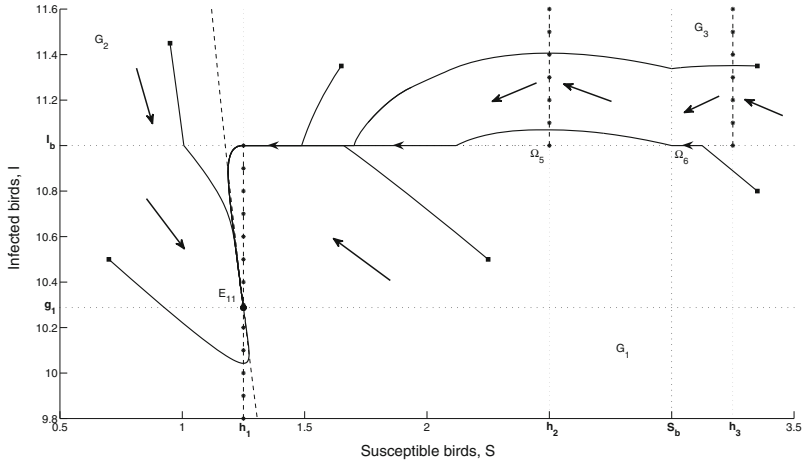

Fig. 14 E_{11} is globally asymptotically stable if $h_2 < S_b < h_3$, $g_3 < g_2 < g_1 < I_b$ and $R_1 > 1$

Theorem 5.6 *E_{11} is globally asymptotically stable if $h_2 < S_b < h_3$, $g_3 < g_2 < g_1 < I_b$ and $R_1 > 1$.*

The proof of this theorem is similar to the proof of Theorem 4.6, and so it is omitted. The phase portrait for this case is given in Fig. 14.

6 Case D: $S_b > h_3$

6.1 Sliding mode on M_1 and its dynamics

There exists a sliding domain $\Omega_5 = \{(S, I) \in M_1 : h_1 < S < h_2\}$ on M_1 and its dynamics are governed by (4.1). The sliding equilibrium $E_{S3} = (h_5, I_b) \in \Omega_5 \subset M_1$ is a pseudoequilibrium if (5.2) is satisfied.

6.2 Sliding mode on M_2 and its dynamics

We have that $\langle n_2, f_2 \rangle > 0$ and $\langle n_2, f_3 \rangle < 0$ for $g_5 < I < g_4$ as in Sect. 3.2. Furthermore, $S_b > h_3$ implies that

$$g_5 = \frac{\Lambda}{\beta S_b} - \frac{\mu + c_1}{\beta} < \frac{\Lambda}{\mu + d + c_3} - \frac{\mu + c_1}{\beta} = g_3$$

and similarly $g_4 < g_2$. Recall that

$$\Omega_2 = \{(S, I) \in M_2 : \max\{g_5, I_b\} < I < g_4\}$$

for $I_b < g_4$, while Ω_2 does not exist if $I_b \geq g_4$. The dynamics on Ω_2 are governed by (3.10). Furthermore, $h_3 < S_b$ implies that

$$g_6 = \frac{c_1(\mu + d + c_3 - \beta S_b)}{\beta(c_3 - c_2)} + \frac{\Lambda - (\mu + c_1)S_b}{\beta S_b} < \frac{\Lambda - (\mu + c_1)S_b}{\beta S_b} = g_5.$$

Thus $E_{S2} = (S_b, g_6)$ is never a pseudoequilibrium for $h_3 < S_b$.

6.3 Stability of the endemic states

The same approach as shown in Sects. 3.3, 4.3 and 5.3 is implemented in this section. E_{31} is always a virtual equilibrium because of $S_b > h_3$. Several numerical simulations are performed in this section by choosing $S_b = 4$.

6.3.1 Case 12: $I_b < g_3 < g_2 < g_1$ or $g_3 < I_b < g_2 < g_1$

There is only one equilibrium at E_{21}. The points E_{11} and E_{31} are virtual equilibria, and E_{S2} and E_{S3} are not pseudoequilibria. A simple analysis with the nullclines as we have done for the proof of Theorem 3.8 gives the following result.

Theorem 6.1 *E_{21} is globally asymptotically stable if $I_b < g_3 < g_2 < g_1$ or $g_3 < I_b < g_2 < g_1$, $S_b > h_3$ and $R_1 > 1$.*

Figure 15 depicts the numerical result of $I_b < g_3 < g_2 < g_1$. We choose $I_b = 1$ in Fig. 15. The numerical result of $g_3 < I_b < g_2 < g_1$ is omitted here since it is similar to Fig. 15.

6.3.2 Case 13: $g_3 < g_2 < I_b < g_1$

In this case, E_{11}, E_{21} and E_{31} are virtual equilibria. As we said before, E_{S2} is not a pseudoequilibrium. There is only one pseudoequilibrium E_{S3} in system (2.1). The phase portrait for this case is given in Fig. 16, where $I_b = 6$.

6.3.3 Case 14: $g_3 < g_2 < g_1 < I_b$

The equilibrium E_{11} is globally asymptotically stable whenever $g_3 < g_2 < g_1 < I_b$. The points E_{21} and E_{31} are virtual equilibrium, and E_{S2} and E_{S3} are not pseudoequilibria.

Theorem 6.2 *E_{11} is globally asymptotically stable if $S_b > h_3$, $g_3 < g_2 < g_1 < I_b$ and $R_1 > 1$.*

The numerical result of this case is relatively similar to the phase portrait given in Fig. 4.

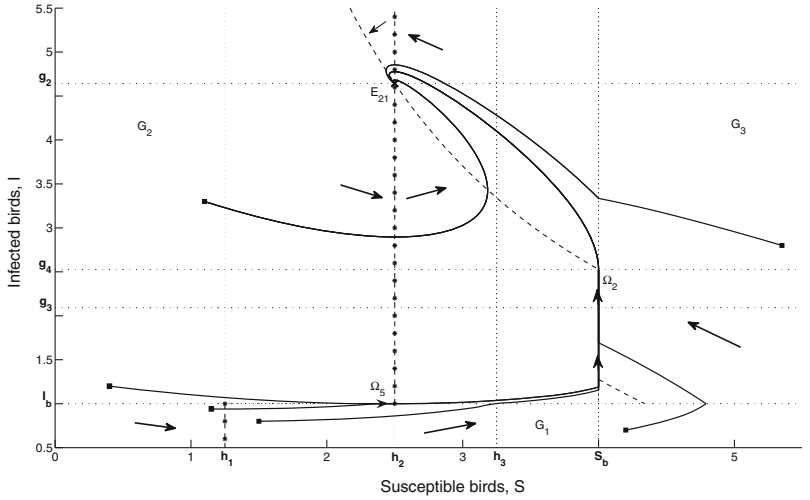

Fig. 15 E_{21} is globally asymptotically stable if $S_b > h_3$, $I_b < g_3 < g_2 < g_1$ and $R_1 > 1$

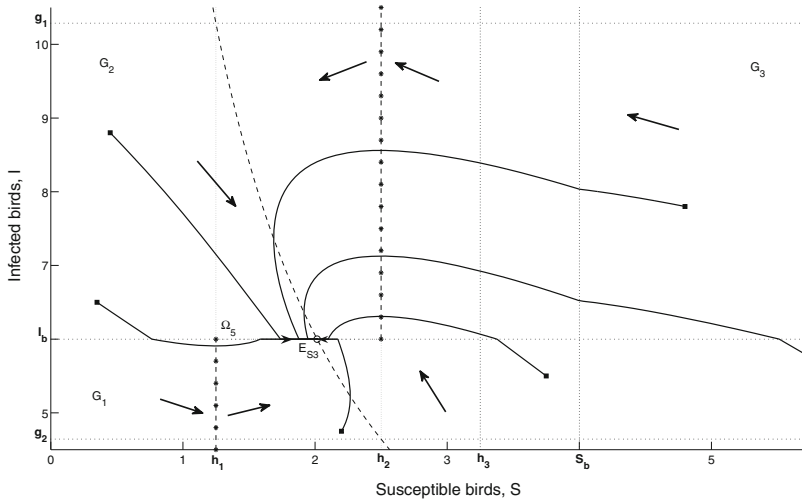

Fig. 16 $E_{S3} \in \Omega_5 \subset M_1$ is globally asymptotically stable if $S_b > h_3$, $g_3 < g_2 < I_b < g_1$ and $R_1 > 1$

7 Conclusion and discussion

The model we considered here used nonlinear ordinary differential equations with discontinuous right-hand sides, extending our previous work (Chong and Smith? 2015) by taking into account culling susceptible birds, instead of only infected birds. Since culling birds is one of the most effective strategies to control the transmission of bird

Table 2 Conclusions for Sects. 3–6

	$S_b < h_1$	$h_1 < S_b < h_2$	$h_2 < S_b < h_3$	$S_b > h_3$
$I_b < g_3$	II	II	IV	II
$g_3 < I_b < g_2$	I	$I_b < g_8$: I	$I_b < g_7 < g_6 < g_4$: III	II
		$g_8 < I_b$: I	$g_7 < I_b < g_6 < g_4$: III	
			$g_6 < I_b$: II	
$g_2 < I_b < g_1$	I	$I_b < g_8 < g_4$: I	I	I
		$g_8 < I_b < g_4$: I		
		$g_8 < g_4 < I_b$: I		
$g_1 < I_b$	I	I	I	I

flu, it was also essential for us to look into other efficient culling strategies that not only control the disease, but reduce the socio-economic impact as well (FAO 2008; Centers for Disease Control and Prevention 2012; International Animal Health Organisation 2015; Gulbudak and Martcheva 2013; Menach et al. 2006). To achieve this objective, the numbers of susceptible and infected birds were employed as reference indices in our disease-management strategy in order to determine whether or not we need to call for culling birds as a control measure.

In this model, depopulation of birds was only carried out if the number of infected birds was greater than the threshold level I_b; no application of culling strategy was carried out whenever the number of infected birds was below the threshold level I_b. When the number of infected birds was above I_b, infected birds were culled with rates c_2 and c_3 if the numbers of susceptible birds were less than or greater than the threshold level S_b, respectively. Moreover, we culled susceptible birds with rate c_1 if the number of susceptible birds exceeded the threshold level S_b, in order to prevent a serious infection among the avian population.

The results from Sects. 3–6 are summarised in Table 2, with the following biological outcomes:

I. For these choices of infected and susceptible threshold levels I_b and S_b, there is no risk of an epidemic because the infected level will always eventually converge to a level below or equal to I_b, as we can see from Figs. 3, 4, 6, 7, 8, 12, 13, 14 and 16. In these cases, there is a globally asymptotically stable equilibrium, pseudoequilibrium or pseudo-attractor below or on $I = I_b$.
II. It is virtually impossible to avoid an epidemic if the infected threshold level I_b is sufficiently low. As can be seen in Figs. 2, 5 and 15, as soon as there are some infected birds, the number will rise above I_b to reach the level of a globally asymptotically stable equilibrium.
III. If there are initially a small number of infected birds, this number may rise but will stay at a level inferior or equal to the infected threshold level I_b. However, if there are initially too many infected birds, the number of infected birds will balloon to a level higher than I_b. As can be seen in Figs. 10 and 11, for initial conditions with the number of infected birds I small enough, the orbits will converge to a pseudo-attractor or a locally stable pseudoequilibrium on $I = I_b$. However, for initial conditions with $I(0)$ large enough, the orbits will converge to the locally asymptotically stable equilibrium above $I = I_b$.

IV. This case is similar to Case II, in the sense that it is impossible to avoid an epidemic. However, the reason for this conclusion is slightly different. As seen in Fig. 9, there are two locally asymptotically stable equilibria. Since both are above the infected threshold level I_b, the number of infected birds will converge to one of these equilibria, depending on initial conditions, and an epidemic will ensue.

In Case I, there is no need to modify the culling policy. The number of infected birds will eventually be below the infected threshold level I_b. In Cases II and IV, the infected threshold level is not realistic for this bird population and must be modified.

In Case III, there may not be any need to modify the culling policy if the initial number of infected birds is kept low. However, there is a risk of epidemic if there is a large inflow of infected birds.

Our model has several limitations, which should be acknowledged. We assumed that the bird inflow in this model was a fixed constant, the culling rate c_3 was greater than the culling rate c_2 and infected birds were presumed not to move to other classes; i.e., the infected birds will only remain within the infected class. We also assumed mass action transmission, which carries with it the assumption of homogeneous contact.

In addition, a deterministic model like (2.1) is valid as long as we consider a large, well-mixed and homogeneous population in a limited area. This is the situation that we have in most large-scale industrial bird farms. If some of these conditions are not respected and the randomness in the evolution of a disease has to be considered, then a stochastic model will become more appropriate. This is, however, out of the scope of this paper. Stochastic effects are important for determining the viability of a population when the number of infected individuals is low or sparsely distributed; an epidemic that would be predicted to balloon may not if there were very few individuals. However, when dealing with large, dense populations, a threshold policy provides guidance for stemming a large-scale outbreak.

Our results have demonstrated that, by choosing appropriate threshold levels S_b and I_b, the avian influenza outbreak could either be prevented or at least stabilized at a desired level. However, we could suppress the infection of avian influenza by culling susceptible and/or infected birds whenever an avian influenza outbreak emerges. Hence, in order for us to combat or eradicate influenza in the avian population efficiently, a good threshold policy is required.

Acknowledgments The authors would like to thank the referees for all their valuable comments. NSC acknowledges support from the Ministry of Higher Education, Malaysia, and the School of Informatics and Applied Mathematics, Universiti Malaysia Terengganu. BD is supported by the University of Ottawa. RJS is supported by an NSERC Discovery Grant. For citation purposes, please note that the question mark in "Smith?" is part of his name.

References

Avian influenza—background (2006) Tech. rep., Food and Agriculture Organization. http://www.fao.org/avianflu/en/background.html

Chong NS, Smith? RJ (2015) Modelling avian influenza using filippov systems to determine culling of infected birds and quarantine. Nonlinear Anal Real World Appl 24:196–218

Dorigatti I, Mulatti P, Rosà R, Pugliese A, Busani L (2010) Modelling the spatial spread of H7N1 avian influenza virus among poultry farms in italy. Epidemics 2:39–35

Fact sheet—avian influenza (2012) Tech. rep., Canadian Food Inspection Agency. http://www.inspection.gc.ca/animals/terrestrial-animals/diseases/reportable/ai/fact-sheet/eng/1356193731667/1356193918453

Filippov AF (1988) Differential equations with discontinuous right-hand sides. Kluwer Academic Dordrecht, The Nertherlands

Food and Agriculture Organization of the United Nations (2011) Approaches to controlling, preventing and eliminating H5N1 highly pathogenic avian influenza in endemic countries. Tech. rep., Food and Agriculture Organization. http://www.fao.org/docrep/014/i2150e/i2150e.pdf

Food-producing animals: disease outbreaks (avian influenza h5n1) (2015) Tech. rep., International Animal Health Organisation—Europe. http://www.ifaheurope.org/food-producing-animals/disease-outbreaks/avianflu.html

Gulbudak H, Martcheva M (2013) Forward hysteresis and backward bifurcation caused by culing in an avian influenza model. Math Biosci 246:202–212

Gumel AB (2009) Global dynamics of a two-strain avian influenza model. Int J Comput Math 86:85–108

Human health issues related to avian influenza in canada (2006) Tech. rep., Public Health Agency of Canada. http://www.phac-aspc.gc.ca/publicat/daio-enia/2-eng.php#jmp-lan2

Iwami S, Takeuchi Y, Korobeinikov A, Liu X (2008) Prevention of avian influenza epidemic: what policy should we choose? J Theor Biol 252:732–741

Iwami S, Takeuchi Y, Liu X (2009) Avian flu pandemic: can we prevent it? J Theor Biol 257:181–190

Jacob JP, Butcher GD, Mather FB, Miles RD (2013) Avian influenza in poultry. University of Florida IFAS Extension ps38. http://edis.ifas.ufl.edu/ps032

Kimman T, Hoek M, de Jong MCM (2013) Assessing and controlling health risks from animal husbandry. NJAS Wagening J Life Sci 66:7–14

Le Menach A, Vergu E, Grais RF, Smith? DL, Flahault A (2006) Key strategies for reducing spread of avian influenza among commercial poultry holdings: lessons for transmission to humans. Proc R Soc B 273:2467–2475

Leine RI (2000) Bifurcations in discontinuous mechanical systems of Filippov-type. The Universiteitsdrukkerij TU Eindhoven, The Netherlands

Li J, Blakeley D, Smith? RJ (2011) The failure of r_0. Comp Math Methods Med ID 527610

Martcheva M (2014) Avian flu: modeling and implications for control. J Bio Syst 22(1):151–175

Perez DR, Garcia-Sastre A (2013) H5N1, a wealth of knowledge to improve pandemic preparedness. Virus Res 178:1–2

Perko L (2001) Differential equations and dynamical systems, 3rd edn. Springer, New York

Seasonal influenza (flu) (2012) Tech. rep., Centers for Disease Control and Prevention. http://www.cdc.gov/flu/avianflu/avian-in-birds.html

Shim E, Galvani AP (2009) Evolutionary repercussions of avian culling on host resistance and influenza virulence. PLoS One 4(5):e5503

Tang S, Xiao Y, Wang N, Wu H (2012) Piecewise HIV virus dynamic model with $CD4^+$ T cell count-guided therapy. Theor Biol 308:123–134

The global strategy for prevention and control of H5N1 highly pathogenic avian influenza (2008) Tech. rep., Food and Agriculture Organization. ftp://ftp.fao.org/docrep/fao/011/aj134e/aj134e00.pdf

Tuncer N, Martcheva M (2013) Modeling seasonality in avian influenza H5N1. J Bio Syst 22(4):1340004

van den Driessche P, Watmough J (2002) Reproduction numbers and sub-threshold endemic equilibria for compartmental models of disease transmission. Math Biosci 180:29–48

Wang A, Xiao Y (2014) A filippov system describing media effects on the spread of infectious diseases. Nonlinear Anal Hybrid Syst 11:84–97

Xiao Y, Xu X, Tang S (2012) Sliding mode control of outbreaks of emerging infectious diseases. Bull Math Biol 74:2403–2422

Xiao Y, Zhao T, Tang S (2013) Dynamics of an infectious diseases with media/psychology induced non-smooth incidence. Math Biosci Eng 10(2):445–461

Zhao T, Xiao Y, Smith? RJ (2013) Non-smooth plant disease models with economic thresholds. Math Biosci 241:34–48

Chapter 6

Discussion, conclusion and future work

We proposed a half-saturated incidence model and Filippov models that incorporated control strategies to examine the spread of avian influenza in bird and human populations. Three Filippov models were introduced; one incorporated a quarantine strategy for the human population, and two used a culling strategy for the bird population. The stability analysis and numerical simulations for each model were performed to give more insight into the dynamics of these models. Furthermore, the results of these models presented some valuable information, particularly for government health agencies, in combating a future avian influenza outbreak effectively.

In order to examine the effect of half-saturation constants in modelling avian influenza, we compared the transmission dynamics of half-saturated and bilinear incidences in Chapter 3. Assuming that the basic reproduction number of the avian-only half-saturated incidence model was greater than unity (i.e., $R_b > 1$), we found that the disease-free equilibria for the avian-only and avian–human half-saturated incidence models (i.e., E_b^0 and E_{ah}^0, respectively) were no longer stable. Although the total number of infected humans for both half-saturated and bilinear incidence models was exponentially decreasing, the disease remained endemic for both models. The bilinear model generated fewer infected people than the half-saturated model for the first approximately 225 days, but both models generated about the same number of infected people on average and stabilized at approximately $e^{3.8}(\approx 45)$ infected people in the long run.

We also studied in Appendix A the stability of the disease-free equilibrium for a half-saturated model by considering the basic reproduction number less than unity. In this study, we found that the total number of infected humans for both half-saturated and bilinear models were decreasing. Both models eventually reached a disease free state, but the half-saturated model took longer and produced more infected people than the bilinear model. Moreover, we discovered that decreasing the

rate at which human-to-human mutant influenza was contracted and increasing the half-saturation constant for humans with the mutant strain would theoretically lead to disease eradication; these parameters played an important role in controlling the basic reproduction number of both models. Several control measures were proposed to control the infection of avian influenza: pharmaceutical (vaccination) and non-pharmaceutical (personal protection and isolation) control strategies. We found that slightly longer time was needed to eliminate avian influenza if we only considered vaccination. Nevertheless, the application of any proposed pharmaceutical or non-pharmaceutical protections would lead theoretically to disease eradication.

We proposed two mathematical models that incorporated control methods on the infected populations in Chapter 4 to study avian influenza in the bird and human populations: an avian-only model with culling of infected birds and an SIIR (Susceptible-Infected-Infected-Recovered) model with quarantine of infected humans. The number of infected birds and the total number of infected humans were used as a guideline in the decision to implement control measures to suppress the outbreak. We applied the control strategy whenever the number of infected individuals exceeded the tolerance threshold to avoid a more severe and dreadful outbreak. However, no control strategy was necessary if the number of infected individuals was less than the tolerance threshold, because it was considered that the disease was manageable in this case. We analyzed the dynamics of the systems of differential equations for these models as we varied the tolerance threshold. We determined the existence of equilibrium points and sliding modes. We analyzed the dynamical system on the discontinuity surface. We also performed numerical simulations and discussed the results. Our findings showed that, by choosing an appropriate tolerance threshold, the avian influenza outbreak could be prevented or at least stabilized at a desired level.

Since culling birds is always considered an effective control measure to reduce the infection rate [65], we further studied culling strategies for the avian population in Chapter 5. We extended the avian-only model with culling of infected birds, which was introduced in Chapter 4, by considering depopulation of both susceptible and infected birds. By stamping out not only infected birds but also susceptible birds, our intention was to avoid more birds getting infected later on and to reduce the severity of the outbreak. Culling infected birds was carried out when the number of infected birds exceeded the tolerance threshold I_b while the number of susceptible birds was less than the tolerance threshold S_b. When both the number of infected birds and the number of susceptible birds exceeded their respective thresholds, culling was applied to both infected and susceptible birds. No culling strategy was conducted when the number of infected birds was less than the tolerance threshold I_b. We study the dynamics of the systems of differential equations for this model as we varied the tolerance thresholds. We examined the existence and stability of equilibria. Furthermore, we proved the existence of sliding modes and analyzed the dynamics

of the system of differential equations on the sliding domains. Our results suggested that, by selecting appropriate values for S_b and I_b, we might have all the orbits of the dynamical system converging to either an equilibrium point in the region below I_b or to one of the pseudoequilibria or pseudo-attractors on the discontinuity surfaces, therefore preventing any outbreak and eliminating the need of a culling strategy. However, for some values of S_b and I_b, some or all the orbits of the dynamical system for this model might converge to an equilibrium point that is located in the region above I_b, forcing the use of culling to control the outbreak. Hence, in order to prevent overkilling birds and to combat outbreaks effectively, a well-defined threshold policy was needed.

For future work, we may consider other types of saturated incidence model to study the transmission dynamics of avian influenza. For instance, we can consider the saturated incidence rate $\frac{\beta SI}{1+\alpha I}$, which is introduced by [66], in modelling avian influenza. $\alpha > 0$ is a parameter that measures the inhibitory effect, β is the infection rate, S is the number of susceptible individuals and I is the number of infected individuals. As I gets large, the infection force $\frac{\beta I}{1+\alpha I}$ approaches the saturation level $\frac{\beta}{\alpha}$; namely, $\frac{\beta I}{1+\alpha I} \to \frac{\beta}{\alpha}$ as $I \to \infty$. This type of incidence rate prevents an unbounded infection force by introducing the possibility of "psychological" and inhibitional effects on the susceptible population when the number of infected individuals is increasing. This change of behaviour may prevent susceptible individuals from getting infected. This is more realistic for a large and nonhomogeneous population than the bilinear incidence rate in the study of avian influenza [66, 67].

It is common to assume that a disease will die out if the outbreak is initiated by only very few infected individuals and effective control methods are available for the disease. However, because of the random nature of the transmission of the disease, there is a possibility in a small population that the outbreak takes off and that the number of infected individuals grows to an unexpected level. In this situation, a stochastic model is more appropriate to study the spread of the disease and the effects of the control measures or interventions. In a very large population, the stochastic effect is generally negligible.

In addition, a mass-action Filippov model (as in Chapters 4 and 5), where we had considered a well-mixed and homogeneous population in a limited area, may not be realistic if we are interested in studying the infection of a disease for a very large but not well-mixed population. In this case, we may consider a standard-incidence Filippov model. Moreover, it will be interesting to develop an avian influenza Filippov model that incorporates several different control measures (such as antiviral treatment, vaccination, biosecurity and isolation).

Gulbudak and Martcheva [64] mentioned that "employment of culling at fixed

times may not be realistic for avian influenza since it ignores the fact that culling occurs as a response to outbreak". A state-dependent impulsive culling model may be more realistic than the impulsive culling at fixed times. According to Gulbudak and Martcheva [64], for this approach, "impulsive culling would occur upon I reaching a threshold value, but culling effort would not vary beyond this impulse switch and limited qualitative results can be obtained in such a model". As a result, a state-dependent impulsive differential inclusion may be a better approach to examine an ideal culling strategy to prevent overkilling birds and stop the outbreak. More precisely, we can use impulsive differential inclusions to model an infectious disease that incorporates control methods. We can apply control measures at either fixed or non-fixed time intervals whenever the number of infected individuals is greater than the tolerance threshold. For instance, to prevent an outbreak from getting worse, we could schedule a pharmaceutical treatment (e.g., vaccination) on a regular basis with a control strategy to determine when a treatment should be skipped.

Appendix A

A mathematical model of avian influenza with half-saturated incidence

A.1 Parameter values

There are several mistakes in the references to parameter values in Table 2 on page 28 of [41] for the half-saturated incidence model (2.1) and the bilinear incidence model (3.1). We list the corrected references in Table A.1 below.

We attach the manuscript [41], which has been published in the Journal *Theory in Biosciences*. The contribution of this work by each author is as follows. The first author analyzed the model, performed all numerical simulations and wrote the manuscript except the introduction and parts of abstract and discussion. The second author designed the study and wrote the introduction, parts of abstract and discussion. The third author designed the study and edited the manuscript.

In this manuscript [41], a large parameter value of additional disease death rate due to avian strain in birds, $\delta_b = 5$, is assumed. As a result, the basic reproduction number for the avian-only model was less than unity (i.e., $R_b < 1$). We only consider the existence of disease-free equilibrium in this model since the endemic equilibrium for this model is located outside the feasibility domain where negative values for the population have no biological meaning.

Parameter	Sample value	Reference
β_a	0.4 per day	Assumed
α	0.06 per day	Assumed
d	1 per day	Assumed
δ_b	5 per day	Assumed
β_b	0.4 per day	Assumed
β_{bh}	0.2 per day	Assumed
β_B	$0.4/200,000$ per individual per day	Assumed
β_A	$0.4/200,000$ per individual per day	Assumed
β_{BH}	0.2/100 per individual per day	Assumed

Table A.1: Corrected references for parameter values of models (2.1) and (3.1) in [41].

Theory Biosci. (2014) 133:23–38
DOI 10.1007/s12064-013-0183-6

ORIGINAL PAPER

A mathematical model of avian influenza with half-saturated incidence

Nyuk Sian Chong · Jean Michel Tchuenche · Robert J. Smith?

Received: 2 November 2012 / Accepted: 19 April 2013 / Published online: 4 June 2013

Abstract The widespread impact of avian influenza viruses not only poses risks to birds, but also to humans. The viruses spread from birds to humans and from human to human In addition, mutation in the primary strain will increase the infectiousness of avian influenza. We developed a mathematical model of avian influenza for both bird and human populations. The effect of half-saturated incidence on transmission dynamics of the disease is investigated. The half-saturation constants determine the levels at which birds and humans contract avian influenza. To prevent the spread of avian influenza, the associated half-saturation constants must be increased, especially the half-saturation constant H_m for humans with mutant strain. The quantity H_m plays an essential role in determining the basic reproduction number of this model. Furthermore, by decreasing the rate β_m at which human-to-human mutant influenza is contracted, an outbreak can be controlled more effectively. To combat the outbreak, we propose both pharmaceutical (vaccination) and non-pharmaceutical (personal protection and isolation) control methods to reduce the transmission of avian influenza. Vaccination and personal protection will decrease β_m, while isolation will increase H_m. Numerical simulations demonstrate that all proposed control strategies will lead to disease eradication; however, if we only employ vaccination, it will require slightly longer to eradicate the disease than only applying non-pharmaceutical or a combination of pharmaceutical and non-pharmaceutical control methods. In conclusion, it is important to adopt a combination of control methods to fight an avian influenza outbreak.

Keywords Avian influenza · Half-saturated incidence · Personal protection · Isolation · Vaccination

N. S. Chong
Department of Mathematics, The University of Ottawa, 585 King Edward Ave, Ottawa, ON K1N 6N5, Canada

J. M. Tchuenche
Department of Mathematics and Statistics, University of Guelph, Guelph, ON N1G 2W1 Canada

R. J. Smith? (✉)
Department of Mathematics, Faculty of Medicine, The University of Ottawa, 585 King Edward Ave, Ottawa, ON K1N 6N5, Canada
e-mail: rsmith43@uottawa.ca

Introduction

Recently, the WHO (World Health Organization) has urged the world to monitor the outbreak of avian influenza and possible mutation of influenza viruses (World Health Organization 2011). The 1918 pandemic was one of the deadliest public health menaces of recorded human history, claiming over 20 million lives (Stuart-Harris 1979). Although subsequent pandemics in 1957 (Asian Flu) and 1968 (Hong Kong Flu) resulted in milder outbreaks (Kilbourne 2006), the recent emergence of the highly pathogenic avian H5N1 influenza A viruses in wild bird populations in several regions of the world, together with recurrent flu cases of H5N1 viruses in humans (arising primarily from direct contact with poultry), have triggered a major scare for a pending pandemic influenza. The current projections of the potential impact of a prospective pandemic are alarming. The highly pathogenic H5N1 influenza A viruses are now endemic in avian populations in Southeast Asia, and human cases continue to rise. H5N1 represents a serious pandemic threat owing to the risk of a mutation generating a virus with increased transmissibility. In humans, avian influenza virus causes similar symptoms

as other types of influenza. These include fever, cough, sore throat, muscle aches, conjunctivitis and, in extreme cases, severe breathing problems and pneumonia that may be fatal (Centers for Disease Control and Prevention 2010; World Health Organization 2011, 2012).

Avian influenza, being an emerging infectious disease in humans, is now receiving significant attention from the mathematical community. Faced with the H5N1 pandemic threat, strategies designed to contain an emerging pandemic should be considered a public health priority. Studies have documented the most significant risk factors for human H5N1 infection to be direct contact with sick or dead poultry or wild birds, or visiting a live poultry market (Centers for Disease Control and Prevention 2007). Since its emergence, a number of mathematical modeling studies, using stochastic as well as deterministic formulations, have been carried out to quantify the burden of a potential flu pandemic and assess various interventions (Alexander et al. 2004, 2008; Chowell et al. 2005; Doyle et al. 2006; Lipsitch et al. 2007; Longini et al. 2004). Nuño et al. (2006) analyzed a model to examine the role of hospital and community control measures, antiviral drugs and vaccination in combating a potential flu pandemic in a population, while a study by Gumel (2009) considered the dynamics of a two-strain influenza model and concluded that the influenza-related burden in humans increased as the mutation rate increased. Although many of these studies tend to emphasize the use of pharmaceutical interventions, it is generally believed that such interventions (antivirals and vaccines) would not be readily and widely available at the onset of the pandemic (Gumel 2009).

Nowadays, the spread of H5N1 virus is known to be under control, but the infection could re-emerge anytime in the future. H5N1 may mutate into a strain capable of efficient person to person transmission (Centers for Disease Control and Prevention 2007). However, none of the mathematical models of avian influenza have considered saturated incidence, which describes the effect of susceptible humans coming into contact with infected birds and or infected humans when effects such as crowding of infectives or protection measures taken by susceptibles are taken into account (Kaddar 2010). Moreover, there will be a potential threat of an uncontrollable outbreak, especially in developing countries where drugs and adequate health facilities for quarantine and isolation are not generally available. Hence it is instructive to carry out modeling studies that focus on the combination of pharmaceutical and non-pharmaceutical interventions with saturated incidence.

Several types of epidemic models have been studied, most of which have investigated the transmission rate of susceptible individuals who have been exposed to infected individuals (Gao et al. 2006; Kaddar 2009; Ruan and Wang 2003). Various incidence functions have been employed in epidemic models, of which the most popular are bilinear and saturated incidences. The bilinear (or mass-action) incidence rate is formulated by βSI where β is a positive constant, and S and I are the number of susceptible and infected individuals, respectively (Zhang et al. 2008; Zhou and Liu 2003). Bilinear incidence is based on the law of mass action, which requires a well-mixed population so that each infected individual has equal probability of infecting each susceptible individual. It has been employed for communicable diseases such as cholera, chickenpox and influenza (Du and Xu 2010). If a population is crowded or saturated with infectives, then saturated incidence is a better option (Gao et al. 2006; Yang et al. 2007). The saturated incidence rate takes the form $\frac{\beta SI}{1+\alpha_1 S}$ or $\frac{\beta SI}{1+\alpha_2 I}$, where α_1, α_2 are positive constants. The saturated incidence rates $\frac{\beta SI}{1+\alpha_1 S}$ and $\frac{\beta SI}{1+\alpha_2 I}$ describe the behavioral change of the disease and saturation effect of the infective and susceptible individuals, respectively, when their numbers increase (Capasso and Serio 1978; Liu and Yang 2012; May and Anderson 1978; Wei and Chen 2008). That is, when S or I is large, $\frac{\beta SI}{1+\alpha_1 S}$ or $\frac{\beta SI}{1+\alpha_2 I}$ will respectively converge to a saturation point.

In this paper, we consider the half-saturated incidence rate $\frac{\beta SI}{H+I}$. The parameter $\beta > 0$ is the transmission rate and H is the half-saturation constant, i.e., the density of infected individuals in the population that yields 50 % possibility of contracting avian influenza. The main goal of this study is to formulate a deterministic mathematical model to interpret the spread of avian influenza from birds to humans using saturated incidence. We assess the potential impact of avian influenza in both the bird and the human populations because two types of outbreak of avian influenza may occur (Gumel 2009; Iwami et al. 2007). Therefore, the specific objectives are: to formulate and analyze a mathematical model of avian influenza that includes both the bird and human populations; to determine the threshold parameter that measures initial disease transmission; and to investigate the effect of saturated incidence on the transmission dynamics of the disease.

The model

The population of birds and humans are represented by $N_b(t)$ and $N_h(t)$, respectively, at time t. The bird population is divided into two sub-populations: susceptible (S_b) and infected (I_b) birds. The number of susceptibles for the bird population is increased by new recruitment (birth), but reduced through natural death and infection (moving to class I_b). On the other hand, the infected bird population is increased by the infection of susceptible birds whereas reduction is caused by natural mortality and death due to

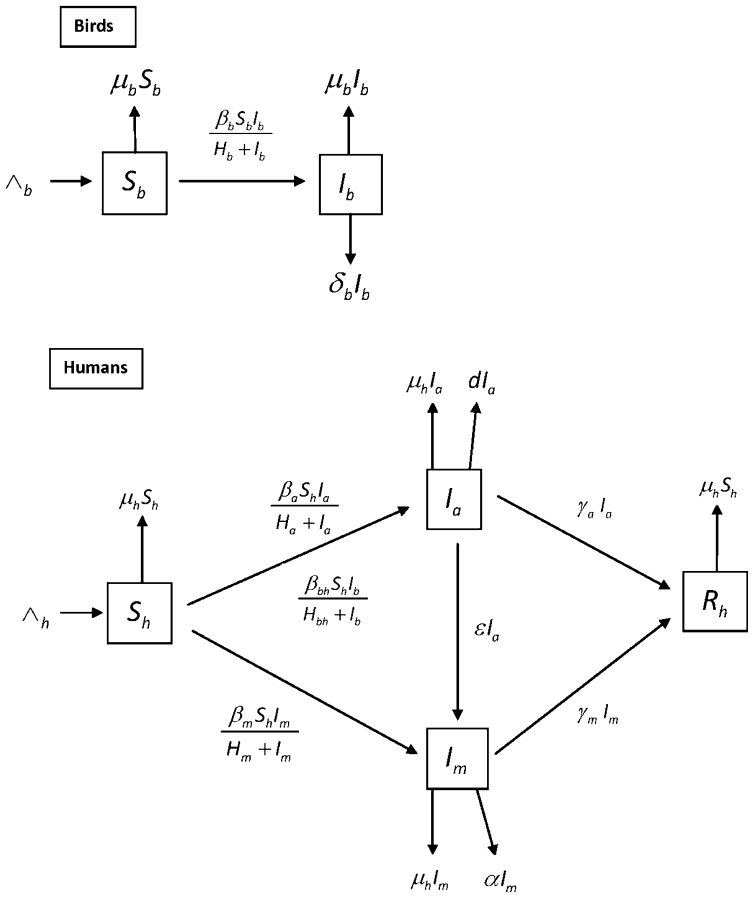

Fig. 1 Flowchart of the model

avian influenza. The total bird population at time t is formulated by $N_b = S_b + I_b$. The human population is subdivided into those who are susceptible (S_h), infected with avian strain (I_a), infected with mutant strain (I_m), and recovered from avian and mutant strains (R_h). The total population of humans at time t is given by $N_h = S_h + I_a + I_m + R_h$. The number of susceptibles for the human population is increased by recruitment, but diminished by infection (moving to class I_a or I_m) and natural death. The number of infected humans with the avian strain is increased by the infection of susceptible humans and reduced through mutation (moving to class I_m), recovery from the disease (moving to class R_h), natural death and disease death. The growth of the population of infected humans with mutant strain is caused by the infection of susceptible humans and mutation of infected humans with the avian strain, but reduced by recovery from the disease (moving to class R_h), natural death and disease death.

A schematic flowchart of this model is depicted in Fig. 1. The descriptions of the variables and associated parameters are given in Table 1.

Model equations

Considering the above formulations and the flow diagram, we have the following system of nonlinear ordinary differential equations:

$$\begin{aligned}
S_b'(t) &= \Lambda_b - \mu_b S_b - \frac{\beta_b S_b I_b}{H_b + I_b} \\
I_b'(t) &= \frac{\beta_b S_b I_b}{H_b + I_b} - (\mu_b + \delta_b) I_b \\
S_h'(t) &= \Lambda_h - \mu_h S_h - \frac{\beta_a S_h I_a}{H_a + I_a} - \frac{\beta_m S_h I_m}{H_m + I_m} - \frac{\beta_{bh} S_h I_b}{H_{bh} + I_b} \\
I_a'(t) &= \frac{\beta_{bh} S_h I_b}{H_{bh} + I_b} + \frac{\beta_a S_h I_a}{H_a + I_a} - (\mu_h + d + \epsilon + \gamma_a) I_a \\
I_m'(t) &= \frac{\beta_m S_h I_m}{H_m + I_m} + \epsilon I_a - (\mu_h + \alpha + \gamma_m) I_m \\
R_h'(t) &= \gamma_a I_a + \gamma_m I_m - \mu_h R_h.
\end{aligned} \tag{2.1}$$

The feasibility of the solution in model (2.1) is given in Appendix 1. In addition, the stability analysis of the avian-only and avian–human models are given in Appendices 2 and 3, respectively.

The effect of half-saturated incidence on the transmission dynamics of the disease

To investigate the effect of half-saturated incidence on the transmission dynamics of avian influenza, we would like to make a comparison of the total number of infected individuals using our model (2.1) and the following bilinear incidence model:

$$\begin{aligned} S_b'(t) &= \Lambda_b - \mu_b S_b - \beta_B S_b I_b \\ I_b'(t) &= \beta_B S_b I_b - (\mu_b + \delta_b) I_b \\ S_h'(t) &= \Lambda_h - \mu_h S_h - \beta_A S_h I_a - \beta_M S_h I_m - \beta_{BH} S_h I_b \\ I_a'(t) &= \beta_{BH} S_h I_b + \beta_A S_h I_a - (\mu_h + d + \epsilon + \gamma_a) I_a \\ I_m'(t) &= \beta_M S_h I_m + \epsilon I_a - (\mu_h + \alpha + \gamma_m) I_m \\ R_h'(t) &= \gamma_a I_a + \gamma_m I_m - \mu_h R_h, \end{aligned} \tag{3.1}$$

where β_B, βA, β_M and β_{BH} are, respectively, the rates at which avian influenza is contracted by birds, human-to-human avian influenza is contracted, human-to-human mutant influenza is contracted and avian influenza is contracted from infected birds. All other parameters are defined in Table 1.

The unit measurements for all four infection rates (β_B, β_A, β_M and β_{BH}) are [number of individuals]$^{-1}$ × [days]$^{-1}$. The transmission parameters of model (3.1) are fixed at $\beta_B = \beta_A = \frac{0.4}{200{,}000}$ per individual per day, $\beta_M = 0.3\ \beta_A$ per individual per day (Gumel 2009) and $\beta_{BH} = \frac{0.2}{100}$ per individual per day (Iwami et al. 2007), whereas the remaining parameter sample values in models (2.1) and (3.1) are as in Table 2. For both models (2.1) and (3.1), we assume the initial populations satisfy $S_b(0) = 2.06 \times 10^9$ and $S_h(0) = 10^9$. In addition, the basic reproduction number of model (3.1) is defined as follows:

$$R_{AH} = \max\left\{\frac{\beta_B \Lambda_b}{\mu_b(\mu_b+\delta_b)}, \frac{\beta_A \Lambda_h}{\mu_h(\mu_h+d+\epsilon+\gamma_a)}, \frac{\beta_M \Lambda_h}{\mu_h(\mu_h+\alpha+\gamma_m)}\right\}. \tag{3.2}$$

Figure 2 illustrates the effects of avian influenza transmission dynamics using bilinear incidence (model 3.1) and half-saturated incidence (model 2.1) It is worth mentioning that the total number of infected humans of the bilinear incidence model is known to decrease exponentially, and both models achieve the outcome of disease eradication. Model (3.1) produces an enormous number of infected humans compared to model (2.1); numerical simulations of model (3.1) produced around 65 % more than the maximum number of infected humans simulated by model (2.1). To achieve the state of disease eradication, half-saturated incidence typically requires more time than bilinear incidence.

Figure 3 describes the effects of the rate of transmission in models (2.1) and (3.1) with respect to each term of R_{ah} in (5.3) and R_{AH} in (3.2). If the natural logarithms of all terms in R_{ah} and R_{AH} are equal to or less than zero, then the disease will die off, whereas if one of these terms is greater than zero, then the disease will persist. Figure 3 shows that β_m and β_M play an essential role in controlling R_{ah} and R_{AH}, respectively. This is because these two parameters are the coefficients of the nonlinear terms in both bilinear and half-saturated incidences. A small change in β_m or β_M will produce a disproportionate change in the outcome. By decreasing β_m and β_M in both models (2.1) and (3.1), the disease will be eradicated. Hence we conclude that $\lim_{\beta_m \to 0} R_{ah} = 0$ and $\lim_{\beta_M \to 0} R_{AH} = 0$.

Sensitivity analysis of R_{ah}

We performed a sensitivity analysis of R_{ah} (given by Eq. 5.3) using Latin Hypercube Sampling with 2,000 simulations per run. The ranges of the parameters are shown in Table 2 while the results are shown in Figs. 4 and 5. From Fig. 4, it can be observed that there are 7 parameters out of 16 to be considered: $\Lambda_h, H_m, \beta_m, H_a, \alpha, d$ and β_a. These parameters are chosen as they have the greatest effect on the outcome. Figure 5 illustrates the sensitivity analysis of R_{ah}, which is highly dependent on the particular seven parameters. From these figures, the simulations suggest that control of avian influenza is most likely to be achieved by lowering the values of Λ_h and β_m. On the other hand, increasing H_a, H_m, α or d, or decreasing β_a is unlikely to eradicate the disease.

Figure 6 illustrates the effect of half-saturation constants (H_b, H_a and H_m) with respect to each term of R_{ah} in (5.3). If all three terms (i.e., ln R_b, ln R_{h1} and ln R_{h2}) are equal to or less than zero, then the disease will die off. Conversely, if one of these terms is greater than zero, then the disease will persist. Figure 6 shows that, within our given ranges, ln R_{h2} always has the largest value compared to ln R_b and ln R_{h1} for every half-saturation constant. Hence, H_m plays an important role in controlling the parameter R_{ah}. For instance, increasing H_m will lead us to disease eradication; that is, whenever $H_m \to \infty$, both $R_{h2} \to 0$ and $R_{ah} \to 0$.

Control strategies

To control the transmission of avian influenza, some control strategies such as pharmaceutical or/and non-pharmaceutical protections have to be considered (Bowman et al. 2005; Yang et al. 2009). For non-pharmaceutical protection, we implement personal protection and isolation, whereas we adopt vaccination for pharmaceutical protection.

Table 1 Description of the variables and associated parameters

Symbol	Description
$S_b(t)$	Susceptible birds
$I_b(t)$	Infected birds
$S_h(t)$	Susceptible humans
$I_a(t)$	Infected humans with avian strain
$I_m(t)$	Infected humans with mutant strain
$R_h(t)$	Recovered humans from avian and mutant strains
$N_b(t)$	Total bird population
$N_h(t)$	Total human population
Λ_b	Bird inflow
Λ_h	Human recruitment rate
μ_b	Natural death rate of birds
μ_h	Natural death rate of humans
β_a	Rate at which human-to-human avian influenza is contracted
β_m	Rate at which human-to-human mutant influenza is contracted
β_{bh}	Rate at which bird-to-human avian influenza is contracted
β_b	Rate at which birds contract avian influenza
H_a	Half-saturation constant for humans with avian strain
H_m	Half-saturation constant for humans with mutant strain
H_b	Half-saturation constant for birds with avian strain
H_{bh}	Half-saturation constant for humans with avian strain contracted from infected birds
α	Additional death rate mediated by mutant strain
ϵ	Mutation rate
d	Additional disease death rate due to avian strain in humans
δ_b	Additional disease death rate due to avian strain in birds
γ_a	Recovery rate of humans with avian strain
γ_m	Recovery rate of humans with mutant strain
ψ_a	Rate of isolation of humans with avian strain
ψ_m	Rate of isolation of humans with mutant strain

Personal protection

There are several potential modes of avian influenza transmission such as the consumption of raw or undercooked infected poultry products, contact with oral/nasal mucous membrane or conjunctiva (for example, through swimming or bathing in a contaminated pond/pool), inhalation of contaminated dust or fine water droplets and human-to-human transmission (Food and Agriculture Organization of the United Nations 2008). Although the exact mode of human-to-human transmission remains unclear, there is reason to believe that unprotected contact with an infected person, respiratory secretions, body fluids or waste poses a higher risk for transmission, especially for health-care workers (HCWs) who are first responders (Food and Agriculture Organization of the United Nations 2008; World Health Organization 2006).

To reduce the mortality and infection rate of avian influenza, the general public—especially HCWs, and workers and employers who are involved in poultry agriculture or have frequent contact with wild birds—is advised to follow strict guidelines for personal protection. For example, one should take precautions for hygiene, using gloves, masks and other protective gear (Centers for Disease Control and Prevention 2012; Government of Ontario 2006; World Health Organization 2006).

As personal protection plays an essential role in preventing an outbreak, we investigated the impact of personal protection on controlling the spread of this disease in humans. We rescaled the transmission coefficients, $(\beta_a, \beta_m, \beta_{bh})$, to $(1 - cq)$ $(\beta_a, \beta_m, \beta_{bh})$, where $0 \leq c \leq 1$ is the fraction of population that has adopted personal protection and $0 < q \leq 1$ is the efficiency of personal protection. For $c = 1$, all the people in a particular community employ personal protection, whereas $c = 0$ means there is no one practicing personal protection. Further, the value $q = 1$ shows that the efficiency of personal protection is 100 %. Hence, the values of c and q are reciprocal to the rate of avian influenza transmission (Bowman et al. 2005).

The number of infected humans with respect to the avian $(I_a(t))$ and mutant strains $(I_m(t))$ are depicted in Figs. 7 and 8, respectively, with $q \in [0.1, 0.5, 0.9]$. Figures 7a and 8a show results for the case of 30 % of the population employing personal protection, whereas Figs. 7b and 8b show results for the case of 80 % of the population employing personal protection. From Figs. 7 and 8, it can be observed that the values of c and q are reciprocal to the maximal points of I_a and I_m. Moreover, more people employing personal protection will reduce the values of I_a and I_m drastically compared to the efficiency of personal protection. Hence, we can conclude that although the efficiency of personal protection plays a role in reducing the rate of avian influenza infection, public awareness is the most effective method for controlling the spread of the disease. See Tchuenche et al. (2011) for more discussion.

Isolation

Before an H5N1 vaccine is ready to be administered to the community to reduce the rate of avian influenza infection, isolation is one of the best choices of control strategy to reduce the transmission rate (World Health Organization 2007). Although the strategy of isolation might not lead to disease eradication, it can reduce the chance of a person making contact with an infected human (Gumel 2009). Hence we consider our model for the population of birds $(S_b'(t)$ and $I_b'(t))$ and humans with isolation as follows:

Table 2 Model parameters

Parameter	Sample value	References	Range
Λ_b	1,000 per day	Bowman et al. (2005)	[100, 2,000]
Λ_h	30 per day	Bowman et al. (2005)	[1, 30]
μ_b	$\frac{1}{100}$ per day	(Gumel 2009)	[0.0005, 0.1]
μ_h	$\frac{1}{70\times365}$ per day	Bowman et al. (2005)	$\left[\frac{1}{75\times365}, \frac{1}{65\times365}\right]$
β_a	0.4 per day	Gumel (2009)	[0.05, 2.5]
β_m	$0.3 \times \beta_a$ per day	Gumel (2009)	[0.01, 0.5]
H_a	150,000 individuals	Assumed	[10,000, 500,000]
H_m	150,000 individuals	Assumed	[10,000, 500,000]
α	0.06 per day	Iwami et al. (2007)	[0.01, 0.1]
ϵ	0.01 per day	Gumel (2009)	[0.005, 0.05]
d	1 per day	Iwami et al. (2007)	[0.05, 2.5]
δ_b	5 per day	Iwami et al. (2007)	[1, 10]
γ_a	0.05 per day	Gumel (2009)	[0.01, 0.1]
γ_m	0.01 per day	Gumel (2009)	[0.005, 0.05]
β_b	0.4 per day	Gumel (2009)	[0.05, 2.5]
H_b	180,000 individuals	Assumed	[10,000, 500,000]
β_{bh}	0.2 per day	Iwami et al. (2007)	N/A
H_{bh}	120,000 individuals	Assumed	N/A

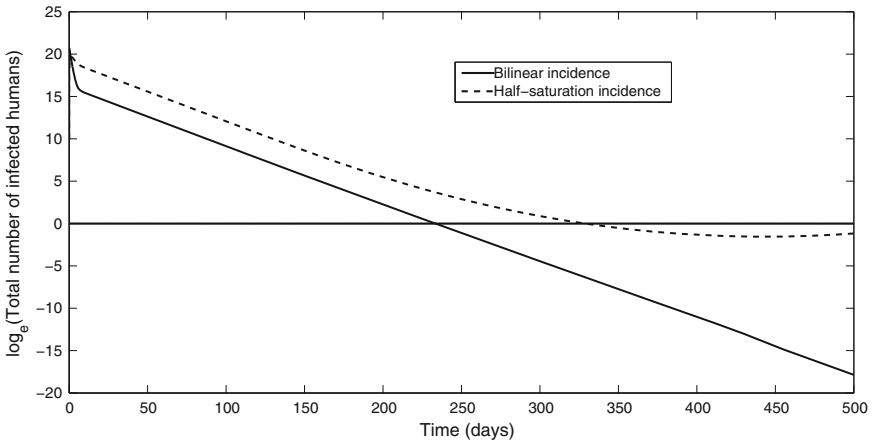

Fig. 2 Comparison between the effects of avian influenza transmission dynamics in models (2.1) and (3.1)

$$
\begin{aligned}
I_a'(t) &= \frac{\beta_{bh} S_h I_b}{H_{bh} + I_b} + \frac{\beta_a S_h I_a}{H_a + I_a} - (\mu_h + d + \epsilon + \psi_a) I_a \\
I_m'(t) &= \frac{\beta_m S_h I_m}{H_m + I_m} + \epsilon I_a - (\mu_h + \alpha + \psi_m) I_m \\
T_a'(t) &= \psi_a I_a - (\mu_h + d + \gamma_a) T_a \\
T_m'(t) &= \psi_m I_m - (\mu_h + \alpha + \gamma_m) T_m \\
R_h'(t) &= \gamma_a T_a + \gamma_m T_m - \mu_h R_h.
\end{aligned} \tag{5.1}
$$

The quantities $T_a(t)$ and $T_m(t)$ represent the populations of isolated humans with avian strain at a rate of ψ_a and mutant strain at a rate of ψ_m at time t, respectively. The basic reproduction number of (5.1) can be expressed as

$$
R_T = \max\left\{ \frac{\beta_a \Lambda_h}{H_a \mu_h (\mu_h + d + \epsilon + \psi_a)}, \frac{\beta_m \Lambda_h}{H_m \mu_h (\mu_h + \alpha + \psi_m)} \right\}.
$$

Several numerical simulations have been performed to validate the effect of the parameters ψ_a and ψ_m; see Figs. 9 and 10. Assuming that the parameters ψ_a and ψ_m are equal, we observe from Fig. 9 that the isolation of infected humans will lead to the reduction of the total number of infected humans (i.e., $I_a(t) + I_m(t) + T_a(t) + T_m(t)$). Thus, the values of ψ_a and ψ_m are reciprocal to the number of infected individuals. However, increasing the rate of isolation will not lead to eradication of the disease.

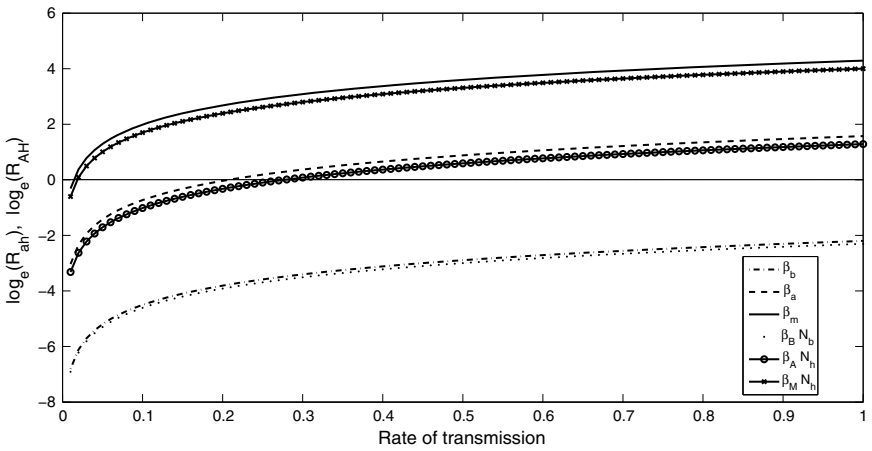

Fig. 3 The effect of the transmission parameters on R_{ah} and R_{AH}

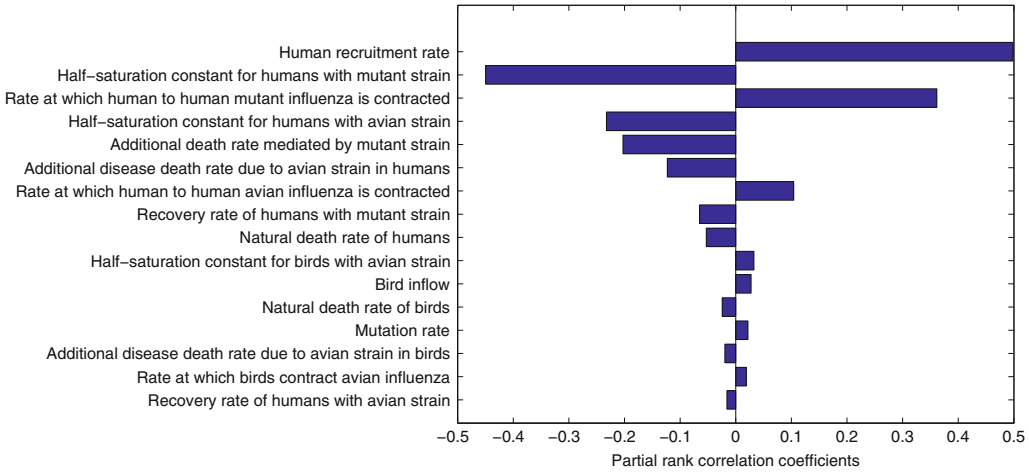

Fig. 4 Sensitivity of R_{ah} to all parameters. Parameters with positive partial rank correlation coefficients will increase R_{ah} when they are increased, while parameters with negative partial rank correlation coefficients will decrease R_{ah} when they are increased

Furthermore, we studied the impact of only isolating infected humans with one strain (i.e., either the avian or mutant strain). Figure 10 shows that increasing the rate of isolation of infected humans with the avian strain gives a better performance in controlling the spread of the disease compared to isolation of those with the mutant strain. From Figs. 9 and 10, we can conclude that the transmission of the disease can be controlled much more efficiently by isolating infected humans with avian and mutant strains. This works better than the countermeasure of isolating infected humans with only one strain; however, it does not lead to disease eradication.

Vaccination

Controlling and diminishing the spread of avian influenza is a challenging task, as the disease is very infectious and able to mutate into highly pathogenic strains (Marangon et al. 2008). Consequently, vaccination of poultry or humans as a tool to manage, prevent or eradicate the disease has been recommended by the United Nations (Food and Agriculture Organization of the United Nations 2004). Here, we consider our model for the population of birds ($S'_b(t)$ and $I'_b(t)$) and vaccination of humans as follows:

$$\begin{aligned} S'_h(t) &= (1-p)\Lambda_h - \mu_h S_h - \frac{\beta_a S_h I_a}{H_a + I_a} - \frac{\beta_m S_h I_m}{H_m + I_m} - \frac{\beta_{bh} S_h I_b}{H_{bh} + I_b} \\ V'_h(t) &= p\Lambda_h - (1-\phi)\frac{\beta_m V_h I_m}{H_m + I_m} - \mu_h V_h \\ I'_m(t) &= \frac{\beta_m I_m}{H_m + I_m}[S_h + (1-\phi)V_h] + \epsilon I_a - (\mu_h + \alpha + \gamma_m) I_m. \end{aligned} \tag{5.2}$$

In this model, $V_h(t)$ represents the population of vaccinated humans, whereas p and ϕ denote the

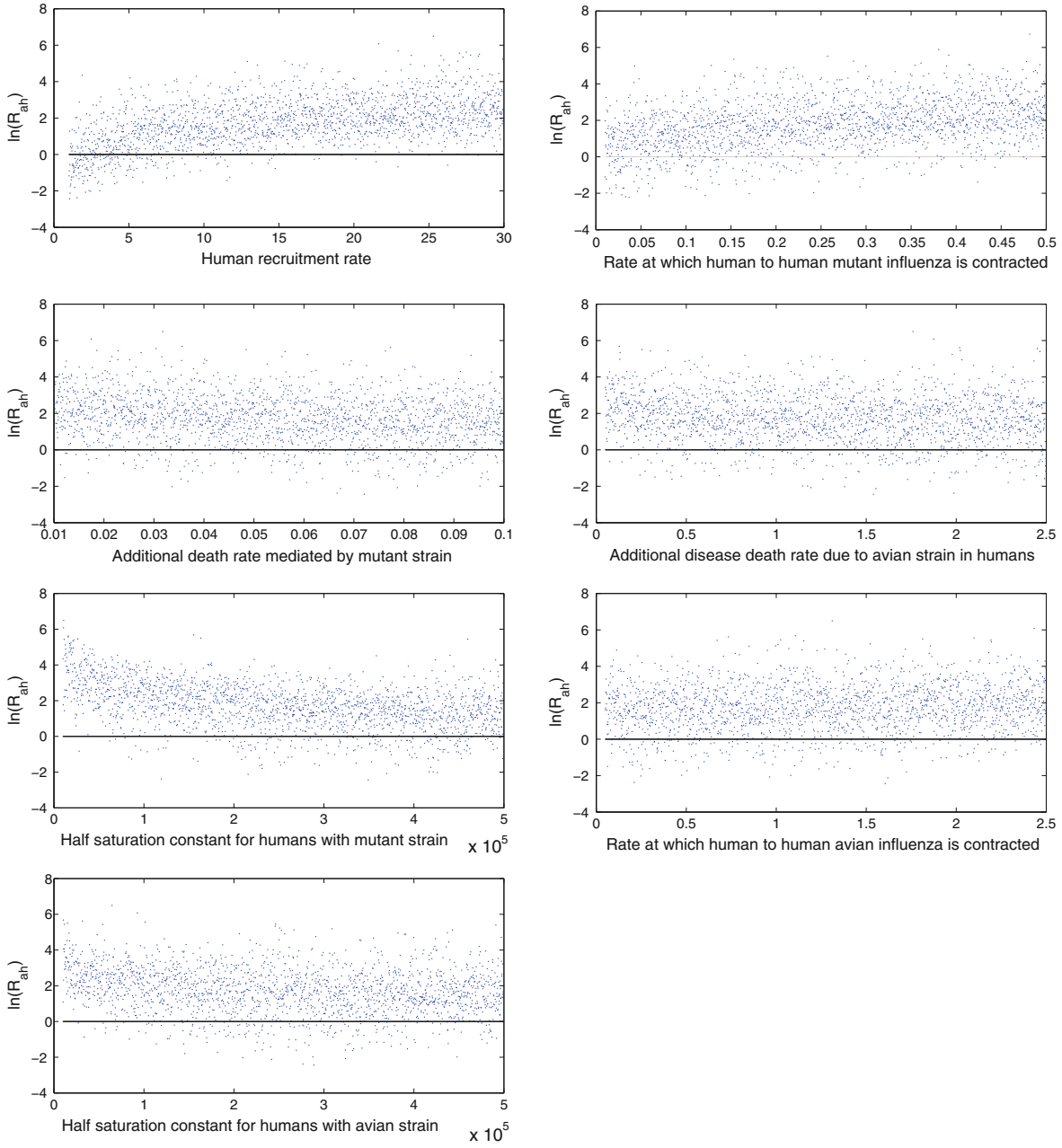

Fig. 5 Sensitivity analysis of R_{ah} to the seven parameters which have the most significant effects on the outcome

prevalence rate of the vaccination program and the efficacy of the vaccine, respectively. Further, we assume that vaccinated humans are fully protected from the avian strain, but partially protected from the mutant strain with a loss of protection effectiveness of the vaccination (Iwami et al. 2009). The basic reproduction number for this model (5.2) is as follows:

$$R_{\mathrm{V}} = \max\left\{\frac{\beta_{\mathrm{b}}\Lambda_{\mathrm{b}}}{H_{\mathrm{b}}\mu_{\mathrm{b}}(\mu_{\mathrm{b}}+\delta_{\mathrm{b}})}, \frac{\beta_{\mathrm{a}}\Lambda_{\mathrm{h}}}{H_{\mathrm{a}}\mu_{\mathrm{h}}(\mu_{\mathrm{h}}+d+\epsilon+\gamma_{\mathrm{a}})}, \frac{\beta_{\mathrm{m}}\Lambda_{\mathrm{h}}[1+p(1-\phi)]}{H_{\mathrm{m}}\mu_{\mathrm{h}}(\mu_{\mathrm{h}}+\alpha+\gamma_{\mathrm{m}})}\right\}.$$

We performed several numerical simulations to examine the effect of ϕ and to compare various control strategies

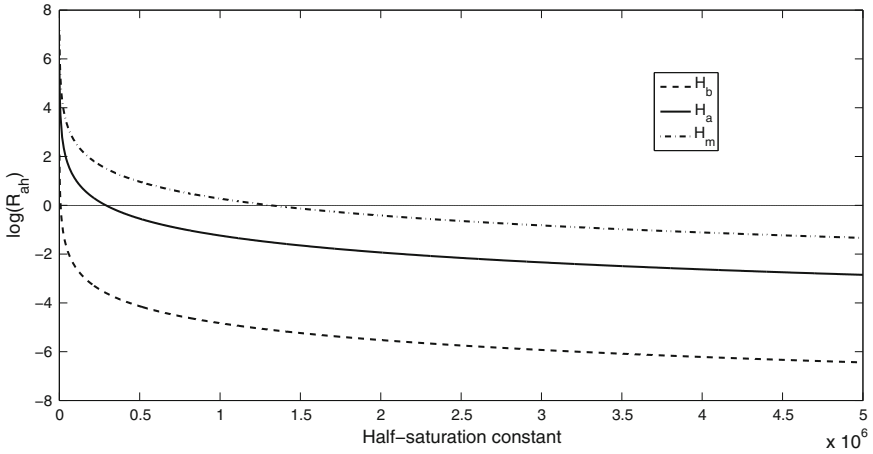

Fig. 6 The effect of parameters H_b, H_a and H_m on each term of R_{ah}. All other parameters are at their sample values in Table 2

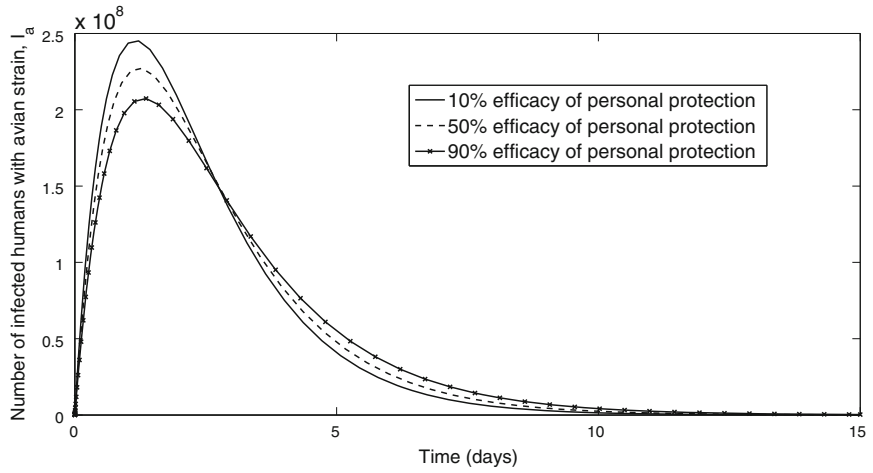

(a) 30% of the population has employed personal protection.

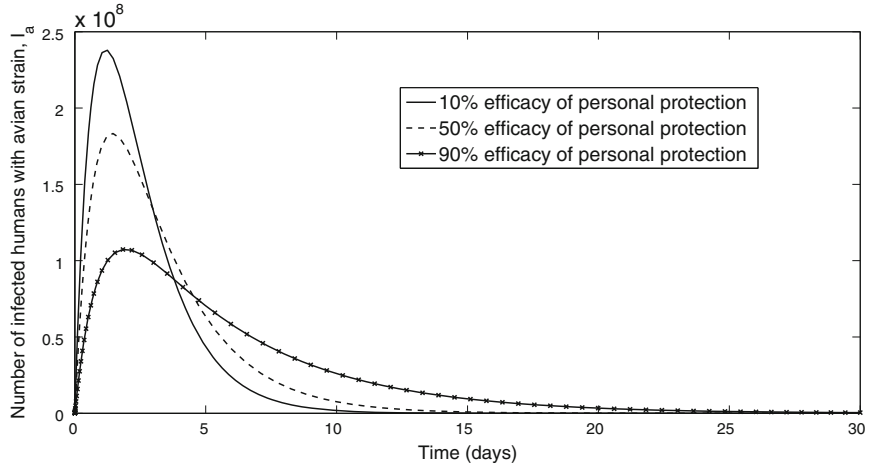

(b) 80% of the population has employed personal protection.

Fig. 7 The effects of personal protection on the avian strain

Fig. 8 The effects of personal protection on the mutant strain

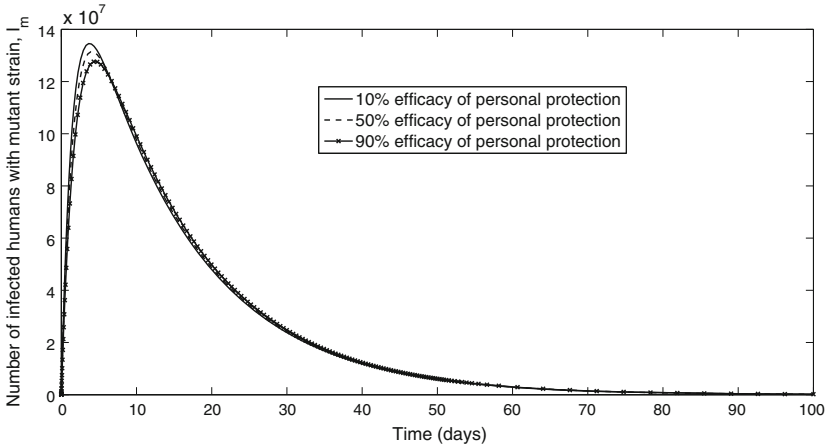

(a) 30% of the population has employed personal protection.

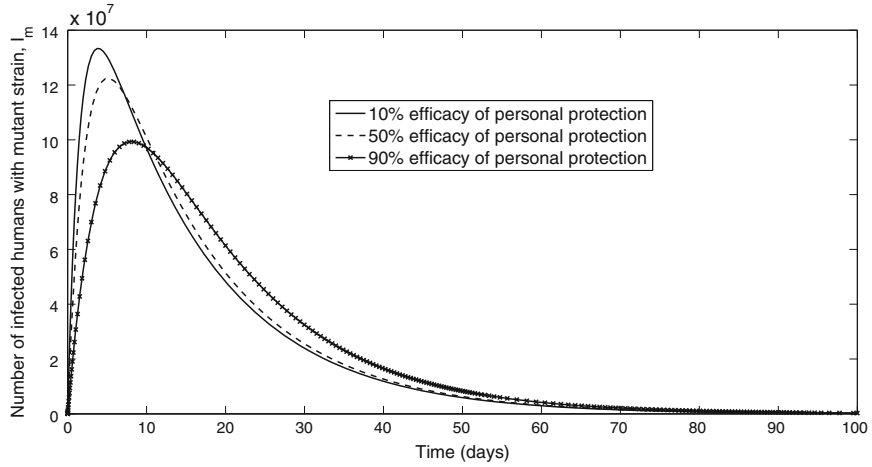

(b) 80% of the population has employed personal protection.

Fig. 9 The effect of isolating infected humans when isolation rates are equal

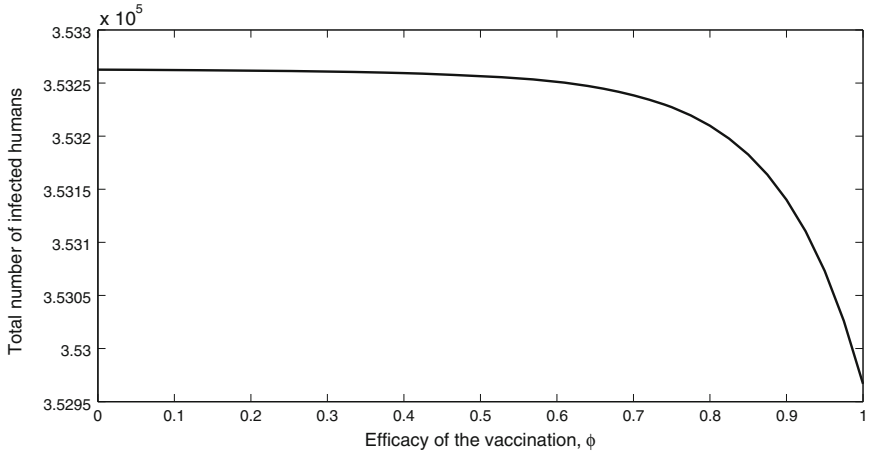

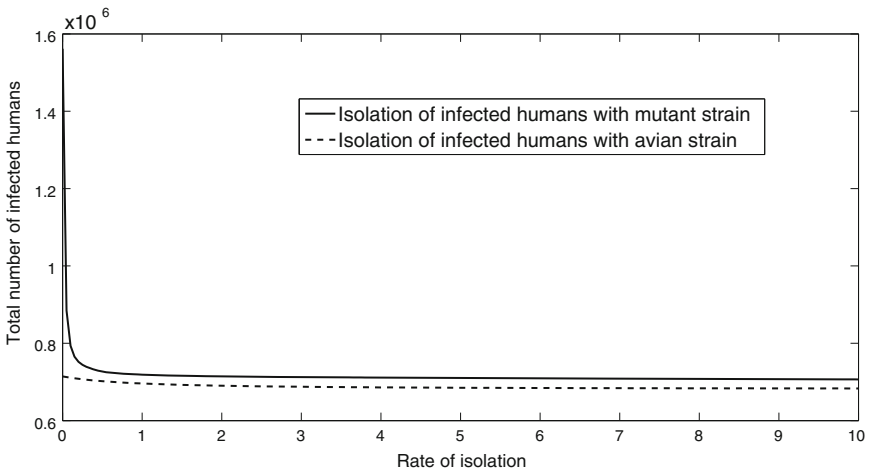

Fig. 10 The impact of isolating humans infected with only one strain

(personal protection, isolation and vaccination). From Fig. 11, we find that the higher the efficacy of vaccine, the fewer the number of infected humans. After 90 days, there is very little reduction in the number of infections, even if 90 % of the population is vaccinated. After 150 days, the number of infections is low if both the efficacy of the vaccine and the vaccination coverage are high. However, if the vaccine only has moderate efficacy (less than 70 %), then very little is gained by vaccinating a large proportion of the population.

In addition, Fig. 12 shows that, if there is an absence of control strategies, then we will need more time to combat the disease compared to those populations which have undergone vaccination. Note that by "combatting" the disease, we mean applying control strategies once infection has begun. Moreover, we cannot guarantee that the disease will not attack the population again in the future if there are no control strategies employed. From the same figure again, we can see that the number of infected humans begins to increase after day 450.

On the other hand, Fig. 13 shows that, by employing non-pharmaceutical interventions (personal protection and isolation) and all of the proposed control methods, less time will be needed to eradicate the disease compared to only employing a pharmaceutical (vaccination) control strategy. In conclusion, the non-pharmaceutical control strategy is more effective than vaccination in battling the disease.

Discussion

In this paper, we have conducted a study focusing on the effect of half-saturated incidence on the transmission dynamics of avian influenza. When half-saturated incidence is included (model 2.1), the effect is a significantly lower peak of the total number of infected humans compared to the case when half-saturated incidence is not included (model 3.1). However, when half-saturation is included, the disease takes longer to die off. Furthermore, the results of the sensitivity analysis of R_{ah} suggest that increasing the half-saturation constants, especially H_m, will lead to disease eradication. Particularly in this case, we obtain $R_{ah} < 1$.

To control the outbreak, we proposed both non-pharmaceutical (personal protection and isolation) and pharmaceutical (vaccination) control strategies. From the outcomes that we have obtained, the total number of infected humans is reciprocal to the following: the fraction of the population that has adopted personal protection, the efficiency of personal protection, the rate of isolation of humans with the avian strain, the rate of isolation of humans with the mutant strain and the efficacy of the vaccine. Hence, by increasing these parameter values, we can control the spread of the disease more effectively and less time is required to battle the outbreak. Although vaccination gives better control of avian influenza transmission than any control strategies not employing vaccination, it takes longer to eradicate the disease compared to employing only non-pharmaceutical or all proposed control methods. However, adopting either pharmaceutical, non-pharmaceutical or all of the proposed control strategies will lead to disease eradication.

The recent H1N1 pandemic provided important lessons for future pandemics. Personal protection and isolation were judged to be successful in Singapore, when well implemented (Hospital Influenza Working Group 2009), but less so in other Asian countries (Chan et al. 2010). Conversely, even once a vaccine became available, distribution was problematic due to hoarding and underutilization (Fisher et al. 2011). This suggests that the recommendations we make here nevertheless need careful implementation once a pandemic occurs.

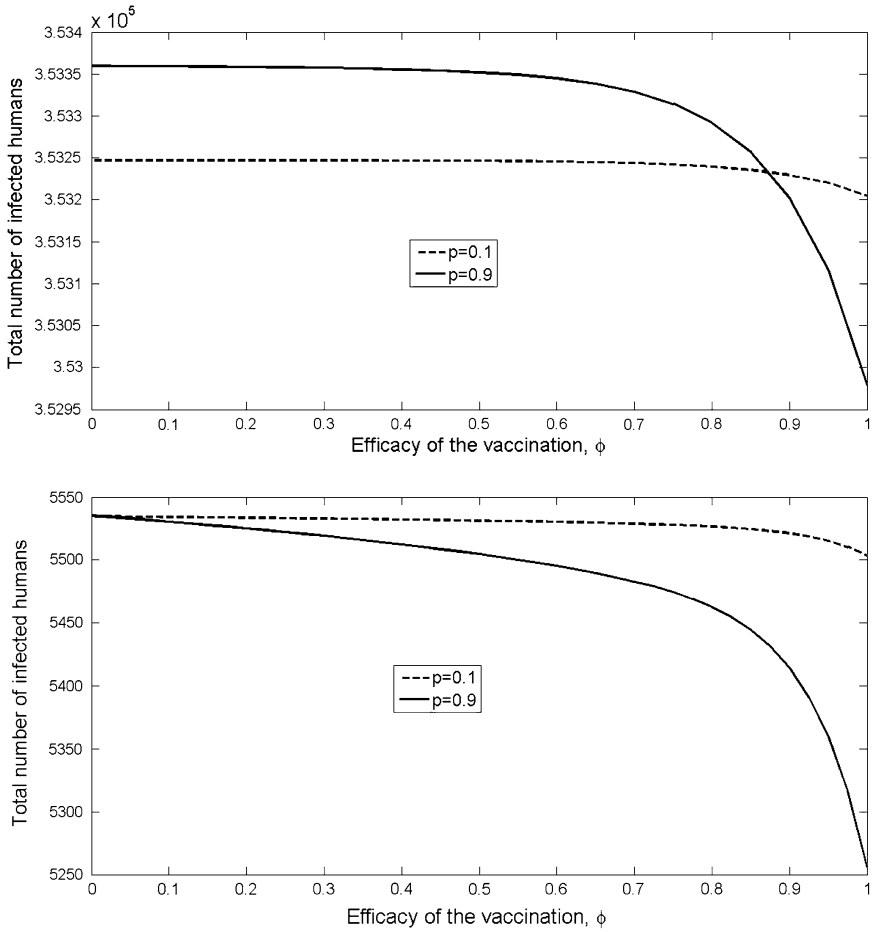

Fig. 11 The impact of ϕ on the total number of infected humans at day 90 (*top figure*) and day 150 (*bottom figure*)

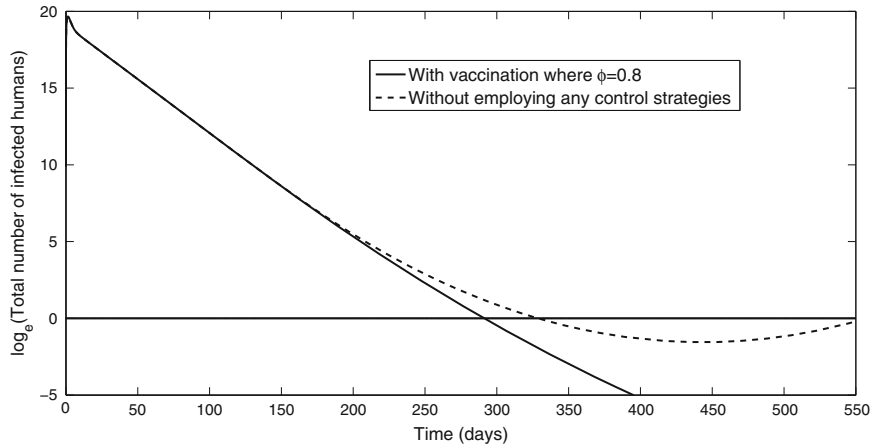

Fig. 12 The effect of vaccination compared to no control methods

This model has several limitations, which should be noted. We have used constant human recruitments and bird inflow. We have also assumed that birds will not be infected with avian influenza from humans and infected birds will remain infected (i.e., infected birds will not move to, for example, a recovered or susceptible class). For the

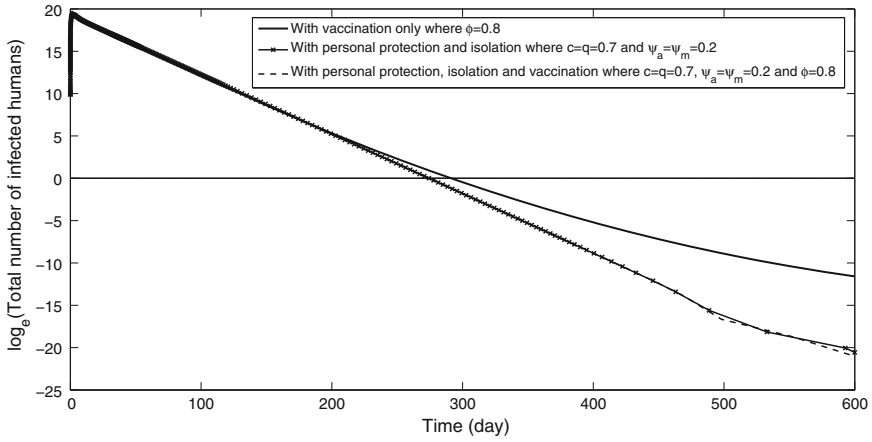

Fig. 13 Comparison between the suggested control strategies

human population, we assumed that immunity was permanent.

If the half-saturation constant, $H_* = \{H_a, H_m, H_b, H_{bh}\}$ tends to infinity, then $\beta_* S_* \frac{I_*}{H_* + I_*}$ tends to zero, where we denote $\beta_* = \{\beta_a, \beta_m, \beta_b, \beta_{bh}\}$, $S_* = \{S_b, S_h\}$ and $I_* = \{I_b, I_a, I_m\}$. That is, the infection does not occur. Thus, the number of susceptibles, S_*, will increase while the number of infected, I_*, will decrease. Moreover, if H_* approaches zero, then we will obtain the peak of infection. It is worth mentioning that the half-saturation constant for humans with the avian strain contracted from infected birds in this model is irrelevant. This is because there are no infected birds to infect humans if the half-saturation constant for birds with the avian strain approaches infinity. Hence, in this case, humans will not contract avian influenza from infected birds.

For future work, we propose a model which incorporates the saturation incidence rate, $\frac{\beta SI}{1+\alpha_1 S}$, where α_1 is a positive constant. In this case, we wish to study the role of the parameter α_1 in controlling the epidemic.

In summary, modeling avian influenza with half-saturated incidence gives insights into disease management that cannot be gleaned from mass-action (bilinear) modeling. By increasing the half-saturation constant for the mutant strain (through isolation techniques such as quarantine), in addition to other protection measures such as vaccination and personal protection, we can make the disease-free equilibrium globally stable and hence theoretically eradicate the disease. A comparison of the two models suggests that eradication is slower in the case of half-saturation. It follows that mass-action models may be overestimating the speed with which we might bring the disease under control.

Acknowledgments NSC acknowledges support from the Ministry of Higher Education, Malaysia, and the Department of Mathematics, University of Malaysia Terengganu. For citation purposes, please note that the question mark in "Smith?" is part of his name.

Appendix 1: Feasibility of the solution

Since the model parameters are non-negative, it is important to show that all state variables remain non-negative for all non-negative initial conditions for $t \geq 0$. From Eq. (2.1), we have

$$\frac{dN_b}{dt} = \Lambda_b - \mu_b N_b - \delta_b I_b \leq \Lambda_b - \mu_b N_b$$
$$\frac{dN_h}{dt} = \Lambda_h - \mu_h N_h - dI_a - \alpha I_m \leq \Lambda_h - \mu_h N_h.$$

The closed set

$$\mathcal{D} = \left\{ (S_b, I_b, S_h, I_a, I_m) \in \mathbb{R}^5_+ : N_b \leq \frac{\Lambda_b}{\mu_b}, N_h \leq \frac{\Lambda_h}{\mu_h} \right\}$$

is a feasible region of the model.

Proposition 1 *The closed set $\mathcal{D}$ is bounded and positively invariant.*

Proof Because $\frac{dN_b}{dt} \leq \Lambda_b - \mu_b N_b$, N_b is bounded above by $\frac{\Lambda_b}{\mu_b}$. Hence $\frac{dN_b}{dt} < 0$ whenever $N_b(t) > \frac{\Lambda_b}{\mu_b}$. Using an integrating factor, we have

$$N_b(t) \leq N_b(0) e^{-\mu_b t} + \frac{\Lambda_b}{\mu_b}(1 - e^{-\mu_b t}).$$

As $t \to \infty$, $e^{-\mu_b t} \to 0$ and hence $\lim_{t\to\infty} N_b(t) \leq \frac{\Lambda_b}{\mu_b}$.

The other case is similar. Thus $\mathcal{D}$ is bounded and positively invariant in $\mathbb{R}^5_+$.

Appendix 2: Stability analysis of the avian-only model

We consider the avian-only model, given by the first two equations of the Eq. (2.1)

A feasible region is defined as

$$\mathcal{D}_b = \left\{ (S_b, I_b) \in \mathbb{R}^2_+ : S_b + I_b \le \frac{\Lambda_b}{\mu_b} \right\}.$$

It can be shown from Proposition 1 that $\mathcal{D}_b$ is bounded and positively invariant over $\mathbb{R}^2_+$. The DFE (disease-free equilibrium) is

$$E^0_b = (S^0_b, I^0_b) = \left(\frac{\Lambda_b}{\mu_b}, 0 \right)$$

and the EE (endemic equilibrium) is

$$E^*_b = (S^*_b, I^*_b) = \left(\frac{\Lambda_b + H_b(\mu_b + \delta_b)}{\mu_b + \beta_b}, \frac{\beta_b \Lambda_b - \mu_b H_b(\mu_b + \delta_b)}{(\mu_b + \beta_b)(\mu_b + \delta_b)} \right).$$

The basic reproduction number (see Li et al. 2011; van den Driessche and Watmough 2002 for further details and some complications) for the avian-only model is thus

$$R_b = \frac{\beta_b \Lambda_b}{\mu_b H_b(\mu_b + \delta_b)}.$$

Next, we would like to determine whether or not the model achieves global stability of the DFE or EE with respect to positive initial conditions.

Theorem 2 (Global stability of the DFE for the avian-only model) *Let* $E^0_b = (S^0_b, I^0_b) = \left(\frac{\Lambda_b}{\mu_b}, 0\right)$. *If* $R_b < 1$, *then the DFE,* E^0_b, *is globally stable in the interior* $\Gamma_b = \{(S_b, I_b) \in \mathbb{R}^2_+ : S_b, I_b \le N_b\}$.

Proof Consider a Lyapunov function, $L(S_b, I_b) = \frac{\Lambda_b}{\mu_b H_b(\mu_b + \delta_b)} I_b$. At the DFE, we have $L(S^0_b, I^0_b) = L\left(\frac{\Lambda_b}{\mu_b}, 0\right) = 0$. Its derivative is

$$\begin{aligned}
\frac{dL}{dt} &= \frac{\Lambda_b}{\mu_b H_b(\mu_b + \delta_b)} \left[\frac{\beta_b S_b I_b}{H_b + I_b} - (\mu_b + \delta_b) I_b \right] \\
&= R_b S_b \frac{I_b}{H_b + I_b} - \frac{\Lambda_b I_b}{\mu_b H_b} \\
&\le R_b S_b \frac{I_b}{H_b} - \frac{\Lambda_b I_b}{\mu_b H_b} \\
&\le R_b \frac{\Lambda_b}{\mu_b} \left(\frac{I_b}{H_b} \right) - \frac{\Lambda_b I_b}{\mu_b H_b} \quad \text{where at the DFE, we have} \\
N_b \le \frac{\Lambda_b}{\mu_b} &\Rightarrow S_b \le \frac{\Lambda_b}{\mu_b} \\
&= \frac{\Lambda_b I_b}{\mu_b H_b} (R_b - 1) \\
&< 0 \quad \text{if } R_b < 1
\end{aligned}$$

Thus a periodic solution for this avian-only model does not exist for $(S_b, I_b) \in \Gamma_b$. Therefore, the global stability of the DFE is satisfied. □

Theorem 3 (Global stability of the EE for the avian-only model) *Let* $E^*_b = (S^*_b, I^*_b)$. *If* $R_b > 1$, *then the EE,* E^*_b, *is globally stable in* $\Gamma_b = \{(S_b, I_b) \in \mathbb{R}^2_+ : S_b \le N_b, I_b \le N_b\}$.

Proof Let $f_1 = \Lambda_b - \mu_b S_b - \frac{\beta_b S_b I_b}{H_b + I_b}$, $f_2 = \frac{\beta_b S_b I_b}{H_b + I_b} - (\mu_b + \delta_b) I_b$ and $B(S_b, I_b) = \frac{1}{I_b}$.

$$\begin{aligned}
\nabla(Bf) &= \frac{\partial}{\partial S_b}(Bf_1) + \frac{\partial}{\partial I_b}(Bf_2) \\
&= -\left[\frac{\mu_b}{I_b} + \frac{\beta_b}{H_b + I_b} + \frac{\beta_b S_b}{(H_b + I_b)^2} \right] < 0 \quad \forall\, (S_b, I_b) \in \Gamma_b.
\end{aligned}$$

As $\nabla(Bf) < 0 \forall\, (S_b, I_b) \in \Gamma_b$, then by Bendixson's Negative Criterion (Perko 2001), no periodic orbit can lie entirely in Γ_b. Since $R_b > 1$, the DFE is unstable and hence, in a two-dimensional system, the EE is globally stable in Γ_b. □

Appendix 3: Stability analysis of the avian–human model

Since R_h decouples from the remaining equations in model (2.1), we consider the first five equations of model (2.1). We denote this as the avian–human model.

The transmission matrix, F, and transition matrix, V, of this model are

$$F = \begin{pmatrix} \frac{\beta_b H_b S_b}{(H_b + I_b)^2} & 0 & 0 \\ \frac{\beta_{bh} H_{hb} S_h}{(H_{bh} + I_b)^2} & \frac{\beta_a H_a S_h}{(H_a + I_a)^2} & 0 \\ 0 & 0 & \frac{\beta_m H_m S_h}{(H_m + I_m)^2} \end{pmatrix}$$

$$V = \begin{pmatrix} \mu_b + \delta_b & 0 & 0 \\ 0 & \mu_h + d + \epsilon + \gamma_a & 0 \\ 0 & -\epsilon & \mu_h + \alpha + \gamma_m \end{pmatrix}.$$

Thus we have

$$FV^{-1} = \begin{pmatrix} \frac{\beta_b H_b S_b}{(\mu_b + \delta_b)(H_b + I_b)^2} & 0 & 0 \\ \frac{\beta_{bh} H_{hb} S_h}{(\mu_b + \delta_b)(H_{bh} + I_b)^2} & \frac{\beta_a H_a S_h}{(\mu_h + d + \epsilon + \gamma_a)(H_a + I_a)^2} & 0 \\ 0 & \frac{\epsilon \beta_m H_m S_h}{(\mu_h + d + \epsilon + \gamma_a)(\mu_h + \alpha + \gamma_m)(H_m + I_m)^2} & \frac{\beta_m H_m S_h}{(\mu_h + \alpha + \gamma_m)(H_m + I_m)^2} \end{pmatrix}.$$

The DFE of this model is

$$E^0_{ah} = (S^0_b, I^0_b, S^0_h, I^0_a, I^0_m) = \left(\frac{\Lambda_b}{\mu_b}, 0, \frac{\Lambda_h}{\mu_h}, 0, 0 \right).$$

At the DFE, we have

$$FV^{-1} = \begin{pmatrix} \frac{\beta_b \Lambda_b}{H_b \mu_b (\mu_b + \delta_b)} & 0 & 0 \\ \frac{\beta_{bh} \Lambda_h}{H_{bh} \mu_h (\mu_b + \delta_b)} & \frac{\beta_a \Lambda_h}{H_a \mu_h (\mu_h + d + \epsilon + \gamma_a)} & 0 \\ 0 & \frac{\epsilon \beta_m \Lambda_h}{H_m \mu_h (\mu_h + d + \epsilon + \gamma_a)(\mu_h + \alpha + \gamma_m)} & \frac{\beta_m \Lambda_h}{H_m \mu_h (\mu_h + \alpha + \gamma_m)} \end{pmatrix}$$

and

$$R_{\mathrm{ah}} \equiv \max\left\{\frac{\beta_{\mathrm{b}}\Lambda_{\mathrm{b}}}{H_{\mathrm{b}}\mu_{\mathrm{b}}(\mu_{\mathrm{b}}+\delta_{\mathrm{b}})}, \frac{\beta_{\mathrm{a}}\Lambda_{\mathrm{h}}}{H_{\mathrm{a}}\mu_{\mathrm{h}}(\mu_{\mathrm{h}}+d+\epsilon+\gamma_{\mathrm{a}})}, \times \frac{\beta_{\mathrm{m}}\Lambda_{\mathrm{h}}}{H_{\mathrm{m}}\mu_{\mathrm{h}}(\mu_{\mathrm{h}}+\alpha+\gamma_{\mathrm{m}})}\right\} \quad (5.3)$$
$$\Rightarrow R_{\mathrm{ah}} = \max\{R_{\mathrm{b}}, R_{\mathrm{h1}}, R_{\mathrm{h2}}\}$$

where $R_{\mathrm{h1}} = \frac{\beta_{\mathrm{a}}\Lambda_{\mathrm{h}}}{H_{\mathrm{a}}\mu_{\mathrm{h}}(\mu_{\mathrm{h}}+d+\epsilon+\gamma_{\mathrm{a}})}$ and $R_{\mathrm{h2}} = \frac{\beta_{\mathrm{m}}\Lambda_{\mathrm{h}}}{H_{\mathrm{m}}\mu_{\mathrm{h}}(\mu_{\mathrm{h}}+\alpha+\gamma_{\mathrm{m}})}$.

Theorem 4 (Global stability of the DFE for the avian–human model) *Let* $E^0_{\mathrm{ah}} = (S^0_{\mathrm{b}}, I^0_{\mathrm{b}}, S^0_{\mathrm{h}}, I^0_{\mathrm{a}}, I^0_{\mathrm{m}}) = \left(\frac{\Lambda_{\mathrm{b}}}{\mu_{\mathrm{b}}}, 0, \frac{\Lambda_{\mathrm{h}}}{\mu_{\mathrm{h}}}, 0, 0\right)$. *If* $R_{\mathrm{ah}} < 1$, *then the DFE,* E^0_{ah}, *is globally stable in the interior* $\Gamma_{\mathrm{ah}} = \{(S_{\mathrm{b}}, I_{\mathrm{b}}, S_{\mathrm{h}}, I_{\mathrm{a}}, I_{\mathrm{m}}) \in \mathbb{R}^5_+ : S_{\mathrm{b}}, I_{\mathrm{b}} \le N_{\mathrm{b}}, S_{\mathrm{h}}, I_{\mathrm{a}}, I_{\mathrm{m}} \le N_{\mathrm{h}}\}$.

Proof Consider a Lyapunov function,

$$L(S_{\mathrm{b}}, I_{\mathrm{b}}, S_{\mathrm{h}}, I_{\mathrm{a}}, I_{\mathrm{m}}) = \frac{\Lambda_{\mathrm{b}}}{H_{\mathrm{b}}\mu_{\mathrm{b}}(\mu_{\mathrm{b}}+\delta_{\mathrm{b}})} I_{\mathrm{b}} + \frac{\Lambda_{\mathrm{h}}}{H_{\mathrm{a}}\mu_{\mathrm{h}}(\mu_{\mathrm{h}}+d+\epsilon+\gamma_{\mathrm{a}})} I_{\mathrm{a}} + \frac{\Lambda_{\mathrm{h}}}{H_{\mathrm{m}}\mu_{\mathrm{h}}(\mu_{\mathrm{h}}+\alpha+\gamma_{\mathrm{m}})} I_{\mathrm{m}}.$$

At the DFE, we have $L(S^0_{\mathrm{b}}, I^0_{\mathrm{b}}, S^0_{\mathrm{h}}, I^0_{\mathrm{a}}, I^0_{\mathrm{m}}) = L\left(\frac{\Lambda_{\mathrm{b}}}{\mu_{\mathrm{b}}}, 0, \frac{\Lambda_{\mathrm{h}}}{\mu_{\mathrm{h}}}, 0, 0\right) = 0$. Its derivative is

$$\begin{aligned}
\frac{\mathrm{d}L}{\mathrm{d}t} &= \frac{\Lambda_{\mathrm{b}}}{H_{\mathrm{b}}\mu_{\mathrm{b}}(\mu_{\mathrm{b}}+\delta_{\mathrm{b}})} I'_{\mathrm{b}} + \frac{\Lambda_{\mathrm{h}}}{H_{\mathrm{a}}\mu_{\mathrm{h}}(\mu_{\mathrm{h}}+d+\epsilon+\gamma_{\mathrm{a}})} I'_{\mathrm{a}} \\
&\quad + \frac{\Lambda_{\mathrm{h}}}{H_{\mathrm{m}}\mu_{\mathrm{h}}(\mu_{\mathrm{h}}+\alpha+\gamma_{\mathrm{m}})} I'_{\mathrm{m}} = \frac{\Lambda_{\mathrm{b}}}{H_{\mathrm{b}}\mu_{\mathrm{b}}(\mu_{\mathrm{b}}+\delta_{\mathrm{b}})} \\
&\quad \times \left[\frac{\beta_{\mathrm{b}} S_{\mathrm{b}} I_{\mathrm{b}}}{H_{\mathrm{b}}+I_{\mathrm{b}}} - (\mu_{\mathrm{b}}+\delta_{\mathrm{b}}) I_{\mathrm{b}}\right] + \frac{\Lambda_{\mathrm{h}}}{H_{\mathrm{a}}\mu_{\mathrm{h}}(\mu_{\mathrm{h}}+d+\epsilon+\gamma_{\mathrm{a}})} \\
&\quad \times \left[\frac{\beta_{\mathrm{bh}} S_{\mathrm{h}} I_{\mathrm{b}}}{H_{\mathrm{bh}}+I_{\mathrm{b}}} + \frac{\beta_{\mathrm{a}} S_{\mathrm{h}} I_{\mathrm{a}}}{H_{\mathrm{a}}+I_{\mathrm{a}}} - (\mu_{\mathrm{h}}+d+\epsilon+\gamma_{\mathrm{a}}) I_{\mathrm{a}}\right] \\
&\quad + \frac{\Lambda_{\mathrm{h}}}{H_{\mathrm{m}}\mu_{\mathrm{h}}(\mu_{\mathrm{h}}+\alpha+\gamma_{\mathrm{m}})} \left[\frac{\beta_{\mathrm{m}} S_{\mathrm{h}} I_{\mathrm{m}}}{H_{\mathrm{m}}+I_{\mathrm{m}}} + \epsilon I_{\mathrm{a}} - (\mu_{\mathrm{h}}+\alpha+\gamma_{\mathrm{m}}) I_{\mathrm{m}}\right] \\
&\le R_{\mathrm{b}} S_{\mathrm{b}} \frac{I_{\mathrm{b}}}{H_{\mathrm{b}}+I_{\mathrm{b}}} - \frac{\Lambda_{\mathrm{b}} I_{\mathrm{b}}}{H_{\mathrm{b}}\mu_{\mathrm{b}}} + R_{\mathrm{h1}} S_{\mathrm{h}} \frac{I_{\mathrm{a}}}{H_{\mathrm{a}}+I_{\mathrm{a}}} - \frac{\Lambda_{\mathrm{h}} I_{\mathrm{a}}}{H_{\mathrm{a}}\mu_{\mathrm{h}}} \\
&\quad + R_{\mathrm{h2}} S_{\mathrm{h}} \frac{I_{\mathrm{m}}}{H_{\mathrm{m}}+I_{\mathrm{m}}} - \frac{\Lambda_{\mathrm{h}} I_{\mathrm{m}}}{H_{\mathrm{m}}\mu_{\mathrm{h}}} \\
&\le R_{\mathrm{b}} \frac{\Lambda_{\mathrm{b}} I_{\mathrm{b}}}{\mu_{\mathrm{b}} H_{\mathrm{b}}} - \frac{\Lambda_{\mathrm{b}} I_{\mathrm{b}}}{H_{\mathrm{b}}\mu_{\mathrm{b}}} + R_{\mathrm{h1}} \frac{\Lambda_{\mathrm{h}} I_{\mathrm{a}}}{\mu_{\mathrm{h}} H_{\mathrm{a}}} - \frac{\Lambda_{\mathrm{h}} I_{\mathrm{a}}}{H_{\mathrm{a}}\mu_{\mathrm{h}}} + R_{\mathrm{h2}} \frac{\Lambda_{\mathrm{h}} I_{m}}{\mu_{\mathrm{h}} H_{\mathrm{m}}} \\
&\quad - \frac{\Lambda_{\mathrm{h}} I_{\mathrm{m}}}{H_{\mathrm{m}}\mu_{\mathrm{h}}} \\
&= \frac{\Lambda_{\mathrm{b}} I_{\mathrm{b}}}{\mu_{\mathrm{b}} H_{b}} (R_{\mathrm{b}} - 1) + \frac{\Lambda_{\mathrm{h}} I_{\mathrm{a}}}{H_{\mathrm{a}}\mu_{\mathrm{h}}} (R_{\mathrm{h1}} - 1) + \frac{\Lambda_{\mathrm{h}} I_{m}}{H_{\mathrm{m}}\mu_{\mathrm{h}}} (R_{\mathrm{h2}} - 1) \\
&< 0 \quad \text{if } R_{\mathrm{b}}, R_{\mathrm{h1}}, R_{\mathrm{h2}} < 1
\end{aligned}$$

Thus, a periodic solution for this avian–human model does not exist for $(S_{\mathrm{b}}, I_{\mathrm{b}}, S_{\mathrm{h}}, I_{\mathrm{a}}, I_{\mathrm{m}}) \in \Gamma_{\mathrm{ah}}$. □

References

Alexander ME, Bowman C, Moghadas SM, Summers R, Gumel AB, Sahai BM (2004) A vaccination model for transmission dynamics of influenza. SIAM J Appl Dyn Syst 3:503–524

Alexander ME, Moghadas SM, Wu J (2008) A delay differential model for pandemic influenza with antiviral treatment. Bull Math Biol 70:382–397

Bowman C, Gumel AB, van den Driessche P, Wu J, Zhu H (2005) A mathematical model for assessing control strategies against West Nile virus. Bull Math Biol 67:1107–1133

Capasso V, Serio G (1978) A generalization of the Kermack–McKendrick deterministic epidemic model. Math Biosci 42:43–61

Centers for Disease Control and Prevention (2007) CDC avian influenza: current H5N1 situation. http://www.cdc.gov/flu/avian/outbreaks/current.htm (Accessed 28 Jan 2013)

Centers for Disease Control and Prevention (2010) Key facts about avian influenza (bird flu) and highly pathogenic avian influenza A (H5N1) virus. http://www.cdc.gov/flu/avian/gen-info/facts.htm (Accessed 28 Jan 2013)

Centers for Disease Control and Prevention (2012) Human infection with avian influenza A (H5N1) virus: advice for travelers. http://wwwnc.cdc.gov/travel/page/human-infection-avian-flu-h5n1-advice-for-travelers-current-situation.htm (Accessed 28 Jan 2013)

Chan YJ, Lee CL, Hwang SJ et al (2010) Seroprevalence of antibodies to pandemic (H1N1) 2009 influenza virus among hospital staff in a medical center in Taiwan. J Chin Med Assoc 73:62–66

Chowell G, Ammon CE, Hengartner NW, Hyman JM (2005) Transmission dynamics of the great influenza pandemic of 1918 in Geneva, Switzerland: assessing the effects of hypothetical interventions. J Theor Biol 241:193–204

Doyle A, Bonmarin I, Lévy-Bruhl D, Le Strat Y, Desenclos J (2006) Influenza pandemic preparedness in France: modelling the impact of interventions. J Epidemiol Commun Health 60:399–404

Du Y, Xu R (2010) A delayed SIR epidemic model with nonlinear incidence rate and pulse vaccination. J Appl Math Inform 28:1089–1099

Fisher D, Hui D, Zhancheng G, Lee C et al (2011) Pandemic Response Lessons from Influenza H1N1 2009 in Asia Respirol 16:876–882

Food and Agriculture Organization of the United Nations (2004) FAO recommendations on the prevention, control and eradication of highly pathogenic avian influenza (HPAI) in Asia (proposed with the support of the OIE). http://www.fao.org/ag/againfo/programmes/en/programmes.htm (Accessed 30 Jan 2013)

Food and Agriculture Organization of the United Nations (2008) Possible modes of transmission of avian viruses to people: studies in experimental models. http://www.fao.org/docs/eims/upload//250678/aj155e00.pdf (Accessed 30 Jan 2013)

Gao S, Chen L, Nieto JJ, Torres A (2006) Analysis of a delayed epidemic model with pulse vaccination and saturation incidence. Vaccine 24:6037–6045

Government of Ontario (2006) Avian influenza: a guide to personal protective clothing and equipment for workers and employers working with or around poultry or wild birds. http://www.health.gov.on.ca/en/pro/programs/emb/avian/docs/avian_ppe_guide.pdf (Accessed 30 Jan 2013)

Gumel AB (2009) Global dynamics of a two-strain avian influenza model. Int J Comput Math 86:85–108

Hospital Influenza Working Group (2009) Management of novel influenza epidemics in Singapore: consensus recommendations

from the hospital influenza (Singapore). Singapore Med J 50:567–580
Iwami S, Takeuchi Y, Liu X (2007) Avian–human influenza epidemic model. Math Biosci 207:1–25
Iwami S, Suzuki T, Takeuchi Y (2009) Paradox of vaccination: is vaccination really effective against avian flu epidemics? PLoS One 4:e4915
Kaddar A (2009) On the dynamics of a delayed SIR epidemic model with a modified saturated incidence rate. Electr J Differ Equ 133:1–7
Kaddar A (2010) Stability analysis in a delayed SIR epidemic model with a saturated incidence rate. Nonlinear Anal Model Control 15(3):299–306
Kilbourne ED (2006) Influenza pandemics of the 20th century. Emerg Infect Dis 12:9–14
Li J, Blakeley D, Smith? RJ (2011) The failure of R_0. Comput Math Methods Med 2011:527610
Lipsitch M, Cohen T, Murray M, Levin BR (2007) Antiviral resistance and the control of pandemic influenza. PLoS Med 4:e15
Liu X, Yang L (2012) Stability analysis of an SEIQV epidemic model with saturated incidence rate. Nonlinear Anal Real World Applic 13:2671–2679
Longini IM, Halloran ME, Nizam A, Yang Y (2004) Containing pandemic influenza with antiviral agents. Am J Epidemiol 159:623–633
Marangon S, Cecchinato M, Capua I (2008) Use of vaccination in avian influenza control and eradication. Zoonoses Public Health 55:65–72
May RM, Anderson RM (1978) Regulation and stability of host–parasite population interactions: II. Destabilizing processes. J Anim Ecol 47:249–267
Nuño M, Chowell G, Gumel AB (2006) Assessing the role of basic control measures, antivirals and vaccine in curtailing pandemic influenza: scenarios for the US, UK and the Netherlands. J R Soc Interface 4:505–521
Perko L (2001) Differential equations and dynamical systems, 3rd edn. Springer, New York
Ruan S, Wang W (2003) Dynamical bahavior of an epidemic model with a nonlinear incidence rate. J Differ Equ 188:135–163
Stuart-Harris C (1979) Epidemiology of influenza in man. Br Med Bull 35:3–8
Tchuenche JM, Dube N, Bhunu CP, Smith? RJ, Bauch CT (2011) The impact of media coverage on the transmission dynamics of human influenza. BMC Public Health 11(Suppl 1):S5
van den Driessche P, Watmough J (2002) Reproduction numbers and sub-threshold endemic equilibria for compartmental models of disease transmission. Math Biosci 180:29–48
Wei C, Chen L (2008) A delayed epidemic model with pulse vaccination. Discrete Dyn Nat Soc 2008:746951
World Health Organization (2006) Avian influenza, including influenza A (H5N1), in humans: WHO interim infection control guideline for health care facilities. https://www.premierinc.com/quality-safety/tools-services/safety/topics/influenza/downloads/07-who-ai-inf-control-guide05-10-07.pdf (Accessed 30 Jan 2013)
World Health Organization (2007) Options for the use of human H5N1 influenza vaccines and the WHO H5N1 vaccine stockpile. http://www.who.int/csr/resources/publications/WHO_HSE_EPR_GIP_2008_1d.pdf (Accessed 30 Jan 2013)
World Health Organization (2011) New: WHO comment on the importance of global monitoring of variant influenza viruses. http://www.who.int/influenza/human_animal_interface/avian_influenza/h5n1-2011_12_19/en/index.html (Accessed 30 Jan 2013)
World Health Organization (2012) H5N1 avian influenza: timeline of major events. http://www.who.int/influenza/human_animal_interface/avian_influenza/H5N1_avian_influenza_update.pdf (Accessed 30 Jan 2013)
Yang J, Zhang F, Wang X (2007) A class of SIR epidemic model with saturation incidence and age of infection. Ninth ACIS international conference on software engineering, artificial intelligence, networking, and parallel/distributed computing, vol 1, pp 146–149
Yang Y, Sugimoto JD, Halloran ME, Basta NE et al (2009) The transmissibility and control of pandemic influenza A (H1N1) virus. Sci Agric 326:729–733
Zhang F, Li Z-Z, Zhang F (2008) Global stability of an SIR epidemic model with constant infectious period. Appl Math Comput 199:285–291
Zhou Y, Liu H (2003) Stability of periodic solutions for an SIS model with pulse vaccination. Math Comput Model 38:299–308

Bibliography

[1] T Shors. *Understanding Viruses*. Jones and Bartlett Publishers, Sudbury, Massachusetts, 2009.

[2] E D Kilbourne. Influenza pandemics of the 20th century. *Emerging Infectious Diseases*, 12(1):9–14, 2006.

[3] J K Taubenberger and D M Morens. 1918 influenza: the mother of all pandemics. *Emerging Infectious Diseases*, 12(1):15–22, 2006.

[4] D A Henderson, B Courtney, T V Inglesby, E Toner, and J B Nuzzo. Public health and medical responses to the 1957–58 influenza pandemic. *Biosecurity and Bioterrorism: Biodefense Strategy, Practice, and Science*, 7(3):265–273, 2009.

[5] C Jackson. History lessons: the Asian flu pandemic. *British Journal of General Practice*, 59(565):622–623, 2009.

[6] Timeline of human flu pandemics. Technical report, National Institute of Allergy and Infectious Diseases, 2006.

[7] Influenza: questions and answers. Technical report, Immunization Action Coalition, 2006.

[8] How human influenza transmits from person to person. Technical report, European Centre for Disease Prevention and Control, 2009.

[9] How flu spreads. Technical report, Centers for Disease Control and Prevention, 2014.

[10] Avian influenza A (H7N9) virus. Technical report, Centers for Disease Control and Prevention, 2014.

[11] Information on avian influenza. Technical report, Centers for Disease Control and Prevention, 2015.

[12] P K S Chan. Outbreak of avian influenza A (H5N1) virus infection in Hong Kong in 1997. *Clinical Infectious Diseases*, 34(Suppl 2):S58–64, 2002.

[13] M Du Ry van Beest Holle, A Meijer, M Koopmans, and C M de Jager. Human-to-human transmission of avian influenza A/H7N7, The Netherlands, 2003. *Euro Surveill*, 10(12):264–268, 2005.

[14] World Health Organization. Weekly epidemiological record. 83(40):357–364, 2008.

[15] S S Y Wong and K Yuen. Avian influenza virus infections in humans. *Chest*, 129(1):156–168, 2006.

[16] L D Sims, T M Ellis, K K Liu, K Dyrting, H Wong, M Peiris, Y Guan, and K F Shortridge. Avian influenza in Hong Kong 1997–2002. *Avian Diseases*, 47:832–838, 2003.

[17] Avian influenza A (H7N9) virus. Technical report, World Health Organization.

[18] J Hu, Y Zhu, B Zhao, J Li, L Liu, K Gu, W Zhang, H Su, Z Teng, S Tang, Z Yuan, Z Feng, and F Wu. Limited human-to-human transmission of avian influenza A (H7N9) virus, Shanghai, China, March to April 2013. *Euro Surveill*, 19(25):pii=20838, 2014.

[19] C A A Beauchemin and A Handel. A review of mathematical models of influenza A infections within a host or cell culture: lessons learned and challenges ahead. *BMC Public Health*, 11(Suppl 1):S7, 2011.

[20] C X Lei, K I Kim, and Z G Lin. The spreading frontiers of avian–human influenza described by the free boundary. *Sci. China Math.*, 57:971–990, 2014.

[21] M V Maciosek, L I Solberg, A B Coffield, N M Edwards, and M J Goodman. Influenza vaccination: health impact and cost effectiveness among adults aged 50 to 64 and 65 and older. *American Journal of Preventive Medicine*, 31(1):72–79, 2006.

[22] M A Penny, J Saurina, I Keller, L Jenni, H-G Bauer, W Fiedler, and J Zinsstag. Transmission dynamics of highly pathogenic avian influenza at Lake Constance (Europe) during the outbreak of winter 2005–2006. *EcoHealth*, 7:275–282, 2010.

[23] B Roche, J M Drake, and P Rohani. An agent-based model to study the epidemiological and evolutionary dynamics of influenza viruses. *BMC Bioinformatics*, 12:87, 2011.

[24] K J Smith and M S Roberts. Cost-effectiveness of newer treatment strategies for influenza. *American Journal of Medicine*, 113:300–307, 2002.

[25] Types of influenza. Technical report, News Medical, 2014.

[26] Types of influenza viruses. Technical report, Centers for Disease Control and Prevention, 2014.

[27] What's the difference between cold and flu? Technical report, Scientific American, 2008.

[28] Cold versus flu. Technical report, Centers for Disease Control and Prevention, 2015.

[29] There's a difference between cold and flu; here's what you need to know to stay healthy. Technical report, Medical Daily, 2015.

[30] The influenza virus: structure and replication. Technical report, Rapid Reference to Influenza, 2006.

[31] Influenza virus types, subtypes, and strains. Technical report, PA Pandemic Influenza Preparedness Planning Summit, 2006.

[32] A E Fiore, A Fry, D Shay, L Gubareva, J S Bresee, and T M Uyeki. Antiviral agents for the treatment and chemoprophylaxis of influenza. *Centers for Disease Control and Prevention MMWR (Morbidity and Mortality Weekly Report)*, 60(1):1–25, 2011.

[33] M Tisdale. *Antimicrobial drug resistance. Volume 1: Mechanisms of drug resistance*. Humana Press, New York, 2009.

[34] J L McKimm-Breschkin. Influenza neuraminidase inhibitors: Antiviral action and mechanisms of resistance. *Influenza and Other Respiratory Viruses*, 7(Suppl. 1), 2012.

[35] M I S Costa and M E M Meza. Application of a threshold policy in the management of multispecies fisheries and predator culling. *Mathematical Medicine and Biology*, 23:63–75, 2006.

[36] V I Utkin. *Sliding Modes in Control and Optimization*. Springer-Verlag Berlin, Heidelberg, 1992.

[37] J P Aubin and A Cellina. *Differential Inclusions*. Springer-Verlag Berlin, Heidelberg, 1984.

[38] A F Filippov. *Differential Equations with Discontinuous Right-hand Sides*. Kluwer Academic Dordrecht, The Nertherlands, 1988.

[39] R I Leine. *Bifurcations in Discontinuous Mechanical Systems of Filippov-Type*. The Universiteitsdrukkerij TU Eindhoven, The Netherlands, 2000.

[40] R J Smith? *Differential Equations and Dynamical Systems Volume 2: Modelling Disease Ecology with Mathematics*. American Institute of Mathematical Sciences, United States of America, 2008.

[41] N S Chong, J M Tchuenche, and R J Smith? A mathematical model of avian influenza with half-saturated incidence. *Theory in Biosciences*, 133(1):23–38, 2014.

[42] N S Chong and R J Smith? Modelling avian influenza using Filippov systems to determine culling of infected birds and quarantine. *Nonlinear Analysis: Real World Applications*, 24:196–218, 2015.

[43] N S Chong, B Dionne, and R J Smith? An avian-only Filippov model incorporating culling of both susceptible and infected birds in combating avian influenza. *Mathematical Biology*, 73:751–784, 2016.

[44] G de Vries, T Hillen, M Lewis, J Müller, and B Schönfisch. *A Course in Mathematical Biology: Quantitative Modeling with Mathematical and Computational Methods*. Society for Industrial and Applied Mathematics, University City Science Center, Philadelphia, 2006.

[45] V Křivan. Dynamic ideal free distribution: effects of optimal patch choice on predator–prey dynamics. *The American Naturalist*, 149(1):164–178, 1997.

[46] C-F Lee, A C Lee, and J Lee. *Handbook of Quantitative Finance and Risk Management*. Springer, New York, 2010.

[47] K Rama Reddy, S B Badami, and V Balasubramanian. *Oscillations and Waves*. Universities Press (India) Limited, India, 1994.

[48] B J Williams. *Hydrobiological Modelling*. University of Newcastle, NSW, Australia, 2006.

[49] T Zhao, Y Xiao, and R J Smith? Non-smooth plant disease models with economic thresholds. *Mathematical Biosciences*, 241:34–48, 2013.

[50] J. K. Hale. *Ordinary Differential Equations*. Robert E. Krieger Publishing Company, Florida, USA, 1980.

[51] Walter Rudin. *Real and Complex Analysis*. McGraw-Hill, Inc., USA, 1974.

[52] Hartmut Logemann and Eugene P. Ryan. Asymptotic behaviour of nonlinear systems. *The American Mathematical Monthly*, 111(10).

[53] E Roxin. Stability in general control systems. *Differential Equations*, 1:115–150, 1965.

[54] D S Boukal and V Křivan. Lyapunov functions for Lotka–Volterra predator-prey models with optimal foraging behavior. *Mathematical Biology*, 39:493–517, 1999.

[55] R I Leine and N van de Wouw. *Stability and Convergence of Mechanical Systems with Unilateral Constraints*. Springer-Verlag Berlin, Heidelberg, 2008.

[56] S. Wiggins. *Introduction to Applied Nonlinear Dynamical Systems and Chaos*. Springer-Verlag, New York, Berlin, Heidelberg, 2003.

[57] L Perko. *Differential Equations and Dynamical Systems*. Springer-Verlag, New York, third edition edition, 2001.

[58] S Iwami, Y Takeuchi, A Korobeinikov, and X Liu. Prevention of avian influenza epidemic: what policy should we choose? *Journal of Theoretical Biology*, 252:732–741, 2008.

[59] S Iwami, Y Takeuchi, and X Liu. Avian flu pandemic: can we prevent it? *Journal of Theoretical Biology*, 257:181–190, 2009.

[60] A B Gumel. Global dynamics of a two-strain avian influenza model. *Int J Computer Math*, 86:85–108, 2009.

[61] J Li, D Blakeley, and R J Smith? The Failure of R_0. *Comp Math Methods Med*, ID 527610, 2011.

[62] P van den Driessche and J Watmough. Reproduction numbers and sub-threshold endemic equilibria for compartmental models of disease transmission. *Math Biosci*, 180:29–48, 2002.

[63] C Bowman, A B Gumel, P van den Driessche, J Wu, and H Zhu. A mathematical model for assessing control strategies against West Nile virus. *Bull. Math. Biol.*, 67:1107–1133, 2005.

[64] H Gulbudak and M Martcheva. Forward hysteresis and backward bifurcation caused by culing in an avian influenza model. *Math Biosci*, 246:202–212, 2013.

[65] D R Perez and A Garcia-Sastre. H5N1, a wealth of knowledge to improve pandemic preparedness. *Virus Research*, 178:1–2, 2013.

[66] V Capasso and G Serio. A generalization of the Kermack–McKendrick deterministic epidemic model. *Math. Biosci.*, 42:43–61, 1978.

[67] X Liu and L Yang. Stability analysis of an SEIQV epidemic model with saturated incidence rate. *Nonlinear Analysis: Real World Applications*, 13:2671–2679, 2012.